WIND TUNNEL INVESTIGATION OF THE PRESSURE DISTRIBUTION ON A TWO-DIMENSIONAL AIRFOIL WITH PYLON-MOUNTED STORES AT MACH NUMBERS FROM 0.7 TO 0.95

D. K. Smith

ARO, Inc.

April 1973

PROPULSION WIND TUNNEL FACILITY
ARNOLD ENGINEERING DEVELOPMENT CENTER
AIR FORCE SYSTEMS COMMAND
ARNOLD AIR FORCE STATION, TENNESSEE

NOTICES

When U. S. Government drawings specifications, or other data are used for any purpose other than a definitely related Government procurement operation, the Government thereby incurs no responsibility nor any obligation whatsoever, and the fact that the Government may have formulated, furnished, or in any way supplied the said drawings, specifications, or other data, is not to be regarded by implication or otherwise, or in any manner licensing the holder or any other person or corporation, or conveying any rights or permission to manufacture, use, or sell any patented invention that may in any way be related thereto.

Qualified users may obtain copies of this report from the Defense Documentation Center.

References to named commercial products in this report are not to be considered in any sense as an endorsement of the product by the United States Air Force or the Government.

WIND TUNNEL INVESTIGATION OF THE PRESSURE DISTRIBUTION ON A TWO-DIMENSIONAL AIRFOIL WITH PYLON-MOUNTED STORES AT MACH NUMBERS FROM 0.7 TO 0.95

D. K. Smith
ARO, Inc.

FOREWORD

The work reported herein was conducted at the Arnold Engineering Development Center (AEDC) under sponsorship of the Air Force Armament Laboratory (DLGC/Capt. V. E. Studwell), Armament Development and Test Center (ADTC), Air Force Systems Command (AFSC), under Program Element 62602F, Project 2567.

The test results presented were obtained by ARO, Inc. (a subsidiary of Sverdrup & Parcel and Associates, Inc.), contract operator of the AEDC, AFSC, Arnold Air Force Station, Tennessee. The test was conducted from October 11 to 17, 1972, under ARO Project No. PA030. The manuscript was submitted for publication on March 9, 1973.

This technical report has been reviewed and is approved.

L. R. KISSLING
Lt Colonel, USAF
Chief Air Force Test Director, PWT
Directorate of Test

A. L. COAPMAN
Colonel, USAF
Director of Test

ABSTRACT

A wind tunnel test was conducted to determine pressure distributions on a two-dimensional airfoil with pylon-mounted stores at Mach numbers from 0.70 to 0.95 and angles of attack from 0 to 14 deg. Four geometrically similar pylon-mounted stores differing in diameter by a factor of about four and four pylons differing in height were tested. Pressure distributions on the airfoil were obtained for the clean airfoil configuration and 12 pylon/store combinations. The pressure distributions were integrated and the lift, drag, and pitching-moment coefficients for the airfoil are presented. Total pressure wake surveys and oil flow photographs were also obtained for the test, and typical data are presented.

CONTENTS

APPENDIXES

Figure | Page

Figure | Page

NOMENCLATURE

b	Airfoil span (assumed 1 in. for calculations)
c	Airfoil chord length, 6 in.
C_A	Airfoil axial-force coefficient, axial force/$q_\infty cb$
C_D	Airfoil drag coefficient, $C_A \cos \alpha + C_N \sin \alpha$
C_{D_T}	Total drag coefficient, integration of total-pressure wake-survey measurements
C_L	Airfoil lift coefficient, $C_N \cos \alpha - C_A \sin \alpha$
C_m	Airfoil pitching-moment coefficient, pitching moment/$q_\infty c^2 b$
C_N	Airfoil normal-force coefficient, normal force/$q_\infty cb$
C_p	Pressure coefficient, $(p - p_\infty)/q_\infty$
C_{p_T}	Total-pressure probe coefficient, $(p_t - p_\infty)/q_\infty$
C_{p_U}	Pressure coefficient on upper surface of airfoil
Loc	Spanwise location of pylon or pylon/store on airfoil, measured spanwise from pressure orifice locations on airfoil, in. (see Fig. 2b)
M_∞	Free-stream Mach number
p	Local pressure on airfoil, psia
p_T	Local total pressure in the wake, psia
p_∞	Free-stream static pressure, psia
q_∞	Free-stream dynamic pressure, psi
Re	Free-stream unit Reynolds number, ft^{-1}
X	Distance to pressure orifice on airfoil measured from the leading edge of the airfoil along the chord, in. (see Fig. 2b); also longitudinal distance between pitot probe and trailing edge of the airfoil, in. (see Fig. 6)
Y	Lateral distance between pitot probe and orifice locations on the airfoil, in. (see Fig. 6)

Z Vertical distance between pitot probe and chord of the airfoil, in. (see Fig. 6)

α Airfoil angle of attack, deg

Note: Force and moment coefficient orientation shown in Fig. 7. Airfoil span is assumed equal to 1 in. for calculating the forces and moments.

SECTION I
INTRODUCTION

Wind tunnel tests were conducted to determine the pressure distributions on a two-dimensional airfoil with pylon-mounted stores in the transonic flow regime. Past experimental work with specific store configurations on particular aircraft has shown that the addition of external stores on wing pylons of high performance aircraft severely restricts the performance of the aircraft.[1] The present test used a family of low drag stores differing in geometric size by a factor of 3.75 and several pylons differing only in height between airfoil and store. The airfoil was a two-dimensional, unswept configuration supported by end plates.

The tests were conducted in the Aerodynamic Wind Tunnel (4T) of the AEDC Propulsion Wind Tunnel Facility (PWT) at Mach numbers from 0.70 to 0.95 and Reynolds numbers per foot of 5.0×10^6. Chordwise pressure distributions were obtained on the airfoil for the clean configuration and for 12 pylon/store combinations at various spanwise positions on the airfoil. The pressure distributions were integrated to obtain normal-force, axial-force, and pitching-moment coefficients at a given Mach number and angle of attack. The airfoil angles of attack were varied from 0 to 14 deg. Wake total pressure data were obtained with a total-pressure probe located two chord lengths downstream from the trailing edge of the airfoil. The probe was attached to the captive trajectory system (CTS) in Tunnel 4T. Oil flow visualization methods were also used to obtain flow patterns on the airfoil.

SECTION II
APPARATUS

2.1 TEST FACILITY

The Aerodynamic Wind Tunnel (4T) is a closed-loop, continuous-flow, variable-density tunnel in which the Mach number can be varied from 0.1 to 1.3. At all Mach numbers, the stagnation pressure can be varied from 300 to 3700 psfa. The test section is 4 ft square and 12.5 ft long with perforated, variable porosity (0.5- to 10-percent open) walls. It is completely enclosed in a plenum chamber from which the air can be evacuated, allowing part of the tunnel airflow to be removed through the perforated walls of the test section.

The airfoil and its support system were attached to the main pitch sector which extends up from the tunnel floor. The pitot tube probe was supported by the CTS which extends down from the tunnel top wall and provided probe movement (six degrees of freedom) independent of the airfoil and its support system. A schematic showing the test section details and the location of the model in the tunnel is shown in Fig. 1 (Appendix I).

---

[1]Weber, William B. "Effect of External Stores on the Stability, Control, and Drag Characteristics of the F-4 Aircraft." Proceeding of Aircraft/Store Compatibility Symposium, November 19-21, 1969, Air Force Armament Laboratory, Eglin Air Force Base, Florida.

2.2 TEST ARTICLES

The airfoil was a two-dimensional (constant chord length and constant profile along the span) airfoil supported by end plates and a sting. A single row of pressure orifices was located in the chordwise direction on both the upper and lower surfaces of the airfoil. There were 24 orifices on the upper surface and 15 orifices on the lower surface. The airfoil also had four spanwise locations for attaching the pylon on the lower surface. These four pylon locations were at spanwise positions of 0.00, 0.25, 0.50, and 0.75 in. with respect to the location of the pressure orifices. The details and dimension of the airfoil along with the pressure orifice locations and pylon attachment locations are shown in Fig. 2.

Four geometrically similar stores differing in diameter and length by a factor of 3.75 and four pylons differing in height were used in the tests. The details and dimensions of the stores and pylons along with their configuration code are shown in Fig. 3.

Details and dimensions of the total-pressure tube used to survey the wake are given in Fig. 4. Photographs of the test articles are shown in Fig. 5.

2.3 INSTRUMENTATION

The 39 pressure measurements on the airfoil were made using the 24 port Scanivalves® and two 15-psi pressure transducers. The wake total pressure measurement was made with a 15-psi pressure transducer connected to the probe. The electrical signals from the pressure measurements were digitized and recorded on magnetic tape, as well as used directly for the on-line data reduction. Translational positions of the pitot probe were obtained from the CTS analog outputs. An angular position indicator on the main pitch sector was used to determine the airfoil angle of attack.

For the oil flow visualization studies, a fluorescent dye and oil base carrier mixture was flowed through four orifices near the leading edge of the airfoil. Ultraviolet light was used to illuminate the model and oil, and the oil then emits light (fluoresces) in the visible (or at least photographicable) spectrum. A 70-mm camera equipped with a filter to stop ultraviolet light was then used to photograph the oil patterns.

SECTION III
TEST DESCRIPTION

3.1 TEST CONDITIONS AND PROCEDURE

The test data were obtained in three separate test phases: the pressure distribution phase, the wake survey phase, and the oil visualization phase. Data for all phases were obtained at nominal free-stream Mach numbers of 0.70, 0.80, 0.85, and 0.90. For the clean airfoil, data were also obtained at Mach numbers of 0.825, 0.875, 0.925, and 0.95. The free-stream Reynolds number per foot was 5.0×10^6 for all Mach numbers. The total temperature varied from 90 to 100°F.

For the pressure distribution phase, chordwise pressure distribution data were obtained on the airfoil for the clean configuration and 12 store/pylon combinations. The tunnel conditions were held constant at the prescribed Mach number and Reynolds number while the angle of attack was varied from 0 to 14 deg. Data were recorded at 2-deg increments of angle of attack. Chordwise pressure distributions were obtained for various spanwise positions of a particular pylon/store combination by moving the pylon/store to the different spanwise locations available on the airfoil (see Fig. 2b).

For the wake survey phase, the total pressure data were obtained in the airfoil wake for the clean configuration and 9 pylon/store combinations. The tunnel conditions were held constant at the prescribed Mach number, Reynolds number, and zero angle of attack while the Y and Z locations of the pressure probe were varied. The probe Y locations used in the tests were Y = 0.00, 0.20, and 0.40 in. Total pressure data were recorded with the probe from Z = 0.6 to -5.0 in. at 0.1-in. increments for each of the three Y locations. The X-position of the probe was 12 in. downstream of the airfoil trailing edge for all wake surveys (see Fig. 6 for total-pressure probe coordinates). Also for all wake surveys, the pylon or pylon/store was attached to the airfoil at location 0.00.

For the oil-flow visualization phase, photographs of the oil-flow patterns on both the lower and upper surfaces of the airfoil were obtained for the clean configuration and 5 pylon/store combinations. The tunnel conditions were held constant at the prescribed Mach number, Reynolds number, and zero angle of attack while the oil was forced through orifices near the leading edge of the airfoil with air pressure.

Table I (Appendix II) gives the configurations (pylon/store combinations) tested for each test phase.

3.2 DATA REDUCTION

The pressure distribution data obtained on the airfoil for a given configuration, Mach number, angle of attack, and spanwise location of the pylon/store were integrated to obtain the normal-force, axial-force, and pitching-moment coefficients of the airfoil assuming unit span. The force and moment coefficients were determined numerically. Since pressures were not measured at the trailing edge of the airfoil, the pressure data were extrapolated to the trailing edge. The moment reference is at the quarter-chord point. The orientation of the lift, drag, and pitching-moment coefficients is shown in Fig. 7.

The wake total-pressure data obtained for a given configuration and Mach number were integrated to calculate the total drag of both the airfoil and pylon/store. Only at Mach numbers of 0.70 and 0.80 could the wake drag integration be done effectively. At the remaining Mach numbers, the survey could not be extended sufficiently far in the positive Z direction (movement of CTS system was limited) for the pressures to return to the free-stream total value.

3.3 PRECISION OF MEASUREMENTS

The precision of the data which can be attributed to the error in the transducer, in setting the tunnel conditions, in the numerical integration, and in the measurement of the pressure orifice locations was determined and is presented below:

δC_p	δC_L	δC_D	δC_m
±0.012	±0.030	±0.010	±0.005

The error in setting the Mach number is within ±0.005. The Mach number variation in the portion of the test section occupied by the model is no greater then ±0.002 for all Mach numbers. The error in setting the angle of attack is ±0.1 deg and in setting the total pressure probe positions is ±0.005 in.

SECTION IV
RESULTS AND DISCUSSION

The objective of the test was to determine the pressure distributions on an airfoil with pylon-mounted stores. The test was conducted in three separate phases which were the pressure distribution phase, the wake survey phase, and the oil flow visualization phase. Table I gives the configurations (pylon/store combinations) tested for each phase.

The data presented were machine plotted and faired with straight lines with the exception of the C_{D_T} versus M_∞ plots. Only a selected portion of the data taken is presented for brevity.

The pressure distributions for the clean airfoil at zero angle of attack for several Mach numbers are shown in Fig. 8. As can be seen in Fig. 8, a shockwave appears on the upper surface of the airfoil at $M_\infty = 0.8$. The shockwave location moves forward on the airfoil as the Mach number is increased up to $M_\infty = 0.875$, then moves aft on the airfoil as the Mach number is further increased. The forward movement of the shockwave location is most likely caused by the increase in the separated region on the aft portion of the airfoil. The pressure distributions for the upper and lower surfaces on the clean airfoil at several angles of attack for Mach numbers 0.70, 0.80, 0.85, 0.90, and 0.95 are presented in Figs. 9 through 13, respectively.

The variation in the pressure distributions on the airfoil with spanwise location of selected pylon/store configurations is shown in Figs. 14 through 25. It should be noted that the data for orifices 7 through 13 (X/c = 0.20 to 0.70) of the lower surface are invalid when the pylon is at location 0.00 since these orifices are covered by the pylon (see Fig. 2b). As can be seen in the figures, the pylon and pylon with store have little effect on the upper surface of the airfoil for $M_\infty = 0.70$ and 0.80 (see Figs. 14, 15, 18, and 19). For $M_\infty = 0.85$ and 0.90, the spanwise positions of the pylon or pylon/store on the airfoil tend to change the location of the shockwave on the upper surface. For

all Mach numbers, the pressure distribution on the lower surface of the airfoil is affected by the spanwise location of the pylon or pylon/store, especially at the leading edge of the airfoil. Data obtained with pylon and pylon plus store at angle of attack are presented in Figs. 22 through 25. The results discussed for the pressure distribution on the airfoil with pylon or pylon/store attached are typical for all the pylon/store combinations tested.

The lift, drag, and pitching-moment coefficients of the clean airfoil are shown in Fig. 26. These data were obtained from the pressure measurements.

The effect of spanwise location of the pylon or pylon/store on the lift, drag, and pitching-moment coefficients of the airfoil is shown in Figs. 27 through 34. As seen in the figures, varying the spanwise location of the pylon or pylon plus store from 0.25 to 0.75 has only a small influence on the lift, drag, and pitching-moment coefficient curves for a given Mach number. But varying the spanwise location of the pylon or pylon/store from 0.00 to 0.25 does have a greater influence on the aerodynamic coefficients, especially the drag coefficient which sometimes has as much as a 100-percent reduction at a given C_L between location 0.00 and 0.25 (for example, see Fig. 27). These results, discussed about the influence of spanwise locations of the pylon or pylon/store, are typical for all the pylon/store combinations tested.

The variation in the aerodynamic coefficients with the different pylons, and with the different pylons plus C store at a given pylon location is presented in Figs. 35 through 42. For the pylons alone case, the lift, drag, and pitching-moment coefficients of the airfoil with A and B pylon produced similar values, and likewise, the coefficients of the airfoil with C and D pylons had similar values (see Figs. 35 through 38). In general, the magnitude of the lift coefficient of the airfoil was greater with the A and B pylons than with the C and D pylons. Moreover, the A and B pylons generally showed a lower drag coefficient at a given lift coefficient. Also the magnitude of the pitching-moment coefficient for the airfoil was less at a given lift coefficient with the A and B pylons than with the C and D pylons. The aerodynamic coefficients obtained with the B pylon plus C store on the airfoil varied considerably from the coefficients obtained with the other pylons plus C store as shown in Figs. 39 through 42. The values of the aerodynamic coefficients obtained with the A, C, and D pylons plus C store on the airfoil were similar. Moreover, the lift coefficient of the airfoil was greater with B pylon plus C store than with the other pylons plus C store, and the drag coefficient was less at a given lift coefficient, and the magnitude of the pitching-moment coefficient was less with B pylon plus C store.

The effect on the lift, drag, and pitching-moment coefficients of the airfoil with different stores and B pylon is shown in Figs. 43 through 46. As shown in the figures, the A and C store with B pylon generally produced a greater lift coefficient with a reduced magnitude in the pitching-moment coefficient on the airfoil as compared to the B and D store with B pylon.

Shown in Figs. 47 through 50 are the effects on the lift, drag, and pitching-moment coefficients produced by changing the longitudinal position of the C store on the B pylon.

In general, moving the C store aft on the B pylon (noted as store configuration C-1) had little effect on the lift coefficient and produced a small increase in drag coefficient at a given lift coefficient as compared to the data obtained with C store at normal position on the B pylon. Moreover, the magnitude of the pitching-moment coefficient was increased somewhat by shifting the C store aft on the B pylon for $M_\infty \geq 0.80$ (see Figs. 47 through 50).

When comparing the lift, drag, and pitching-moment coefficients between the clean airfoil and the airfoil with pylon or pylons with stores, the following results were noted at all Mach numbers: in general, the lift coefficient showed a small decrease with pylon or pylon/store added, the drag coefficient showed a slight increase at a given lift coefficient with pylon or pylon/stores added, and the pitching-moment coefficient showed a positive increase with pylon or pylon/stores added. It should be mentioned that the coefficients obtained on the airfoil with some of the pylon/store combinations were reasonably close to the coefficients obtained with the clean airfoil; for instance, the A and B pylon alone, the B pylon with A or C store. In all cases the break in the lift curve occurred earlier with pylon/stores on the airfoil than for the clean airfoil.

The total pressure wake surveys for the clean airfoil and selected pylon/store combinations on the airfoil are shown in Figs. 51 through 53. As expected, the total pressure loss for configurations with pylon/store decreases as the survey moves laterally away from the pylon/store location (decreases as Y increases). The wake survey results shown in the figures for B pylon alone and C pylon plus C store are typical for all the pylon/store configurations tested.

The total drag coefficients calculated from the wake surveys versus Mach number for different pylon/store combinations are shown in Fig. 54. The total drag coefficient could only be calculated for $M_\infty = 0.70$ and 0.80 because at the higher Mach numbers the survey could not be extended far enough in the positive Z direction to return to free-stream total pressure (see Figs. 51 through 53). The drag coefficients calculated from the total-pressure wake surveys usually increased as the size of the pylon increased (see Fig. 54). Also the drag coefficient decreased significantly as the store position was moved aft on the pylon (store configuration C-1).

Photographs of the oil-flow patterns on both the upper and lower surfaces of the airfoil with and without pylon are shown in Figs. 55 through 57. The photographs show that the flow is separated on the upper surface from the shockwave location back to the trailing edge for Mach number ≥ 0.85 (see Fig. 55). The flow pattern shown in Fig. 56 for the upper surface and clean airfoil configuration is also typical for all upper surface flows with pylon/store attached. The photographs show that the flow is separated on the lower surface for $M_\infty = 0.90$ (see Figs. 56 and 57). Figure 57 shows the flow around the pylon for $M_\infty = 0.80$ and 0.90 which was typical for all pylon/store configurations.

SECTION V
CONCLUDING REMARKS

Based on the airfoil test results with pylon-mounted stores, the following conclusions are made:

1. The shockwave location on the upper surface of the airfoil moved forward on the airfoil as the Mach number was increased from 0.80 to 0.875 (caused by the increase of the separated region); then the shockwave location moved aft as the Mach number was further increased.

2. In general, the use of the smaller pylons (A and B) and B pylon with either A or C store produced the least changes in the aerodynamic coefficients compared with the clean airfoil. In all cases, the break in the lift curve occurred earlier with pylon/stores on the airfoil than for the clean airfoil.

3. The rearward location of the C store (store configuration C-1) on the B pylon resulted in lower total-drag coefficients.

APPENDIXES

I. ILLUSTRATIONS

II. TABLE

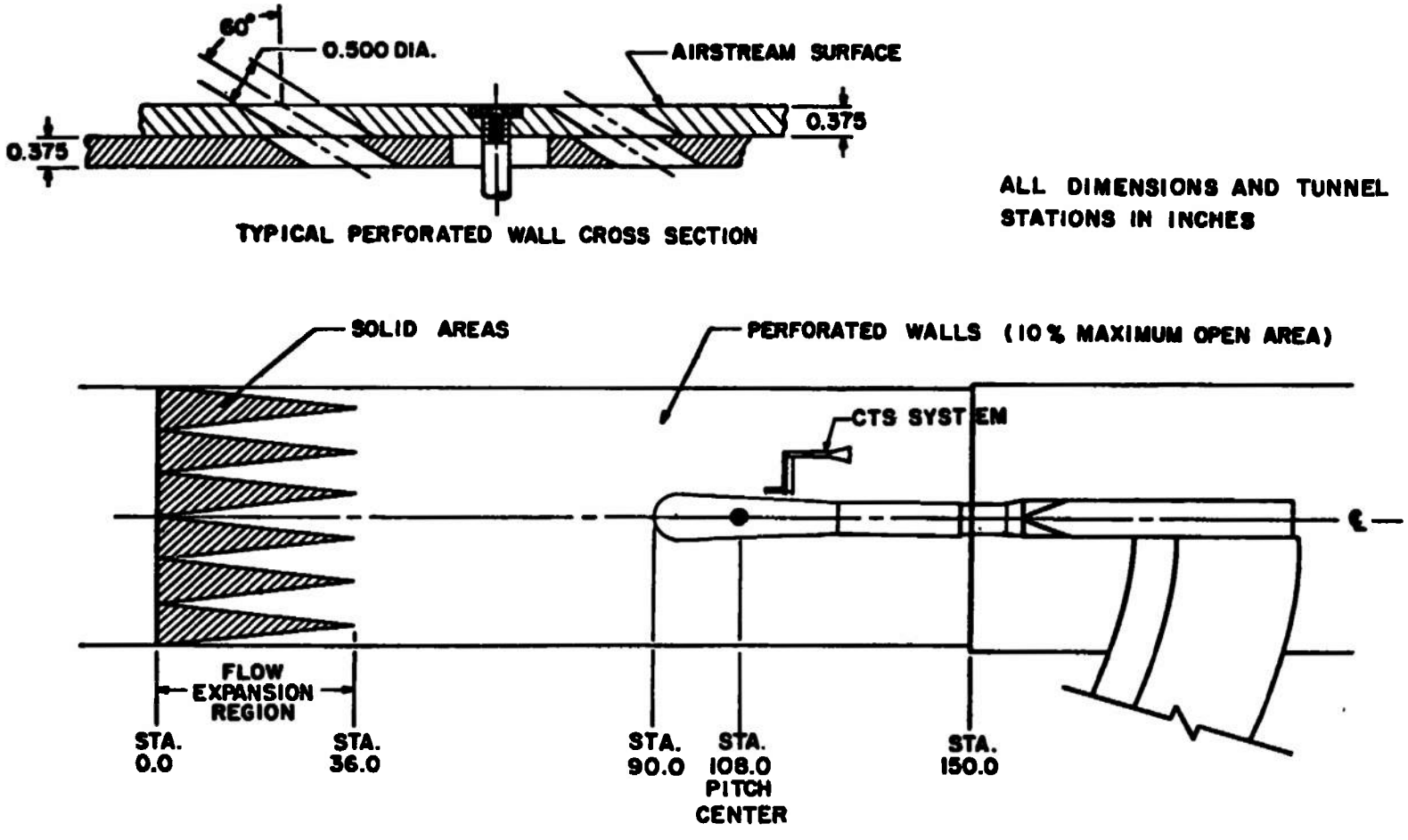

Fig. 1 Schematic of the Tunnel Test Section Showing Model Location

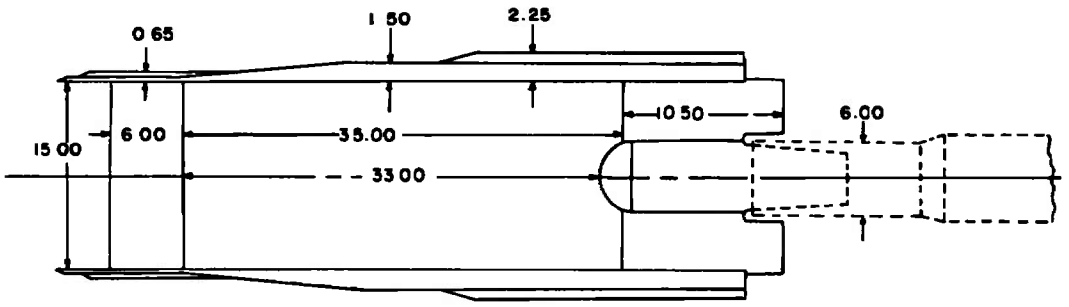

TOP VIEW

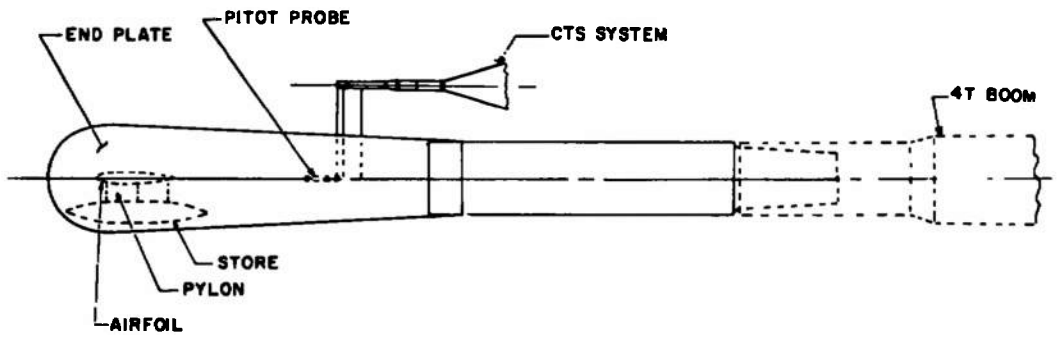

SIDE VIEW WITH PITOT PROBE AND CTS SYSTEM

ALL DIMENSIONS IN INCHES

a. Airfoil and Support System

Fig. 2 Details and Dimensions of Airfoil

Orifice No.	Top Surface X	Bottom Surface X
1	0	0
2	0.150	0.150
3	0.300	0.300
4	0.450	0.450
5	0.600	0.600
6	0.900	0.900
7	1.200	1.200
8	1.500	1.500
9	1.800	1.800
10	2.100	2.400
11	2.700	3.000
12	3.000	3.600
13	3.300	4.200
14	3.480	4.800
15	3.600	5.400
16	3.750	
17	3.900	
18	4.080	
19	4.200	
20	4.380	
21	4.500	
22	4.800	
23	5.400	
24	5.670	

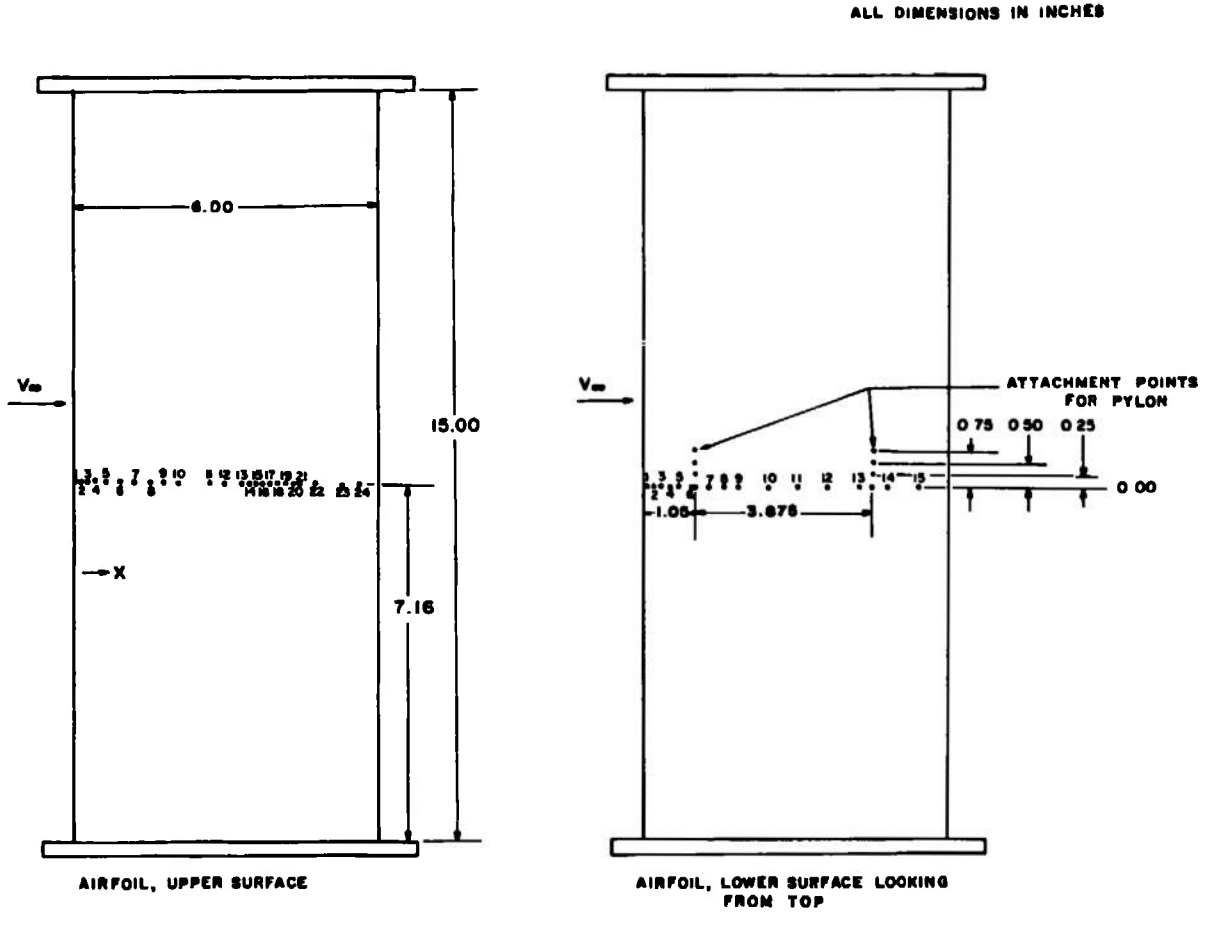

b. Airfoil Showing Orifice Locations and Pylon Attachment Points
Fig. 2 Continued

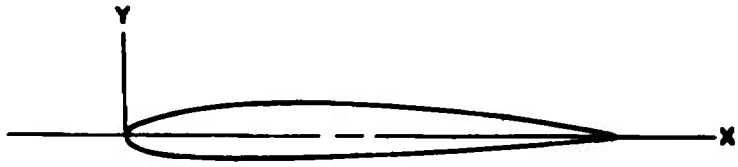

AIRFOIL SECTION COORDINATES

UPPER SURFACE		LOWER SURFACE	
X Coordinate	Y Coordinate	X Coordinate	Y Coordinate
-.0018	.0275	-.0030	-.0190
-.0048	.0387	-.0054	-.0269
-.0078	.0479	-.0102	-.0380
-.0108	.0551	-.0186	-.0524
-.0318	.0859	-.0354	-.0715
-.0456	.1010	-.0594	-.0924
-.0672	.1193	-.0990	-.1167
-.0960	.1396	-.1302	-.1318
-.1398	.1652	-.2238	-.1639
-.2880	.2248	-.4086	-.2039
-.4368	.2675	.5616	-.2262
-.5868	.3002	-.6228	-.2334
.7068	.3225	.7452	-.2458
-.8868	.3500	-.9282	-.2609
1.1874	.3861	1.0500	-.2688
-1.4880	.4130	-1.2318	-.2779
-1.7880	.4320	1.5342	-.2891
2.0880	.4444	-1.8354	-.2956
-2.3874	.4510	2.1360	-.2970
2.6862	.4510	2.4348	-.2943
-2.9844	.4444	-2.7324	-.2871
3.2820	.4320	-3.0288	-.2760
-3.5790	.4130	3.3246	-.2616
3.8766	.3874	-3.6150	-.2419
-4.1772	.3560	3.9126	-.2189
4.4790	.3179	-4.1070	-.2012
-4.7802	.2714	4.3482	-.1822
-5.0832	.2157	-4.7076	-.1475
-5.3856	.1541	5.0046	-.1180
-5.9916	.0111	-5.2020	-.0970
		5.3994	-.0747
		-5.4984	-.0629
		-5.7906	-.0256
		-5.8932	-.0125

ALL DIMENSIONS IN INCHES

c. Airfoil Section Coordinates

Fig. 2 Concluded

2.5 CALIBER OGIVE NOSE AND TAIL

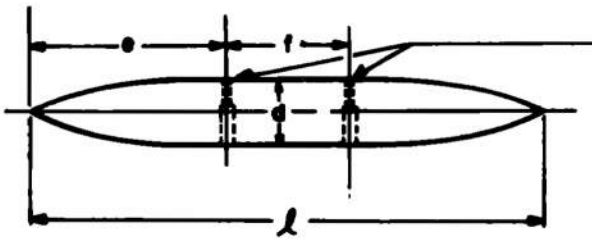

STORE	ℓ	d	e	f
A	3.16	0.40	1.23	0.70
B	6.32	0.80	2.41	1.50
C	6.21	1.04	3.35	1.50
D	11.80	1.50	5.15	1.50
C-1*	6.21	1.04	2.10	1.50

*NOTE: C STORE MOVED AFT ON THE PYLON

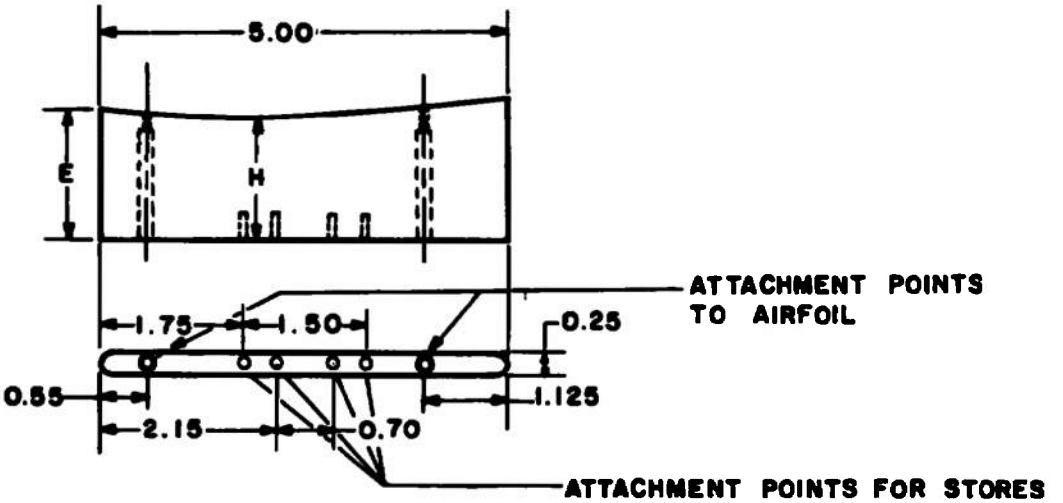

PYLON	E	H
A	0.277	0.20
B	0.577	0.50
C	1.077	1.00
D	1.577	1.50

ALL DIMENSIONS IN INCHES

Fig. 3 Details and Dimensions of Pylons and Stores

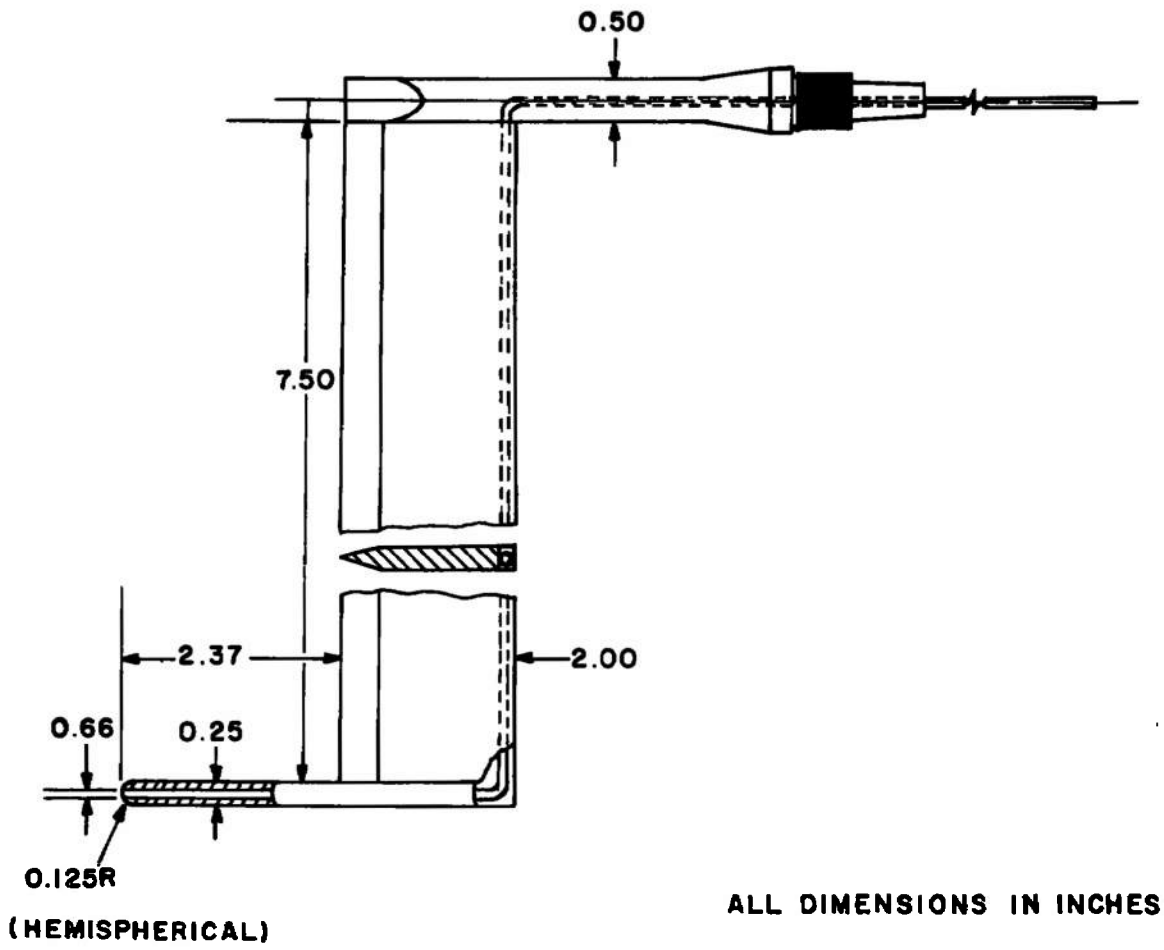

Fig. 4 Details and Dimensions of Total Pressure Probe

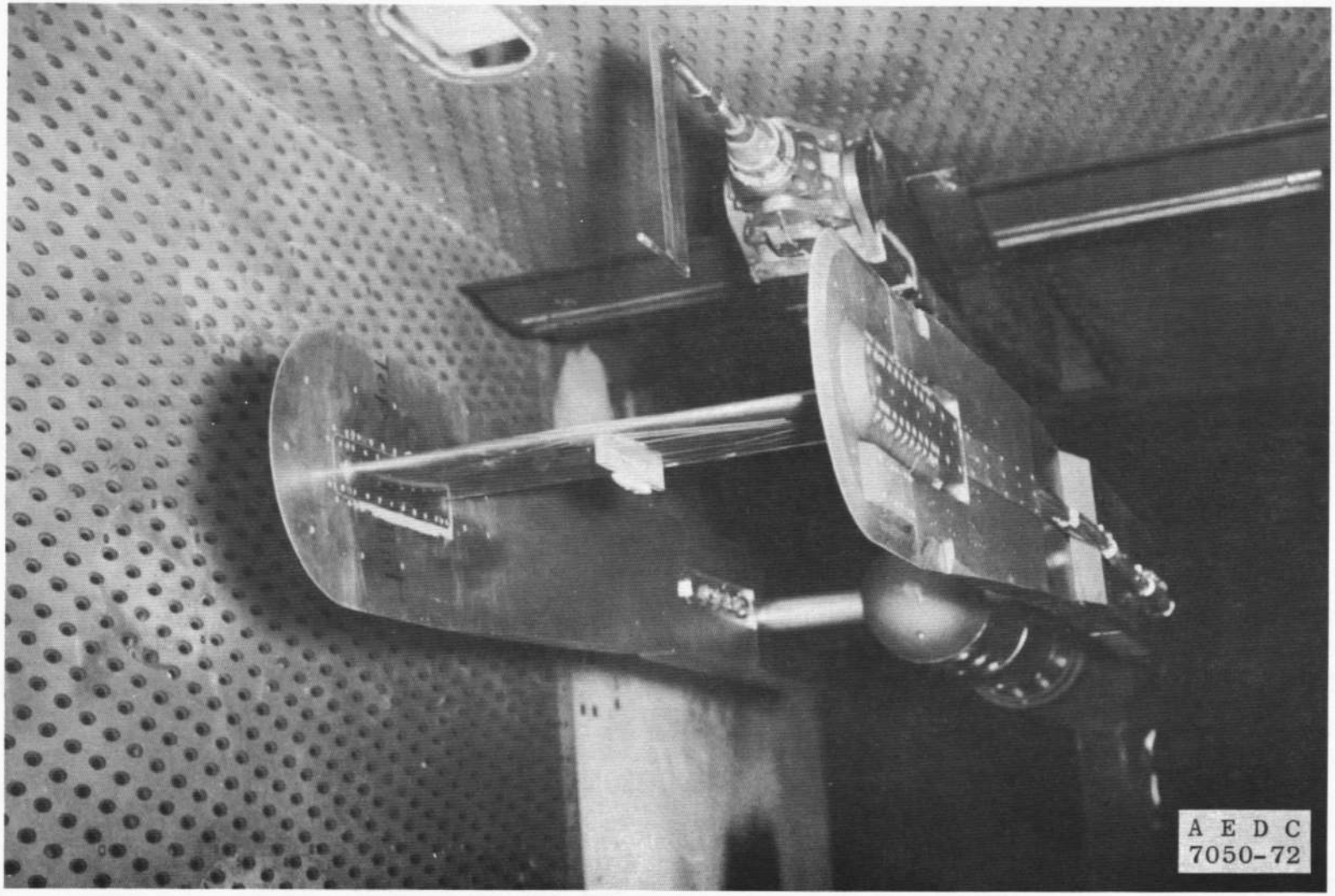

a. Airfoil with B Pylon and A Store

Fig. 5 Photographs of Model Installation in Test Section

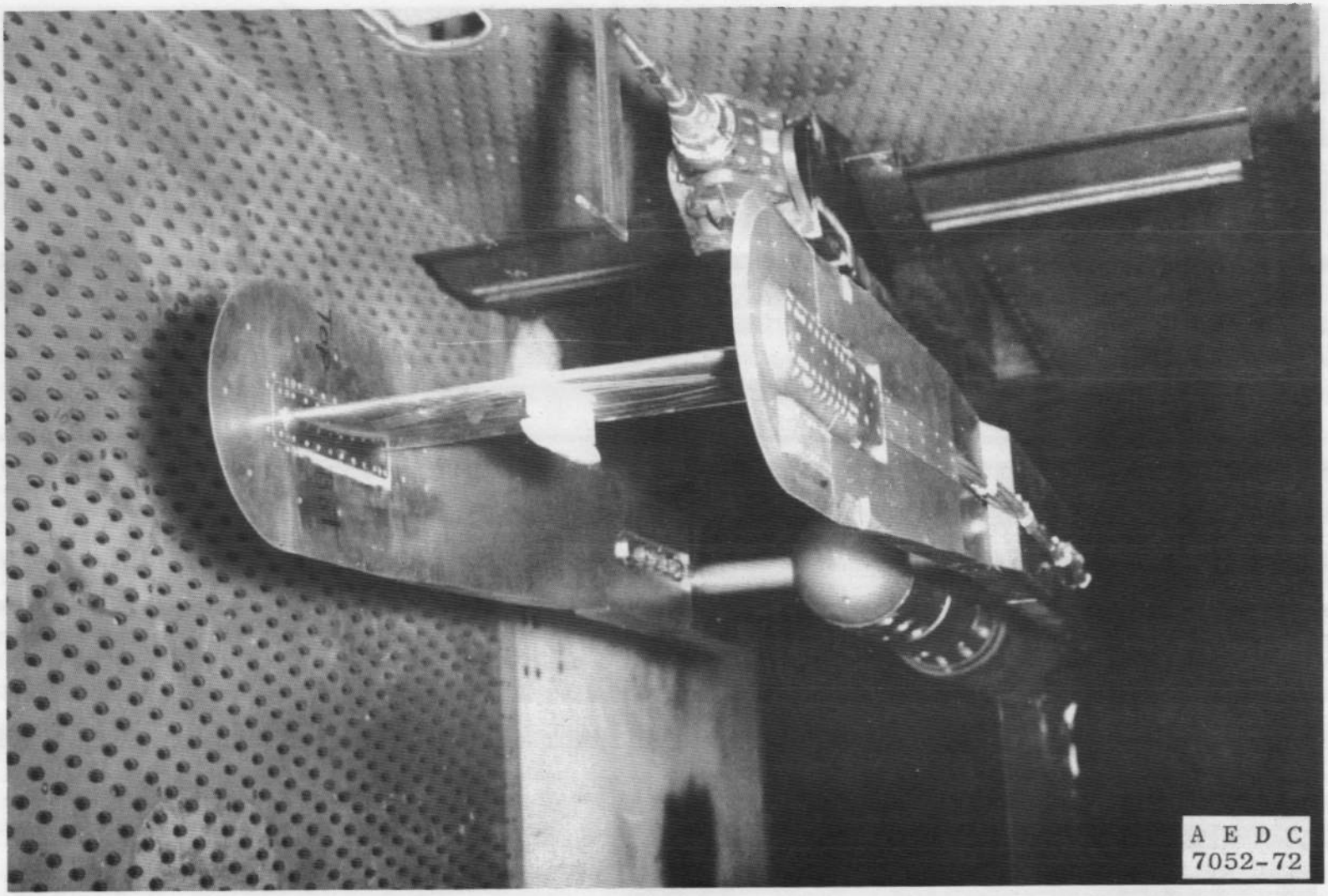

b. Airfoil with B Pylon and B Store
Fig. 5 Continued

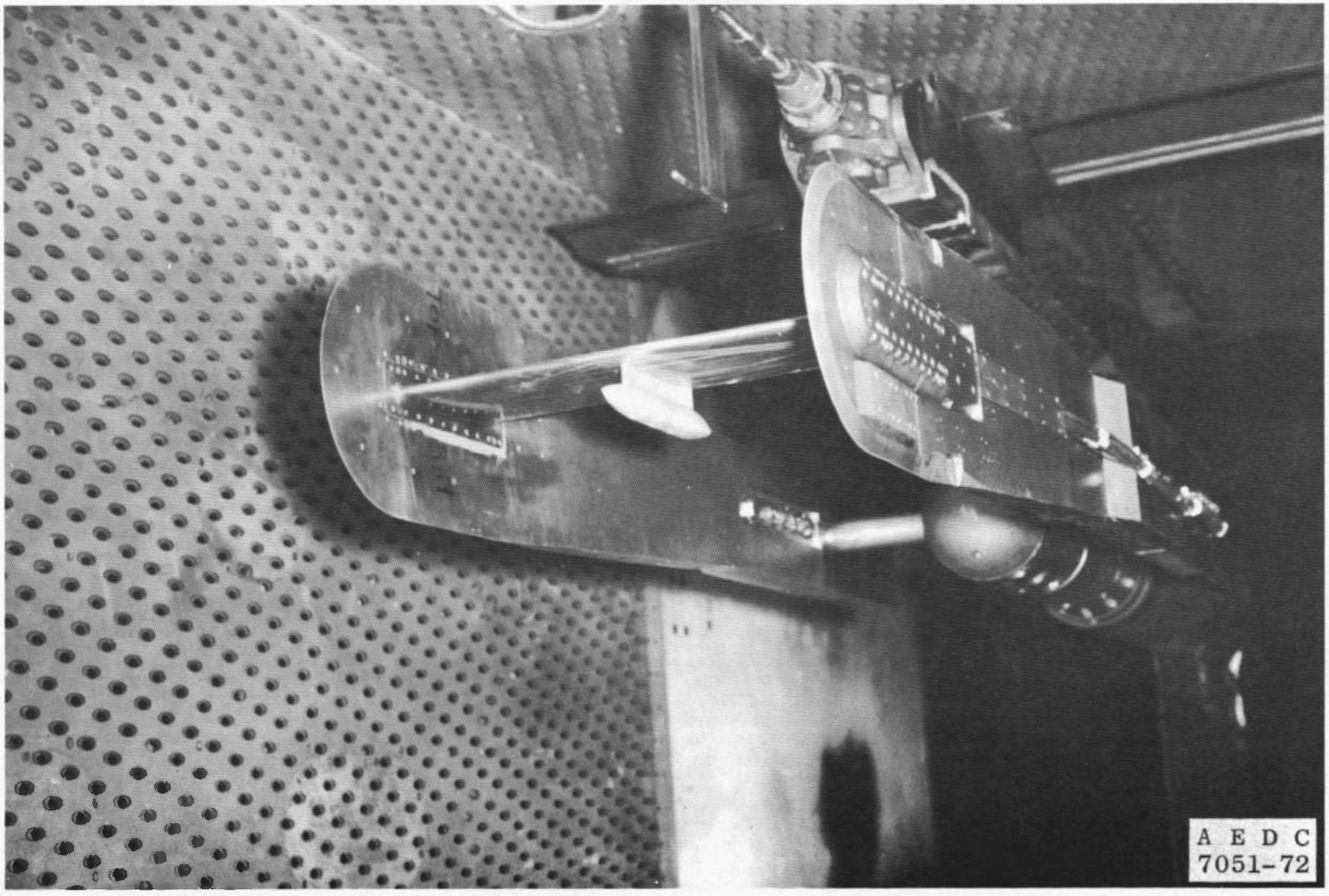

c. Airfoil with B Pylon and C Store
Fig. 5 Continued

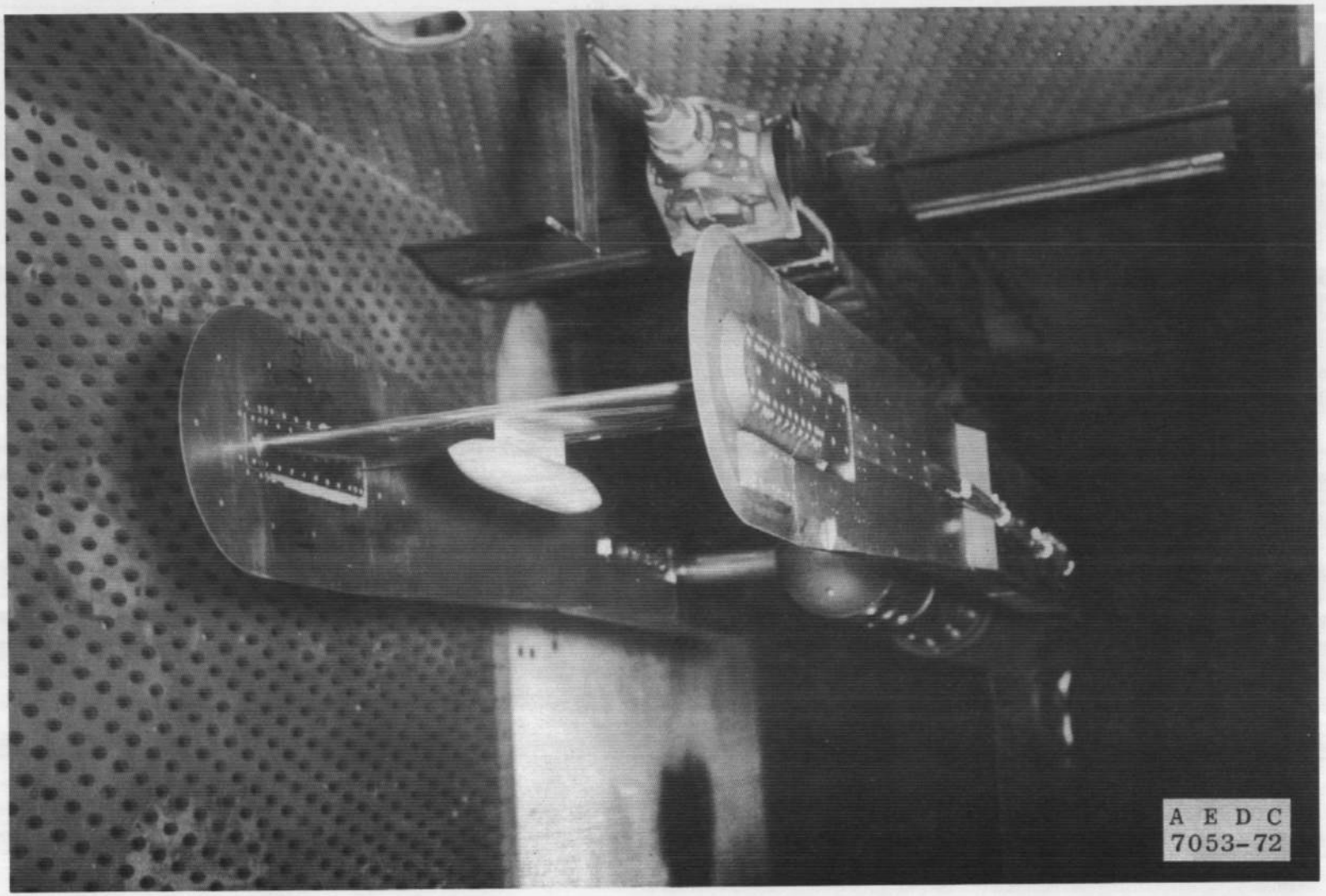

d. Airfoil with B Pylon and D Store
Fig. 5 Continued

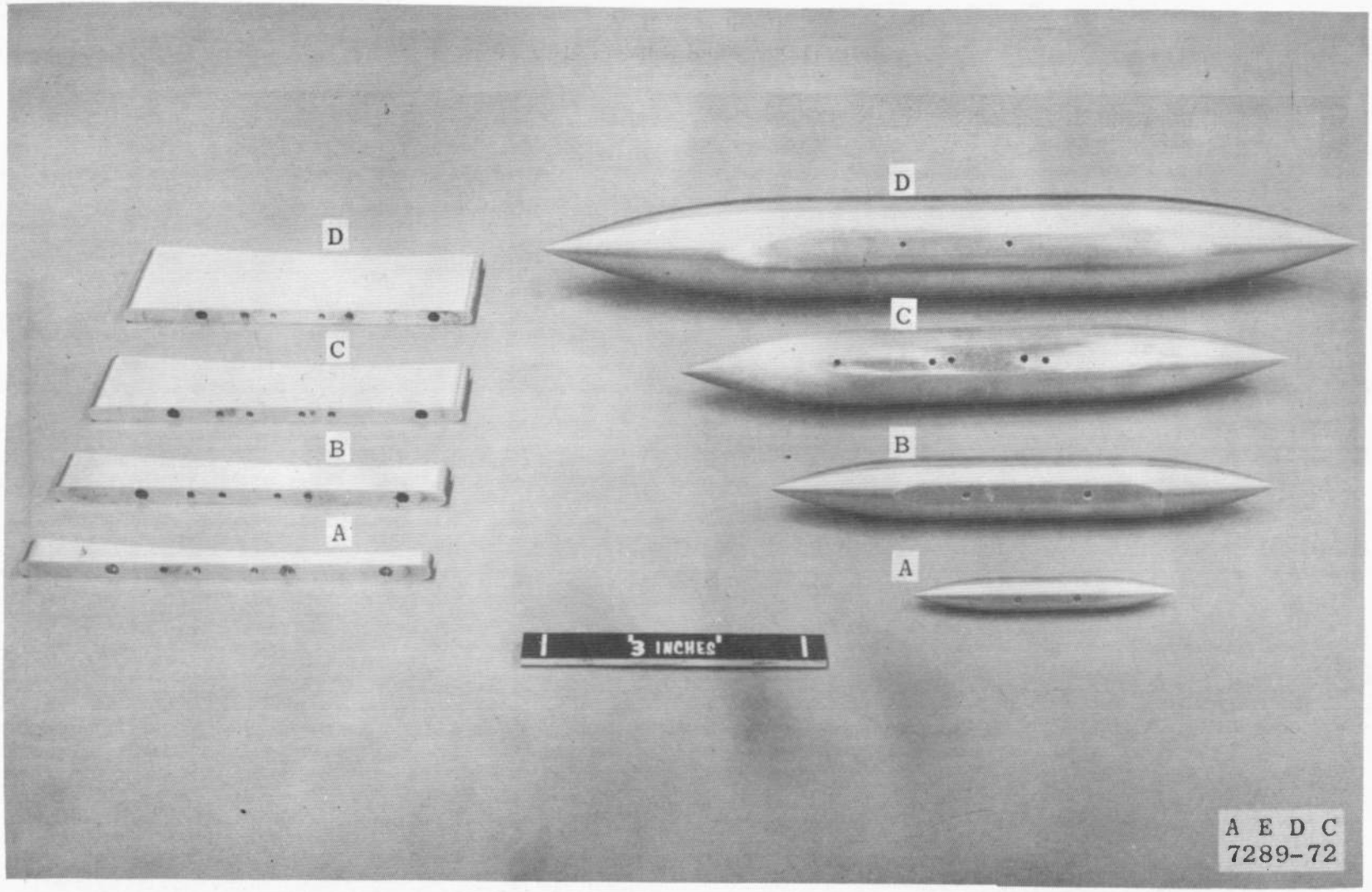

e. Pylons and Stores
Fig. 5 Concluded

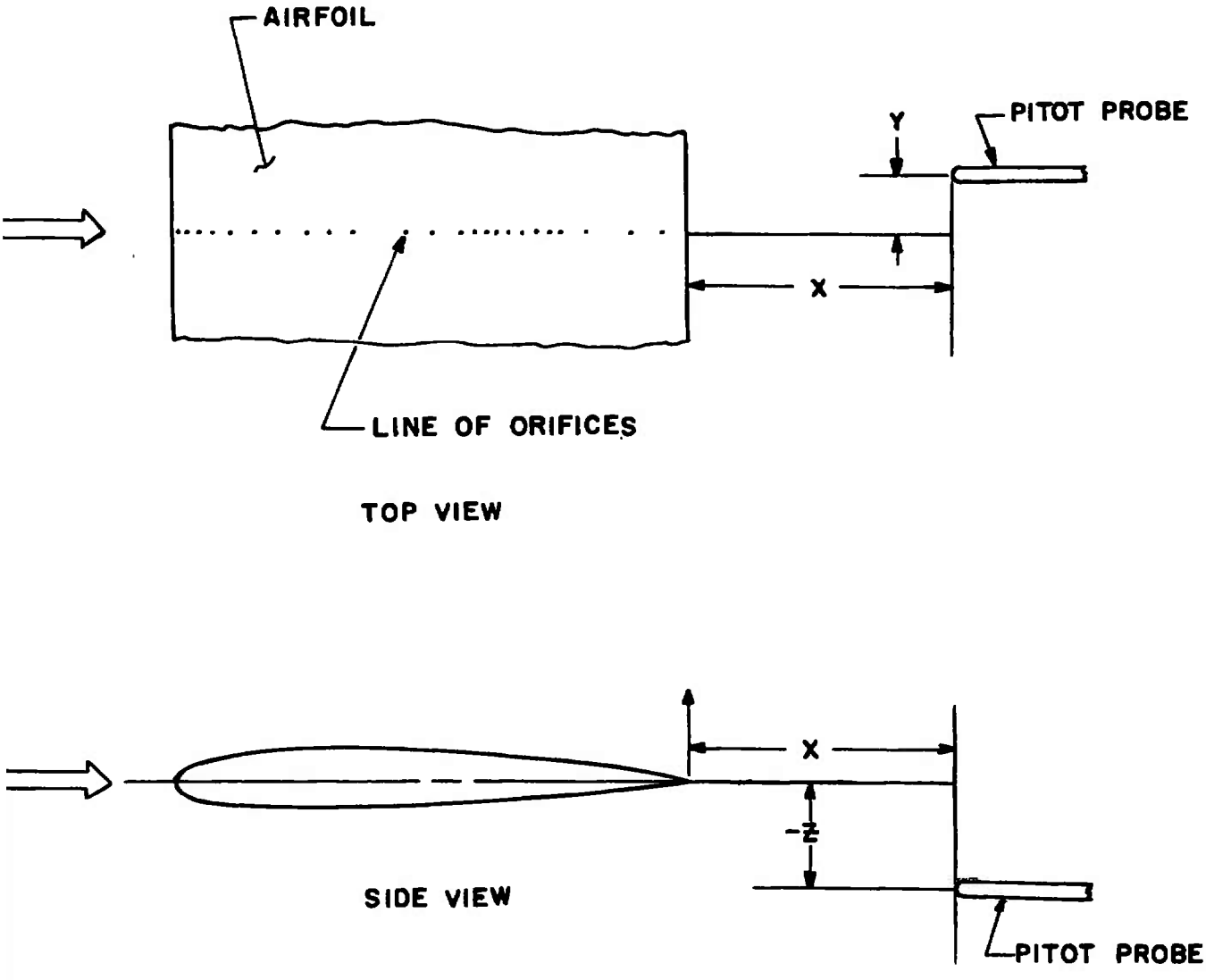

Fig. 6 Pitot Probe Coordinate System

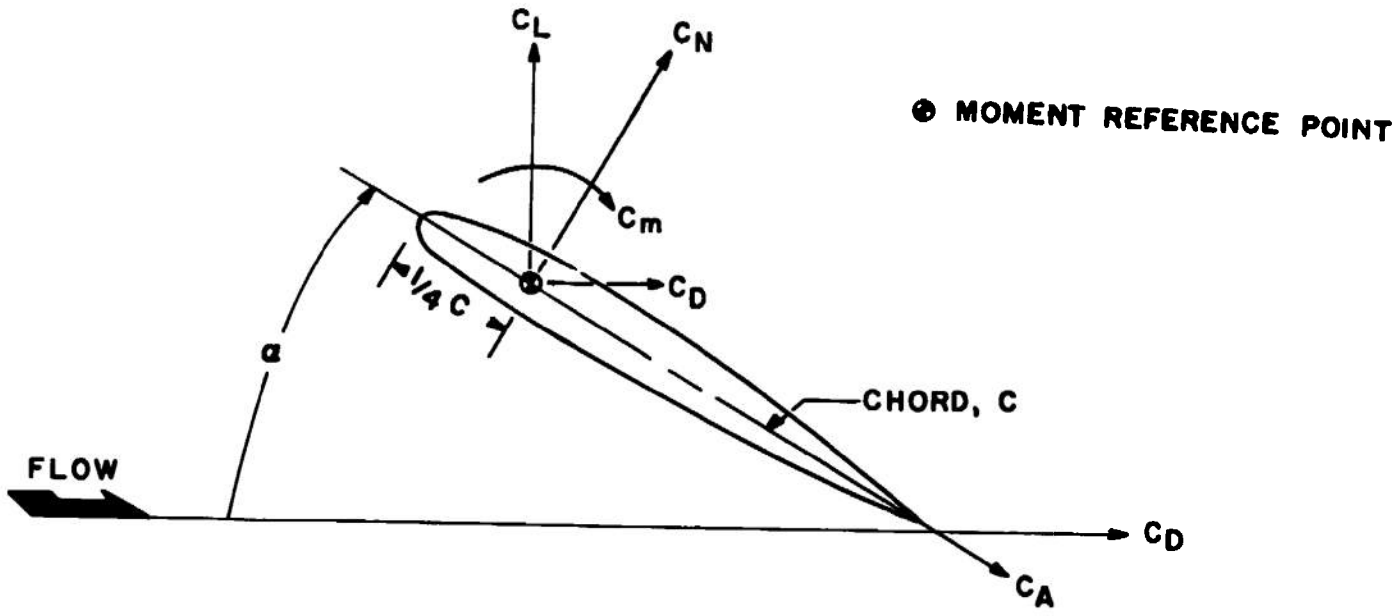

Fig. 7 Force and Moment Orientation

SYMBOL	M_∞	PYLON	STORE	LOC	α
□	0.70	NONE	NONE	NA	0
○	0.80	NONE	NONE	NA	0
△	0.85	NONE	NONE	NA	0
◇	0.90	NONE	NONE	NA	0
◁	0.95	NONE	NONE	NA	0

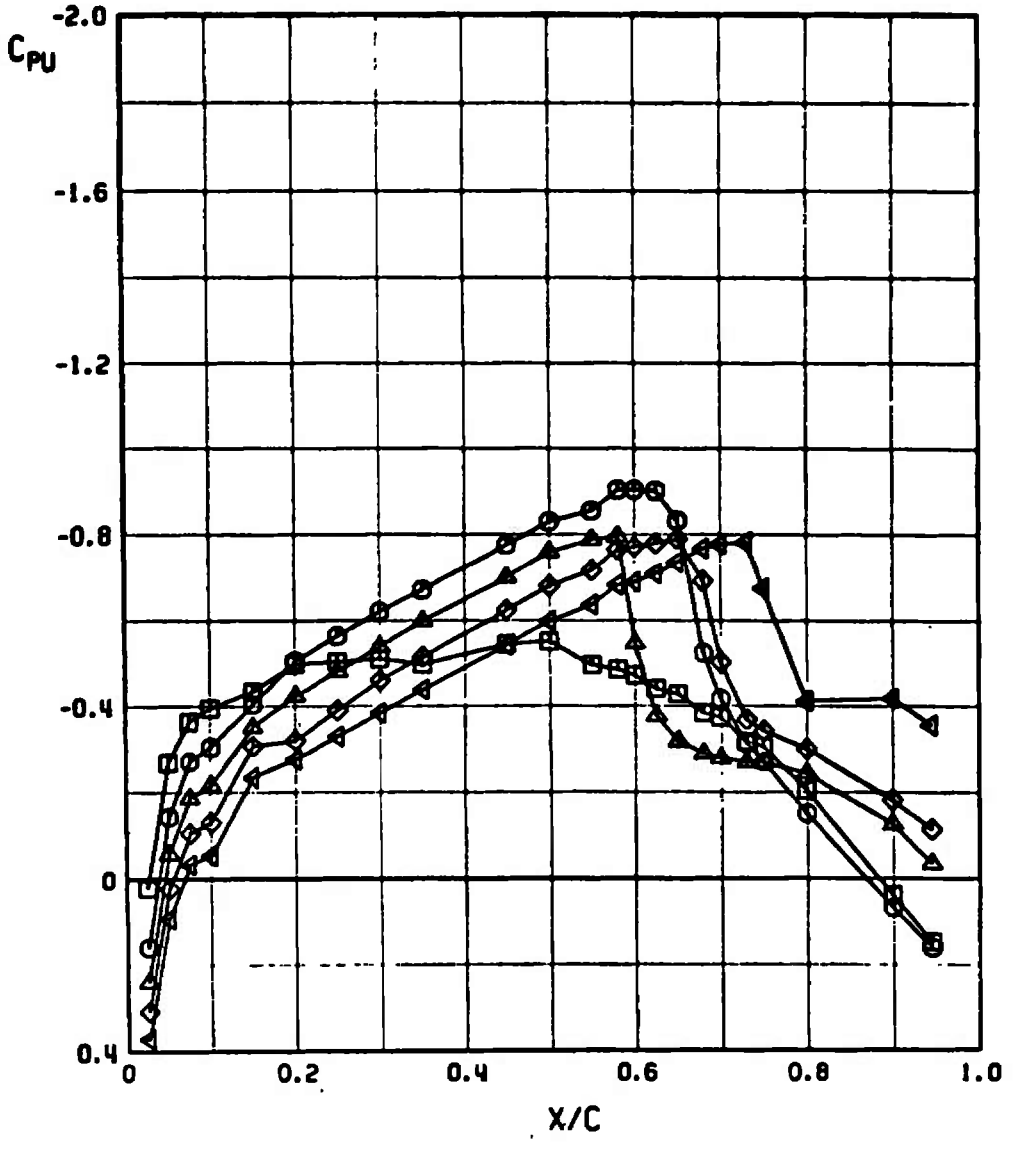

Fig. 8 Pressure Distributions on the Clean Airfoil for Different Mach Numbers at Zero Angle of Attack

SYMBOL	M_∞	PYLON	STORE	LOC	α
○	0.800	NONE	NONE	NA	0
△	0.825	NONE	NONE	NA	0
◇	0.850	NONE	NONE	NA	0
◁	0.875	NONE	NONE	NA	0
▽	0.900	NONE	NONE	NA	0
▷	0.925	NONE	NONE	NA	0
□	0.950	NONE	NONE	NA	0

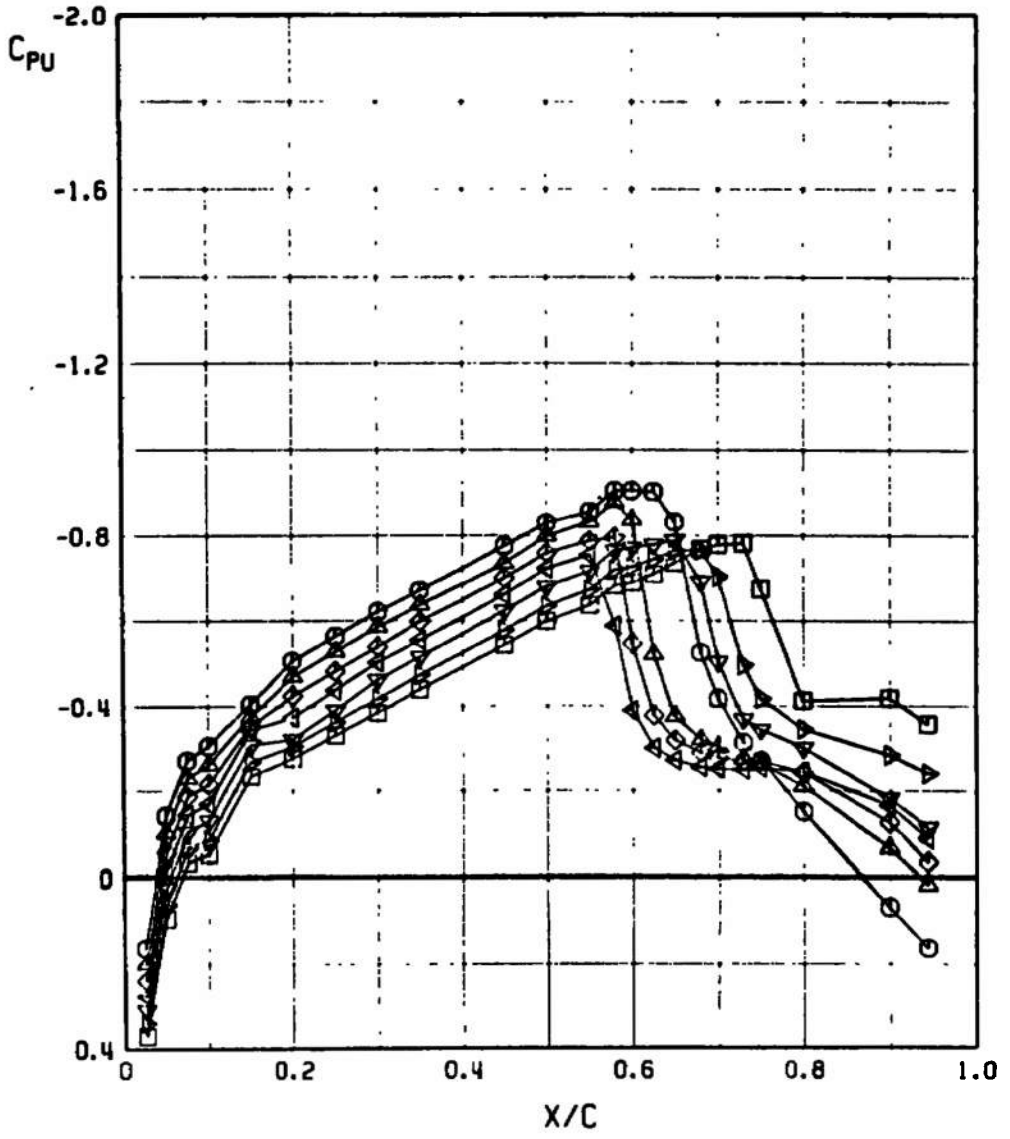

Fig. 8 Continued

SYMBOL	M_∞	PYLON	STORE	LOC	α
□	0.70	NONE	NONE	NA	0
○	0.80	NONE	NONE	NA	0
△	0.85	NONE	NONE	NA	0
◇	0.90	NONE	NONE	NA	0
◁	0.95	NONE	NONE	NA	0

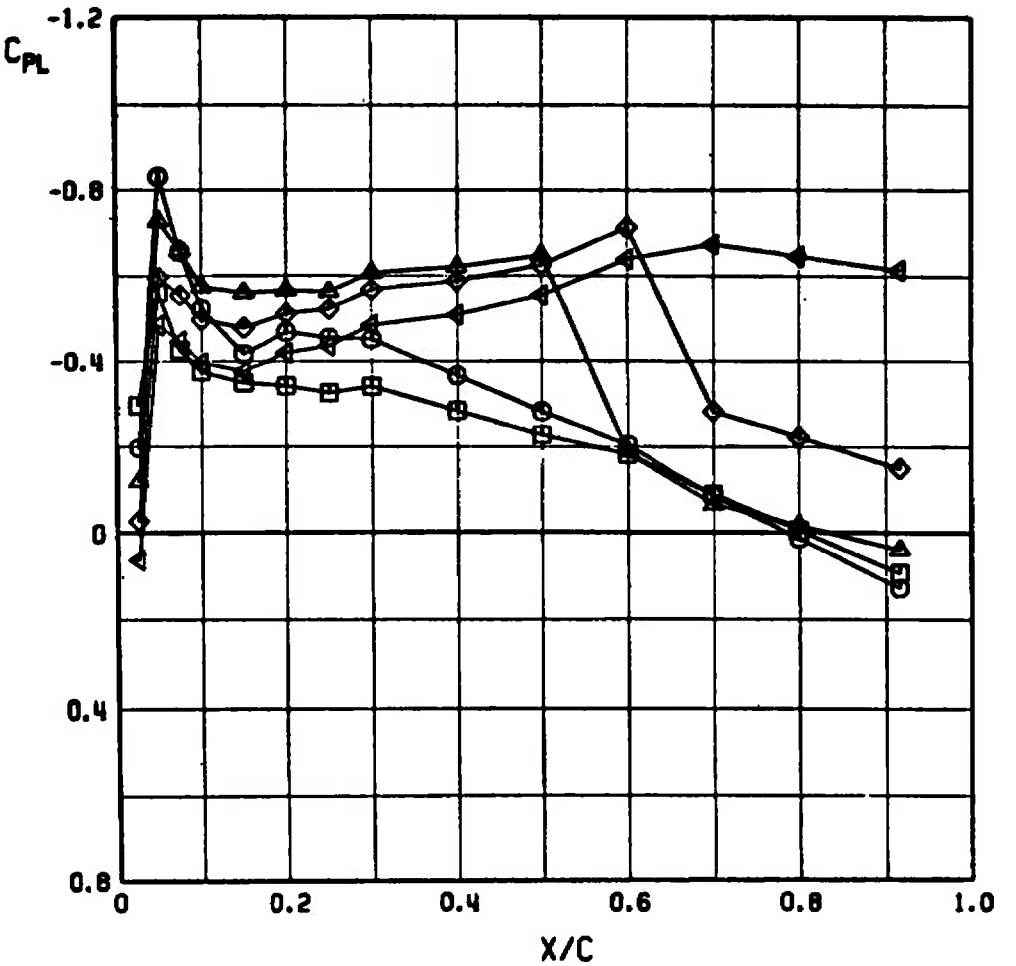

Fig. 8 Continued

SYMBOL	M_∞	PYLON	STORE	LOC	α
○	0.800	NONE	NONE	NA	0
△	0.825	NONE	NONE	NA	0
◇	0.850	NONE	NONE	NA	0
◁	0.875	NONE	NONE	NA	0
▽	0.900	NONE	NONE	NA	0
▷	0.925	NONE	NONE	NA	0
□	0.950	NONE	NONE	NA	0

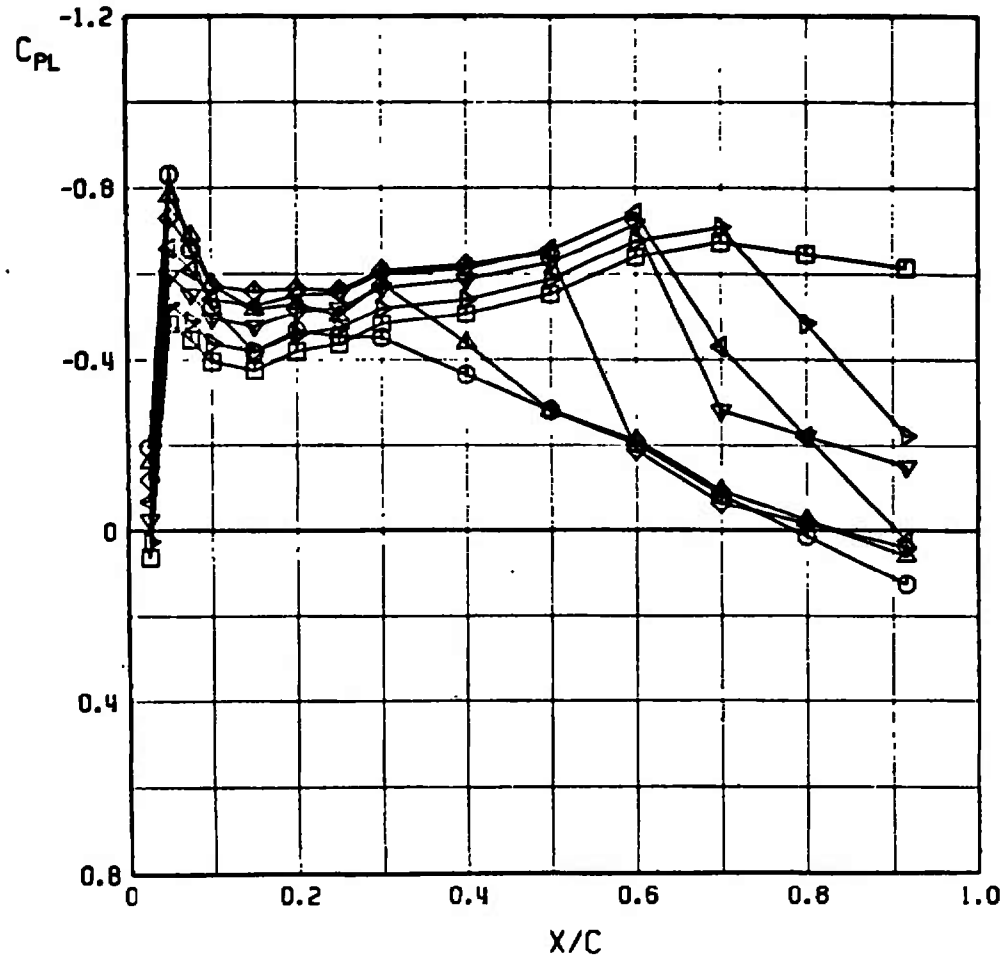

Fig. 8 Concluded

SYMBOL	M_∞	PYLON	STORE	LOC	α
□	0.70	NONE	NONE	NA	0
○	0.70	NONE	NONE	NA	2
△	0.70	NONE	NONE	NA	4
◇	0.70	NONE	NONE	NA	6
◁	0.70	NONE	NONE	NA	8
▽	0.70	NONE	NONE	NA	10

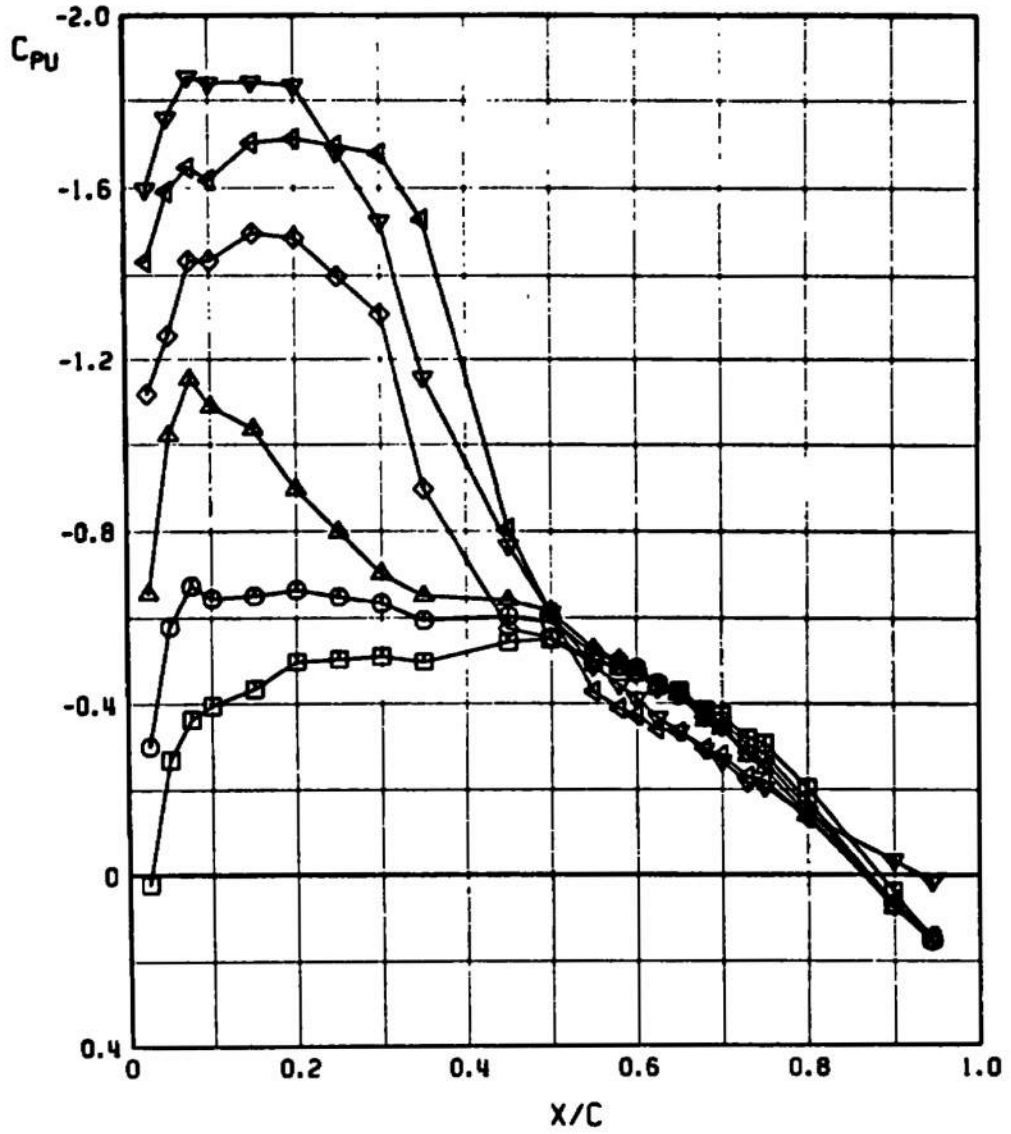

Fig. 9 Pressure Distributions on the Clean Airfoil for Different Angles of Attack, M_∞ = 0.7

SYMBOL	M_∞	PYLON	STORE	LOC	α
□	0.70	NONE	NONE	NA	0
○	0.70	NONE	NONE	NA	2
△	0.70	NONE	NONE	NA	4
◇	0.70	NONE	NONE	NA	6
◁	0.70	NONE	NONE	NA	8
▽	0.70	NONE	NONE	NA	10

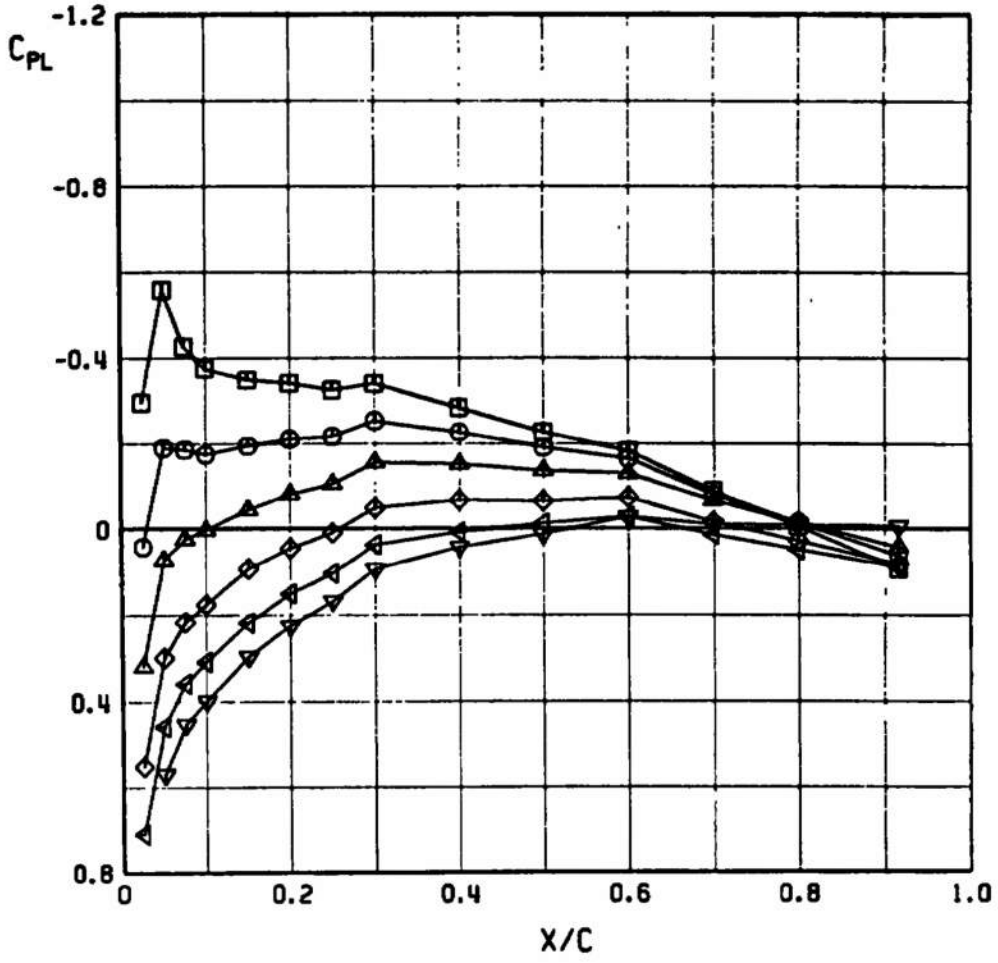

Fig. 9 Concluded

SYMBOL	M_∞	PYLON	STORE	LOC	α
□	0.80	NONE	NONE	NA	0
○	0.80	NONE	NONE	NA	2
△	0.80	NONE	NONE	NA	4
◇	0.80	NONE	NONE	NA	6
◁	0.80	NONE	NONE	NA	8
▽	0.80	NONE	NONE	NA	10

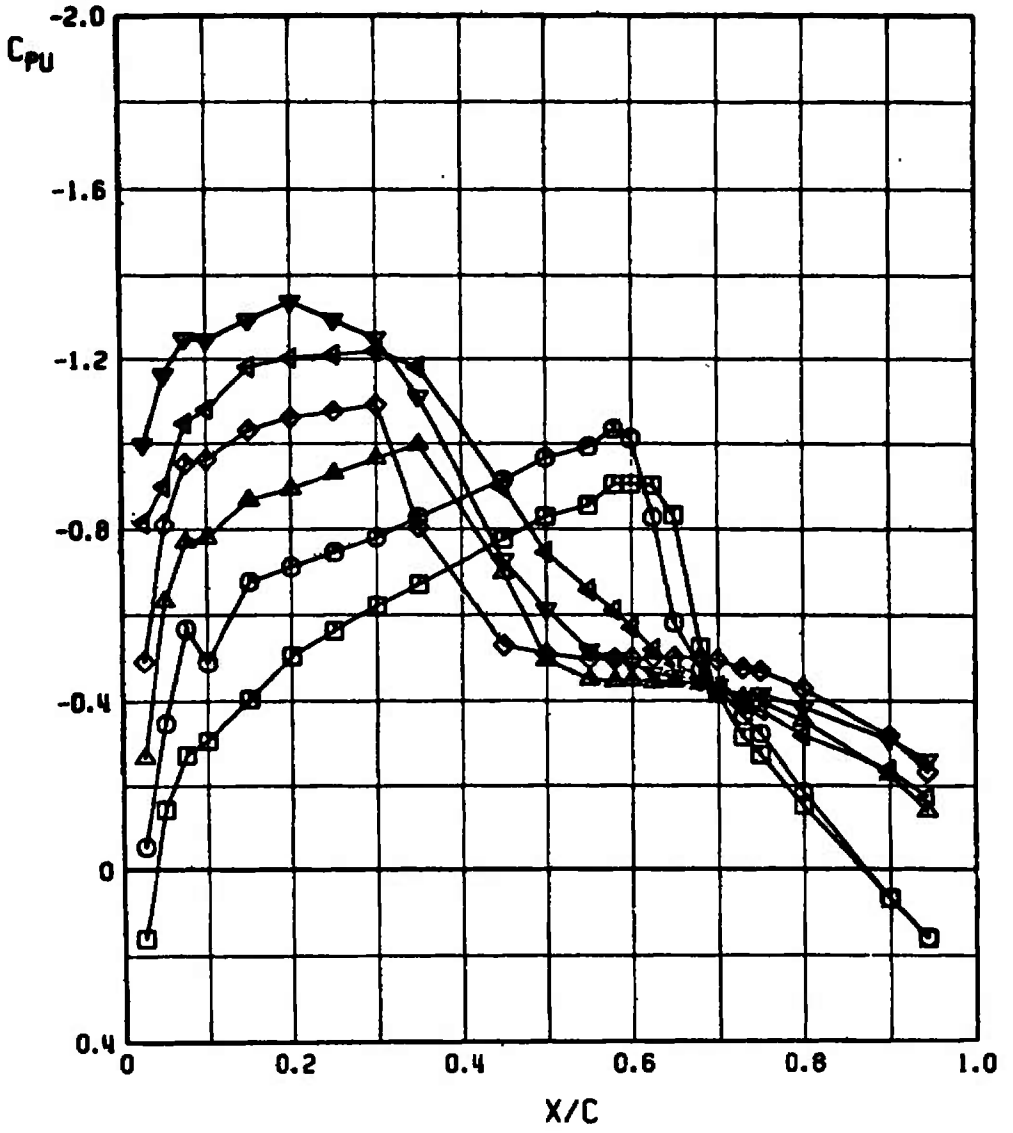

Fig. 10 Pressure Distributions on the Clean Airfoil for Different Angles of Attack, M_∞ = 0.8

SYMBOL	M_∞	PYLON	STORE	LOC	α
□	0.80	NONE	NONE	NA	0
○	0.80	NONE	NONE	NA	2
△	0.80	NONE	NONE	NA	4
◇	0.80	NONE	NONE	NA	6
◁	0.80	NONE	NONE	NA	8
▽	0.80	NONE	NONE	NA	10

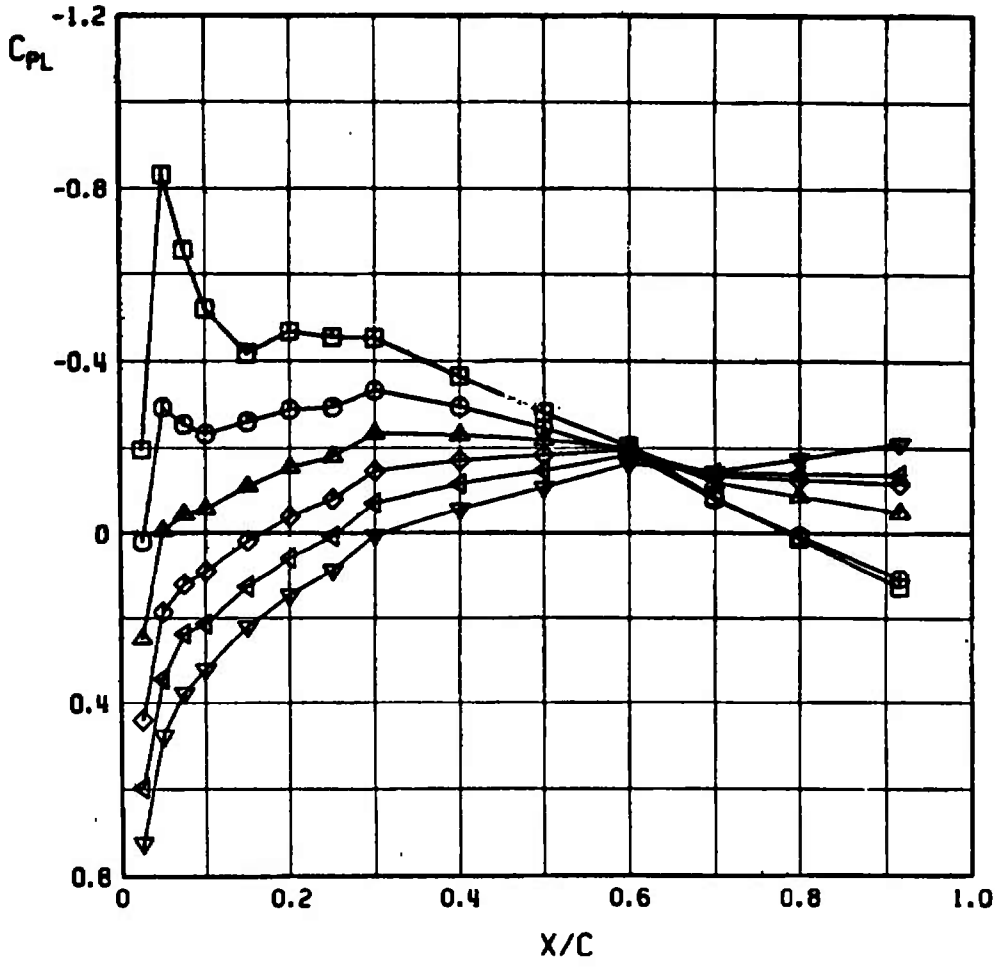

Fig. 10 Concluded

SYMBOL	M_∞	PYLON	STORE	LOC	α
□	0.85	NONE	NONE	NA	0
○	0.85	NONE	NONE	NA	2
△	0.85	NONE	NONE	NA	4
◇	0.85	NONE	NONE	NA	6
◁	0.85	NONE	NONE	NA	8
▽	0.85	NONE	NONE	NA	10

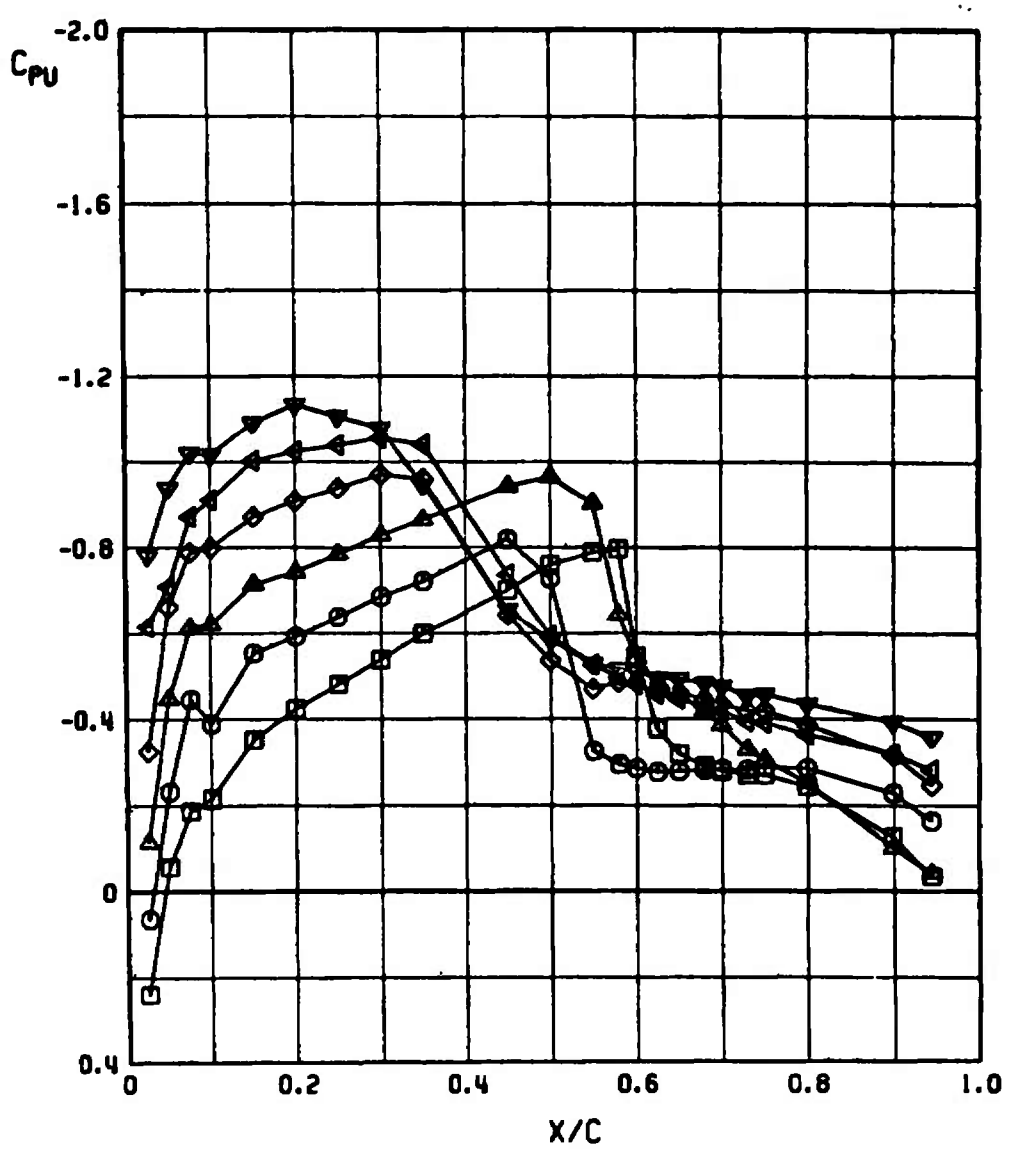

Fig. 11 Pressure Distributions on the Clean Airfoil for Different Angles of Attack, M_∞ = 0.85

SYMBOL	M_∞	PYLON	STORE	LOC	α
□	0.85	NONE	NONE	NA	0
○	0.85	NONE	NONE	NA	2
△	0.85	NONE	NONE	NA	4
◇	0.85	NONE	NONE	NA	6
◁	0.85	NONE	NONE	NA	8
▽	0.85	NONE	NONE	NA	10

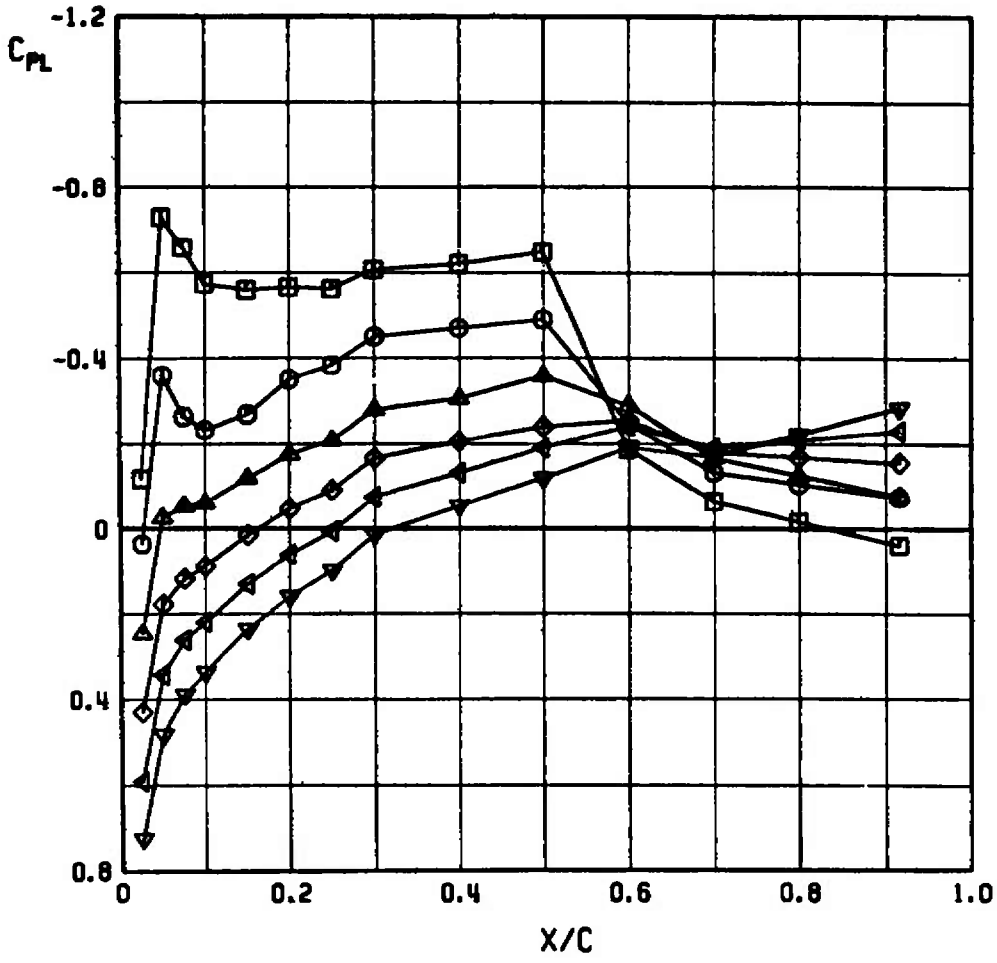

Fig. 11 Concluded

SYMBOL	M_∞	PYLON	STORE	LOC	α
□	0.90	NONE	NONE	NA	0
○	0.90	NONE	NONE	NA	2
△	0.90	NONE	NONE	NA	4
◇	0.90	NONE	NONE	NA	6
◁	0.90	NONE	NONE	NA	8
▽	0.90	NONE	NONE	NA	10

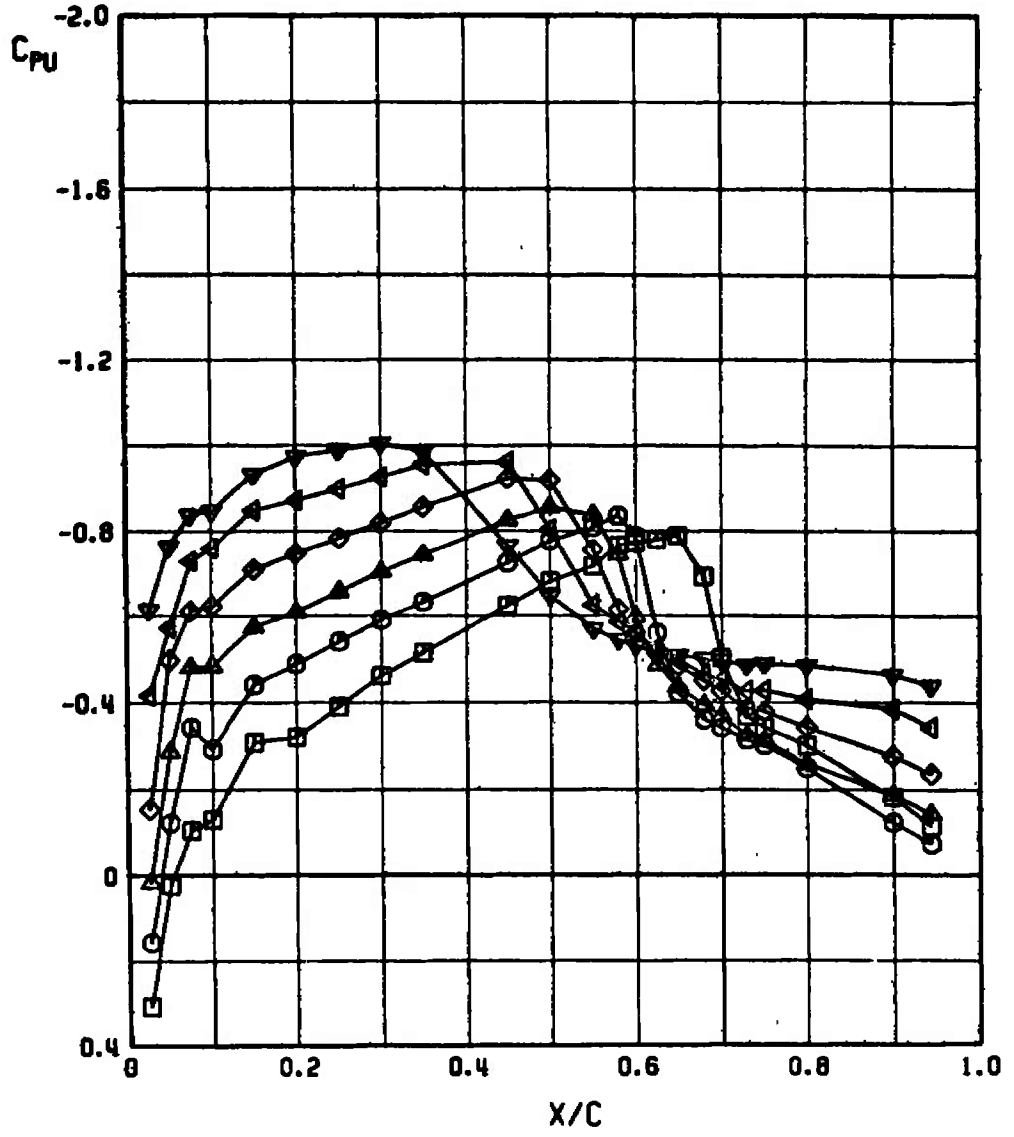

Fig. 12 Pressure Distributions on the Clean Airfoil for Different Angles of Attack, $M_\infty = 0.9$

SYMBOL	M_∞	PYLON	STORE	LOC	α
□	0.90	NONE	NONE	NA	0
○	0.90	NONE	NONE	NA	2
△	0.90	NONE	NONE	NA	4
◇	0.90	NONE	NONE	NA	6
◁	0.90	NONE	NONE	NA	8
▽	0.90	NONE	NONE	NA	10

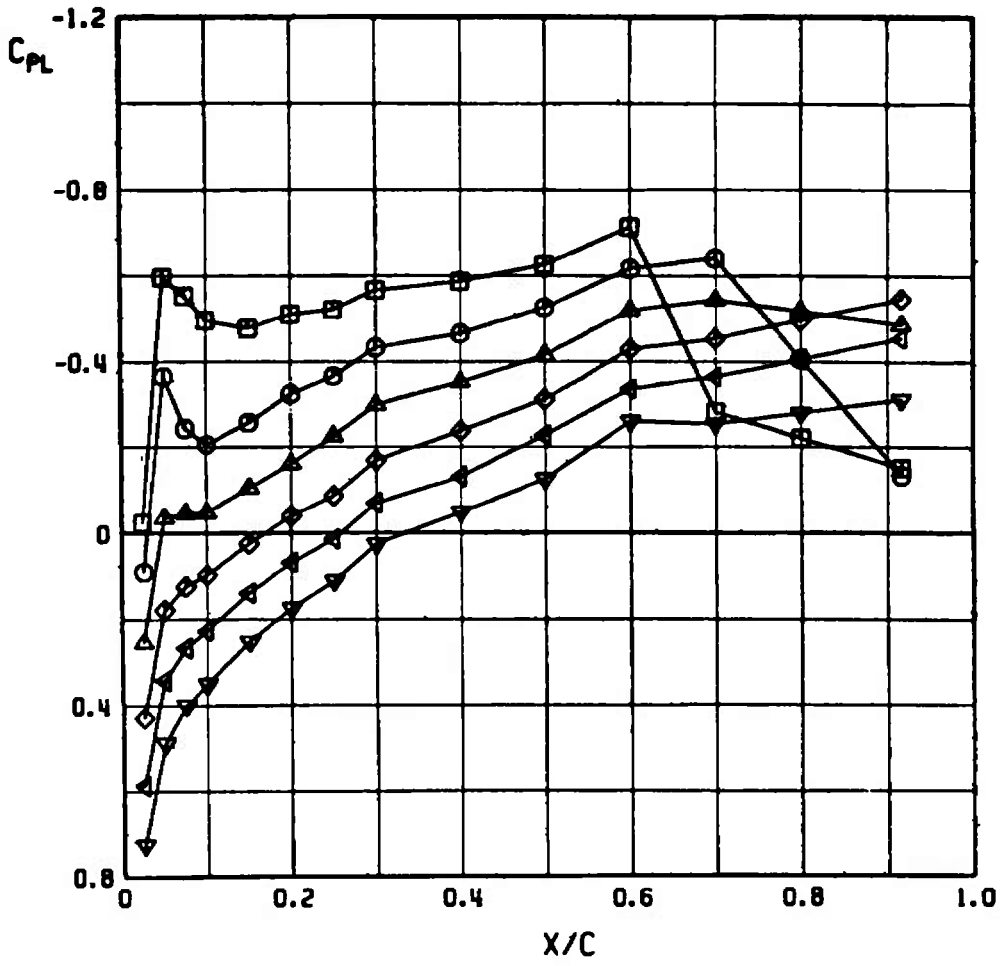

Fig. 12 Concluded

SYMBOL	M_∞	PYLON	STORE	LOC	α
□	0.95	NONE	NONE	NA	0
○	0.95	NONE	NONE	NA	2
△	0.95	NONE	NONE	NA	4
◇	0.95	NONE	NONE	NA	6
◁	0.95	NONE	NONE	NA	8
▽	0.95	NONE	NONE	NA	10

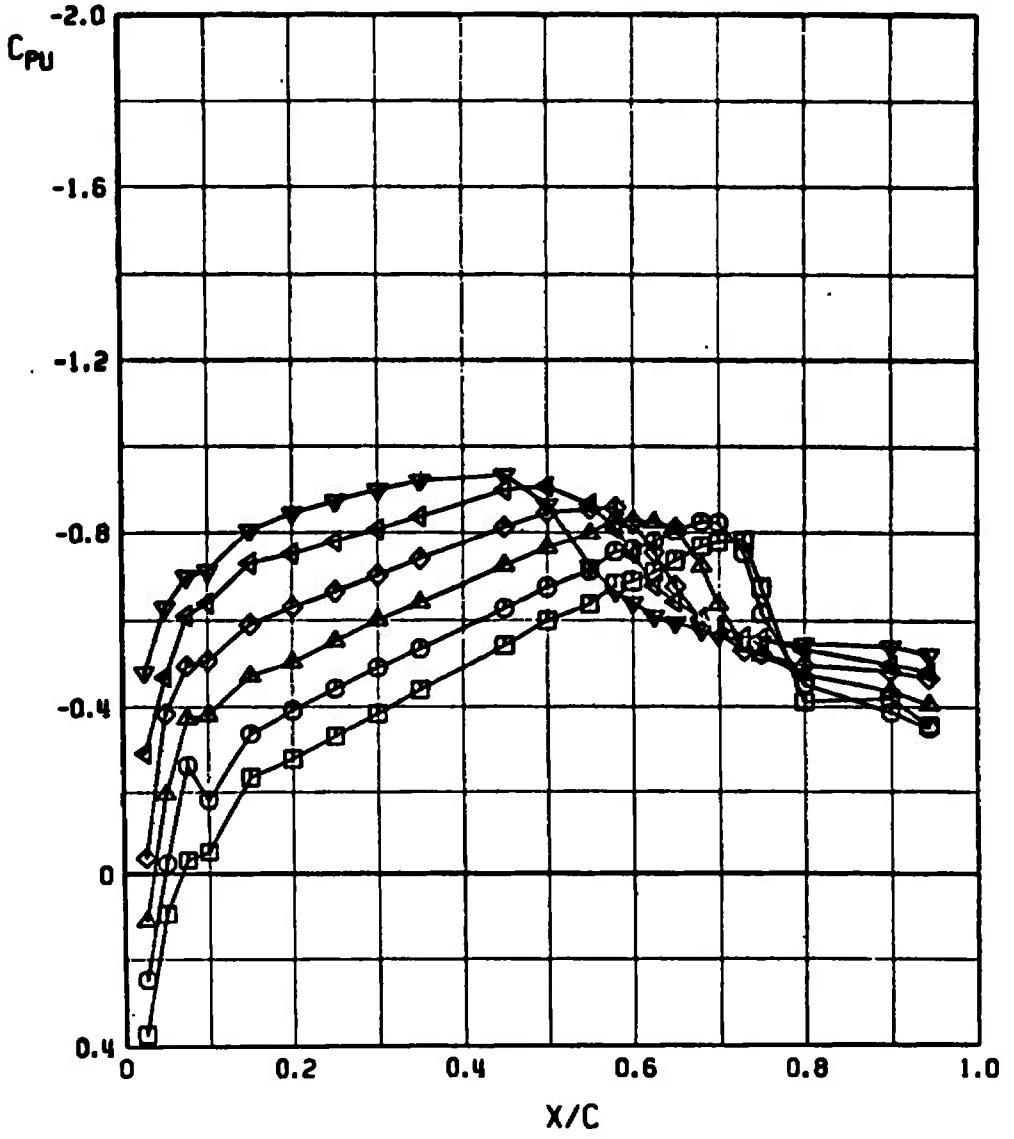

Fig. 13 Pressure Distributions on the Clean Airfoil for Different Angles of Attack, M_∞ = 0.95

SYMBOL	M_∞	PYLON	STORE	LOC	α
□	0.95	NONE	NONE	NA	0
○	0.95	NONE	NONE	NA	2
△	0.95	NONE	NONE	NA	4
◇	0.95	NONE	NONE	NA	6
◁	0.95	NONE	NONE	NA	8
▽	0.95	NONE	NONE	NA	10

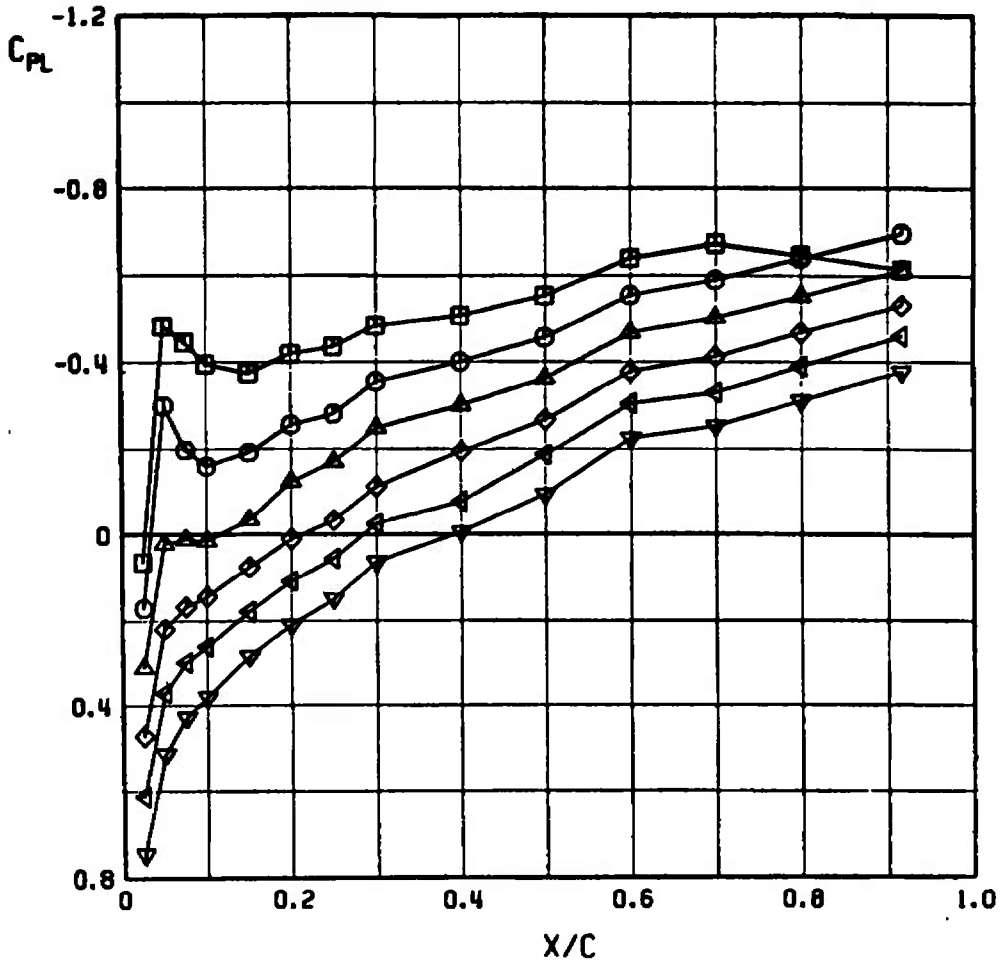

Fig. 13 Concluded

SYMBOL	M_∞	PYLON	STORE	LOC	α
□	0.70	B	NONE	0.00	0
○	0.70	B	NONE	0.25	0
△	0.70	B	NONE	0.50	0
◇	0.70	B	NONE	0.75	0

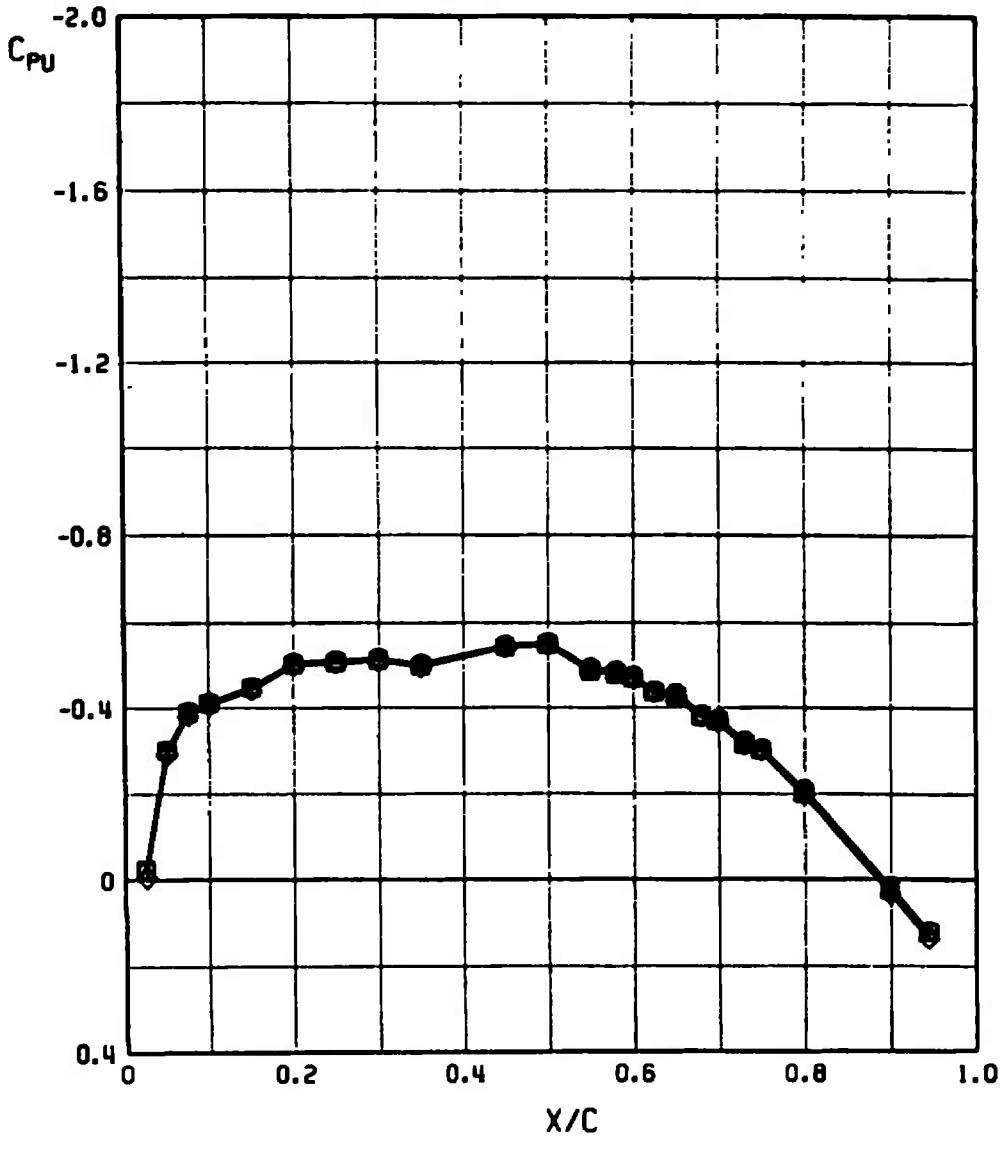

Fig. 14 Pressure Distributions on the Airfoil with B Pylon at Different Spanwise Positions, M_∞ = 0.7

SYMBOL	M_∞	PYLON	STORE	LOC	α
□	0.70	B	NONE	0.00	0
○	0.70	B	NONE	0.25	0
△	0.70	B	NONE	0.50	0
◇	0.70	B	NONE	0.75	0

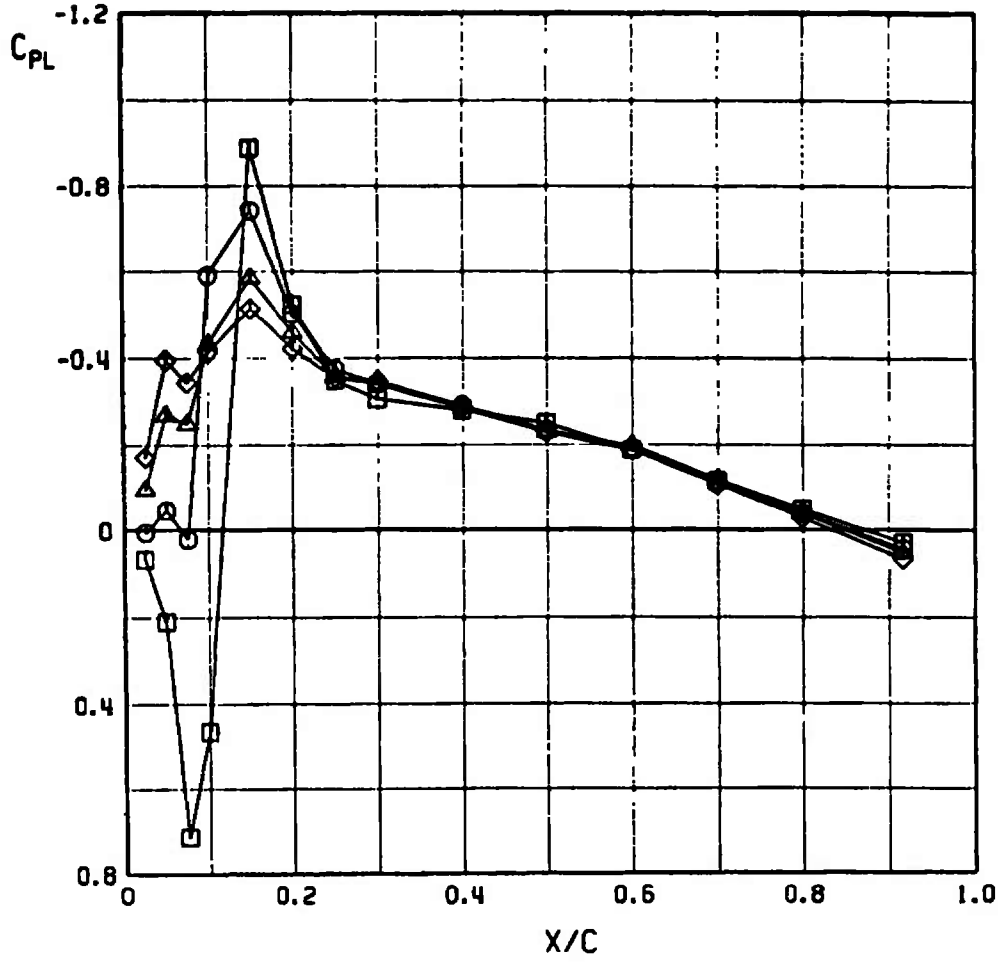

Fig. 14 Concluded

SYMBOL	M_∞	PYLON	STORE	LOC	α
□	0.80	B	NONE	0.00	0
○	0.80	B	NONE	0.25	0
△	0.80	B	NONE	0.50	0
◇	0.80	B	NONE	0.75	0

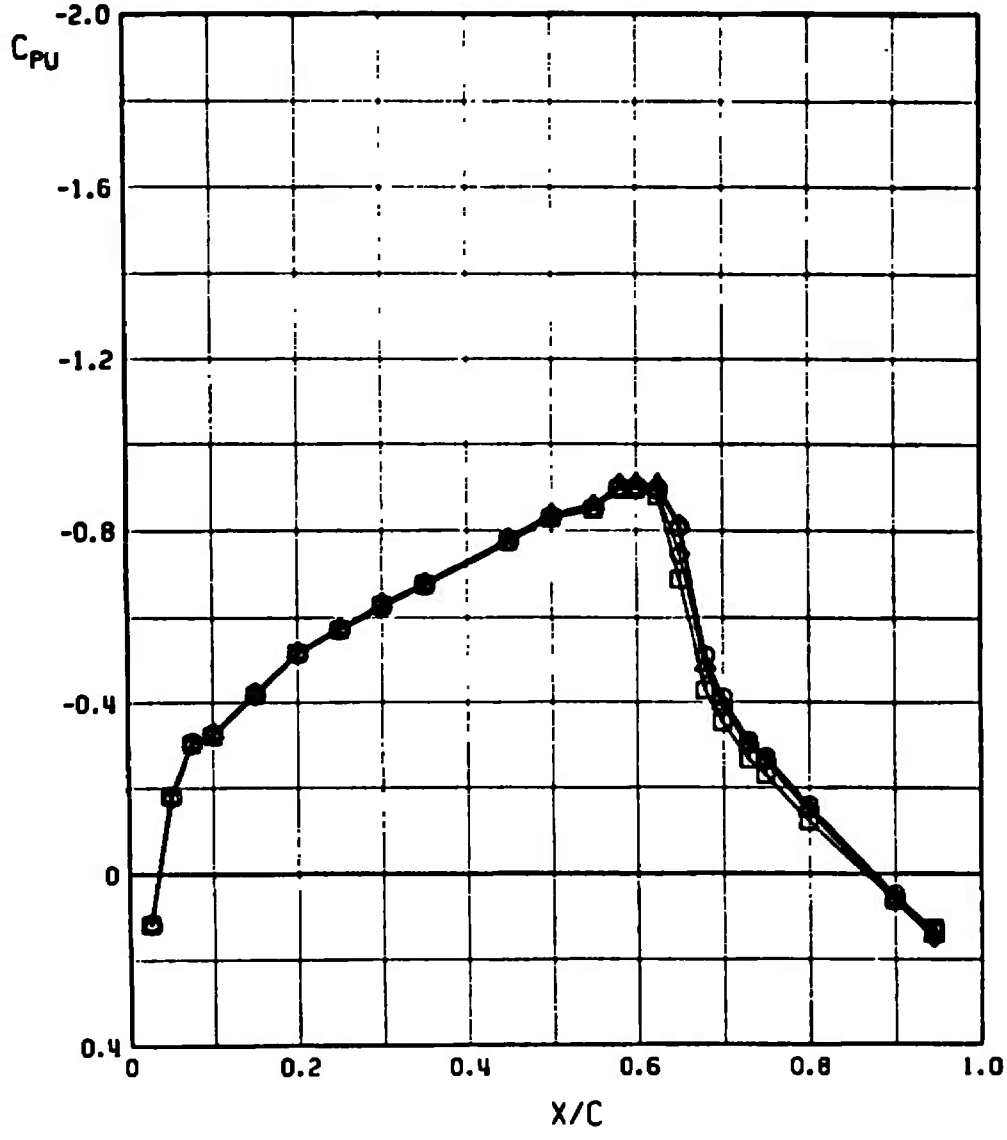

Fig. 15 Pressure Distributions on the Airfoil with B Pylon at Different Spanwise Positions, M_∞ = 0.8

SYMBOL	M_∞	PYLON	STORE	LOC	α
□	0.80	B	NONE	0.00	0
○	0.80	B	NONE	0.25	0
△	0.80	B	NONE	0.50	0
◇	0.80	B	NONE	0.75	0

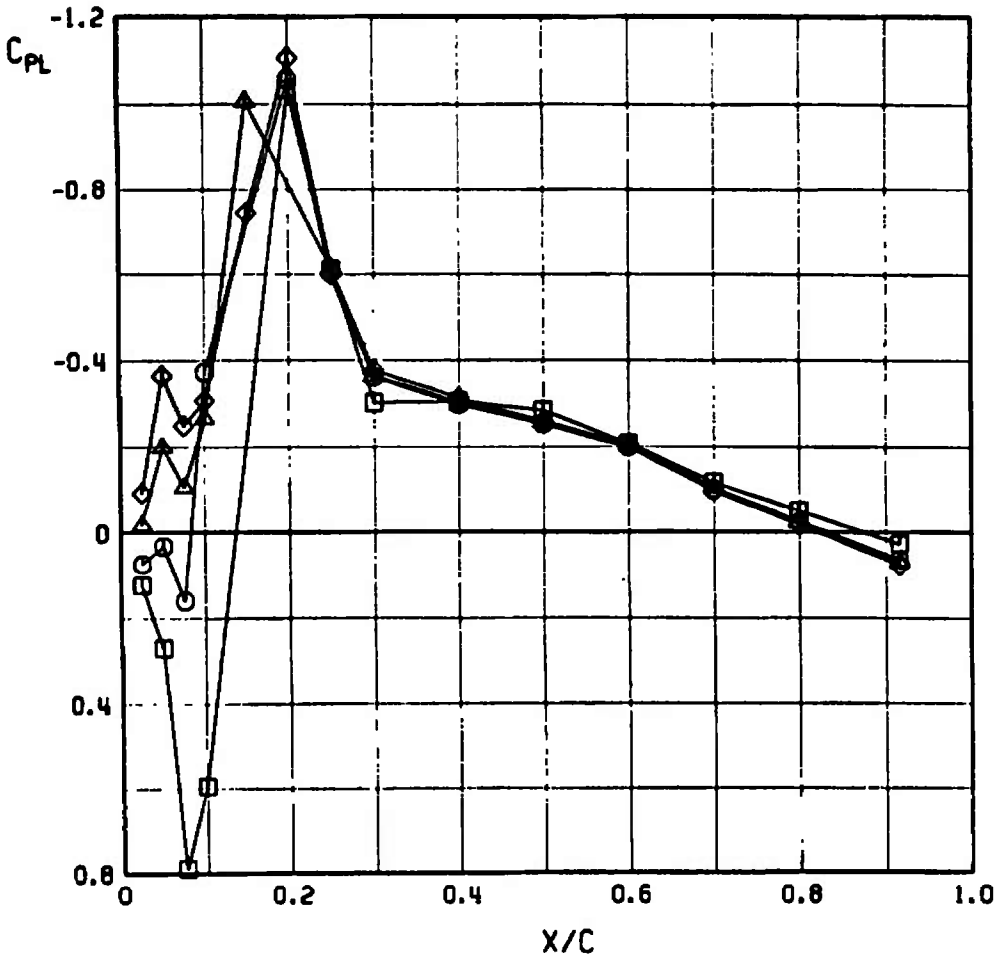

Fig. 15 Concluded

SYMBOL	M_∞	PYLON	STORE	LOC	α
□	0.85	B	NONE	0.00	0
○	0.85	B	NONE	0.25	0
△	0.85	B	NONE	0.50	0
◇	0.85	B	NONE	0.75	0

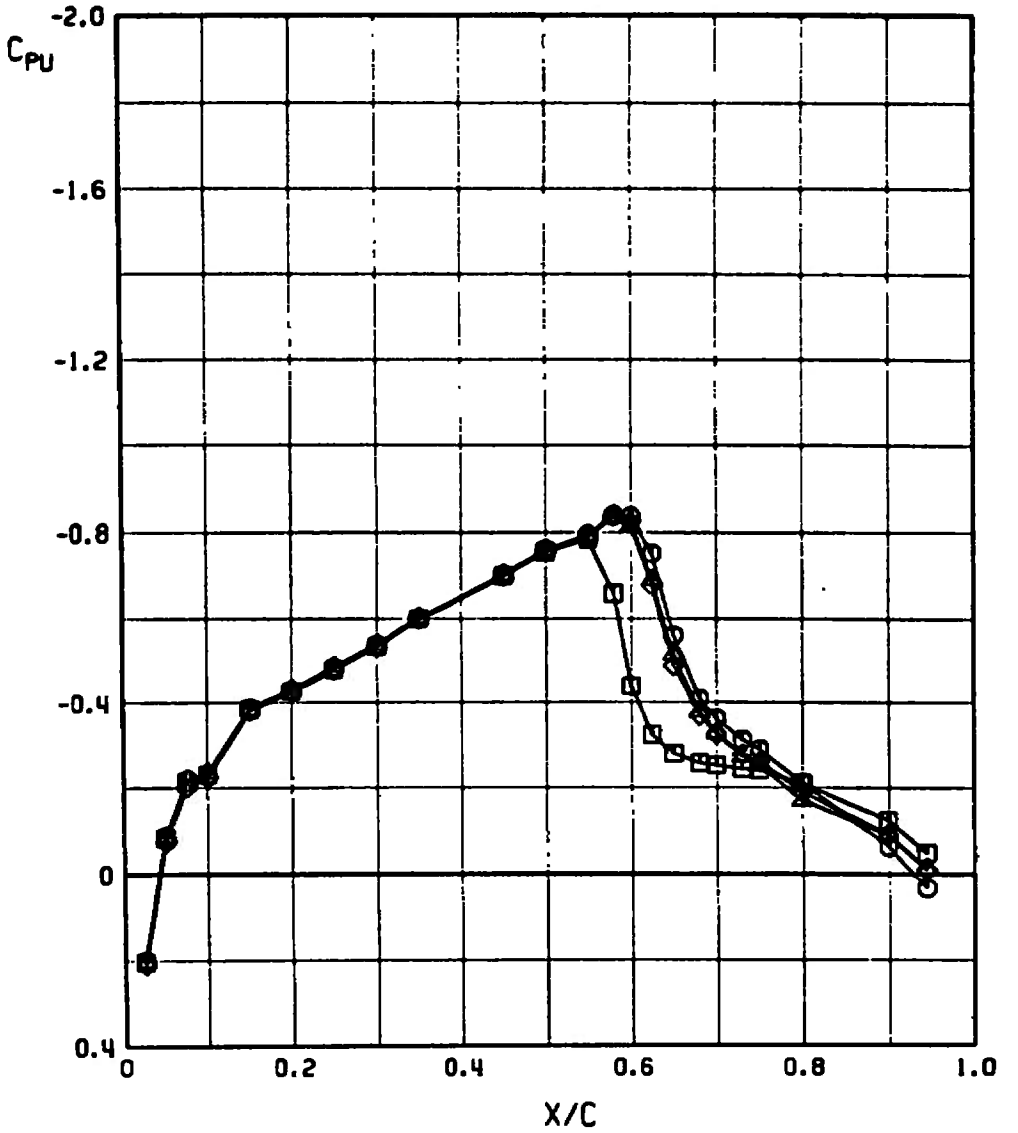

Fig. 16 Pressure Distributions on the Airfoil with B Pylon at Different Spanwise Positions, M_∞ = 0.85

SYMBOL	M_∞	PYLON	STORE	LOC	α
□	0.85	B	NONE	0.00	0
○	0.85	B	NONE	0.25	0
△	0.85	B	NONE	0.50	0
◇	0.85	B	NONE	0.75	0

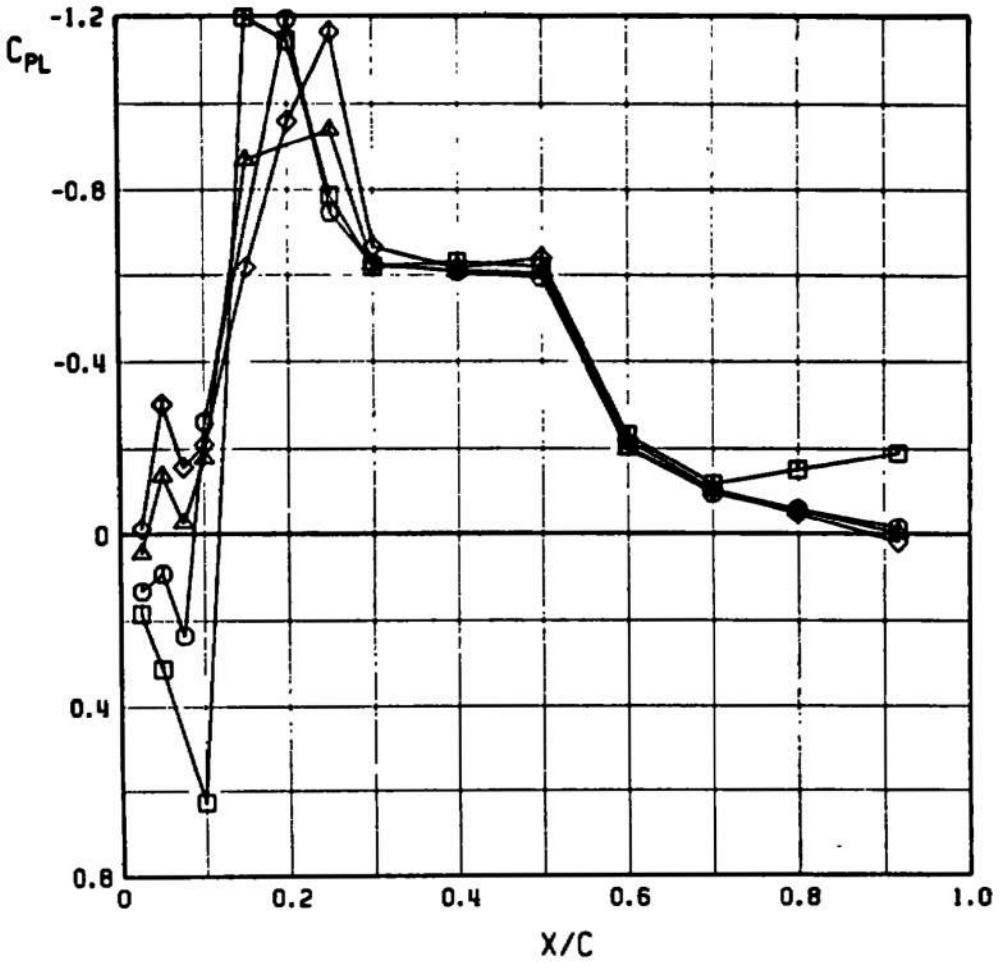

Fig. 16 Concluded

SYMBOL	M_∞	PYLON	STORE	LOC	α
○	0.90	B	NONE	0.25	0
△	0.90	B	NONE	0.50	0
◇	0.90	B	NONE	0.75	0

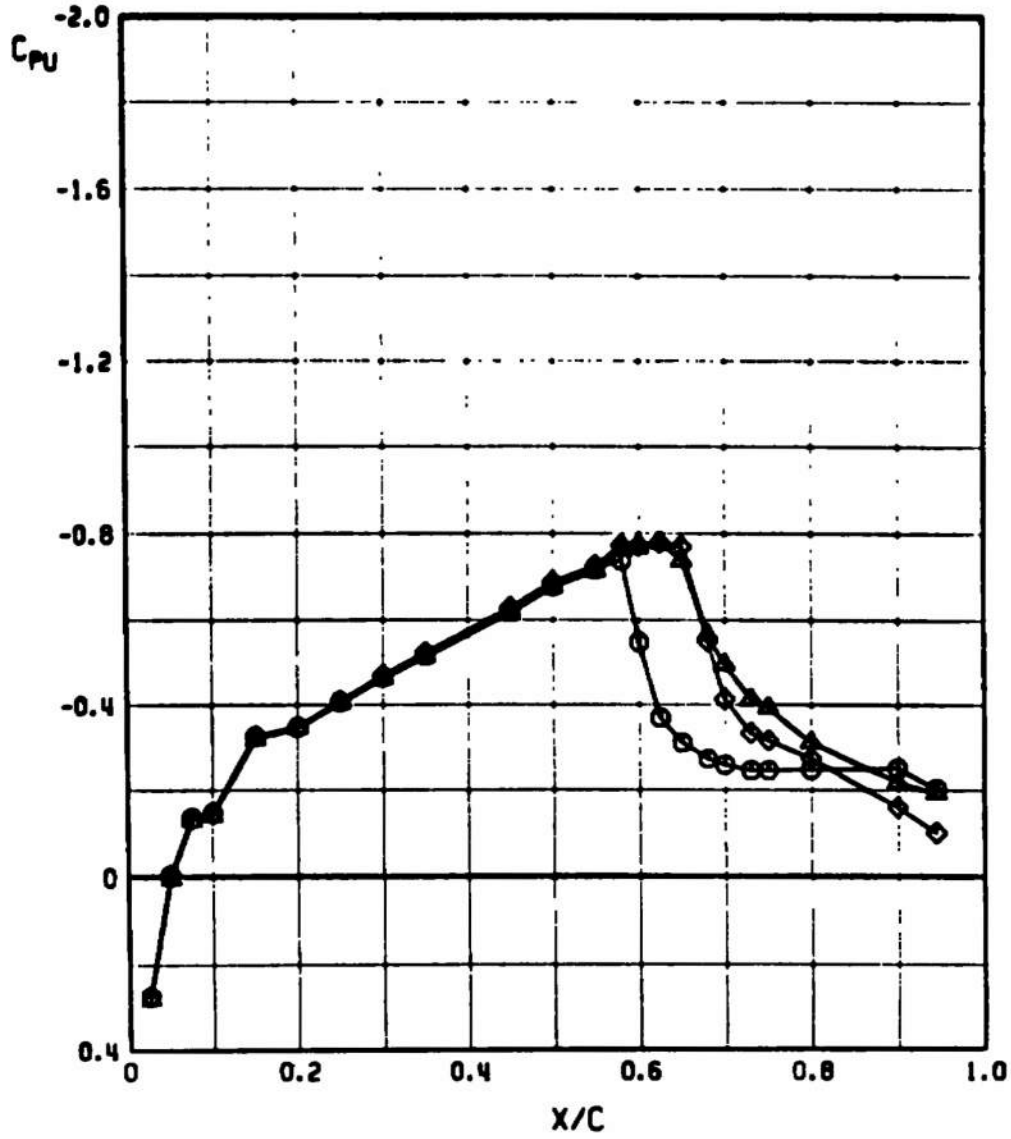

Fig. 17 Pressure Distributions on the Airfoil with B Pylon at Different Spanwise Positions, M_∞ = 0.9

SYMBOL	M_∞	PYLON	STORE	LOC	α
⊙	0.90	B	NONE	0.25	0
△	0.90	B	NONE	0.50	0
◇	0.90	B	NONE	0.75	0

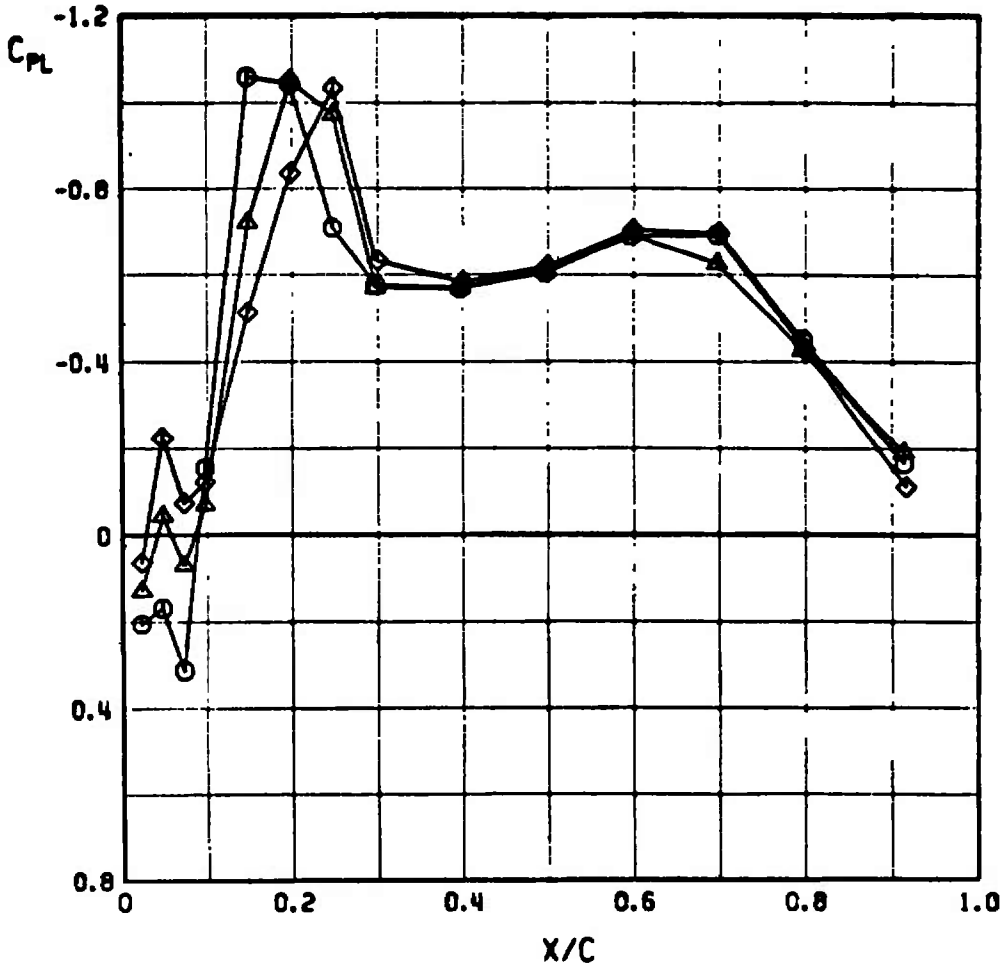

Fig. 17 Concluded

SYMBOL	M_∞	PYLON	STORE	LOC	α
□	0.70	B	C	0.00	0
○	0.70	B	C	0.25	0
△	0.70	B	C	0.50	0
◇	0.70	B	C	0.75	0

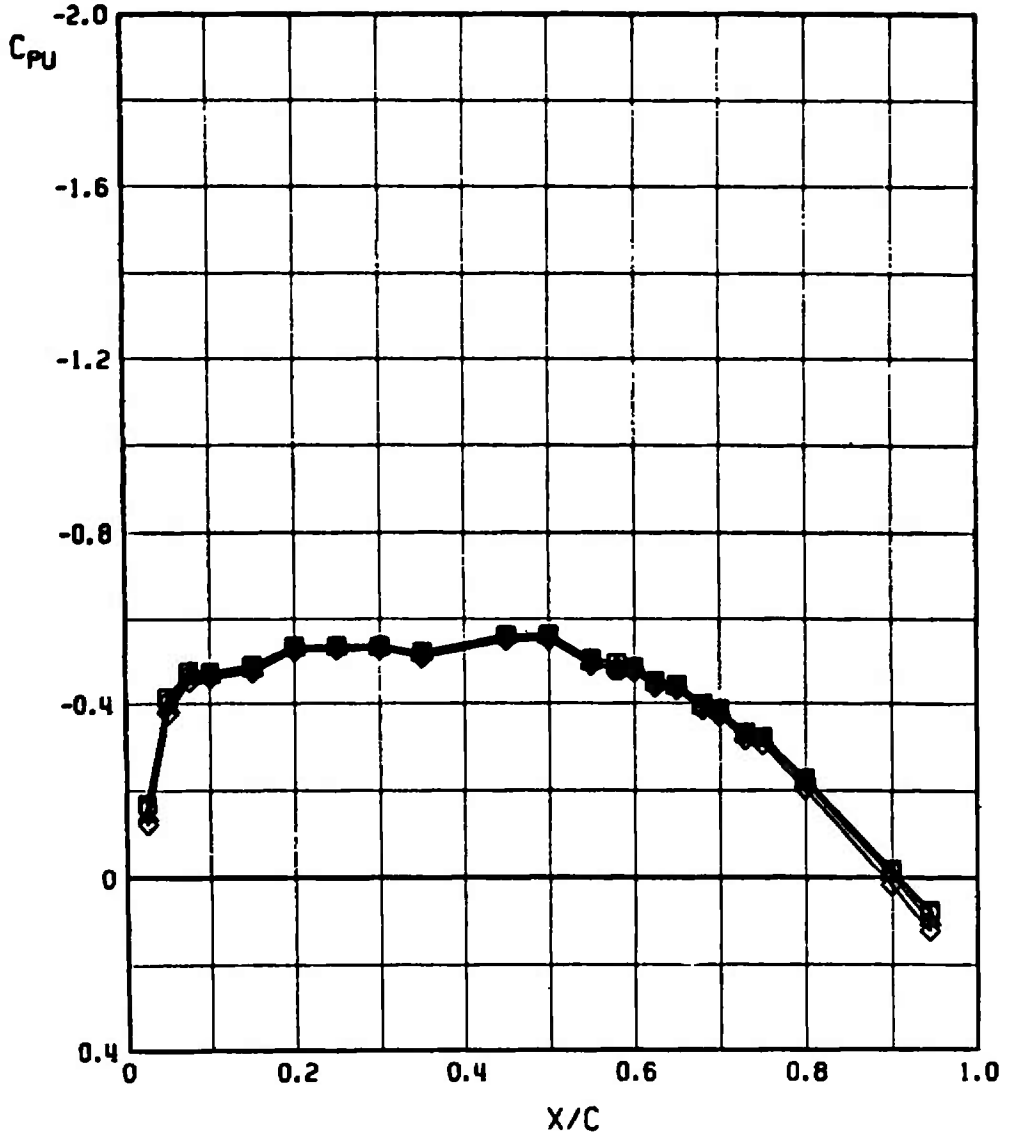

Fig. 18 Pressure Distributions on the Airfoil with B Pylon and C Store at Different Spanwise Positions, M_∞ = 0.7

SYMBOL	M_∞	PYLON	STORE	LOC	α
□	0.70	B	C	0.00	0
○	0.70	B	C	0.25	0
△	0.70	B	C	0.50	0
◇	0.70	B	C	0.75	0

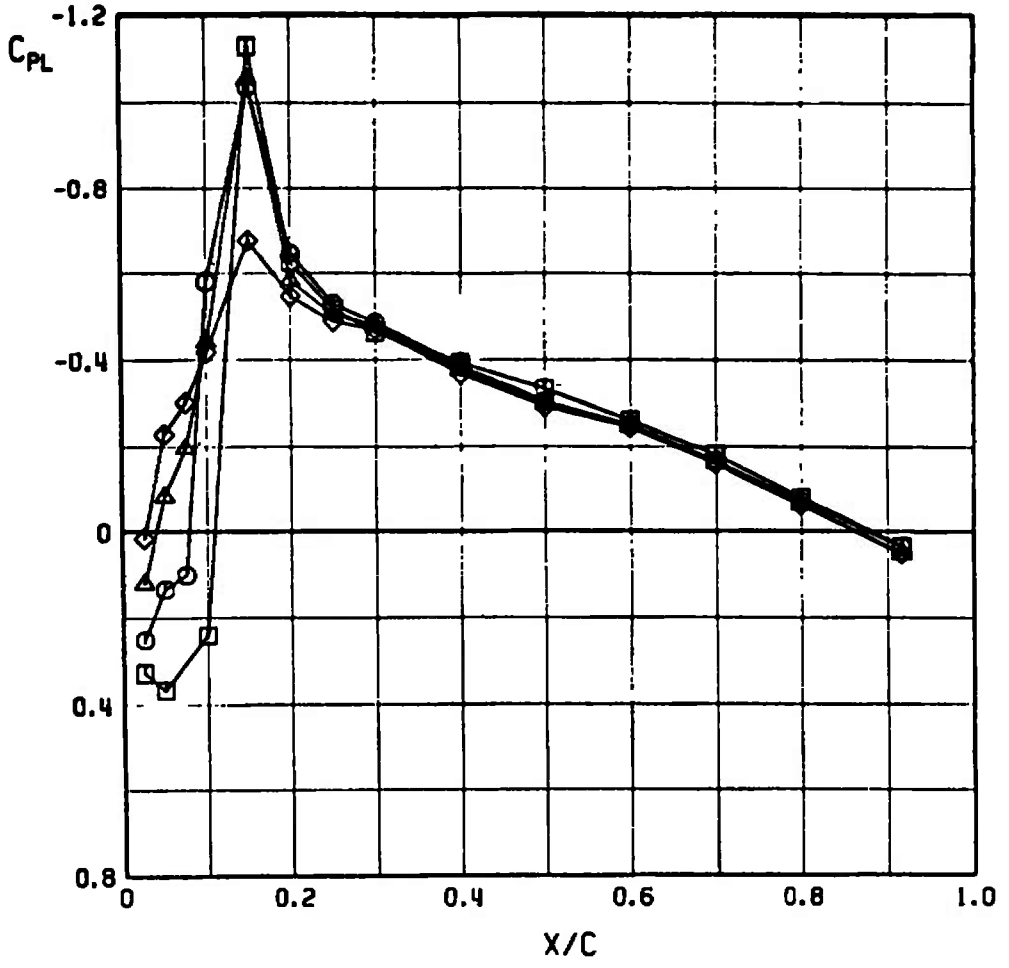

Fig. 18 Concluded

SYMBOL	M_∞	PYLON	STORE	LOC	α
□	0.80	B	C	0.00	0
○	0.80	B	C	0.25	0
△	0.80	B	C	0.50	0
◇	0.80	B	C	0.75	0

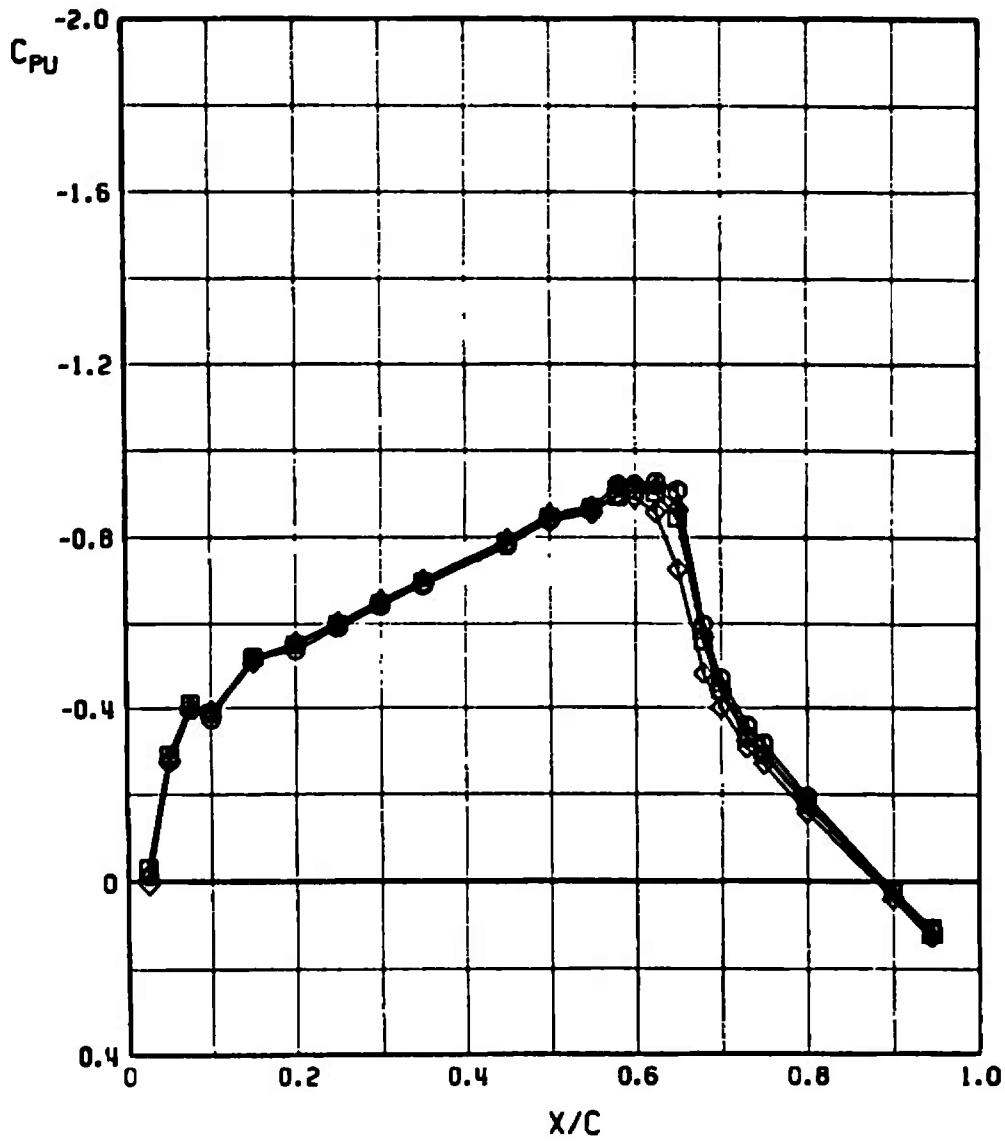

Fig. 19 Pressure Distributions on the Airfoil with B Pylon and C Store at Different Spanwise Positions, M_∞ = 0.8

SYMBOL	M_∞	PYLON	STORE	LOC	α
□	0.80	B	C	0.00	0
○	0.80	B	C	0.25	0
△	0.80	B	C	0.50	0
◇	0.80	B	C	0.75	0

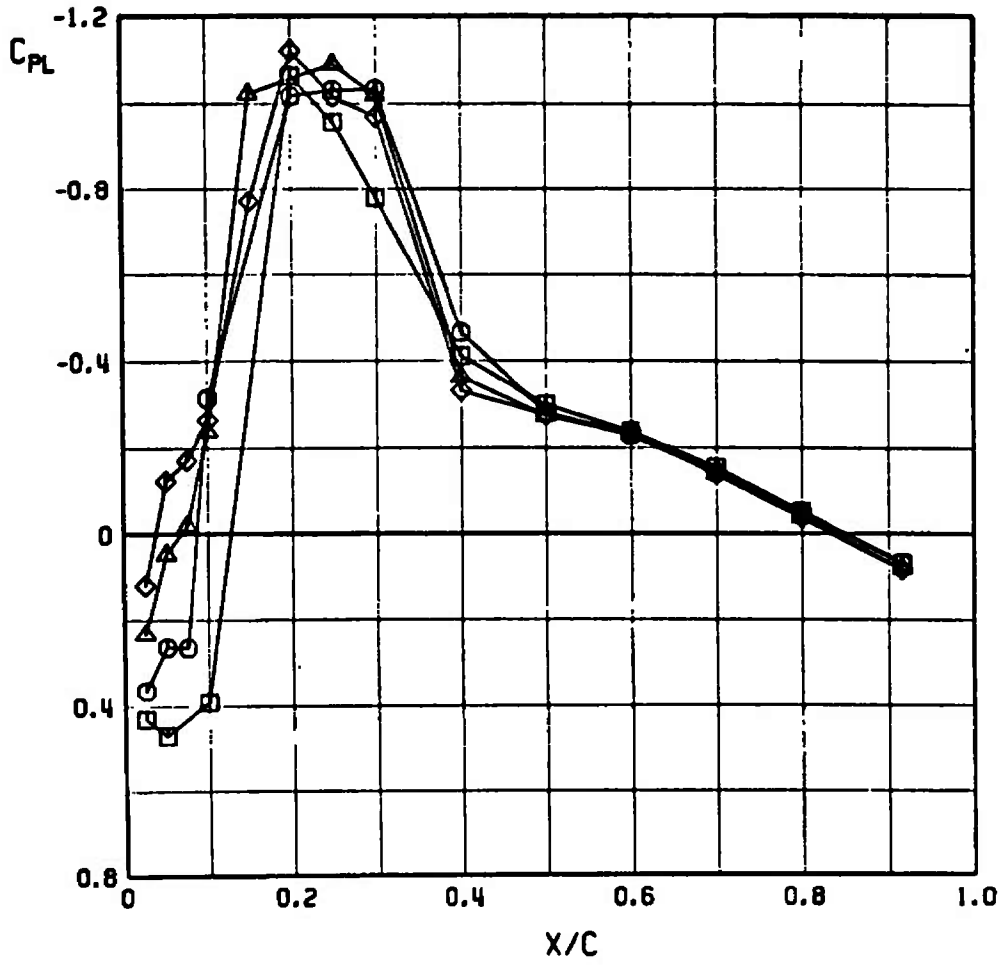

Fig. 19 Concluded

SYMBOL	M_∞	PYLON	STORE	LOC	α
□	0.85	B	C	0.00	0
○	0.85	B	C	0.25	0
△	0.85	B	C	0.50	0
◇	0.85	B	C	0.75	0

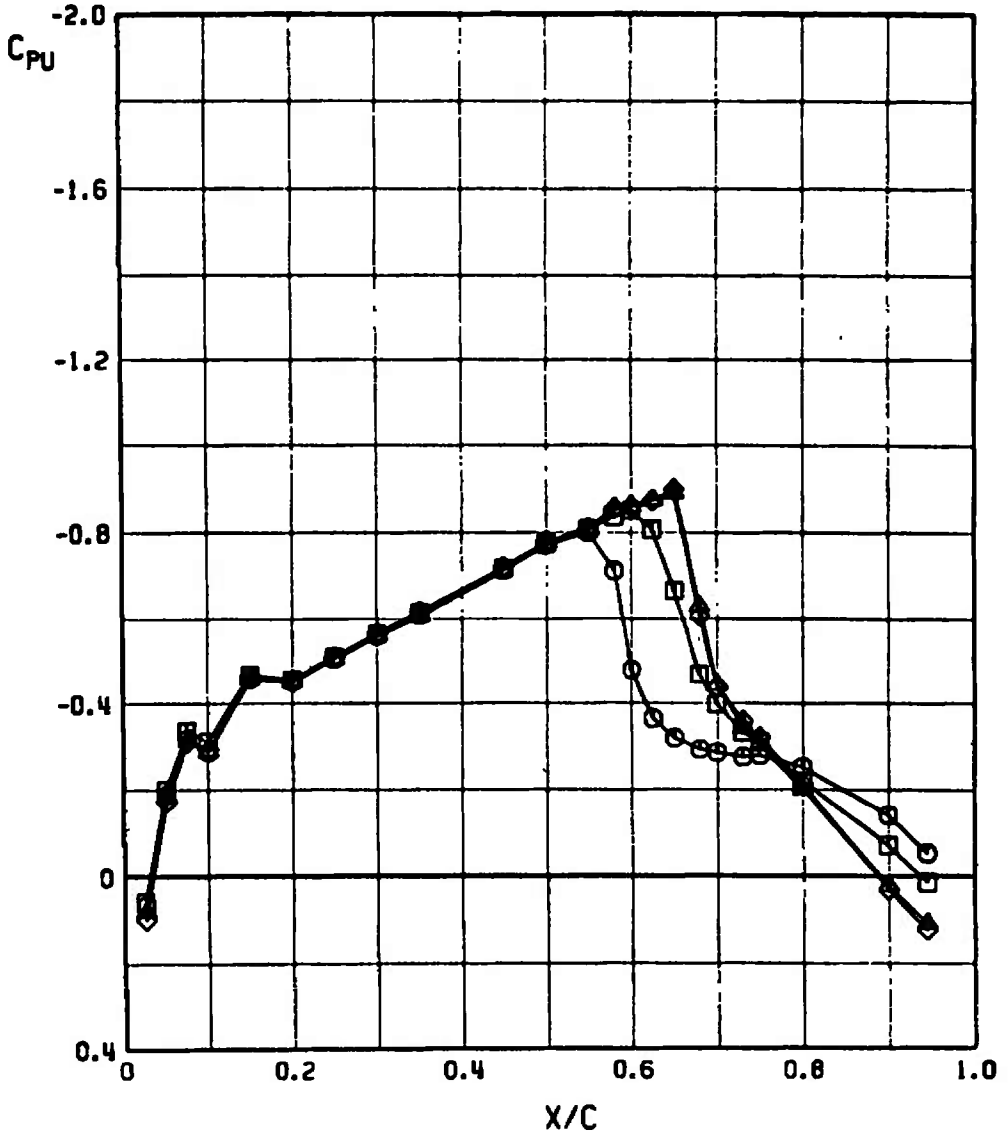

Fig. 20 Pressure Distributions on the Airfoil with B Pylon and C Store at Different Spanwise Positions, M_∞ = 0.85

SYMBOL	M_∞	PYLON	STORE	LOC	α
□	0.85	B	C	0.00	0
○	0.85	B	C	0.25	0
△	0.85	B	C	0.50	0
◇	0.85	B	C	0.75	0

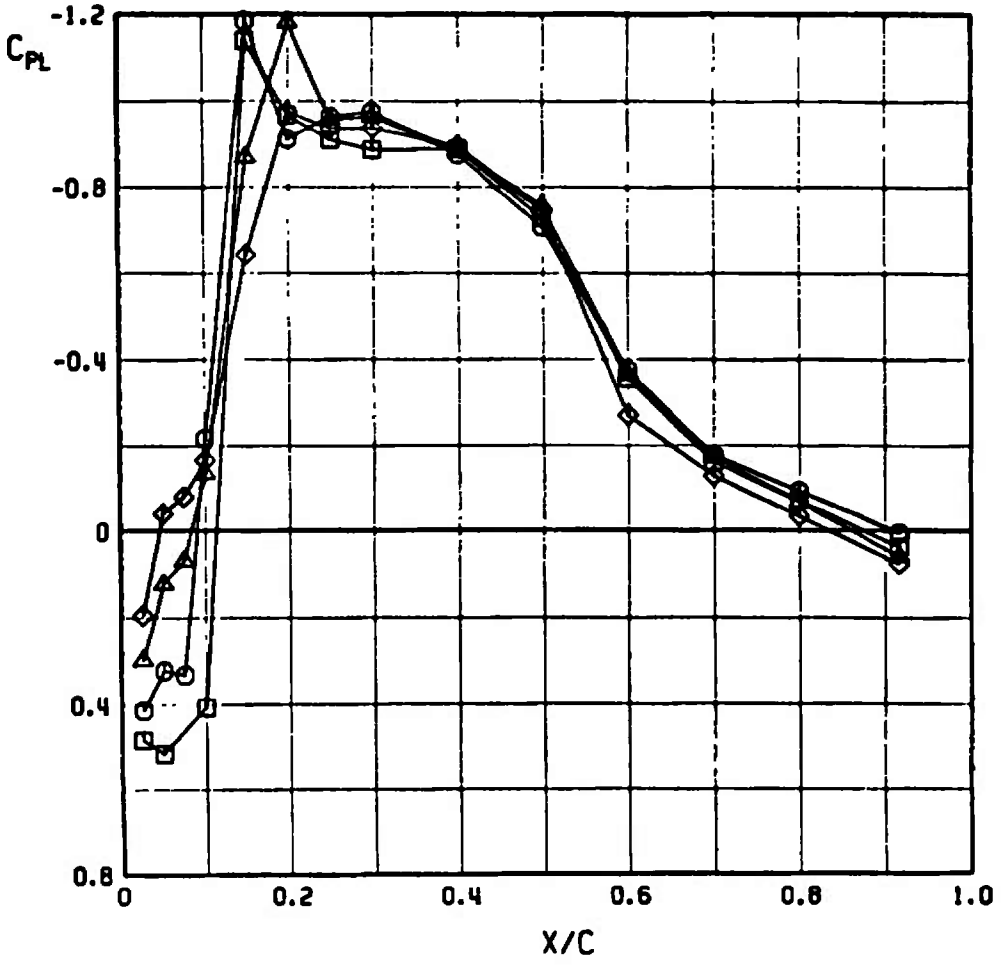

Fig. 20 Concluded

SYMBOL	M_∞	PYLON	STORE	LOC	α
□	0.90	B	C	0.00	0
○	0.90	B	C	0.25	0
△	0.90	B	C	0.50	0
◇	0.90	B	C	0.75	0

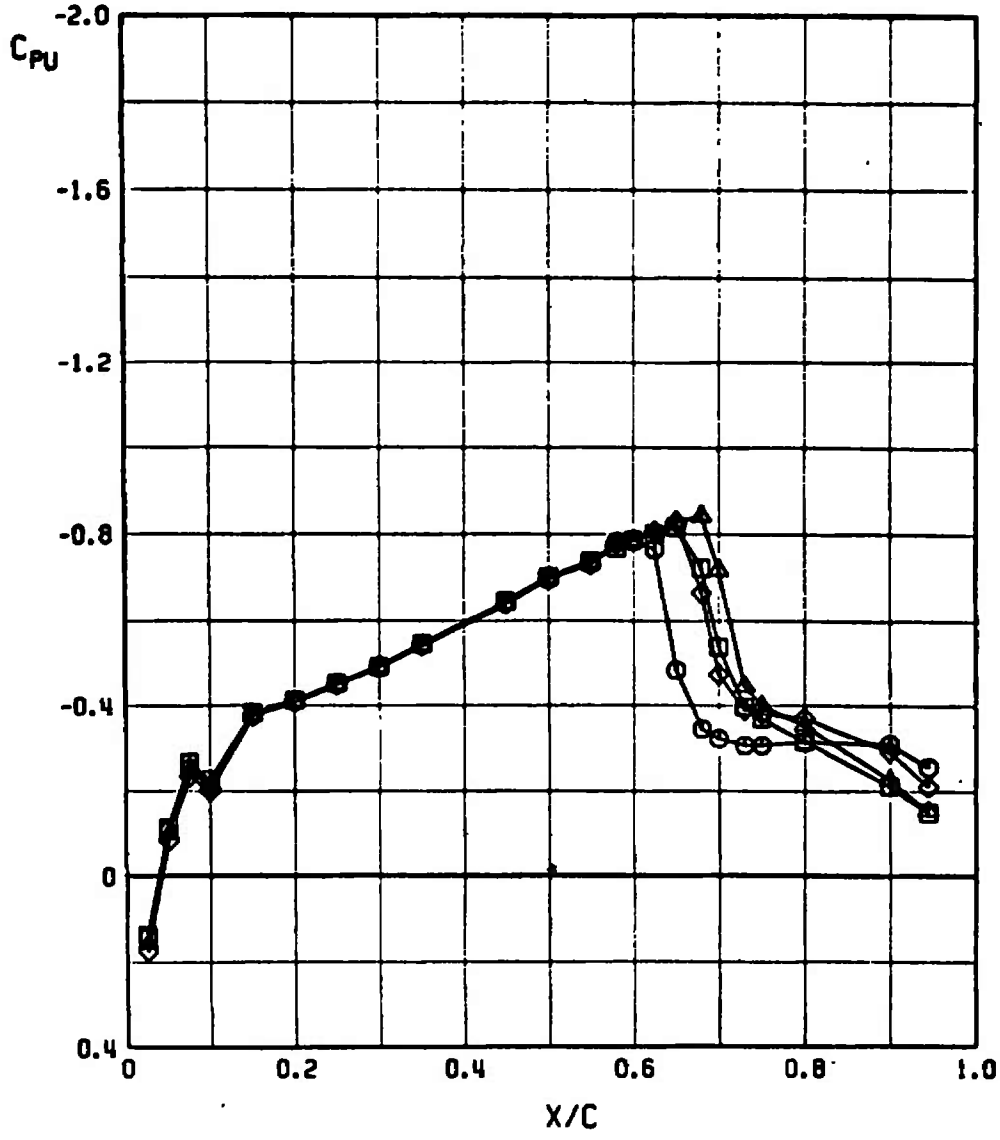

Fig. 21 Pressure Distributions on the Airfoil with B Pylon and C Store at Different Spanwise Positions, $M_\infty = 0.9$

SYMBOL	M_∞	PYLON	STORE	LOC	α
□	0.90	B	C	0.00	0
○	0.90	B	C	0.25	0
△	0.90	B	C	0.50	0
◇	0.90	B	C	0.75	0

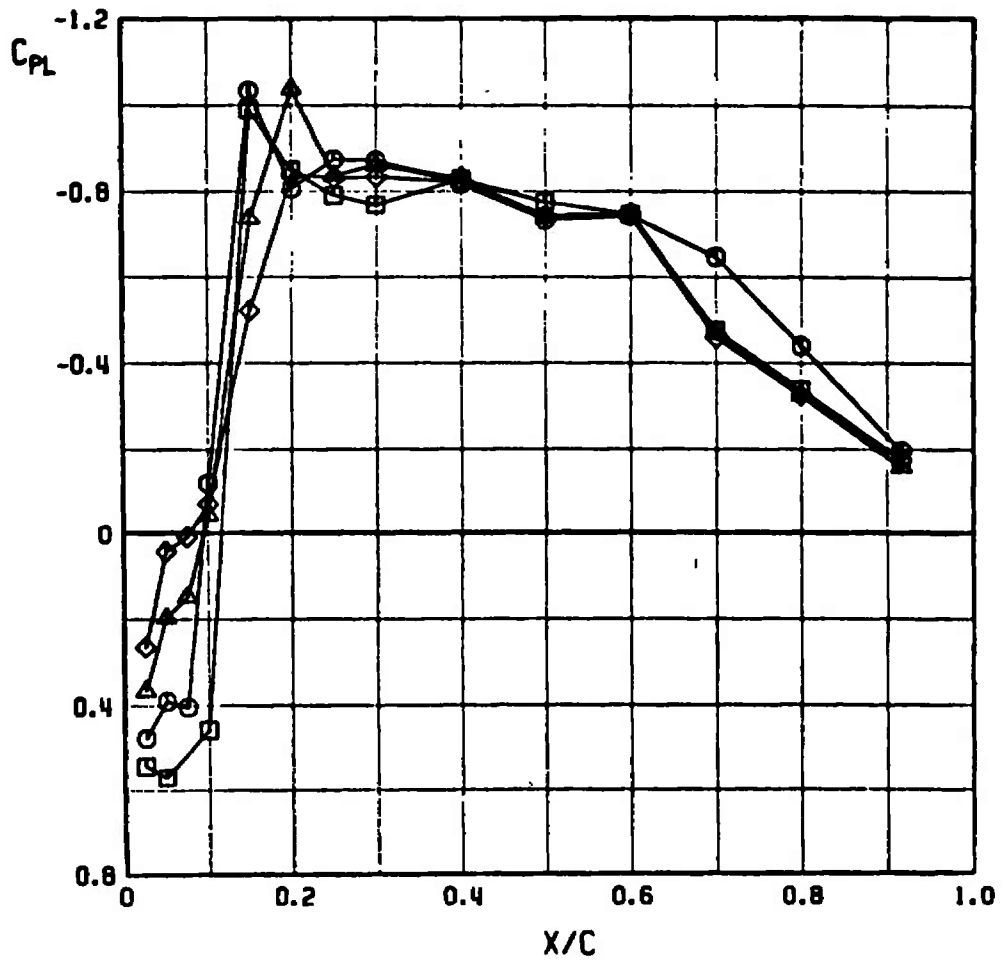

Fig. 21 Concluded

SYMBOL	M_∞	PYLON	STORE	LOC	α
□	0.85	B	NONE	0.00	4
○	0.85	B	NONE	0.25	4
△	0.85	B	NONE	0.50	4
◇	0.85	B	NONE	0.75	4

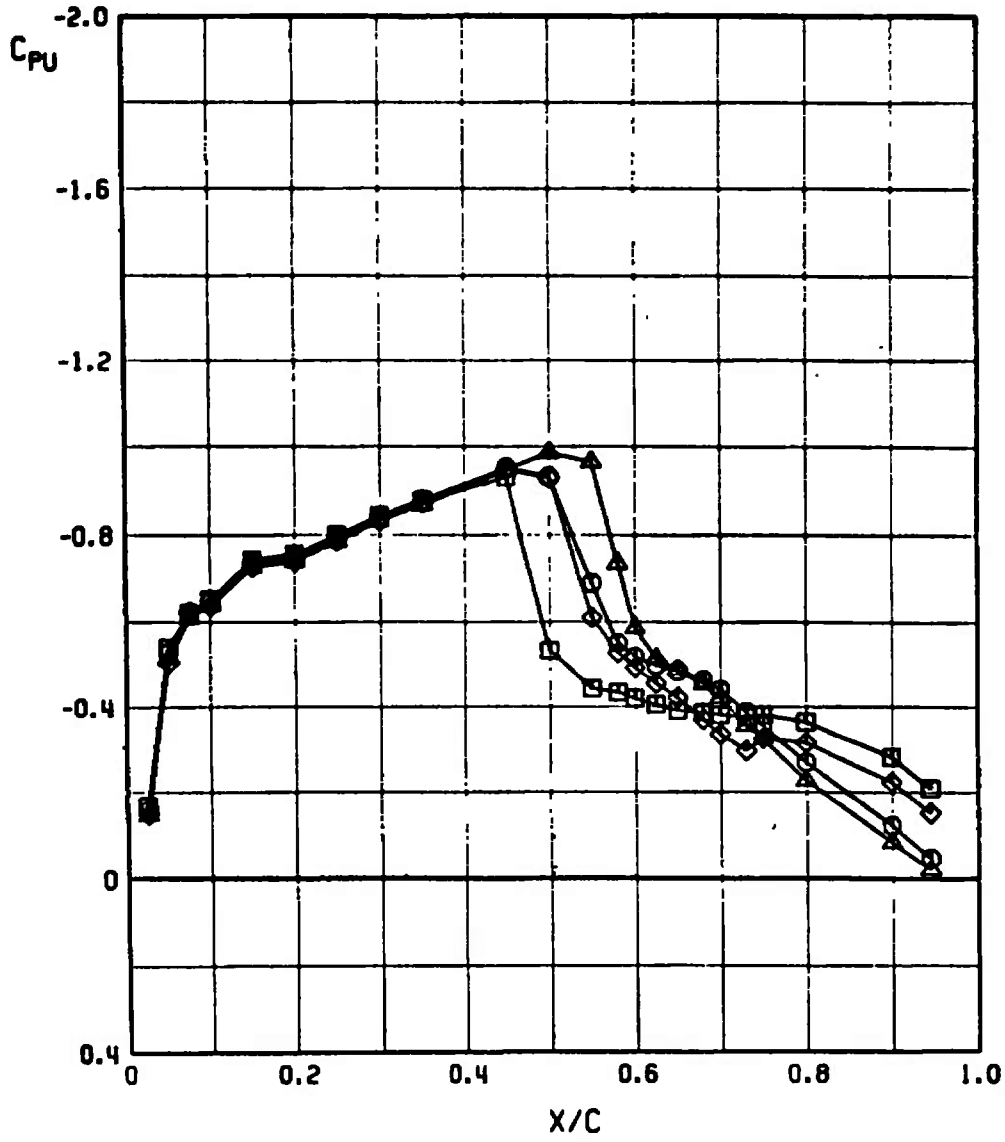

Fig. 22 Pressure Distributions on the Airfoil with B Pylon at Different Spanwise Positions, $M_\infty = 0.85$, $\alpha = 4$ deg

SYMBOL	M_∞	PYLON	STORE	LOC	α
□	0.85	B	NONE	0.00	4
○	0.85	B	NONE	0.25	4
△	0.85	B	NONE	0.50	4
◇	0.85	B	NONE	0.75	4

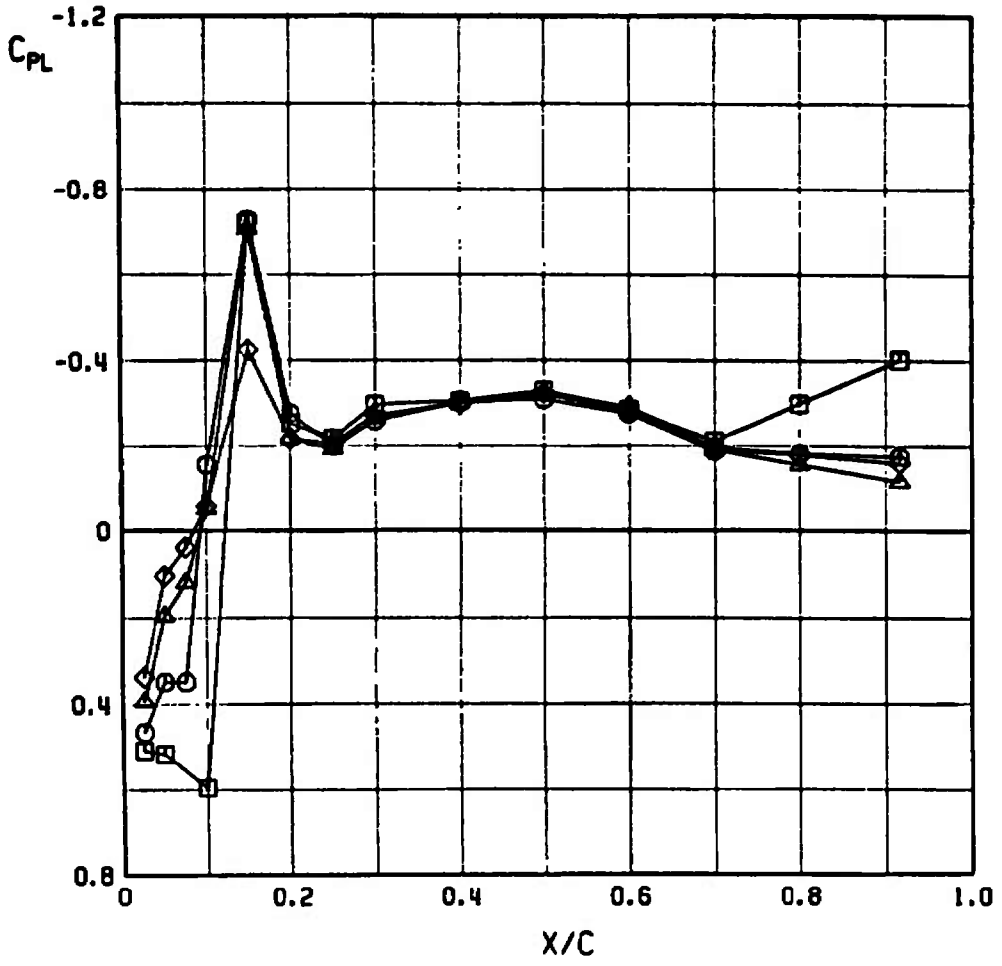

Fig. 22 Concluded

SYMBOL	M_∞	PYLON	STORE	LOC	α
□	0.85	B	NONE	0.00	8
○	0.85	B	NONE	0.25	8
△	0.85	B	NONE	0.50	8
◇	0.85	B	NONE	0.75	8

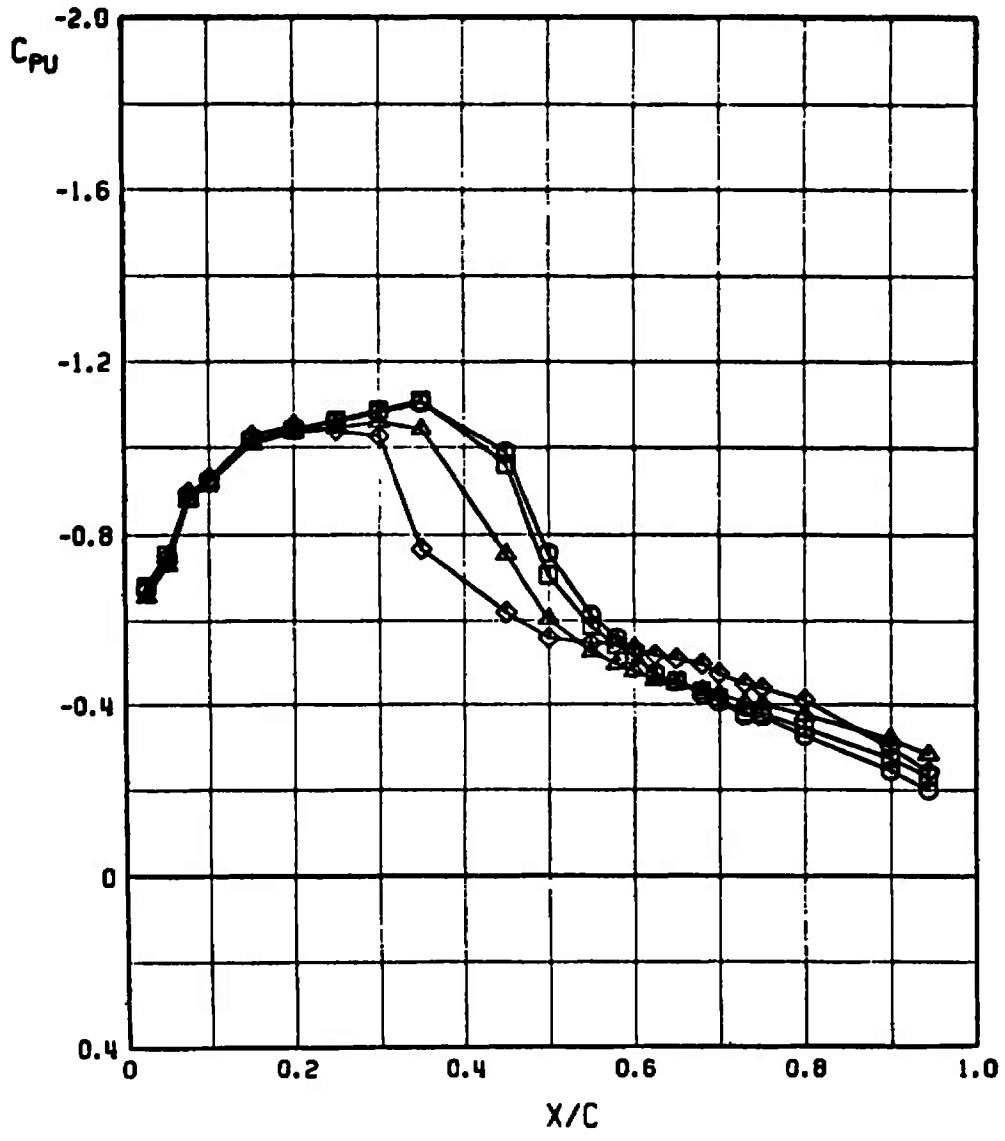

Fig. 23 Pressure Distributions on the Airfoil with B Pylon at Different Spanwise Positions, M_∞ = 0.85, α = 8 deg

SYMBOL	M_∞	PYLON	STORE	LOC	α
□	0.85	B	NONE	0.00	8
○	0.85	B	NONE	0.25	8
△	0.85	B	NONE	0.50	8
◇	0.85	B	NONE	0.75	8

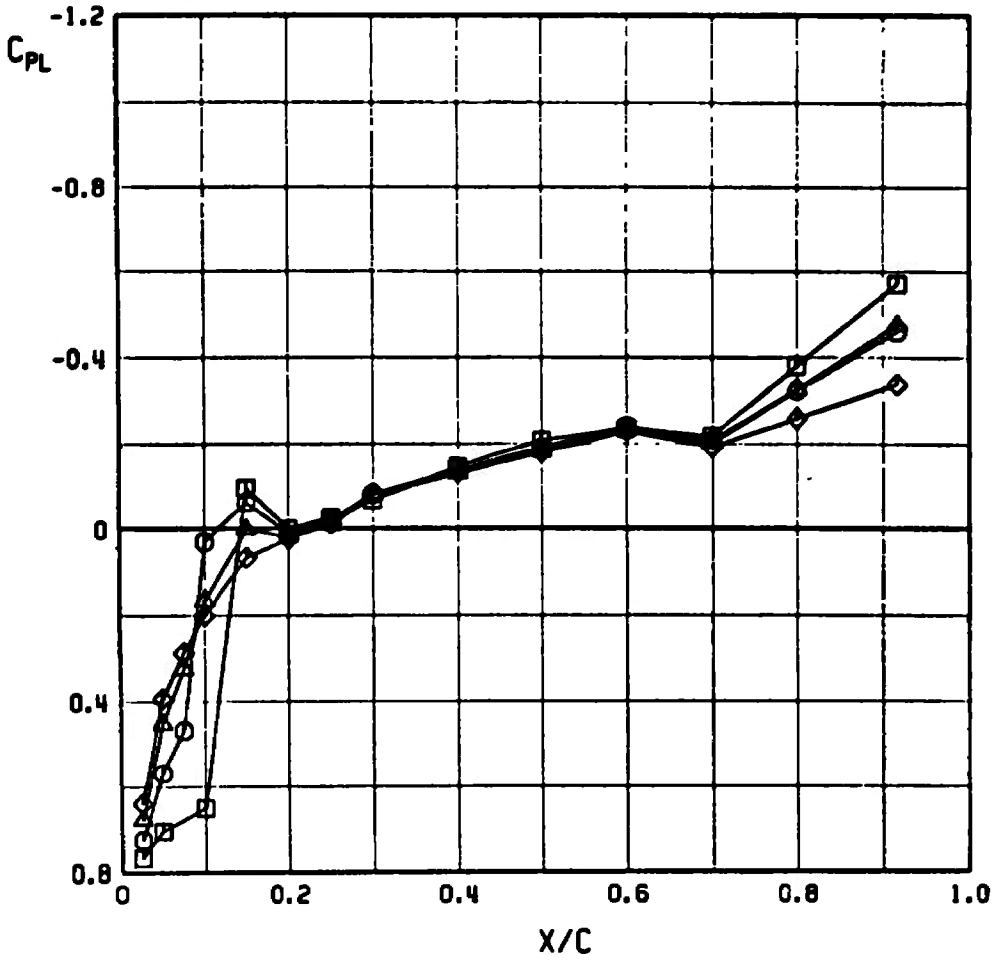

Fig. 23 Concluded

SYMBOL	M_∞	PYLON	STORE	LOC	α
□	0.85	B	C	0.00	4
○	0.85	B	C	0.25	4
△	0.85	B	C	0.50	4
◇	0.85	B	C	0.75	4

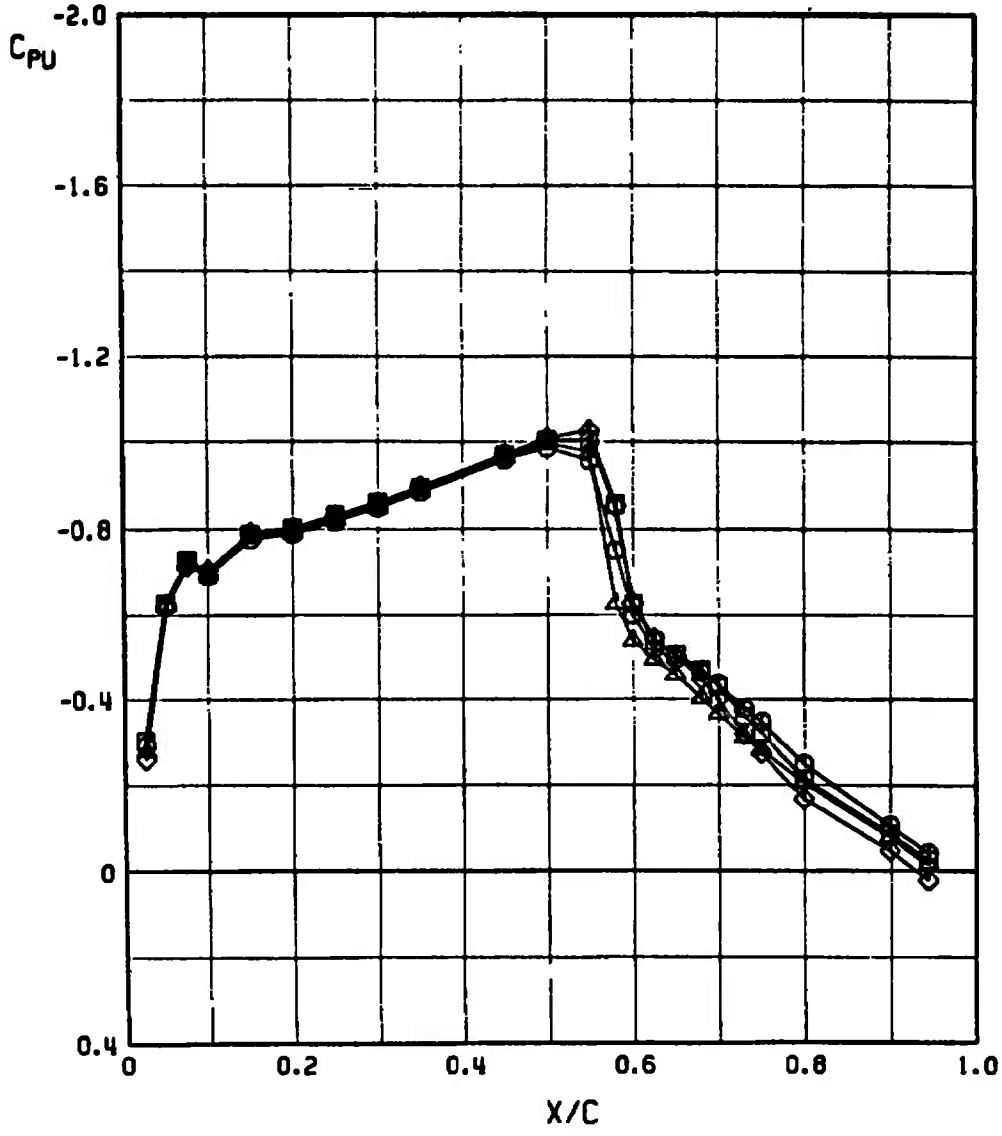

Fig. 24 Pressure Distributions on the Airfoil with B Pylon and C Store at Different Spanwise Positions, $M_\infty = 0.85$, $\alpha = 4$ deg

SYMBOL	M_∞	PYLON	STORE	LOC	α
⊡	0.85	B	C	0.00	4
⊙	0.85	B	C	0.25	4
△	0.85	B	C	0.50	4
◇	0.85	B	C	0.75	4

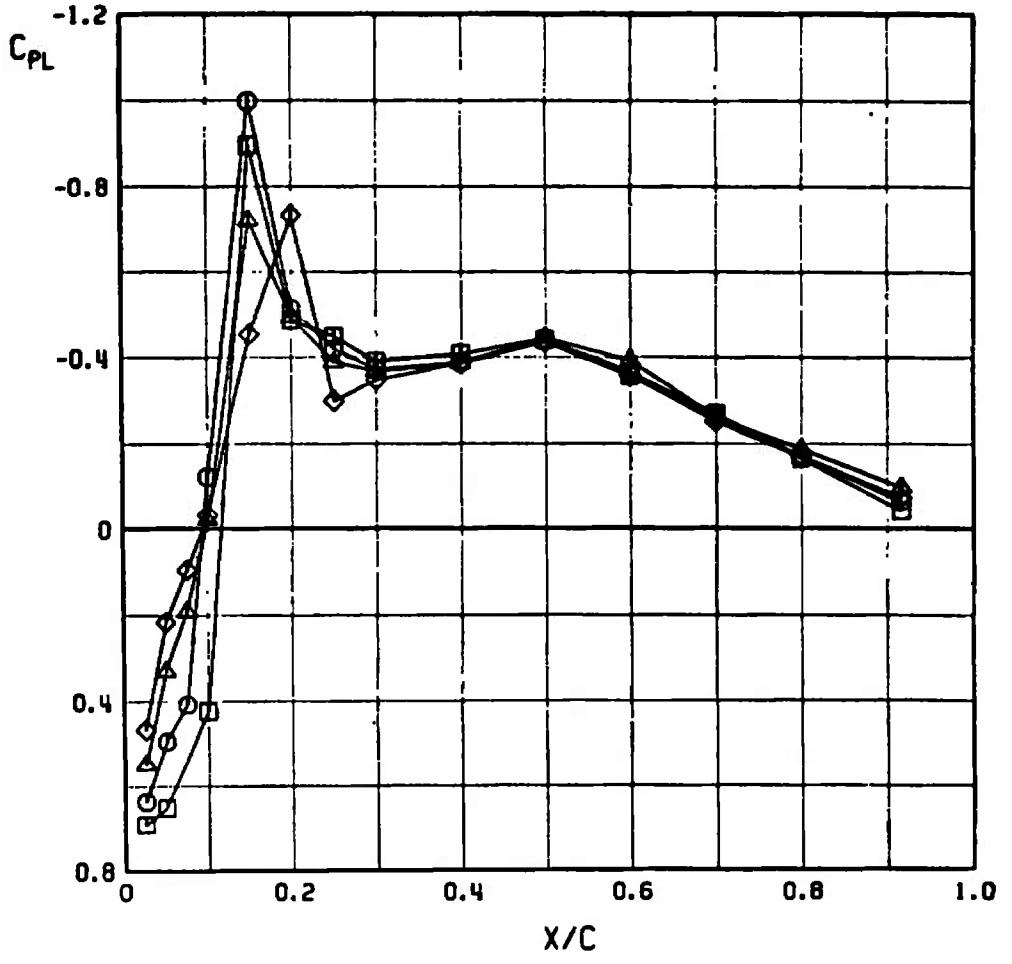

Fig. 24 Concluded

SYMBOL	M_∞	PYLON	STORE	LOC	α
□	0.85	B	C	0.00	8
○	0.85	B	C	0.25	8
△	0.85	B	C	0.50	8
◇	0.85	B	C	0.75	8

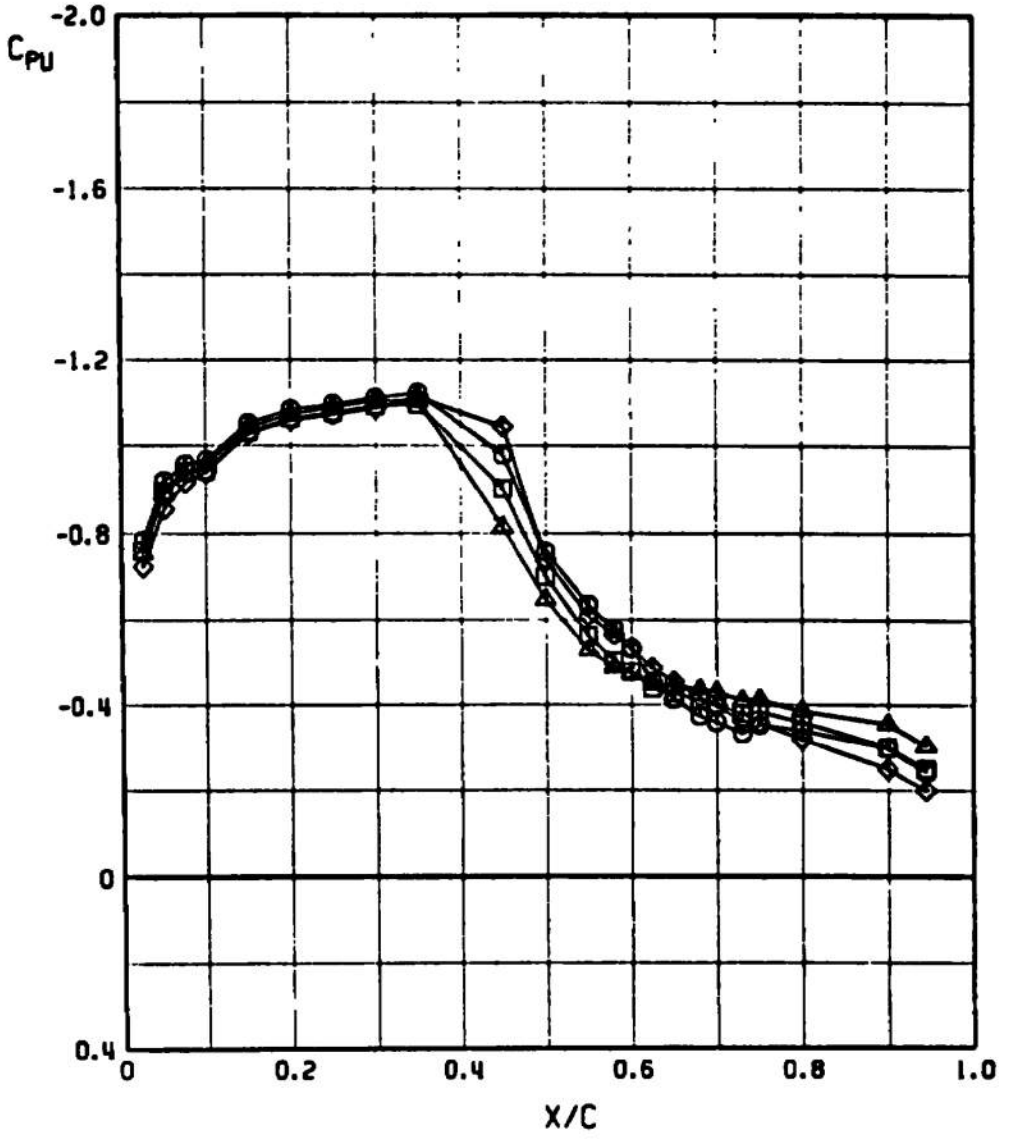

Fig. 25 Pressure Distributions on the Airfoil with B Pylon and C Store at Different Spanwise Positions, M_∞ = 0.85, α = 8 deg

SYMBOL	M_∞	PYLON	STORE	LOC	α
□	0.85	B	C	0.00	8
○	0.85	B	C	0.25	8
△	0.85	B	C	0.50	8
◇	0.85	B	C	0.75	8

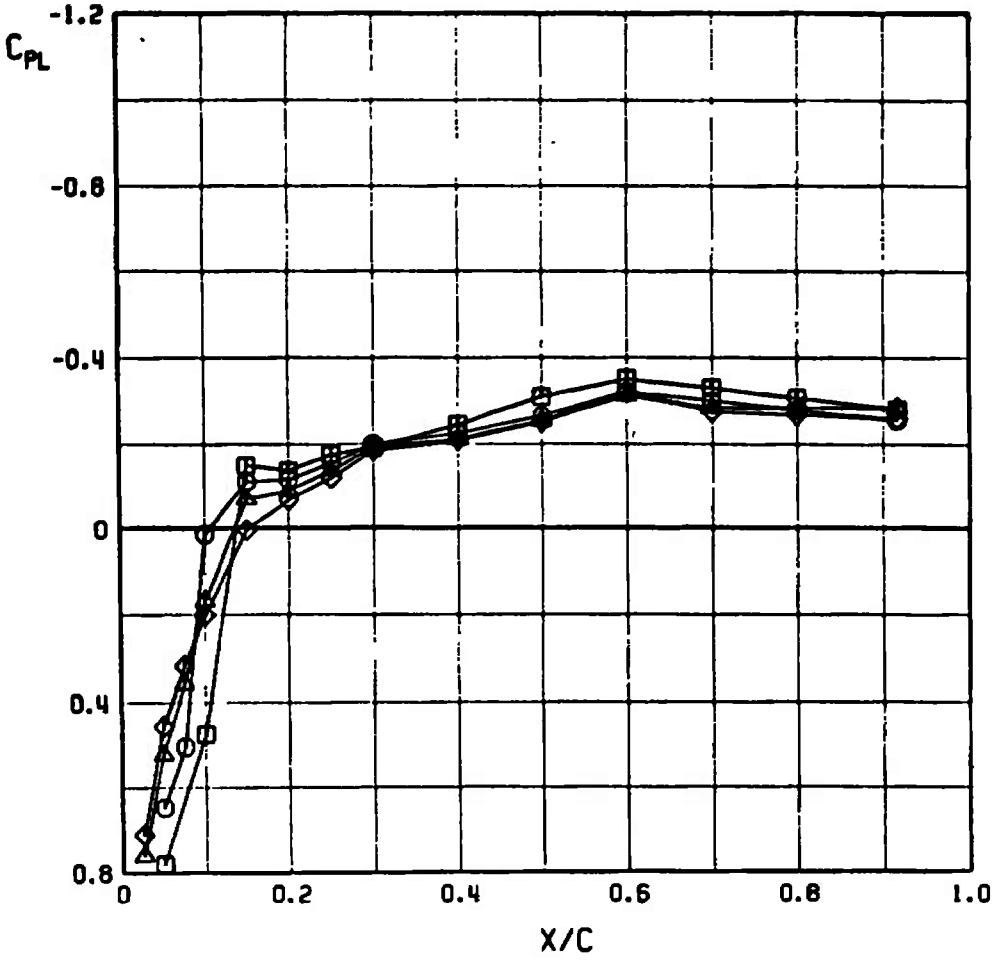

Fig. 25 Concluded

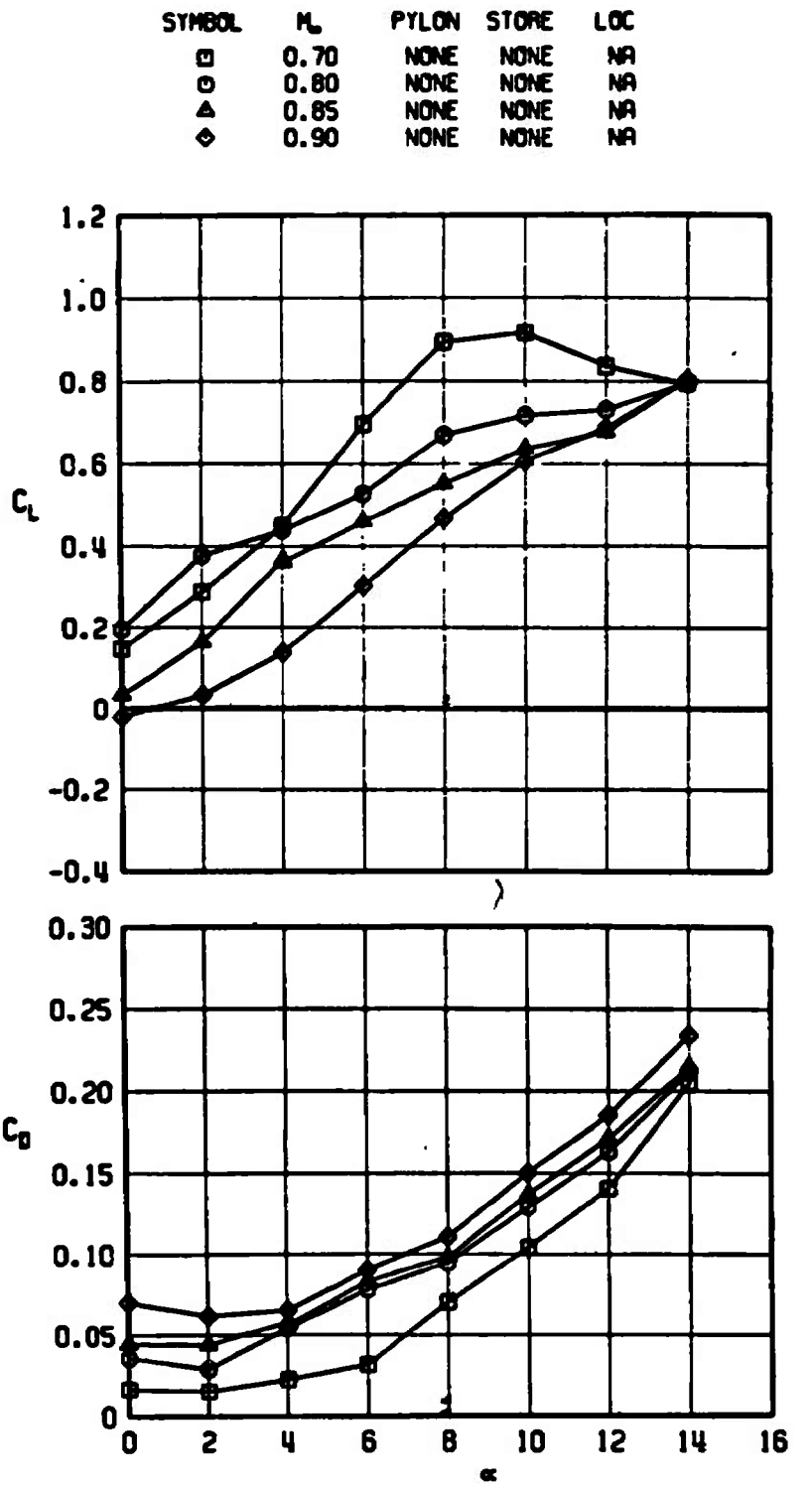

Fig. 26 Effect of Mach Number on the Lift, Drag, and Pitching-Moment Coefficients of the Clean Airfoil

SYMBOL	M_∞	PYLON	STORE	LOC
□	0.825	NONE	NONE	NA
○	0.875	NONE	NONE	NA
△	0.925	NONE	NONE	NA
◇	0.950	NONE	NONE	NA

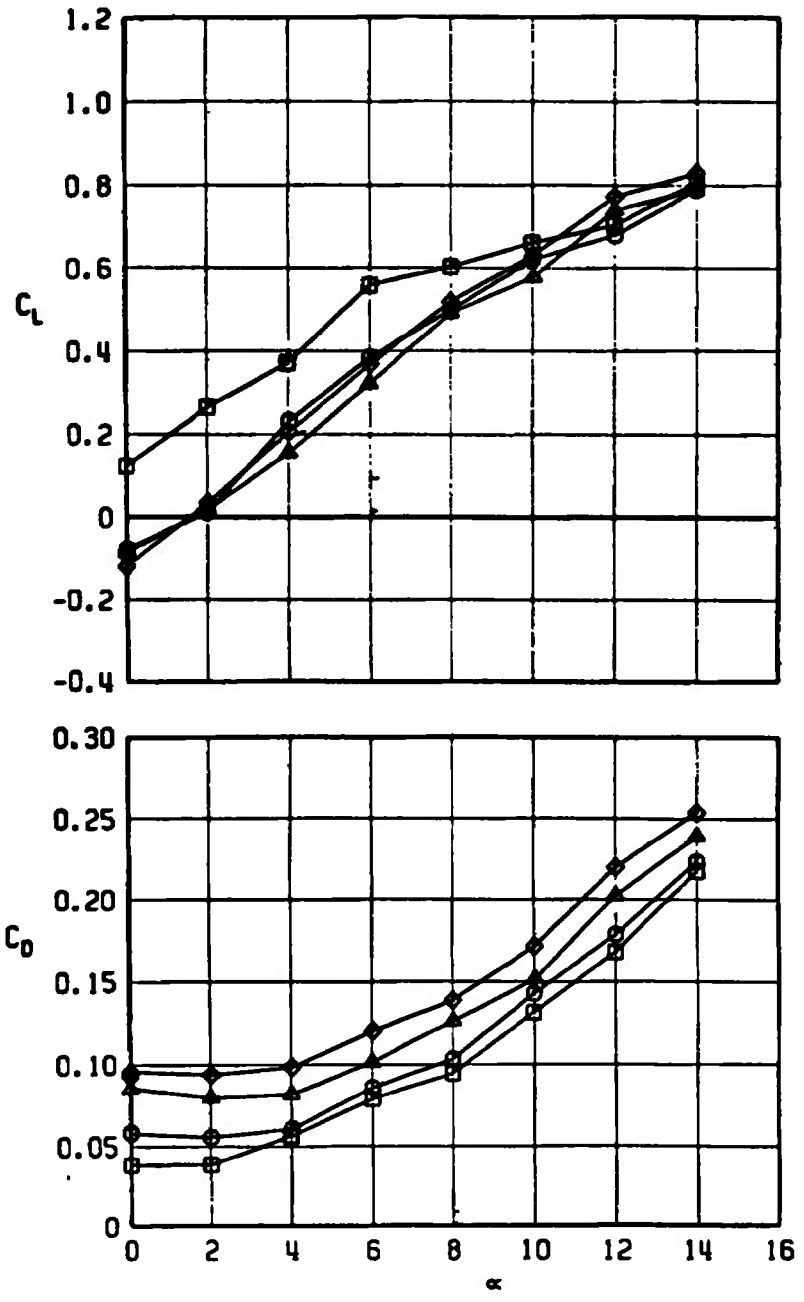

Fig. 26 Continued

SYMBOL	M_∞	PYLON	STORE	LOC
□	0.70	NONE	NONE	NA
○	0.80	NONE	NONE	NA
△	0.85	NONE	NONE	NA
◇	0.90	NONE	NONE	NA

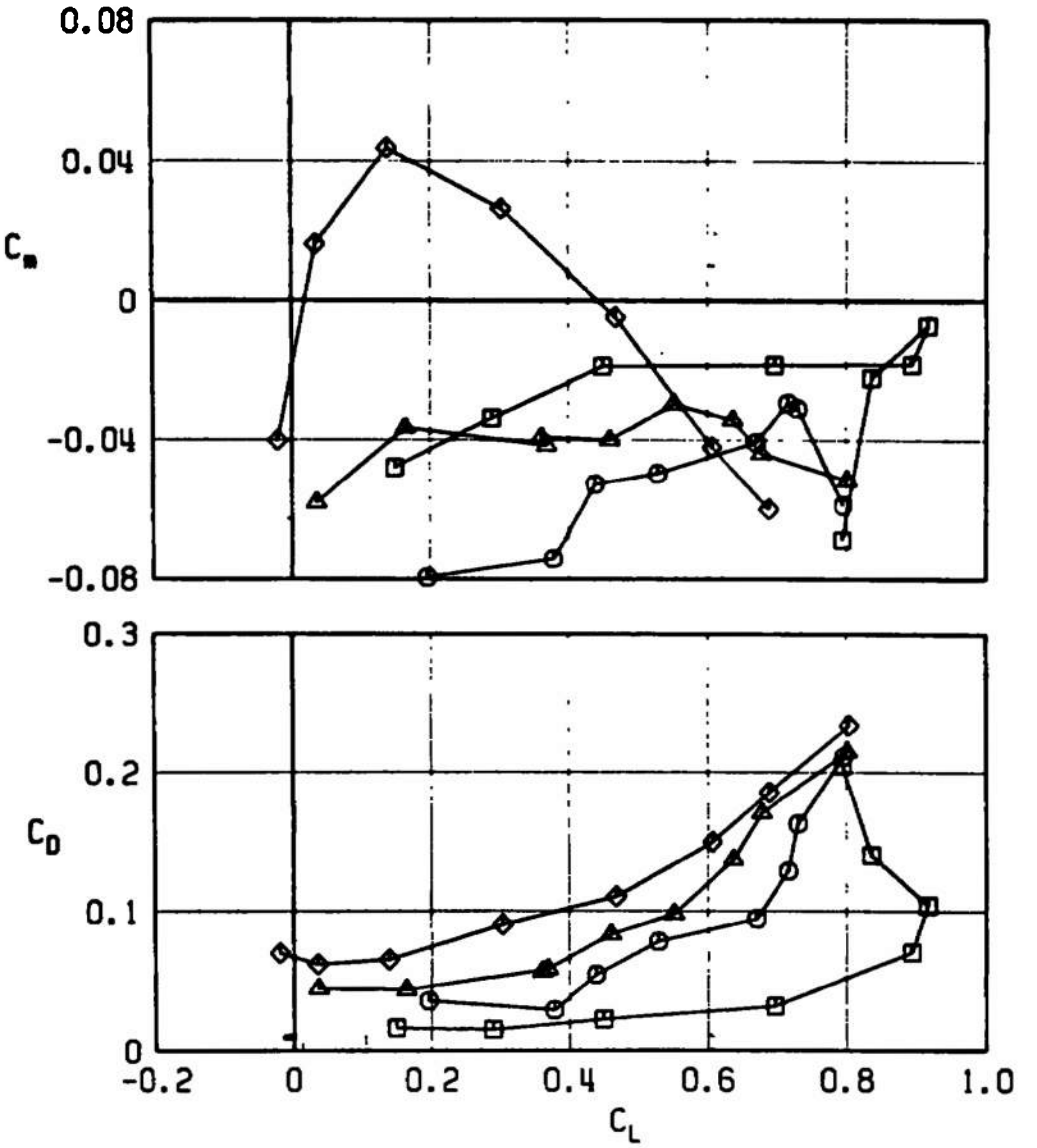

Fig. 26 Continued

SYMBOL	M_∞	PYLON	STORE	LOC
□	0.825	NONE	NONE	NA
○	0.875	NONE	NONE	NA
△	0.925	NONE	NONE	NA
◇	0.950	NONE	NONE	NA

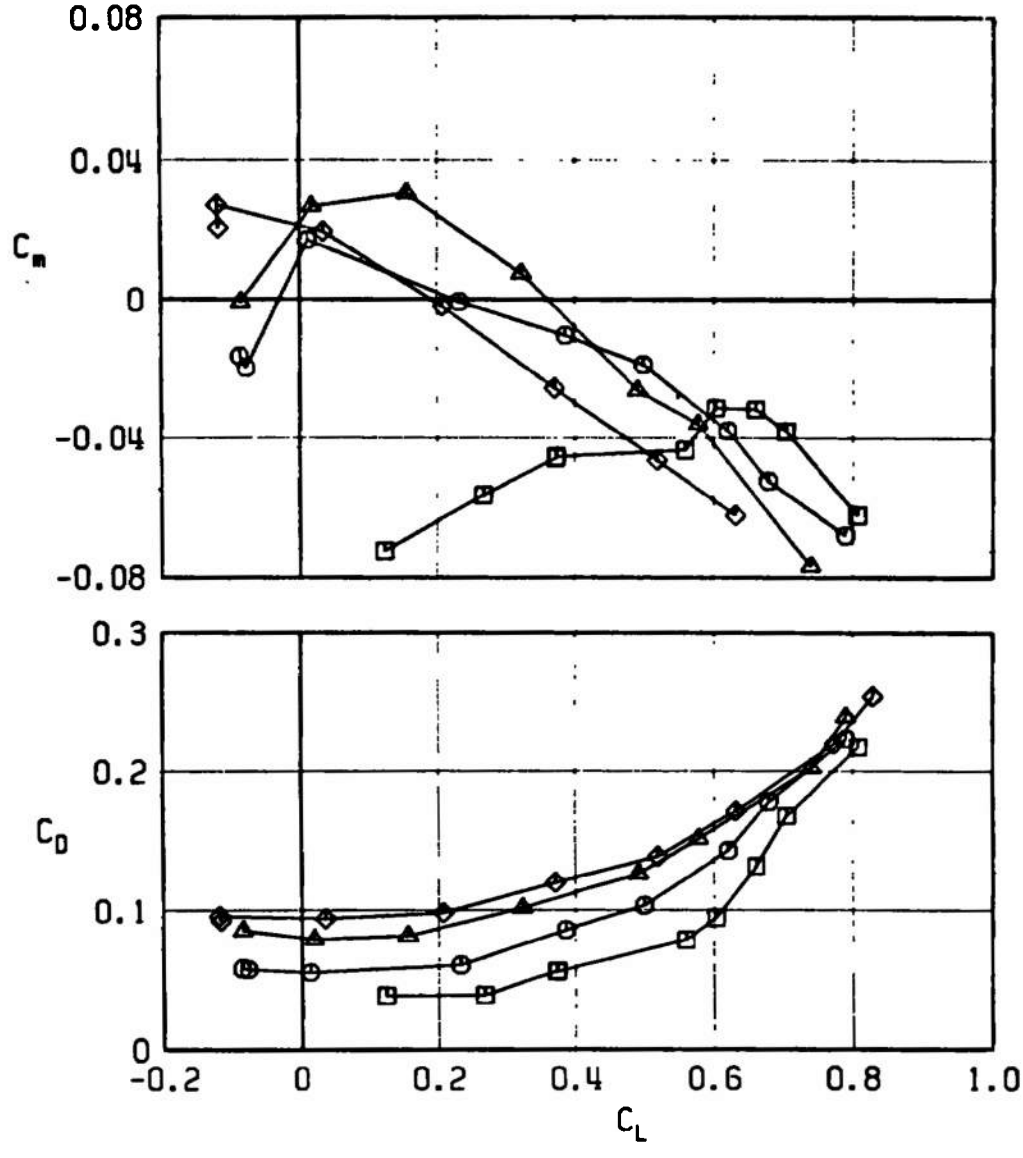

Fig. 26 Concluded

SYMBOL	M_∞	PYLON	STORE	LOC
⊡	0.70	B	NONE	0.00
⊙	0.70	B	NONE	0.25
△	0.70	B	NONE	0.50
◇	0.70	B	NONE	0.75

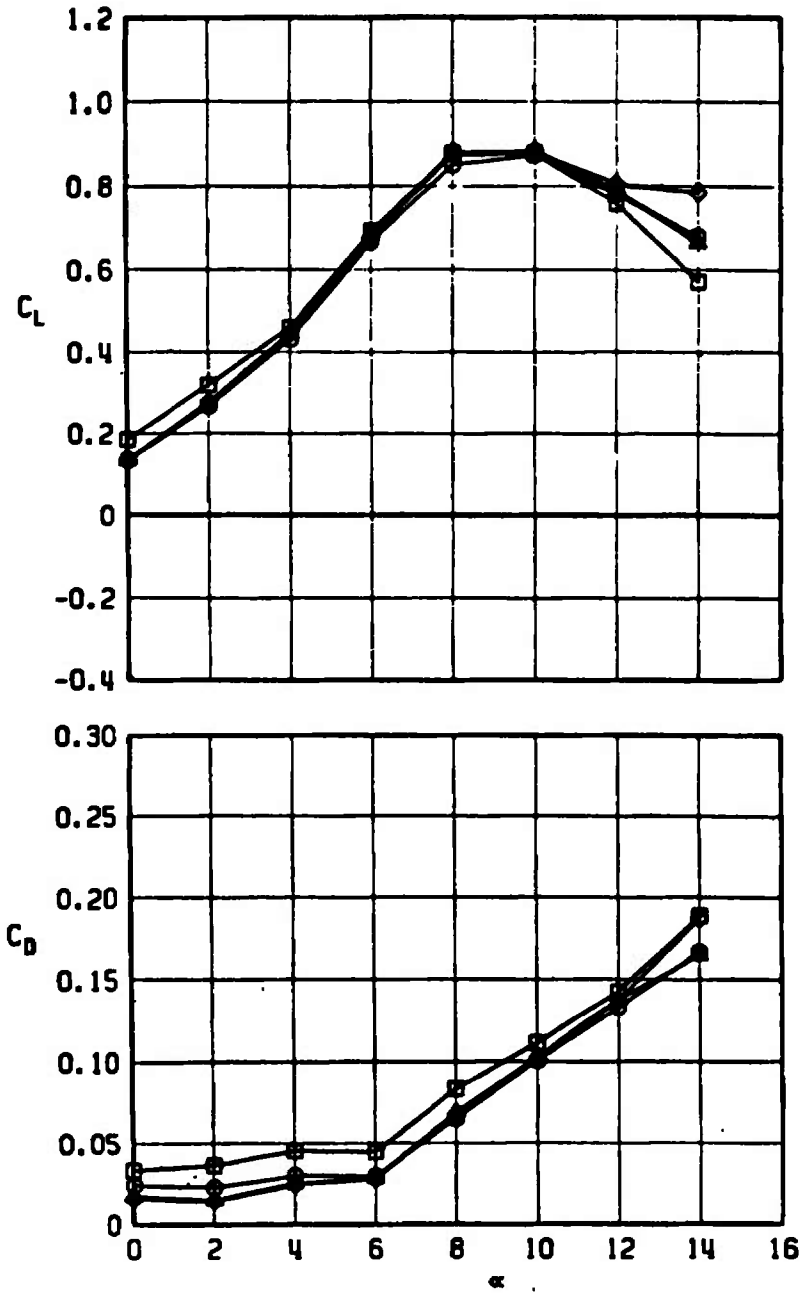

Fig. 27 Effect of Spanwise Location of the B Pylon on the Lift, Drag, and Pitching-Moment Coefficients of the Airfoil, $M_\infty = 0.7$

SYMBOL	M_∞	PYLON	STORE	LOC
□	0.70	B	NONE	0.00
○	0.70	B	NONE	0.25
△	0.70	B	NONE	0.50
◇	0.70	B	NONE	0.75

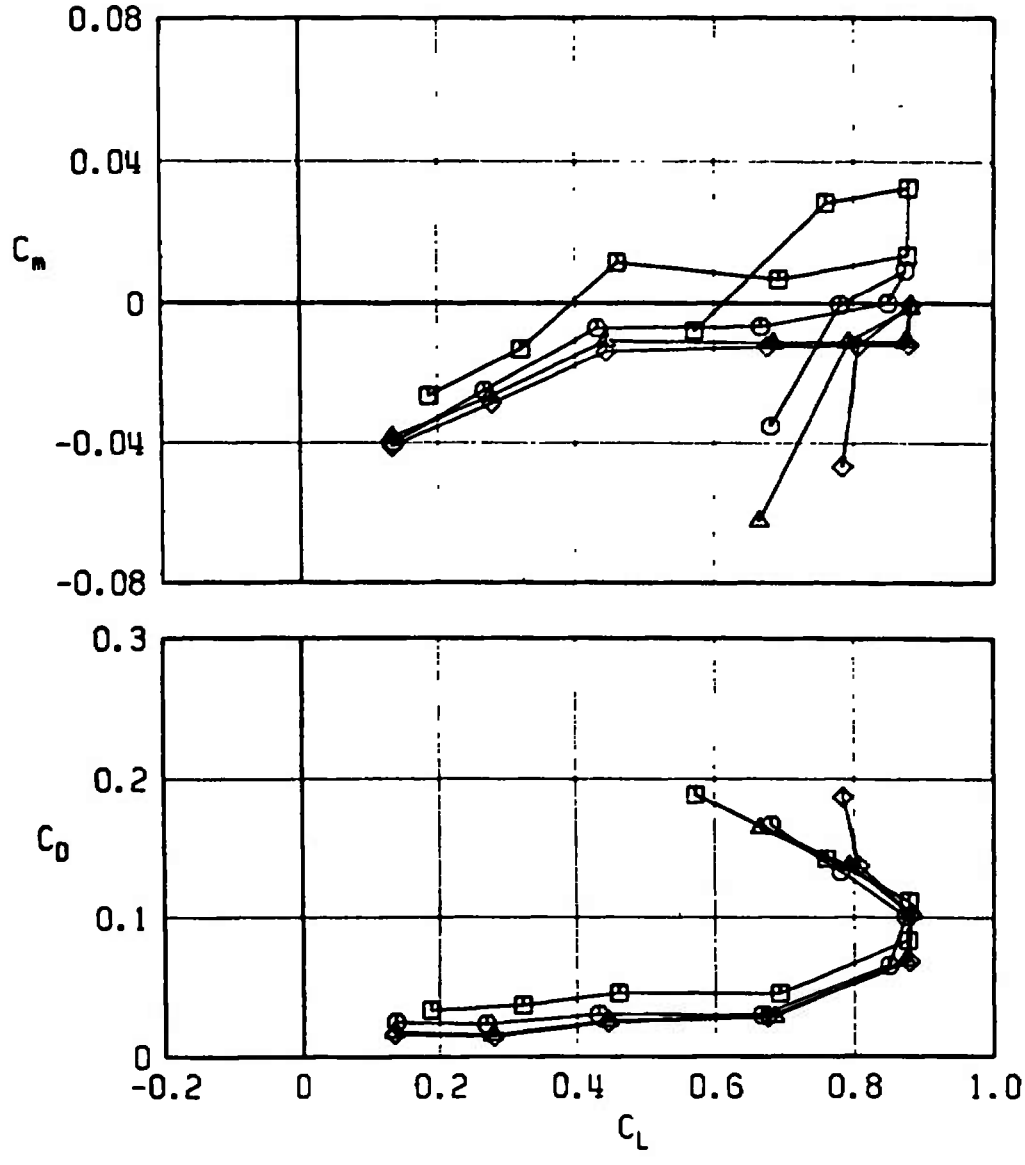

Fig. 27 Concluded

SYMBOL	M_∞	PYLON	STORE	LOC
⊡	0.80	B	NONE	0.00
⊙	0.80	B	NONE	0.25
△	0.80	B	NONE	0.50
◇	0.80	B	NONE	0.75

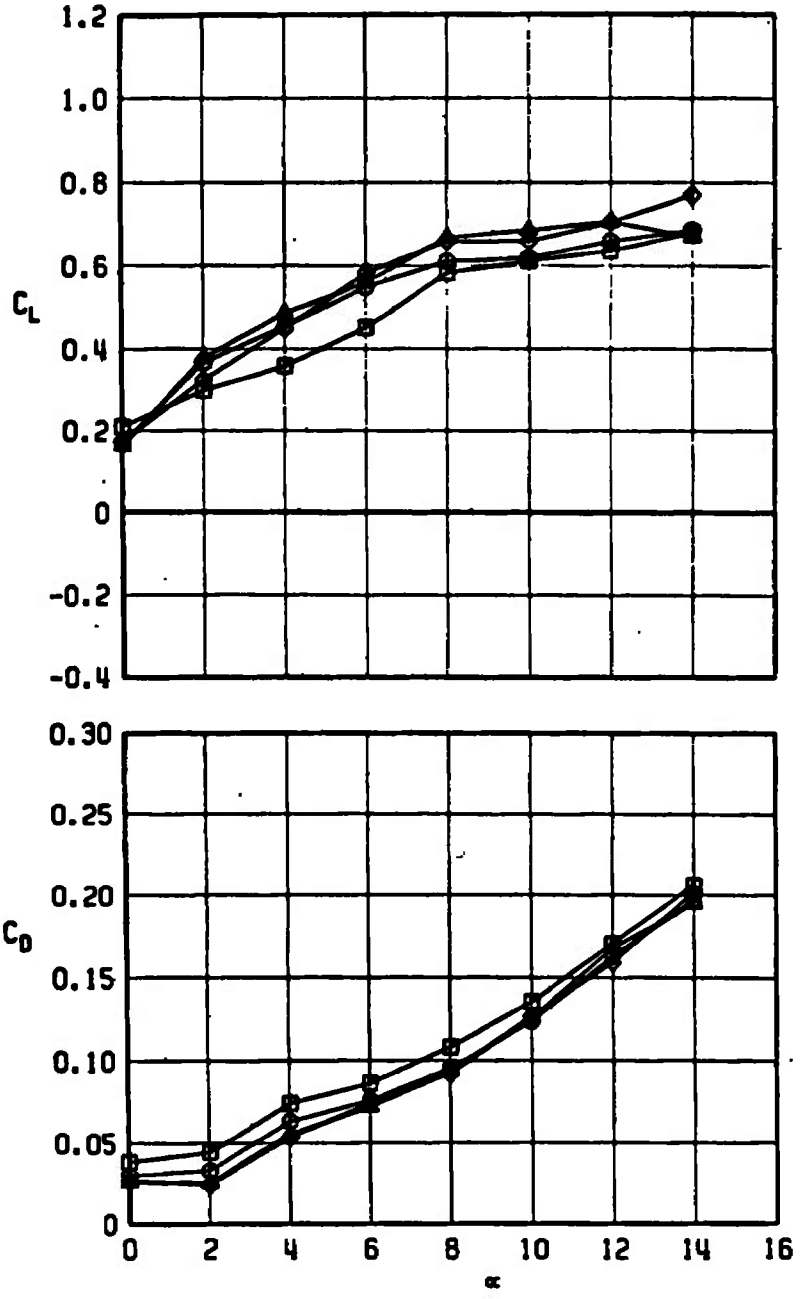

Fig. 28 Effect of Spanwise Location of the B Pylon on the Lift, Drag, and Pitching-Moment Coefficients of the Airfoil, $M_\infty = 0.8$

SYMBOL	M_∞	PYLON	STORE	LOC
□	0.80	B	NONE	0.00
○	0.80	B	NONE	0.25
△	0.80	B	NONE	0.50
◇	0.80	B	NONE	0.75

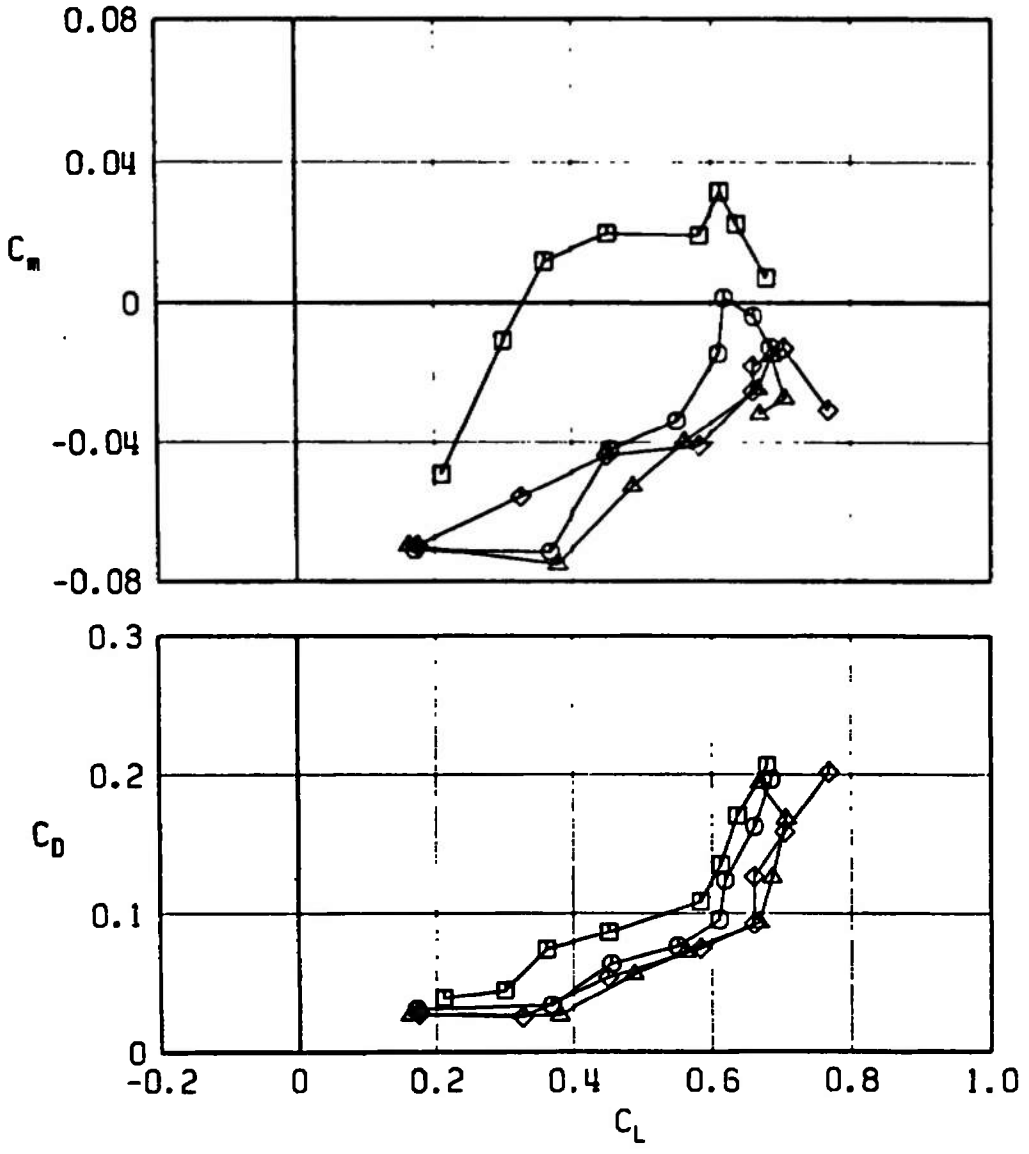

Fig. 28 Concluded

SYMBOL	M_∞	PYLON	STORE	LOC
□	0.85	B	NONE	0.00
○	0.85	B	NONE	0.25
△	0.85	B	NONE	0.50
◇	0.85	B	NONE	0.75

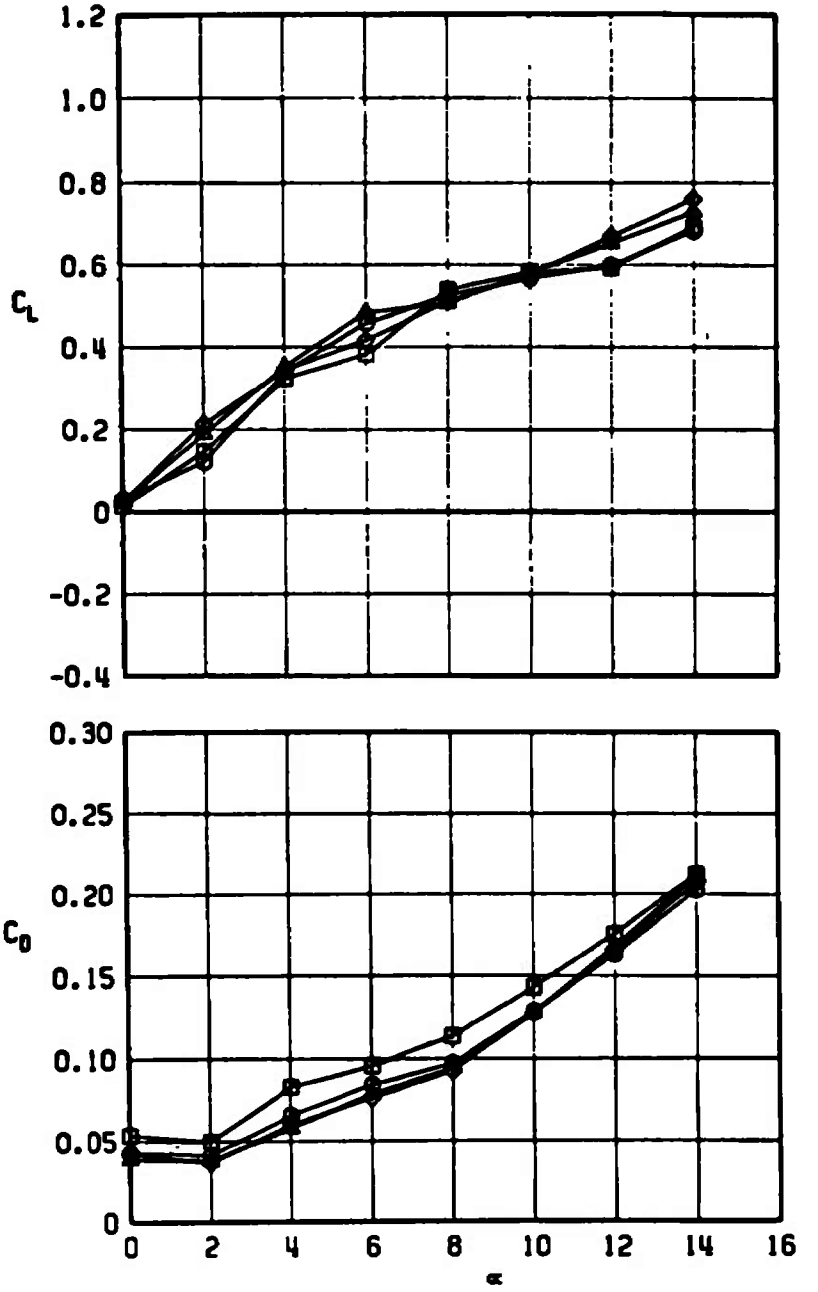

Fig. 29 Effect of Spanwise Location of the B Pylon on the Lift, Drag, and Pitching-Moment Coefficients of the Airfoil, $M_\infty = 0.85$

SYMBOL	M_∞	PYLON	STORE	LOC
□	0.85	B	NONE	0.00
○	0.85	B	NONE	0.25
△	0.85	B	NONE	0.50
◇	0.85	B	NONE	0.75

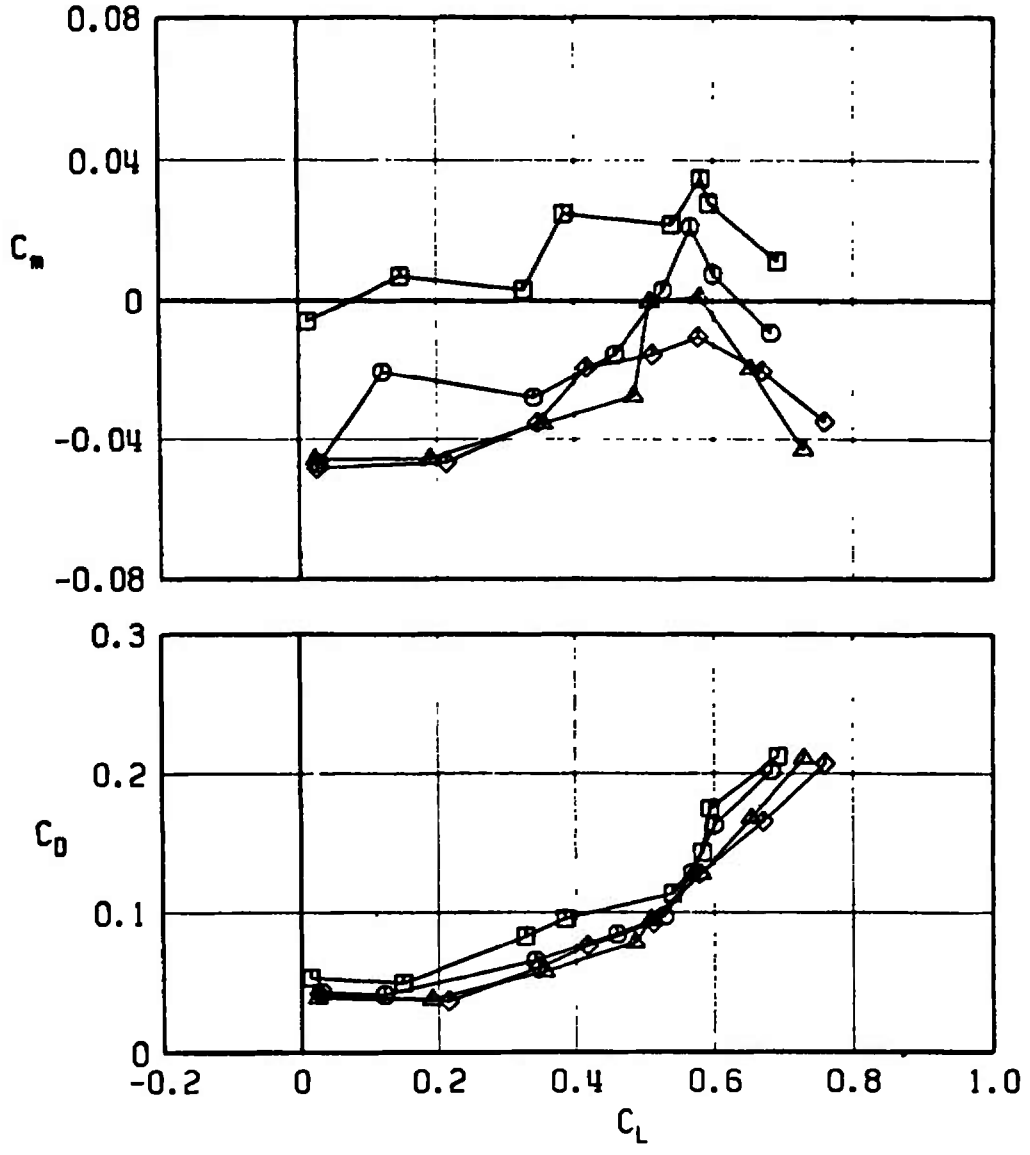

Fig. 29 Concluded

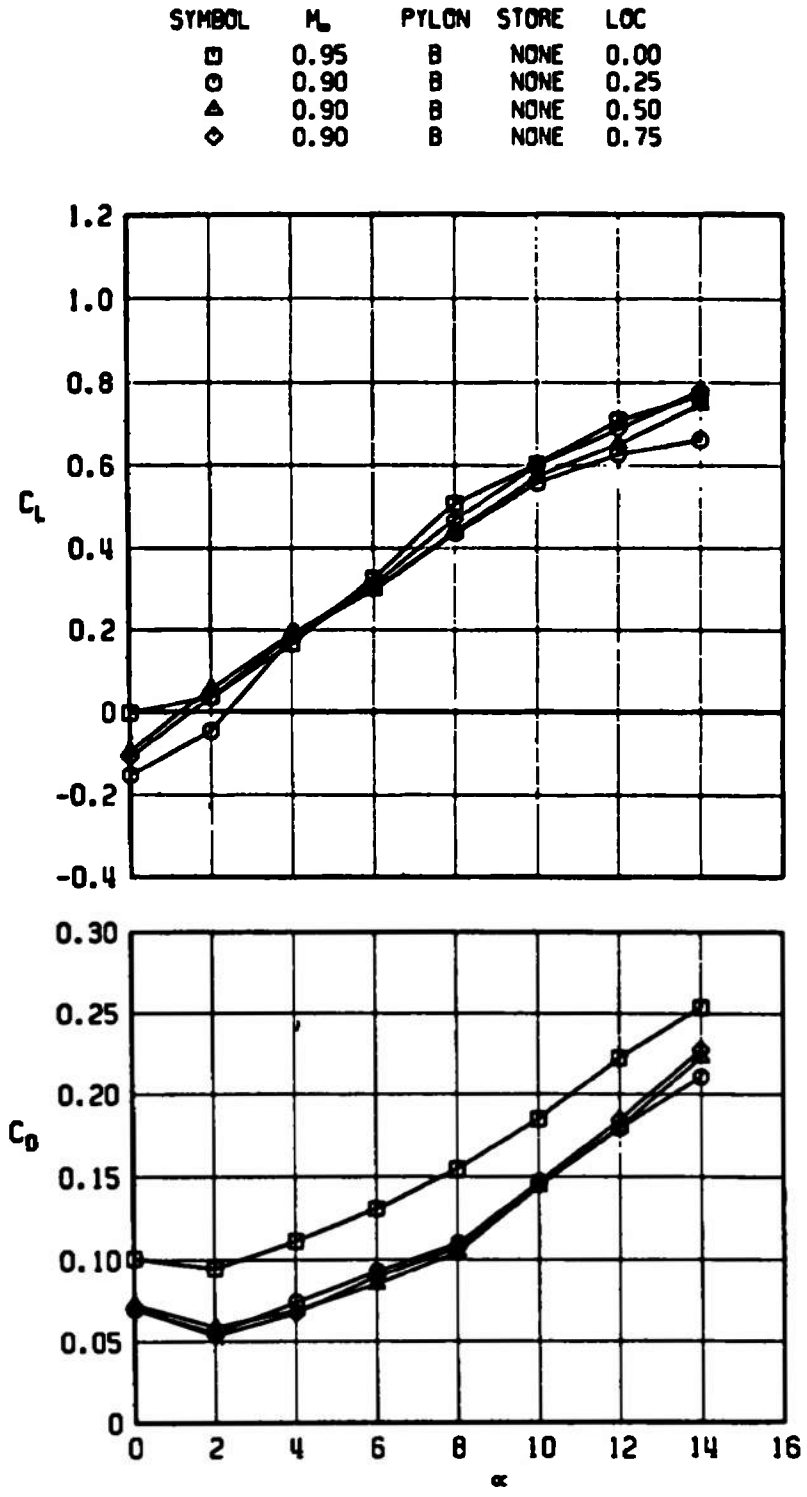

Fig. 30 Effect of Spanwise Location of the B Pylon on the Lift, Drag, and Pitching-Moment Coefficients of the Airfoil, $M_\infty = 0.9$

SYMBOL	M_∞	PYLON	STORE	LOC
□	0.95	B	NONE	0.00
○	0.90	B	NONE	0.25
△	0.90	B	NONE	0.50
◇	0.90	B	NONE	0.75

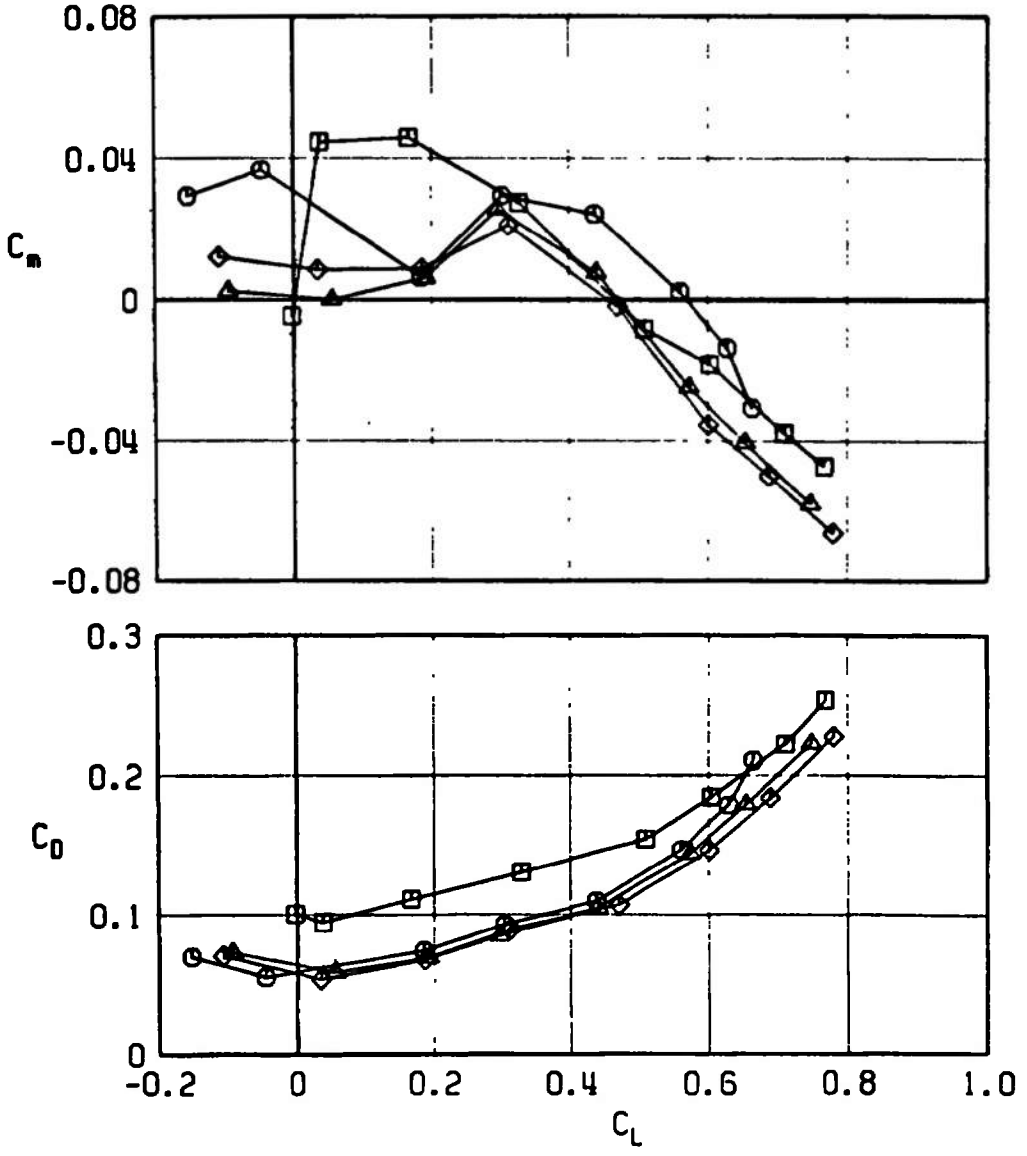

Fig. 30 Concluded

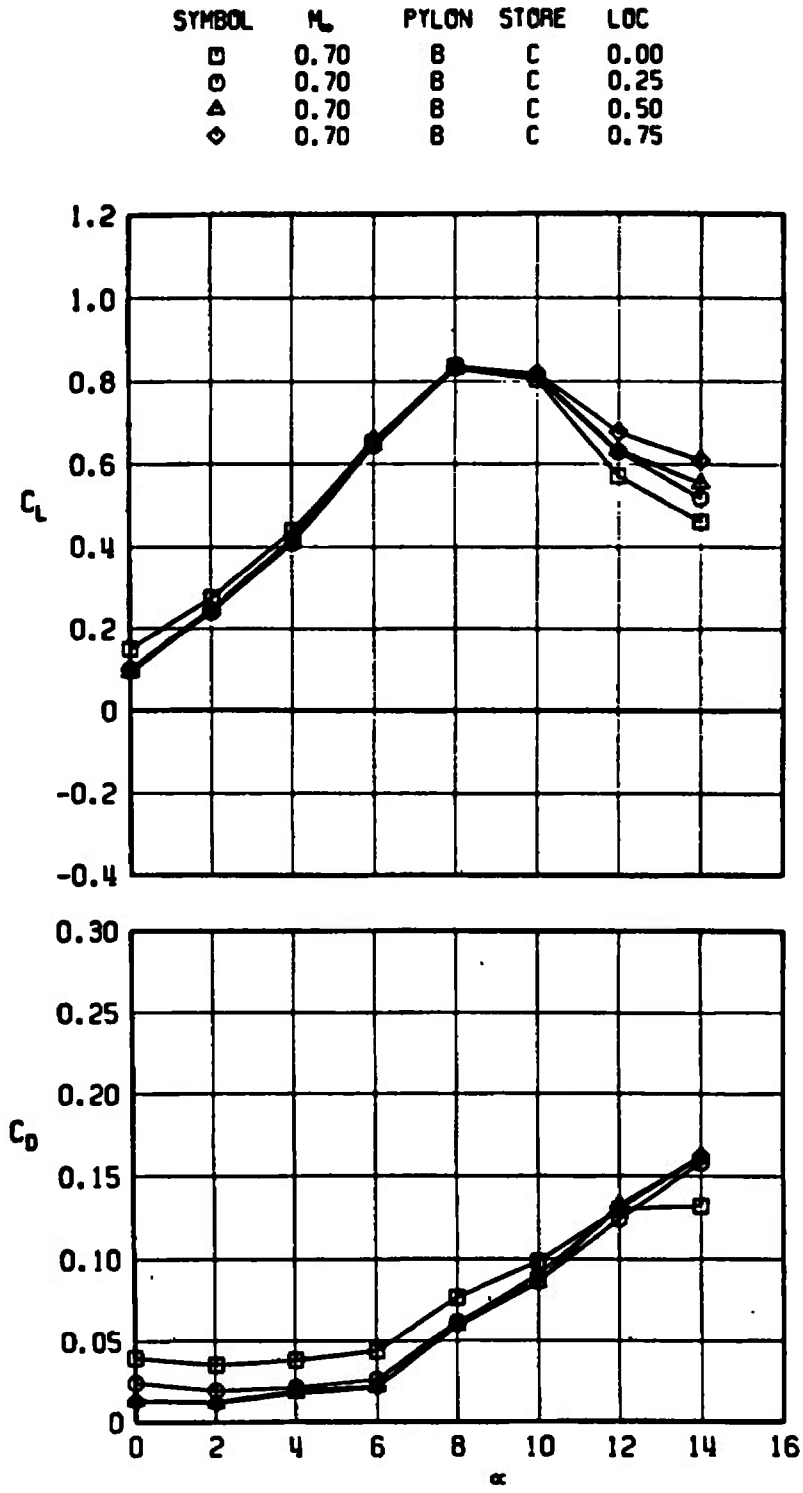

Fig. 31 Effect of Spanwise Location of the B Pylon with C Store on the Lift, Drag, and Pitching-Moment Coefficients of the Airfoil, M_∞ = 0.7

SYMBOL	M_∞	PYLON	STORE	LOC
□	0.70	B	C	0.00
○	0.70	B	C	0.25
△	0.70	B	C	0.50
◇	0.70	B	C	0.75

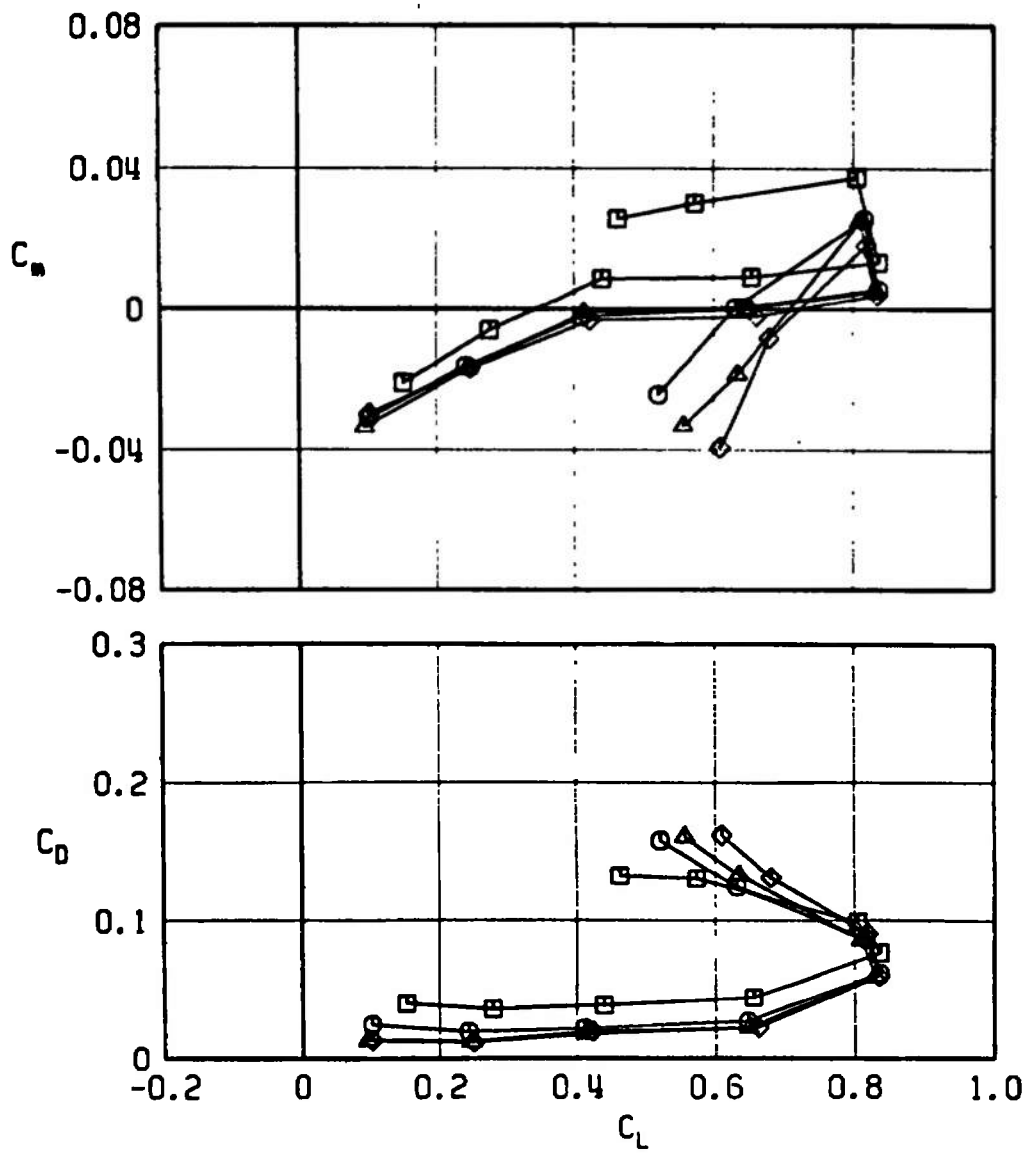

Fig. 31 Concluded

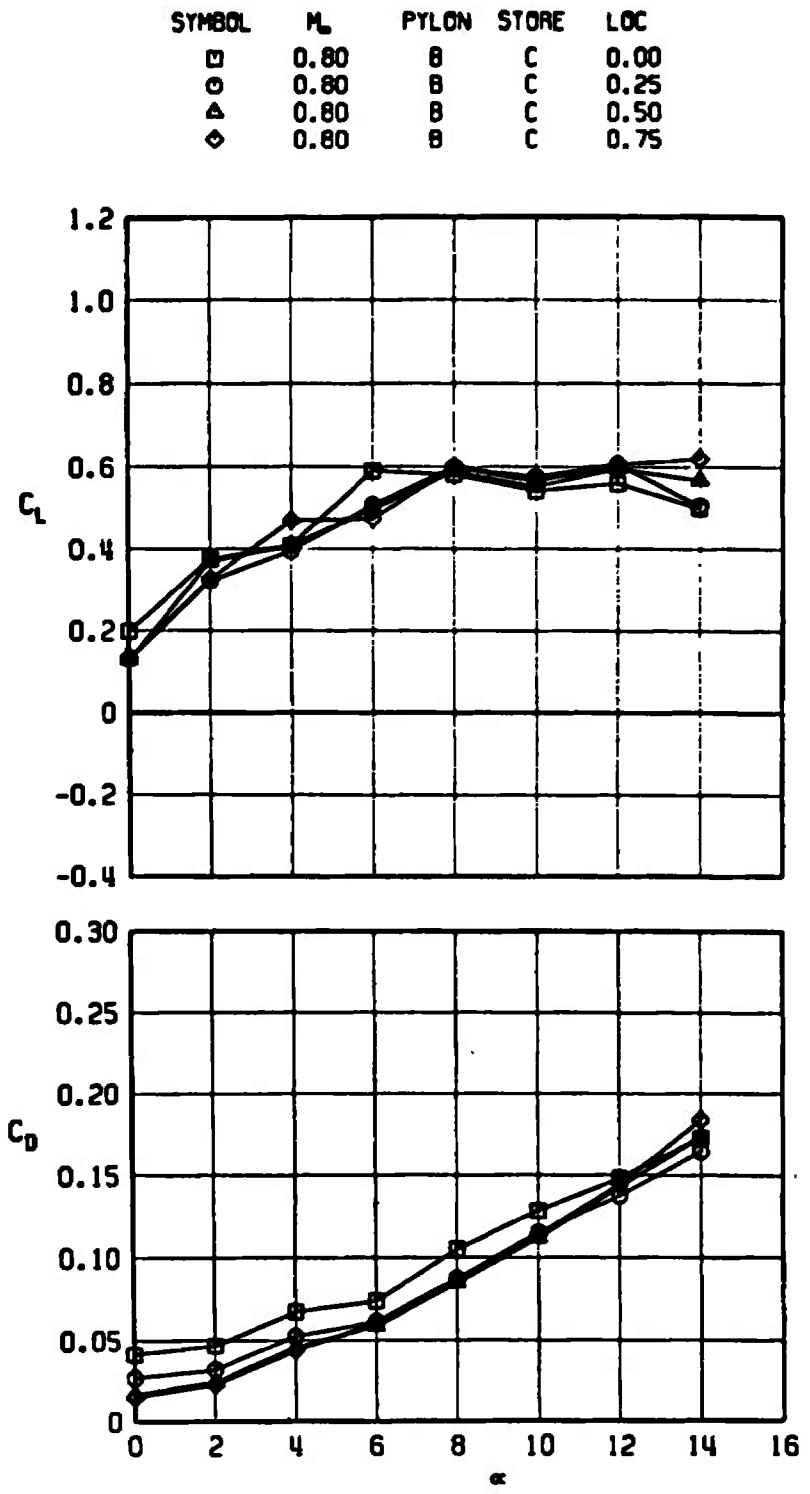

Fig. 32 Effect of Spanwise Location of the B Pylon with C Store on the Lift, Drag, and Pitching-Moment Coefficients of the Airfoil, M_∞ = 0.8

SYMBOL	M_∞	PYLON	STORE	LOC	
□	0.80	B	C	0.00	48
○	0.80	B	C	0.25	58
△	0.80	B	C	0.50	68
◇	0.80	B	C	0.75	79

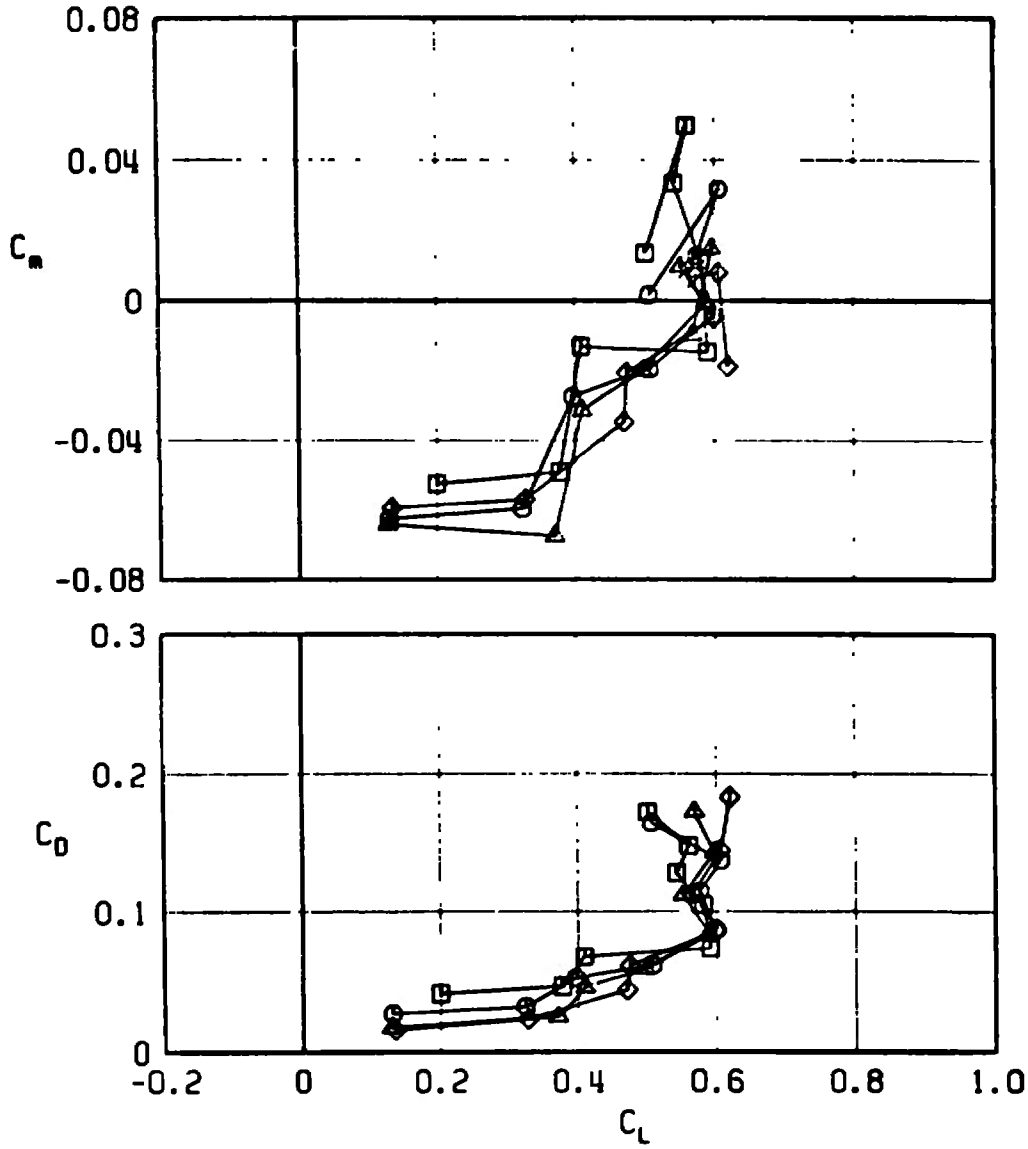

Fig. 32 Concluded

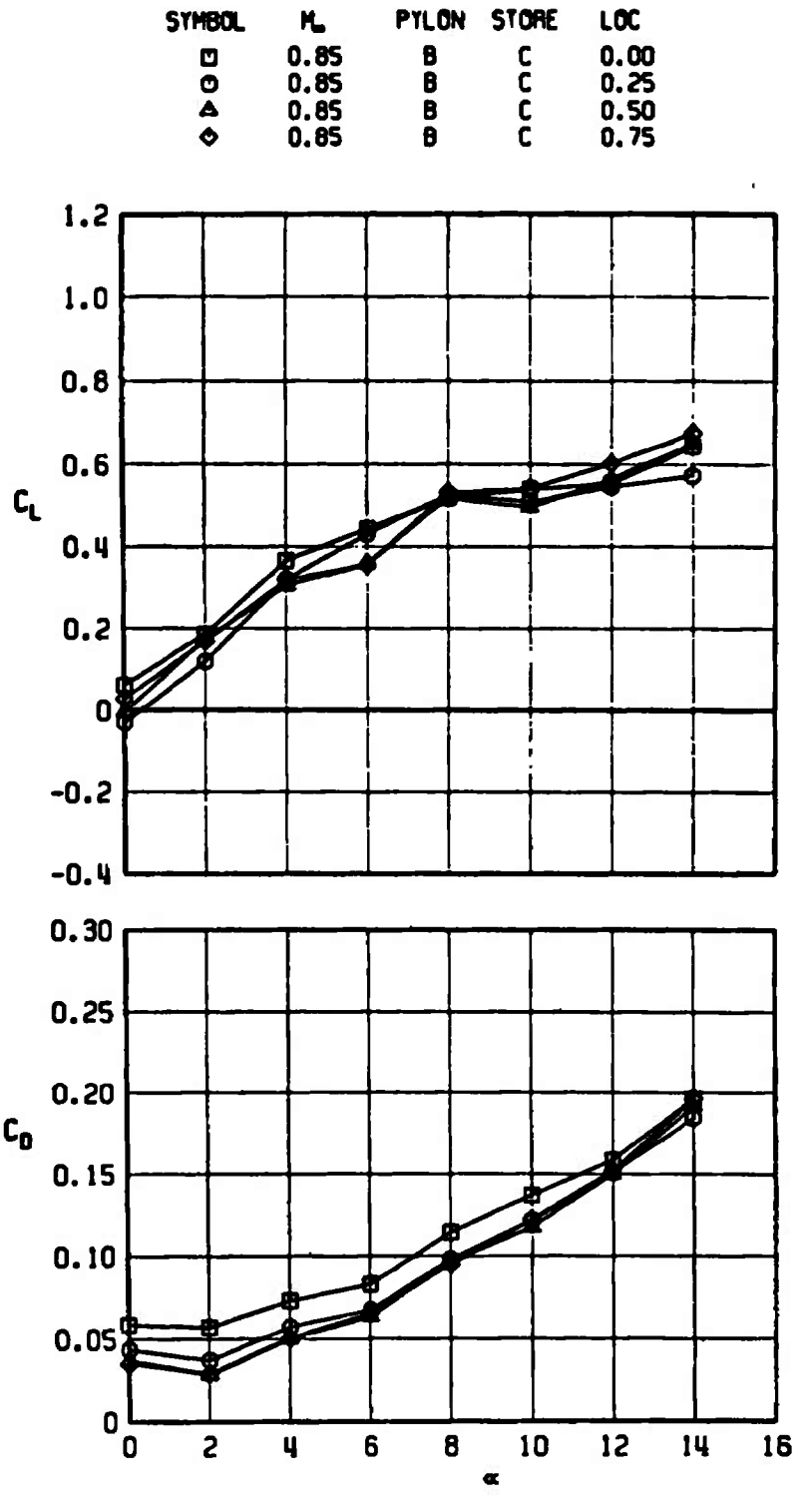

Fig. 33 Effect of Spanwise Location of the B Pylon with C Store on the Lift, Drag, and Pitching-Moment Coefficients of the Airfoil, $M_\infty = 0.85$

SYMBOL	M_∞	PYLON	STORE	LOC
□	0.85	B	C	0.00
○	0.85	B	C	0.25
△	0.85	B	C	0.50
◇	0.85	B	C	0.75

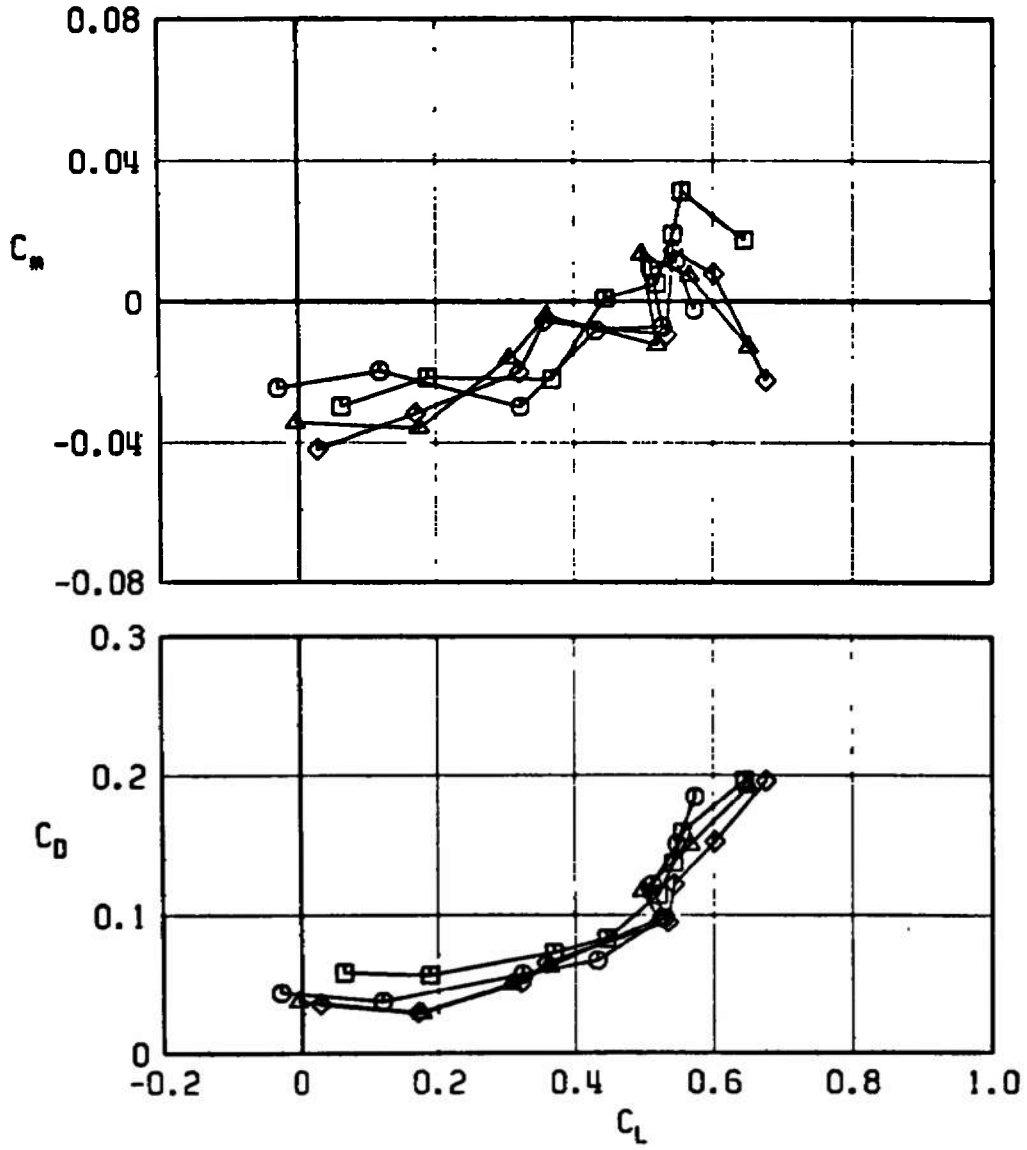

Fig. 33 Concluded

SYMBOL	M_∞	PYLON	STORE	LOC
□	0.90	B	C	0.00
○	0.90	B	C	0.25
△	0.90	B	C	0.50
◇	0.90	B	C	0.75

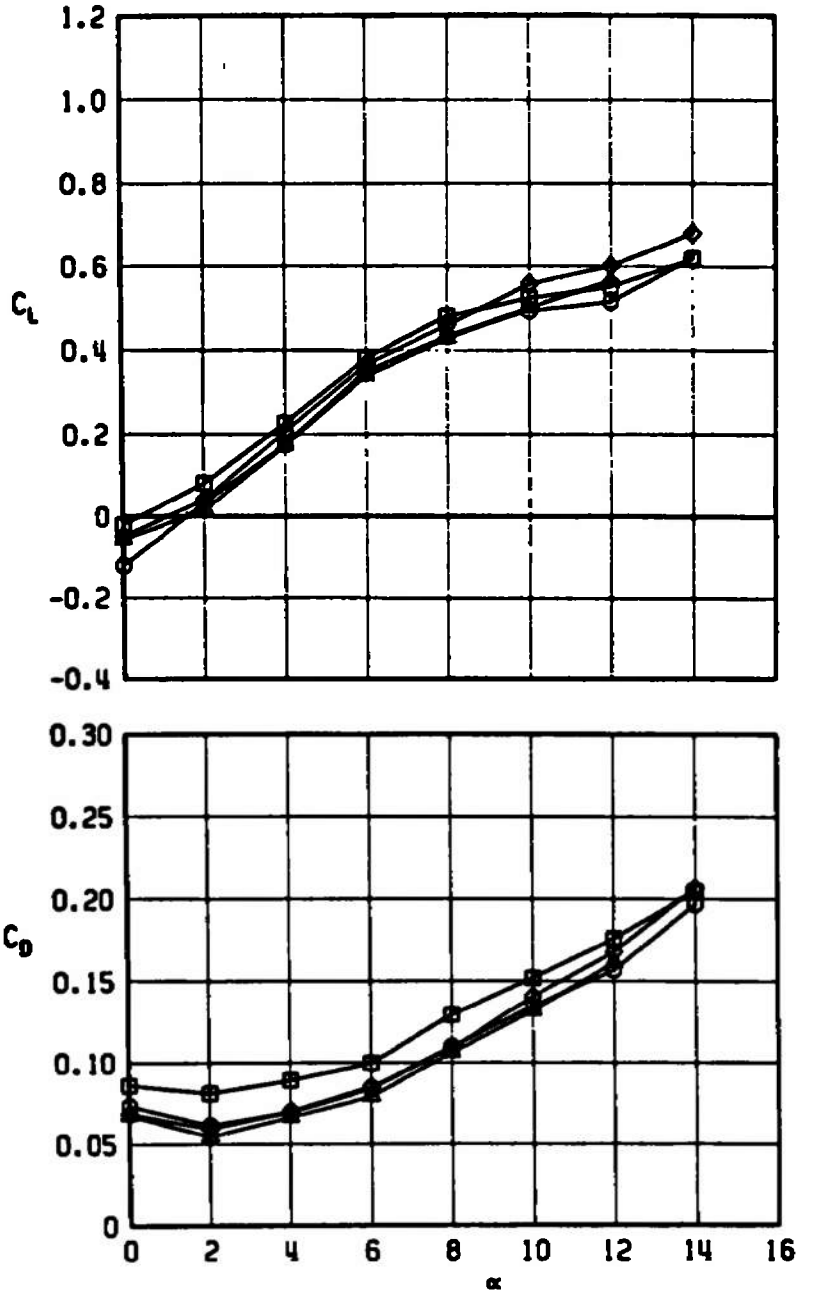

Fig. 34 Effect of Spanwise Location of the B Pylon with C Store on the Lift, Drag, and Pitching-Moment Coefficients of the Airfoil, M_∞ = 0.9

SYMBOL	M_∞	PYLON	STORE	LOC
□	0.90	B	C	0.00
○	0.90	B	C	0.25
△	0.90	B	C	0.50
◇	0.90	B	C	0.75

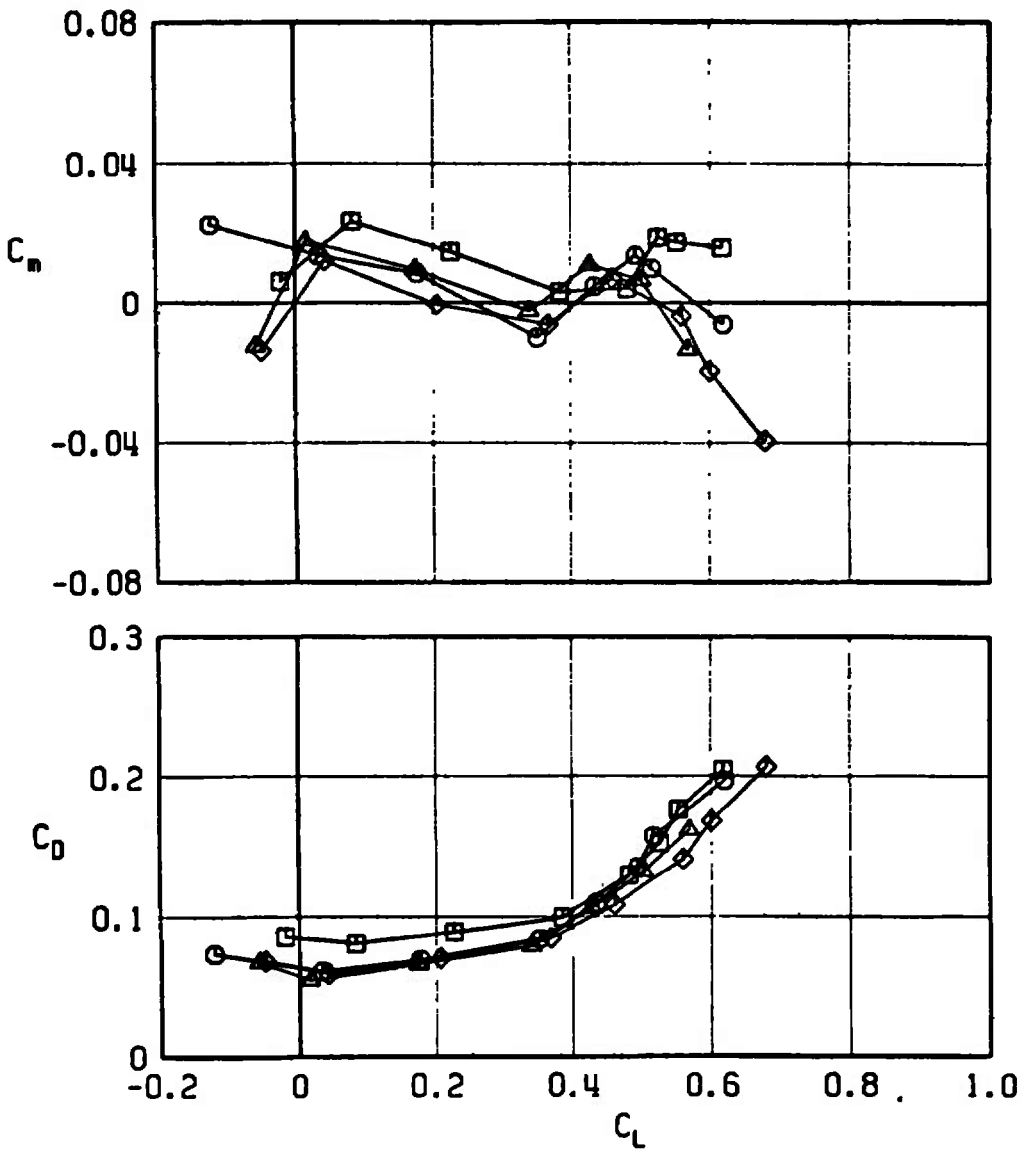

Fig. 34 Concluded

SYMBOL	M_∞	PYLON	STORE	LOC
□	0.70	A	NONE	0.25
○	0.70	B	NONE	0.25
△	0.70	C	NONE	0.25
◇	0.70	D	NONE	0.25

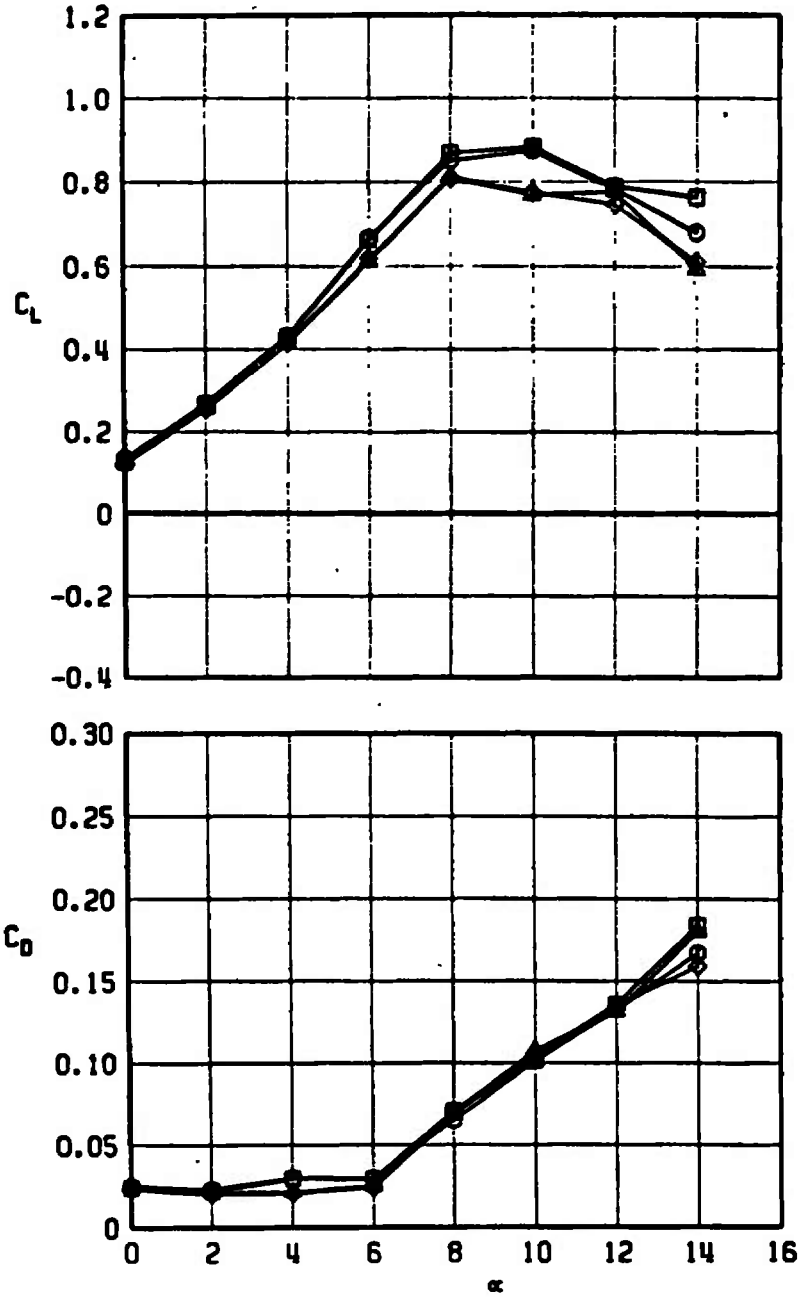

Fig. 35 Effect of Different Pylons on the Lift, Drag, and Pitching-Moment Coefficients of the Airfoil, $M_\infty = 0.7$

SYMBOL	M_∞	PYLON	STORE	LOC
□	0.70	A	NONE	0.25
○	0.70	B	NONE	0.25
△	0.70	C	NONE	0.25
◇	0.70	D	NONE	0.25

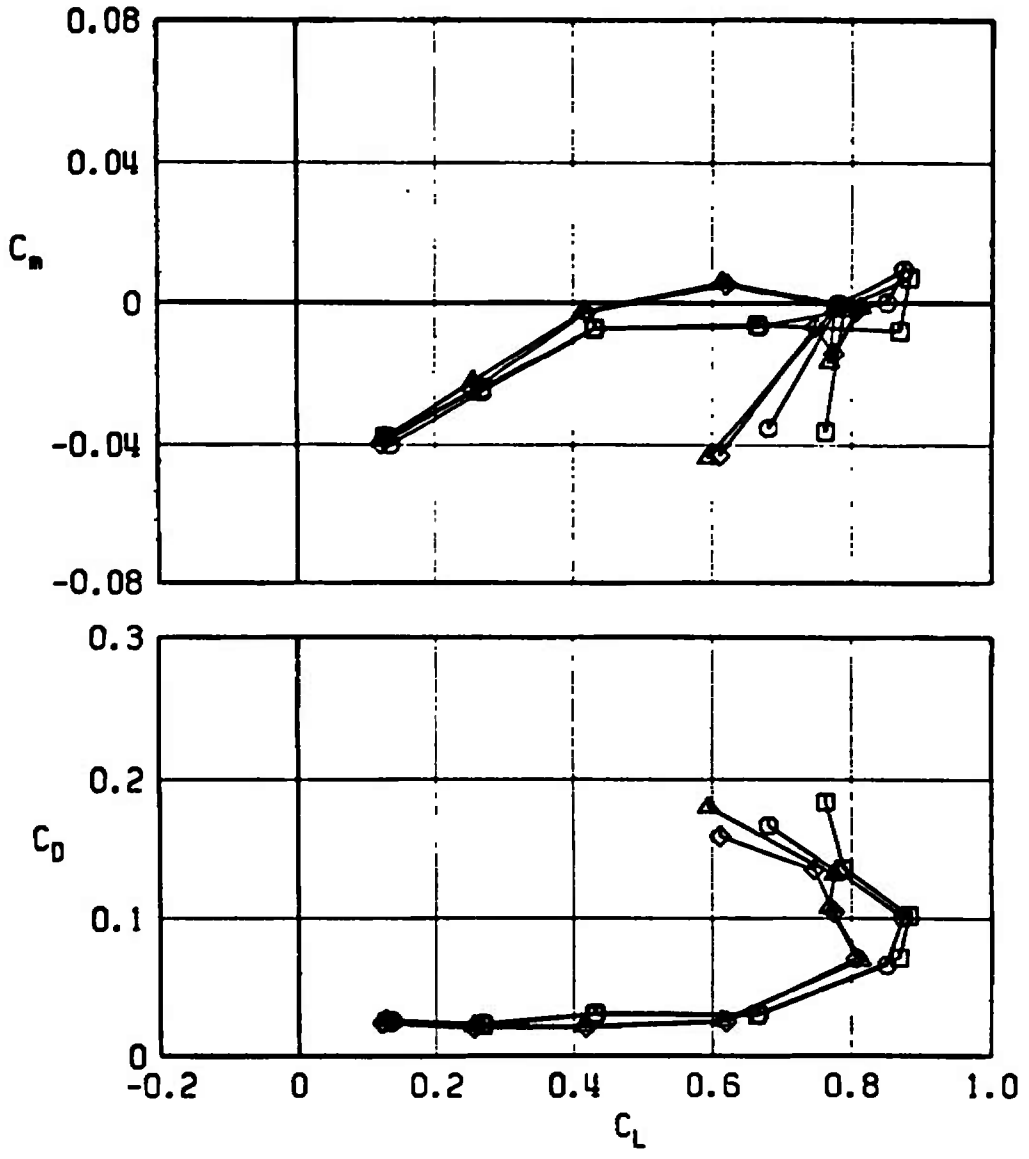

Fig. 35 Concluded

SYMBOL	M_∞	PYLON	STORE	LOC
⊡	0.80	A	NONE	0.25
⊙	0.80	B	NONE	0.25
△	0.80	C	NONE	0.25
◇	0.80	D	NONE	0.25

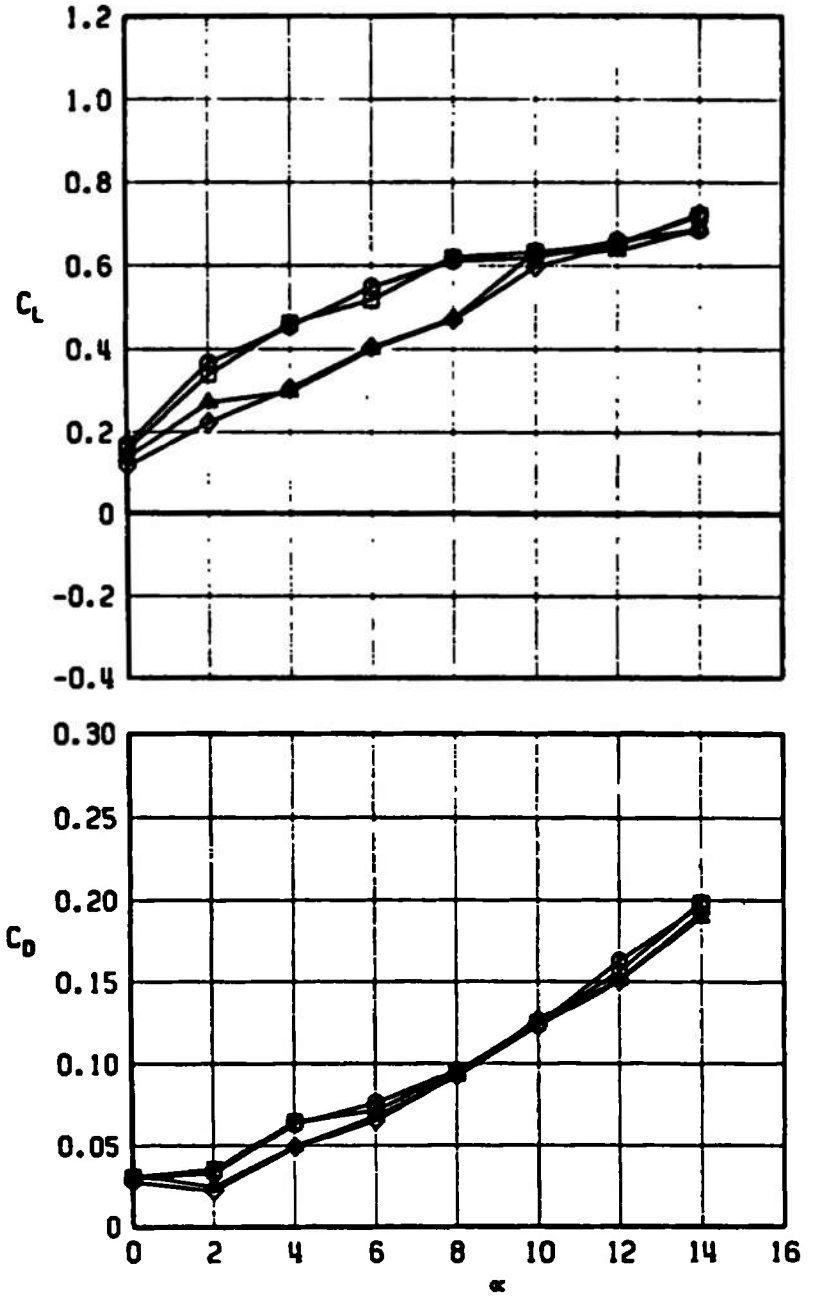

Fig. 36 Effect of Different Pylons on the Lift, Drag, and Pitching-Moment Coefficients of the Airfoil, $M_\infty = 0.8$

SYMBOL	M_∞	PYLON	STORE	LOC
□	0.80	A	NONE	0.25
○	0.80	B	NONE	0.25
△	0.80	C	NONE	0.25
◇	0.80	D	NONE	0.25

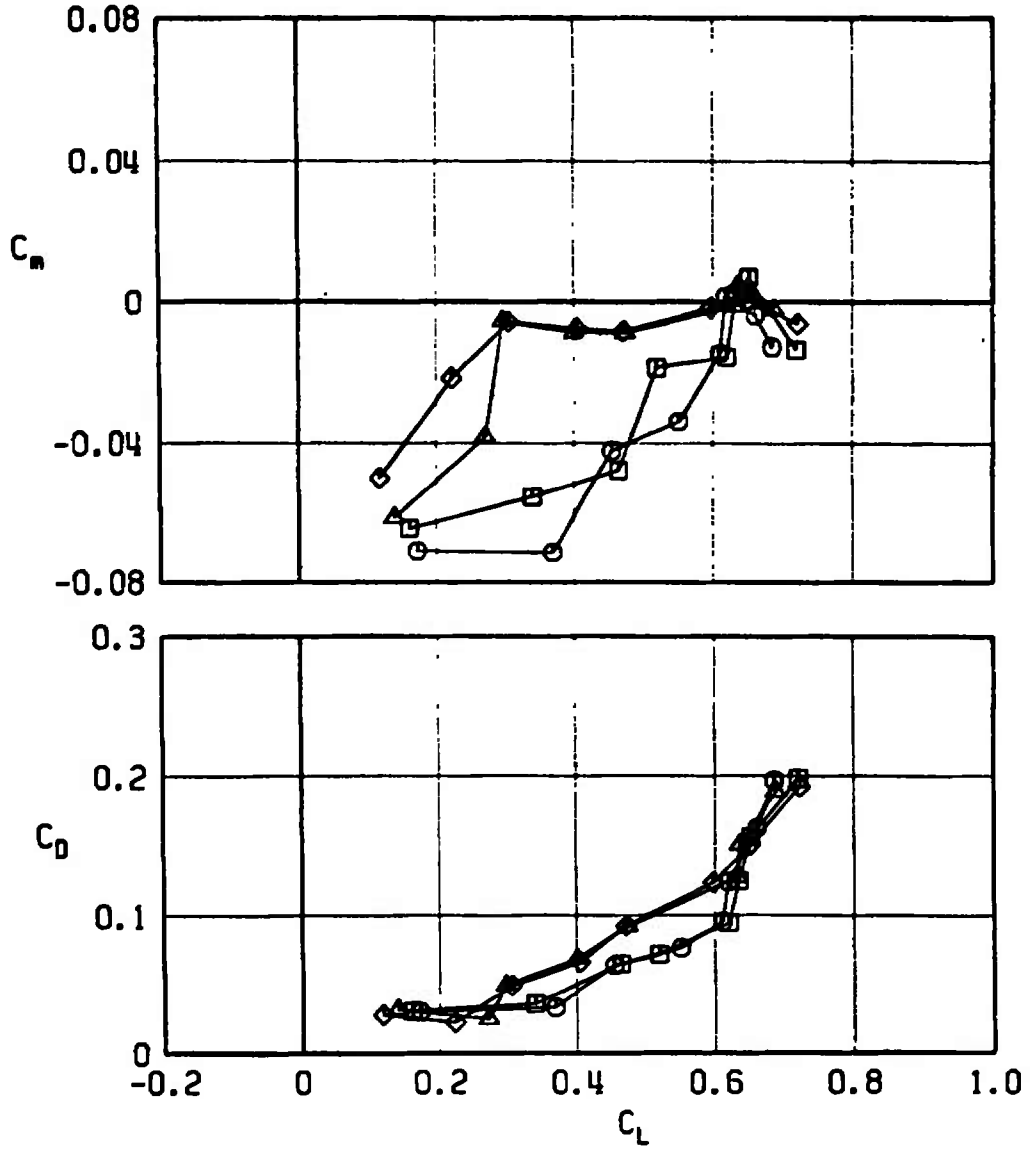

Fig. 36 Concluded

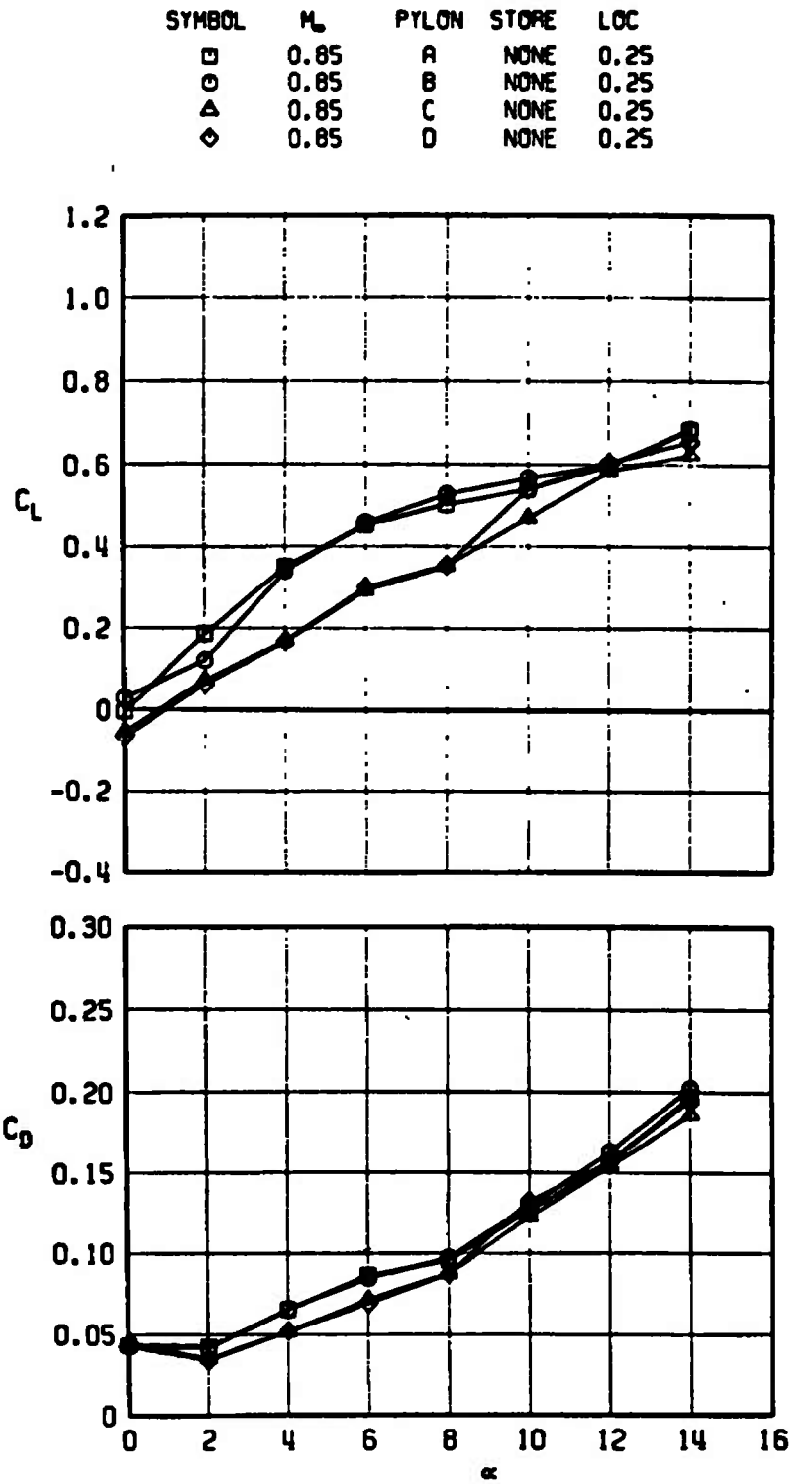

Fig. 37 Effect of Different Pylons on the Lift, Drag, and Pitching-Moment Coefficients of the Airfoil, $M_\infty = 0.85$

SYMBOL	M_∞	PYLON	STORE	LOC
□	0.85	A	NONE	0.25
○	0.85	B	NONE	0.25
△	0.85	C	NONE	0.25
◇	0.85	D	NONE	0.25

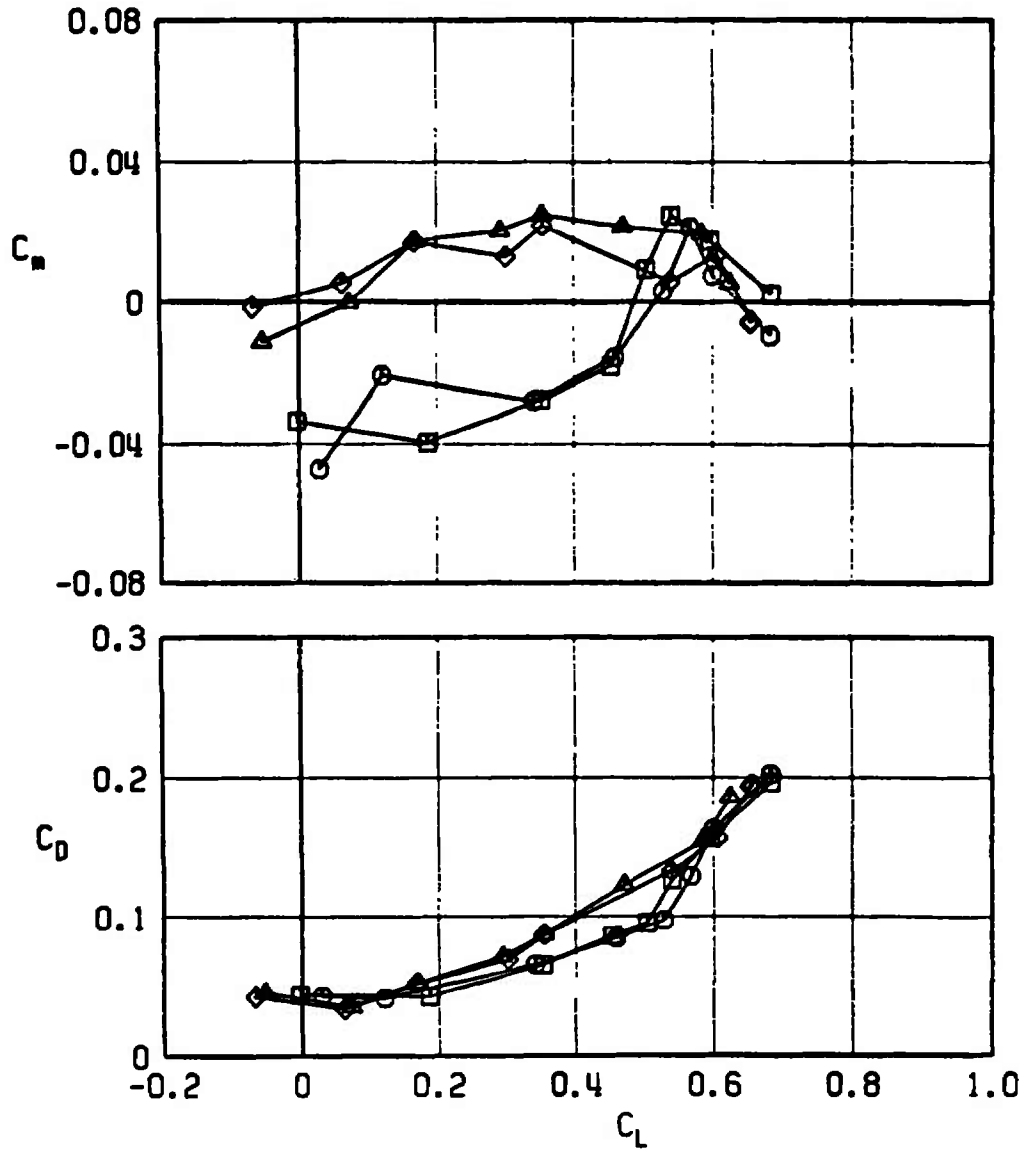

Fig. 37 Concluded

SYMBOL	M_∞	PYLON	STORE	LOC
□	0.90	A	NONE	0.25
○	0.90	B	NONE	0.25
△	0.90	C	NONE	0.25
◇	0.90	D	NONE	0.25

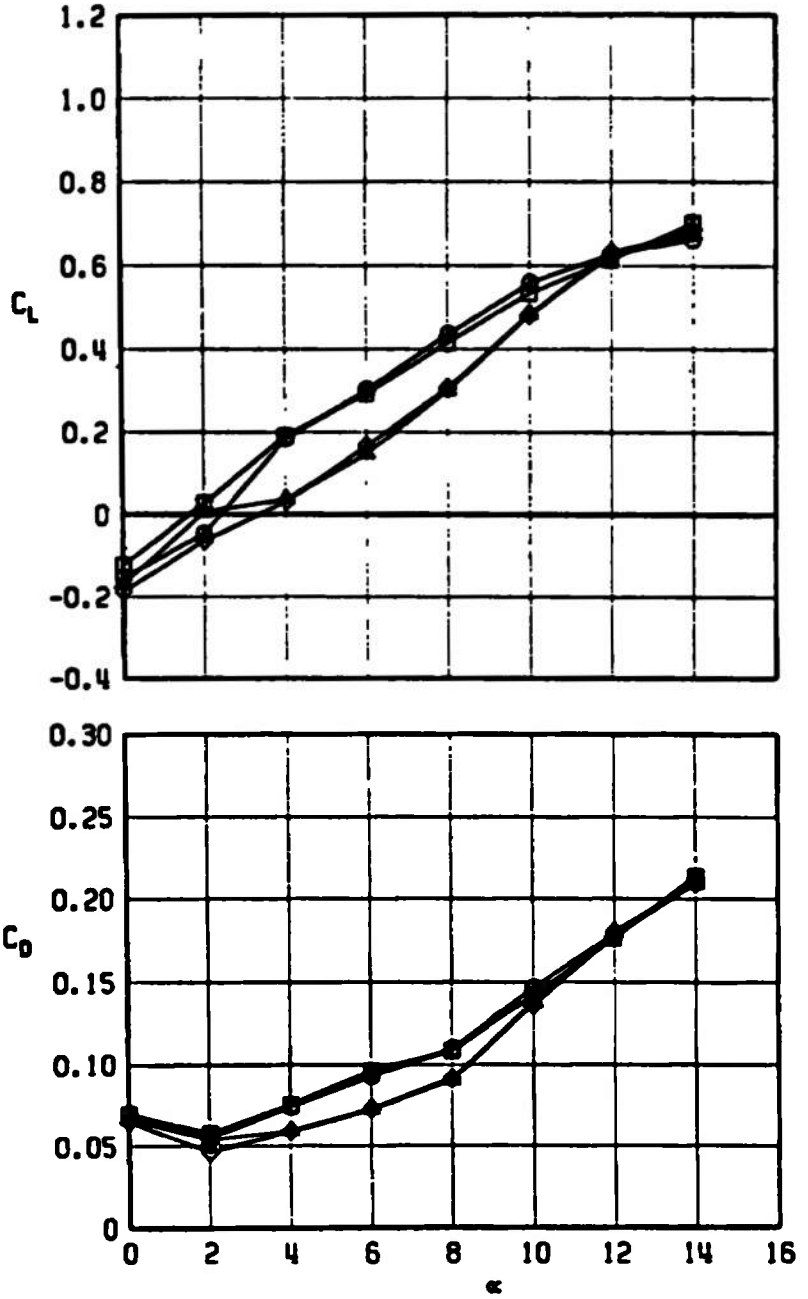

Fig. 38 Effect of Different Pylons on the Lift, Drag, and Pitching-Moment Coefficients of the Airfoil, M_∞ = 0.9

SYMBOL	M_∞	PYLON	STORE	LOC
□	0.90	A	NONE	0.25
○	0.90	B	NONE	0.25
△	0.90	C	NONE	0.25
◇	0.90	D	NONE	0.25

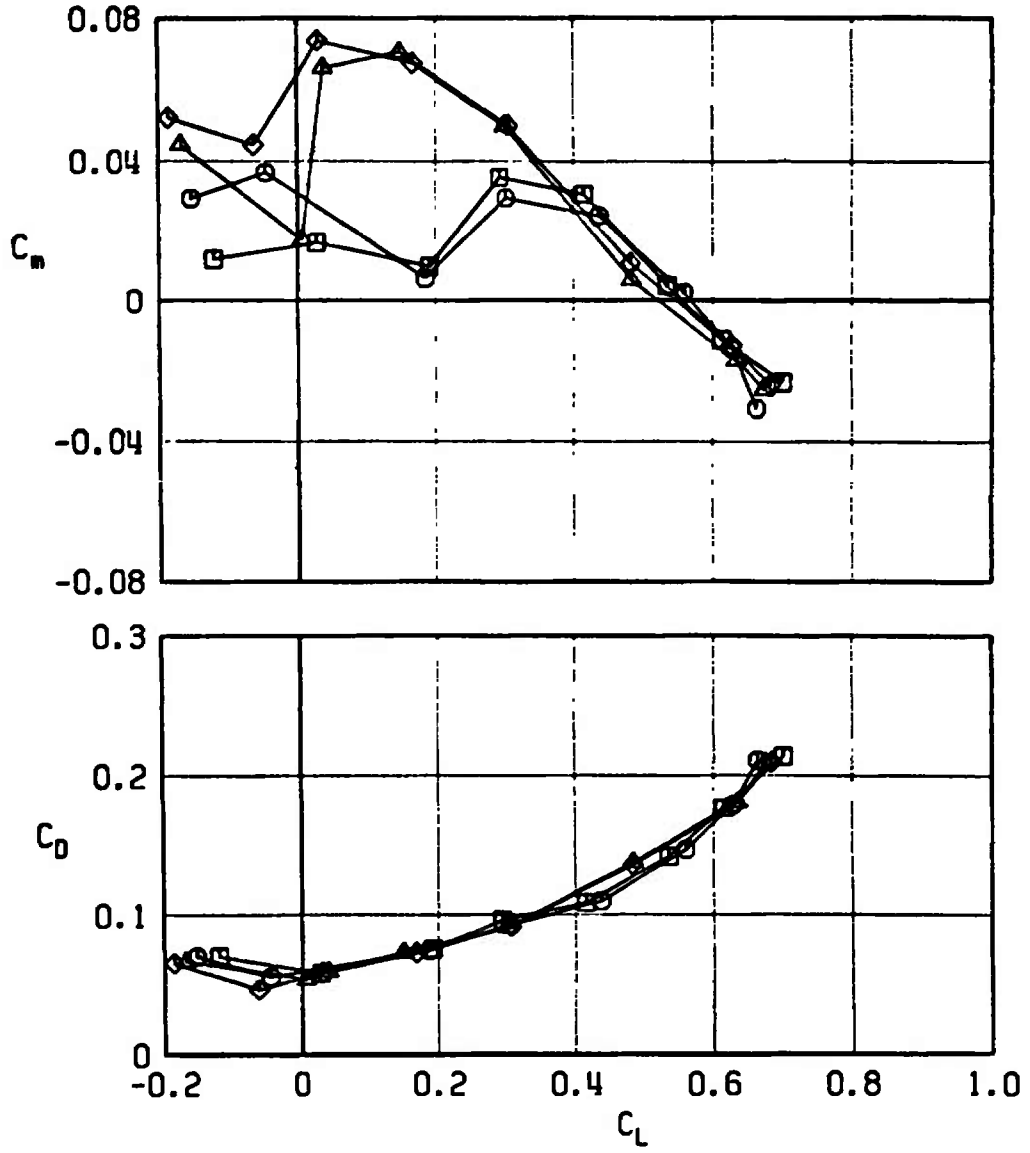

Fig. 38 Concluded

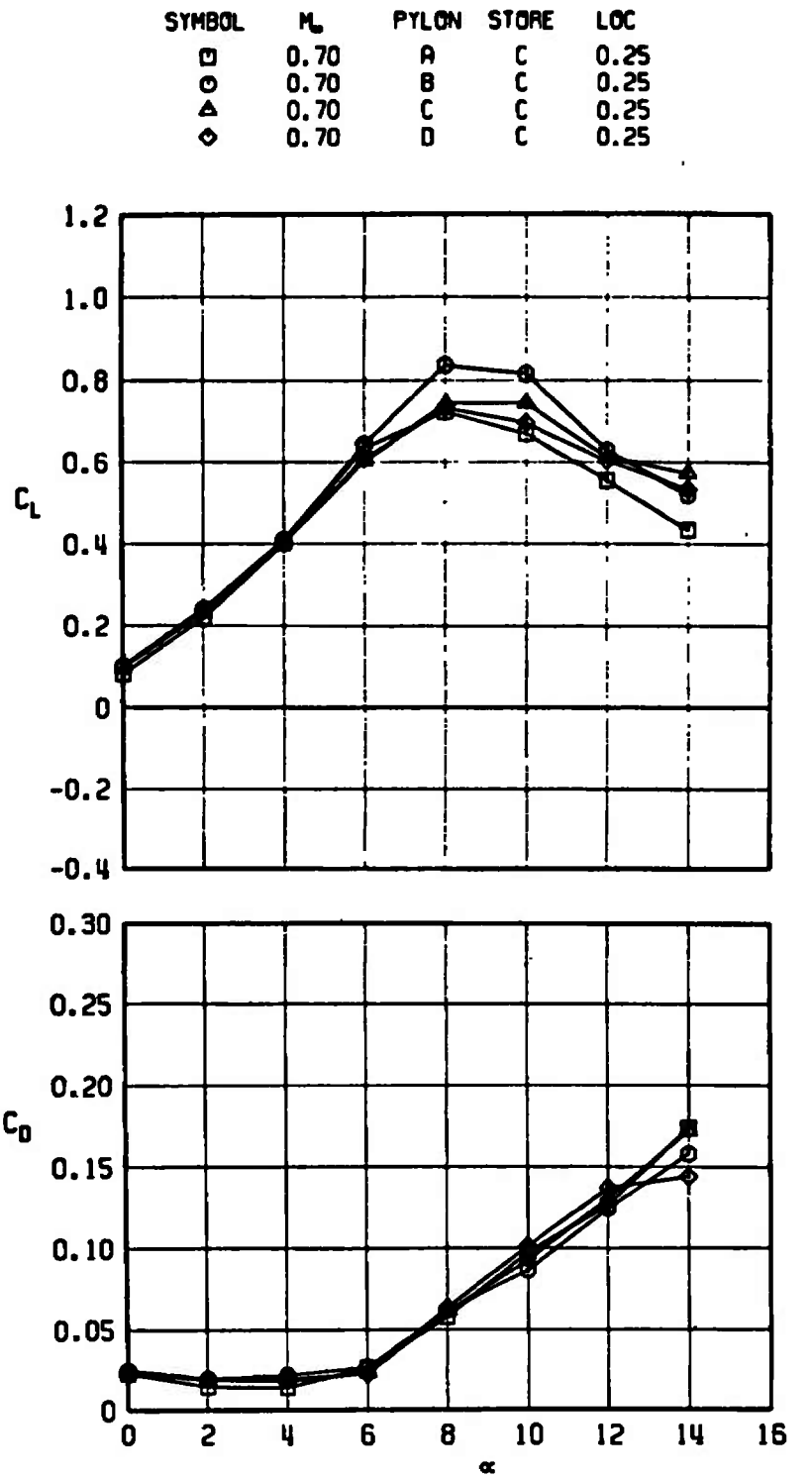

Fig. 39 Effect of Different Pylons with C Store on the Lift, Drag, and Pitching-Moment Coefficients of the Airfoil, $M_\infty = 0.7$

SYMBOL	M_∞	PYLON	STORE	LOC
□	0.70	A	C	0.25
○	0.70	B	C	0.25
△	0.70	C	C	0.25
◇	0.70	D	C	0.25

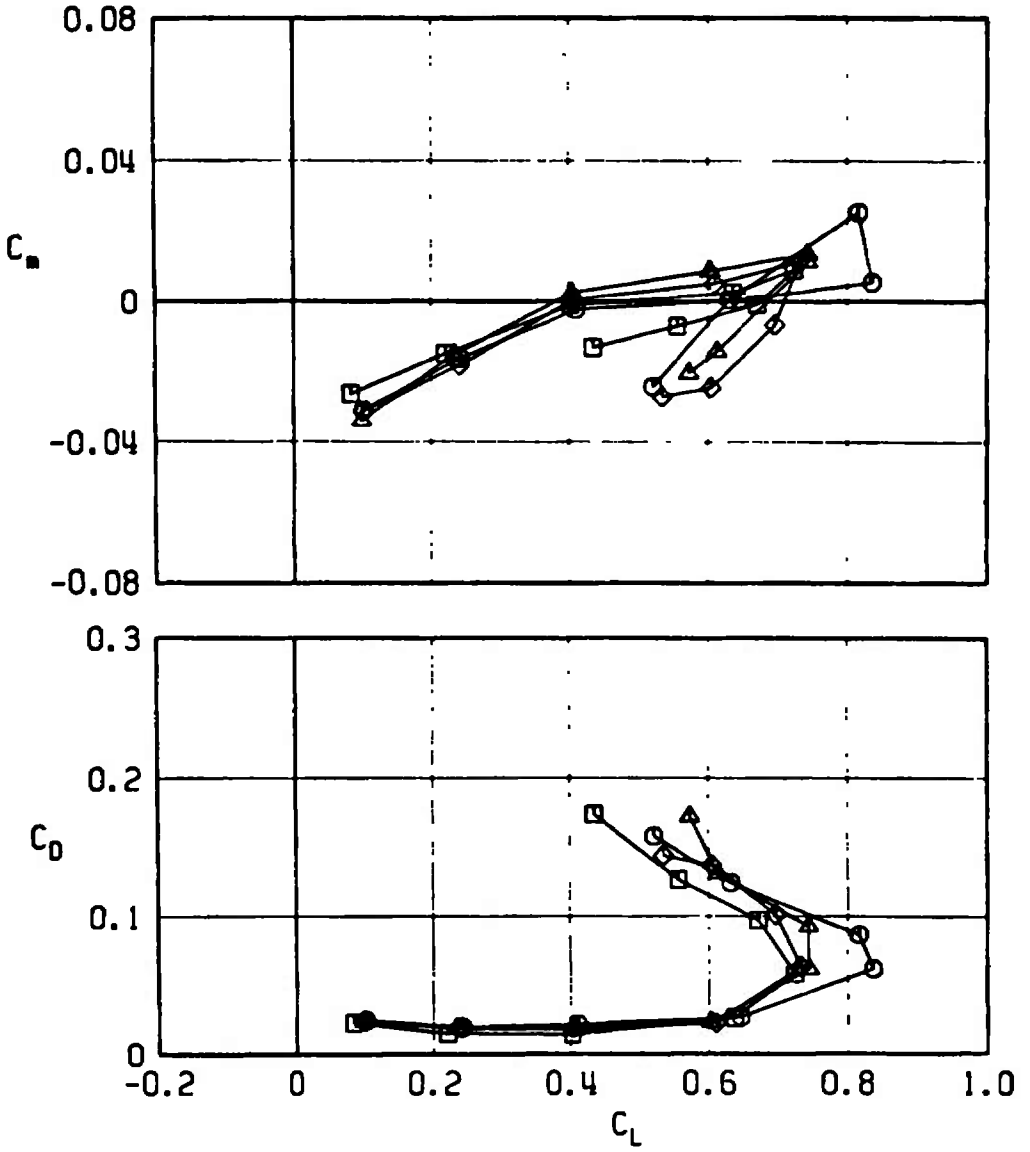

Fig. 39 Concluded

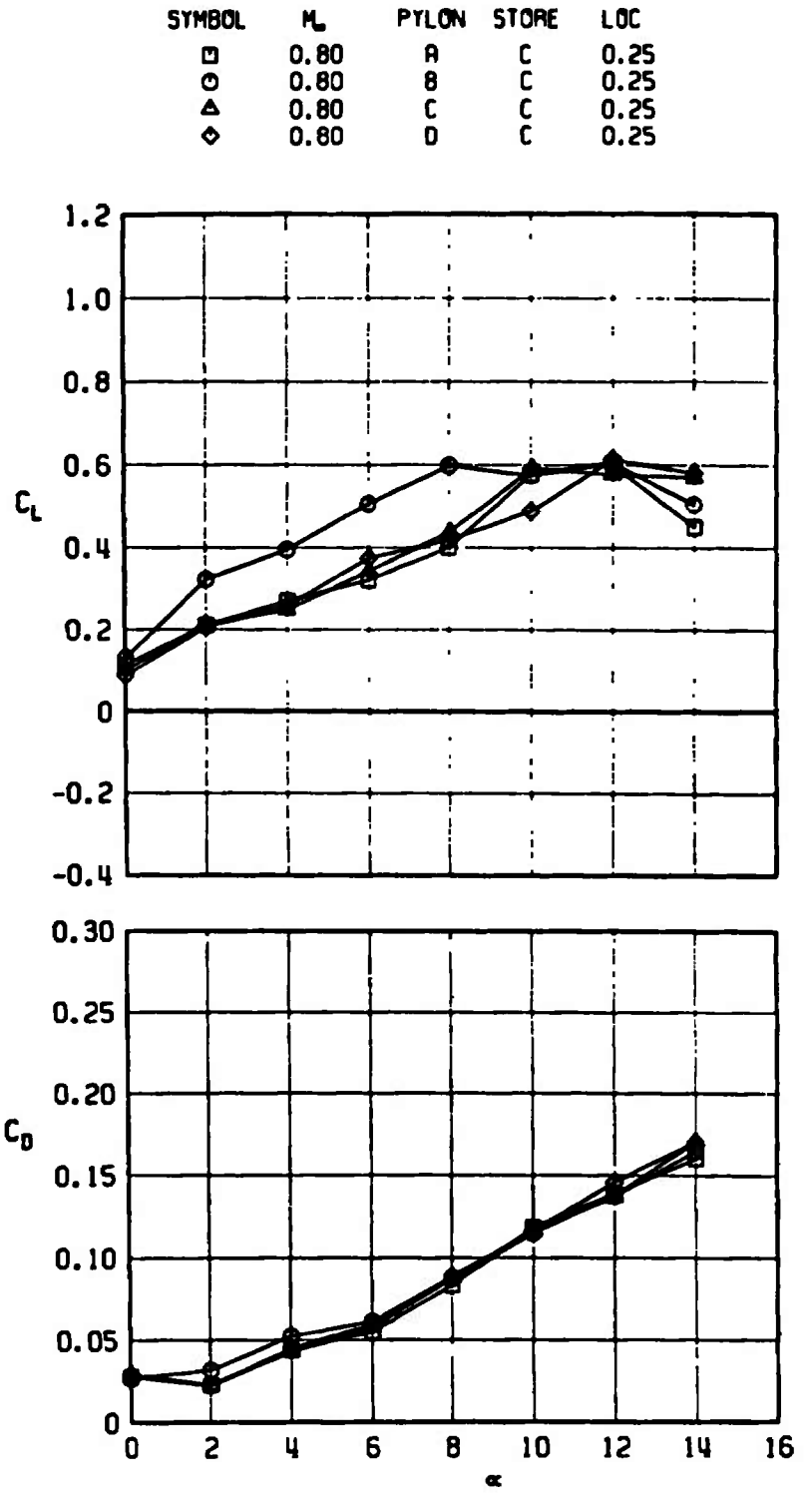

Fig. 40 Effect of Different Pylons with C Store on the Lift, Drag, and Pitching-Moment Coefficients of the Airfoil, $M_\infty = 0.8$

SYMBOL	M_∞	PYLON	STORE	LOC
□	0.80	A	C	0.25
○	0.80	B	C	0.25
△	0.80	C	C	0.25
◇	0.80	D	C	0.25

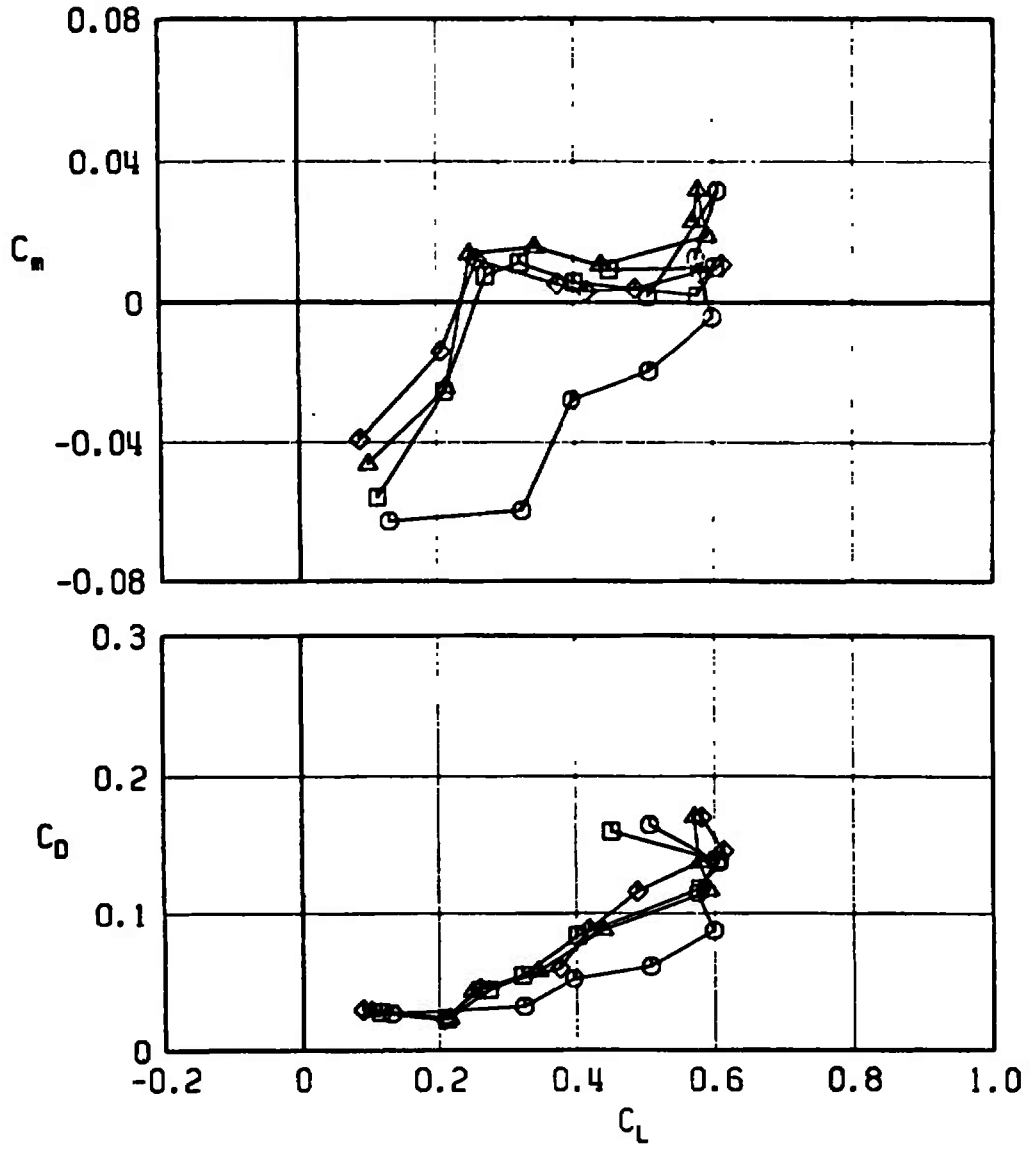

Fig. 40 Concluded

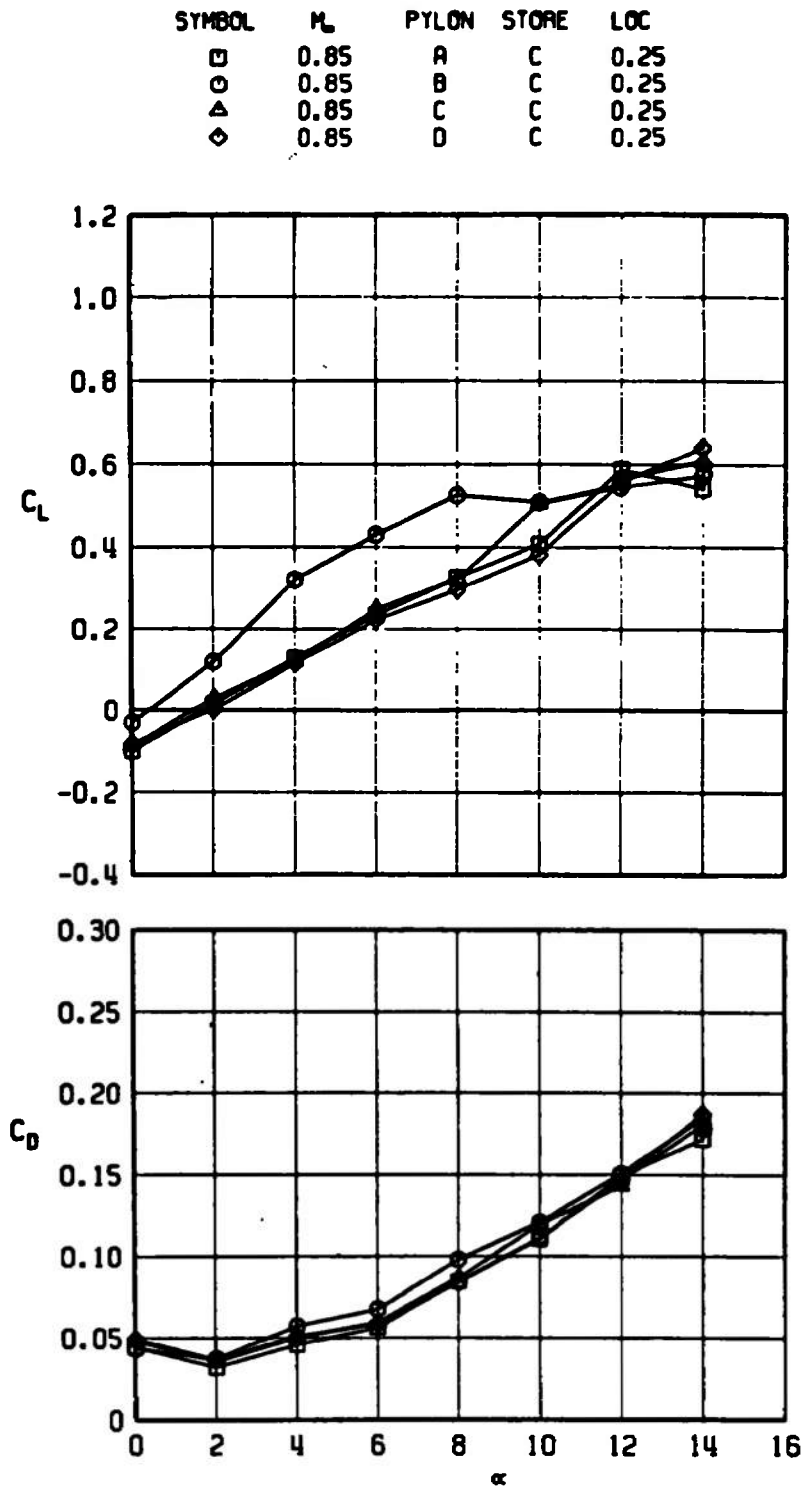

Fig. 41 Effect of Different Pylons with C Store on the Lift, Drag, and Pitching-Moment Coefficients of the Airfoil, M_∞ = 0.85

SYMBOL	M_∞	PYLON	STORE	LOC
□	0.85	A	C	0.25
○	0.85	B	C	0.25
△	0.85	C	C	0.25
◇	0.85	D	C	0.25

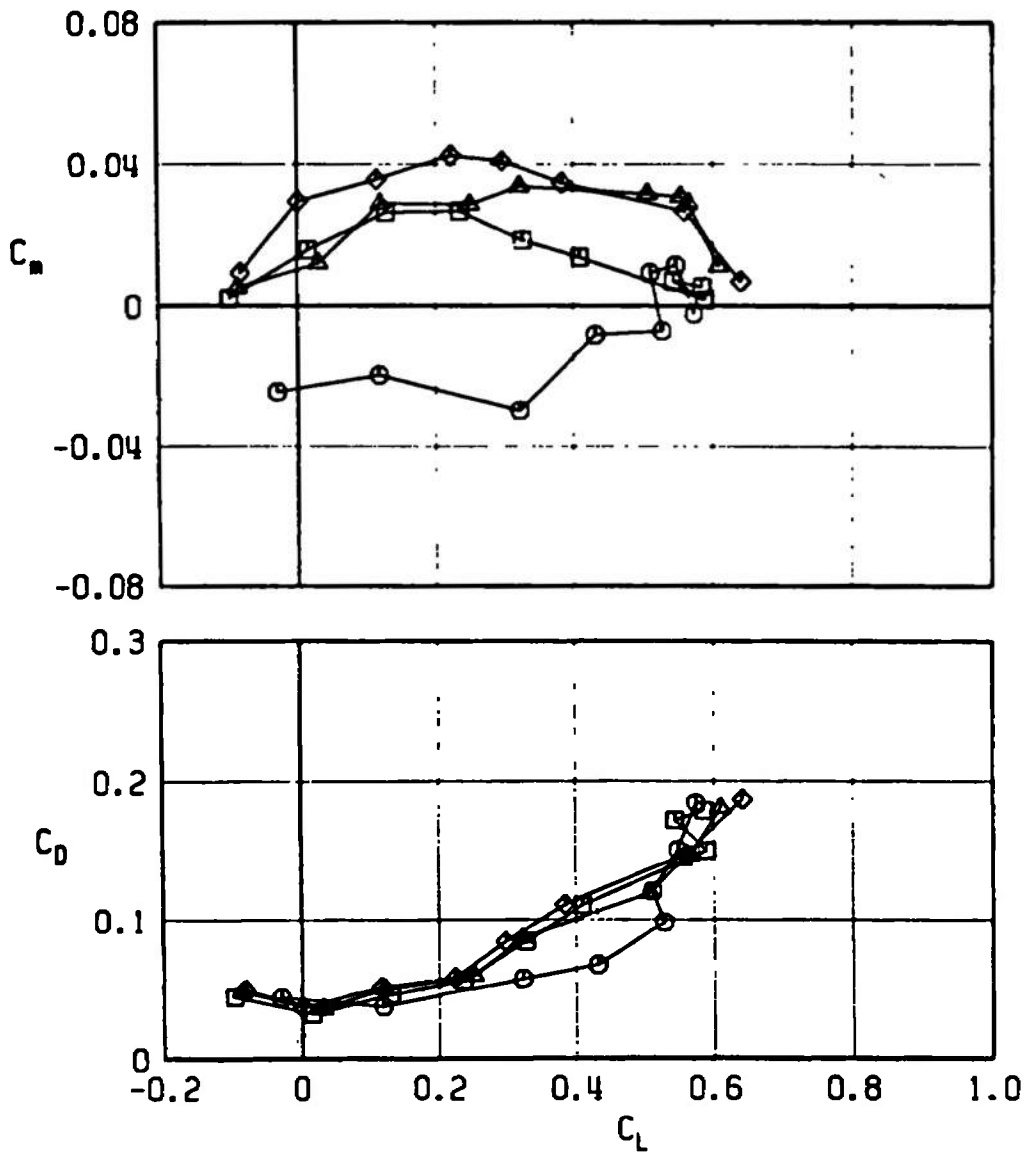

Fig. 41 Concluded

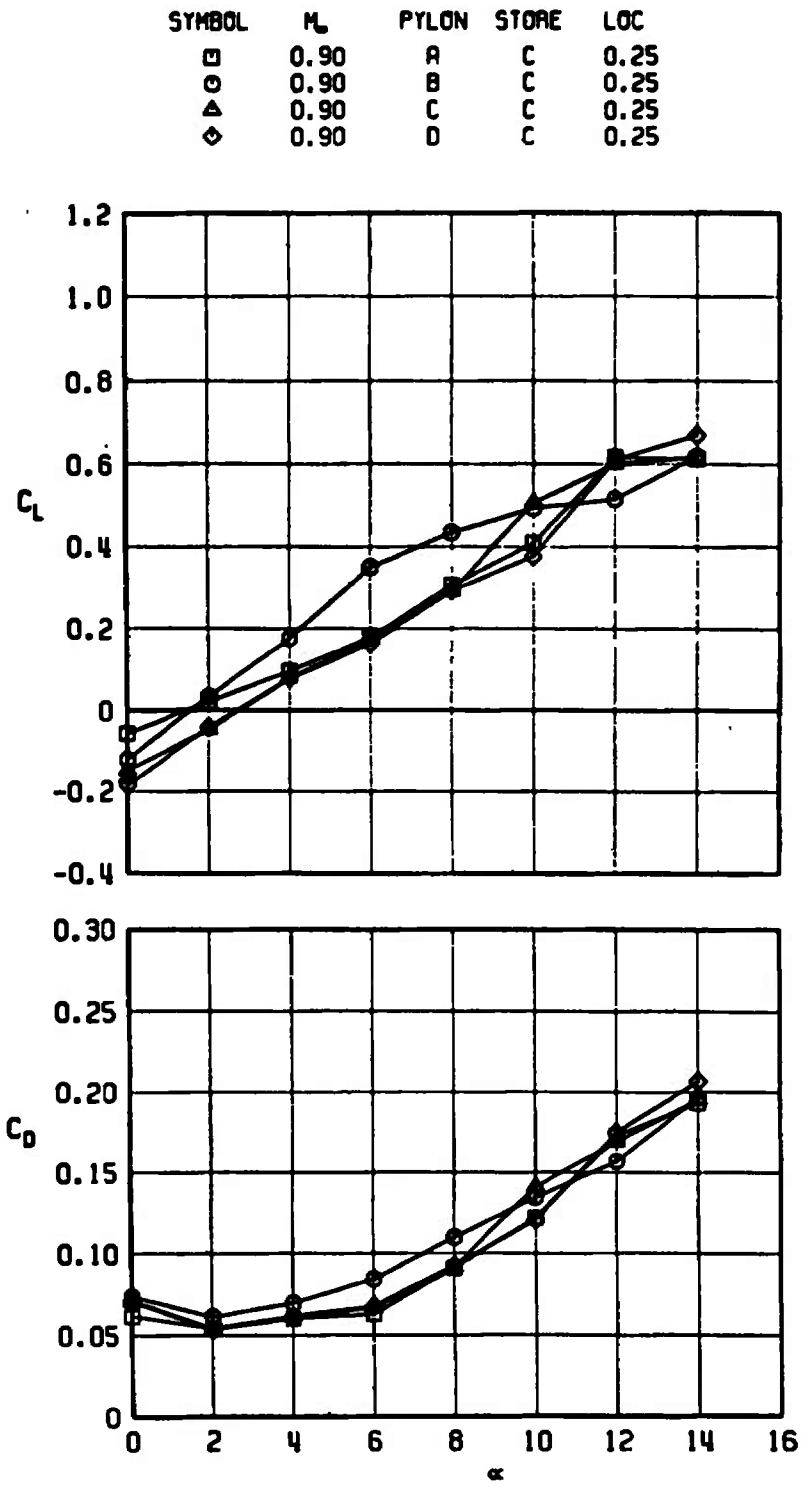

Fig. 42 Effect of Different Pylons with C Store on the Lift, Drag, and Pitching-Moment Coefficients of the Airfoil, $M_\infty = 0.9$

SYMBOL	M_∞	PYLON	STORE	LOC
□	0.90	A	C	0.25
○	0.90	B	C	0.25
△	0.90	C	C	0.25
◇	0.90	D	C	0.25

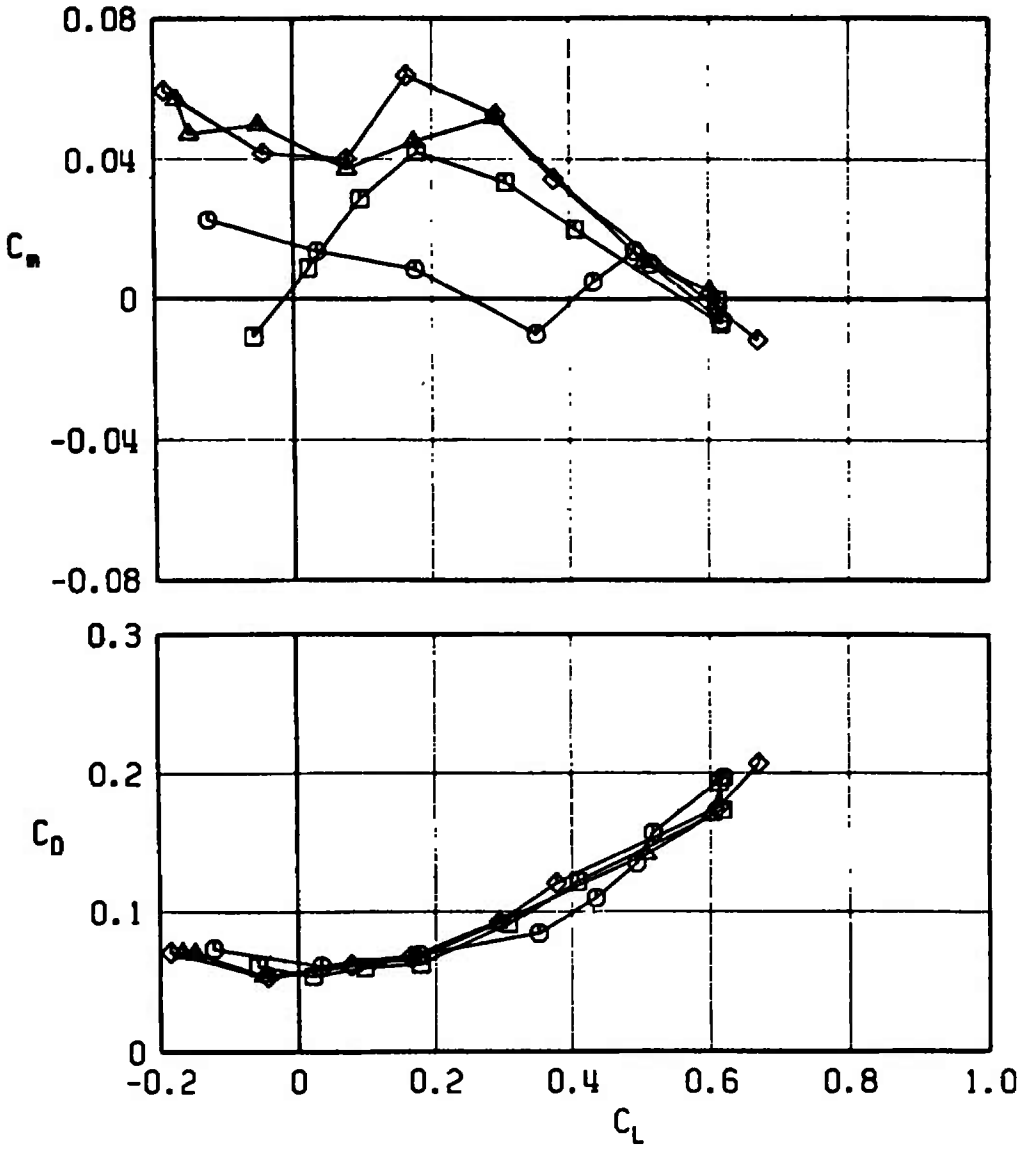

Fig. 42 Concluded

SYMBOL	M_∞	PYLON	STORE	LOC
□	0.70	B	A	0.25
○	0.70	B	B	0.25
△	0.70	B	C	0.25
◇	0.70	B	D	0.25

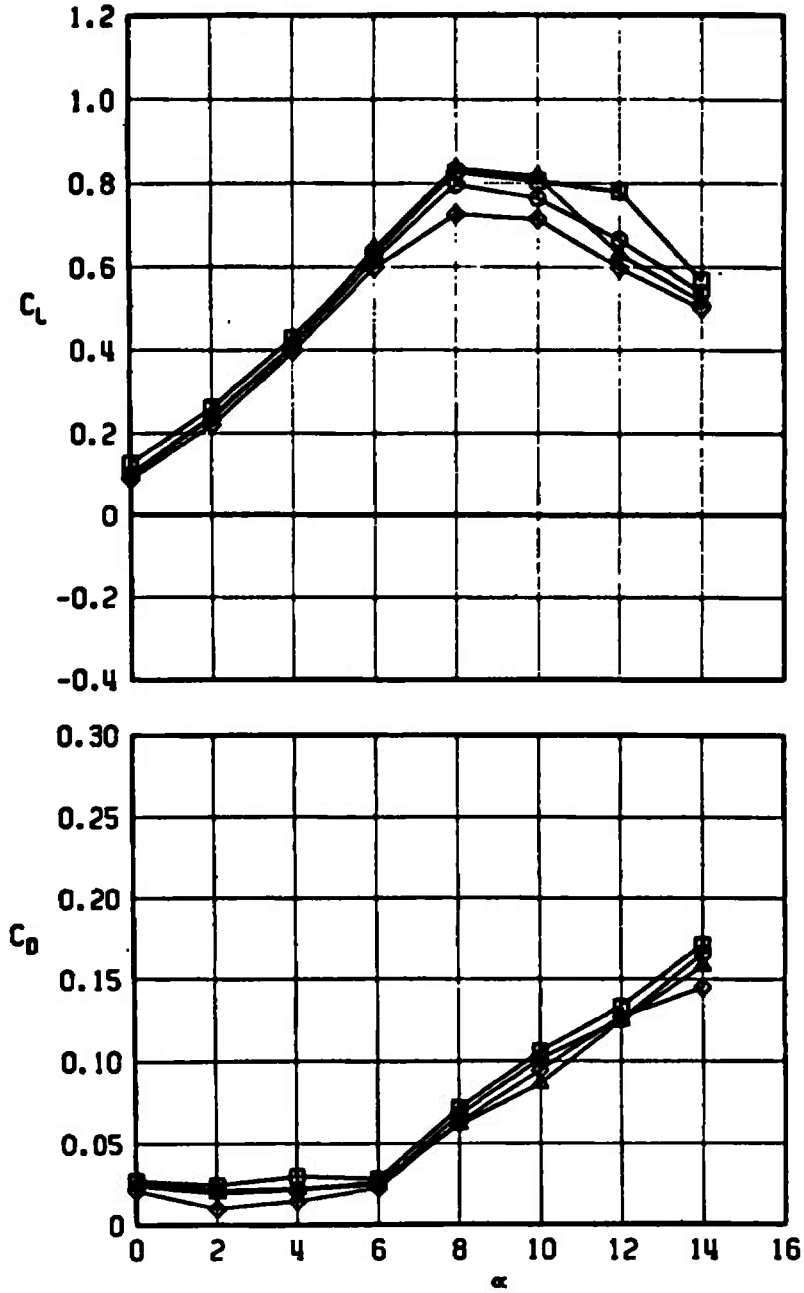

Fig. 43 Effect of Different Stores and B Pylon on the Lift, Drag, and Pitching-Moment Coefficients of the Airfoil, $M_\infty = 0.7$

SYMBOL	M_∞	PYLON	STORE	LOC
□	0.70	B	A	0.25
○	0.70	B	B	0.25
△	0.70	B	C	0.25
◇	0.70	B	D	0.25

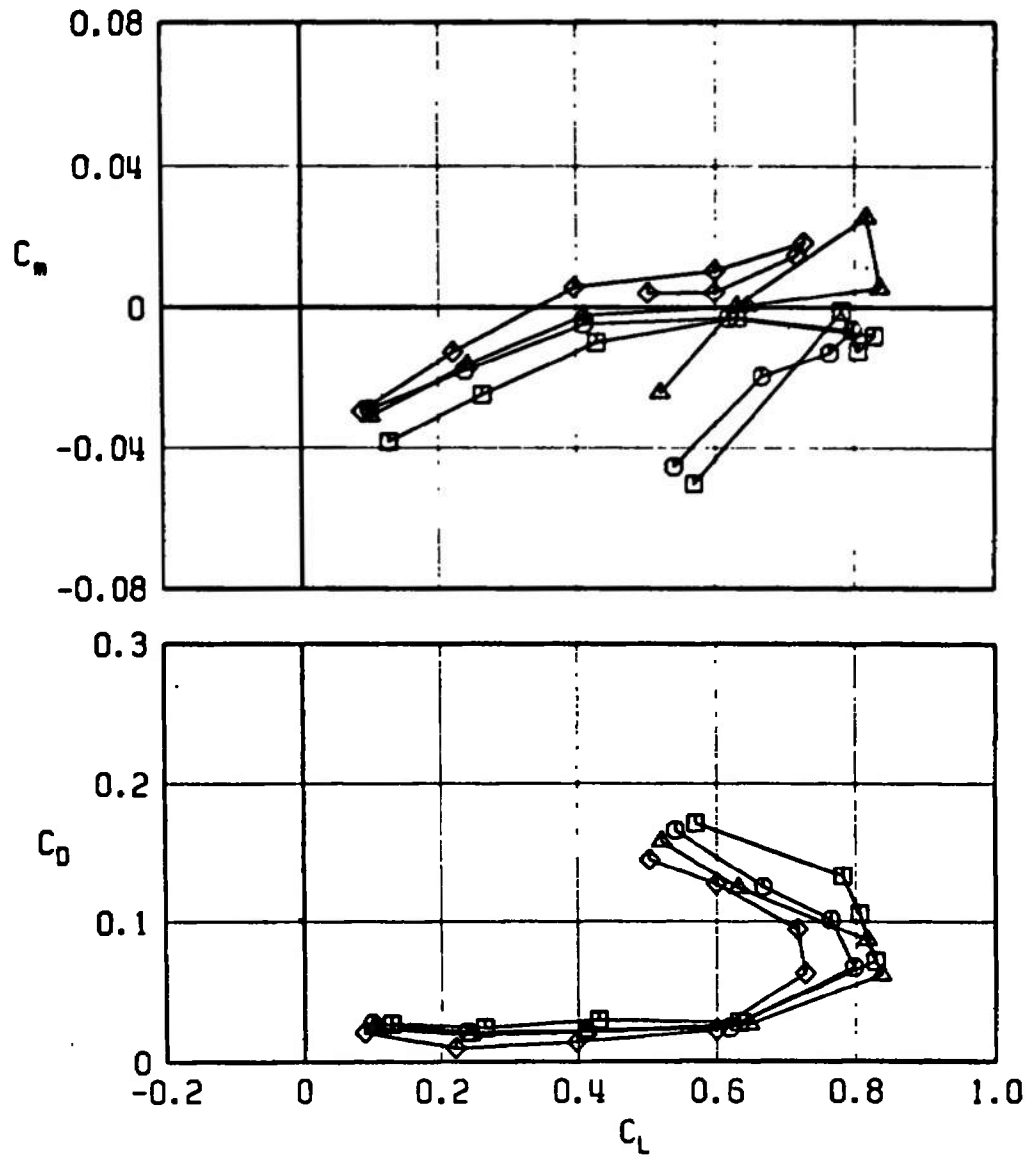

Fig. 43 Concluded

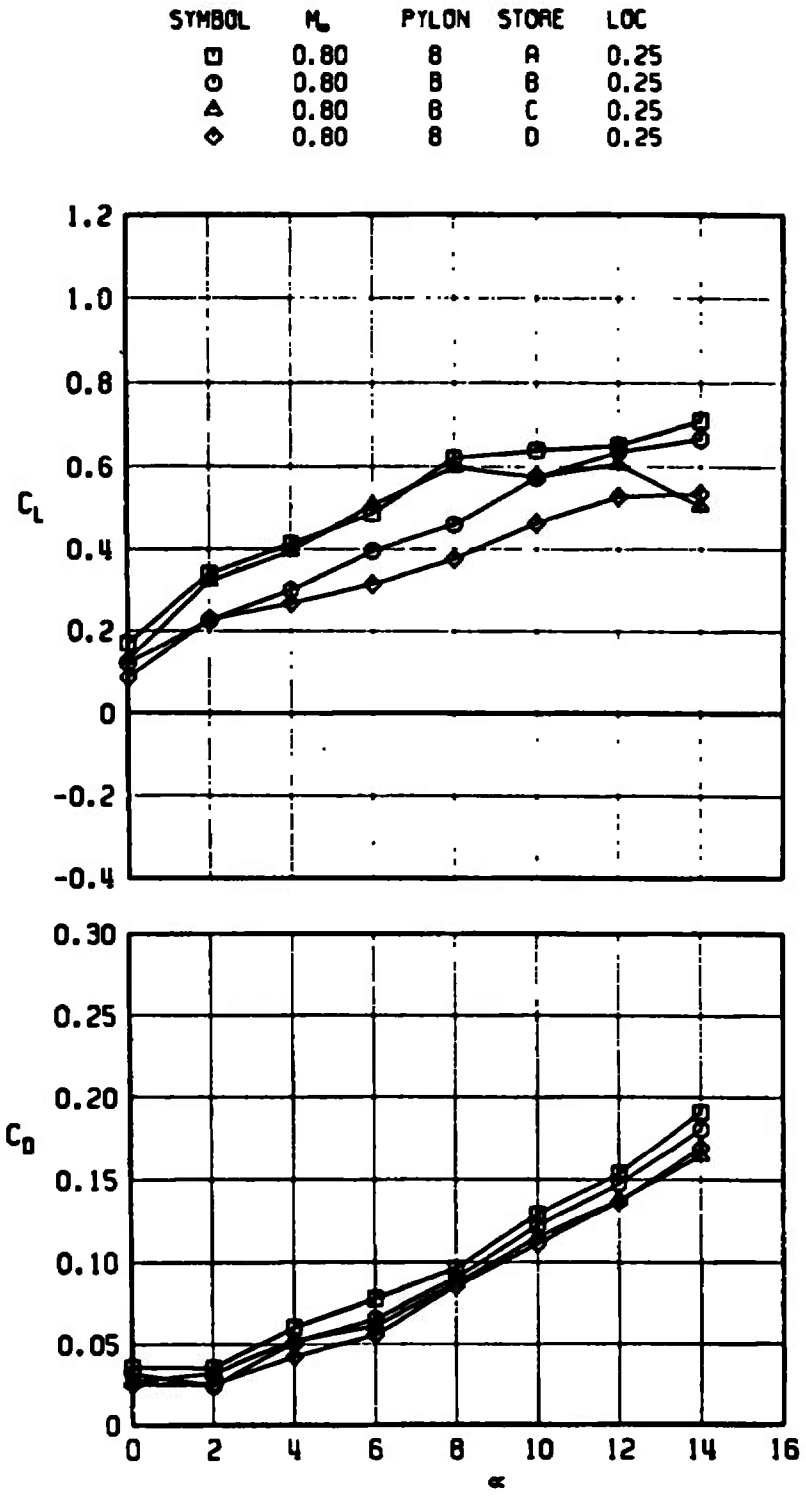

Fig. 44 Effect of Different Stores and B Pylon on the Lift, Drag, and Pitching-Moment Coefficients of the Airfoil, $M_\infty = 0.8$

SYMBOL	M_∞	PYLON	STORE	LOC
□	0.80	B	A	0.25
○	0.80	B	B	0.25
△	0.80	B	C	0.25
◇	0.80	B	D	0.25

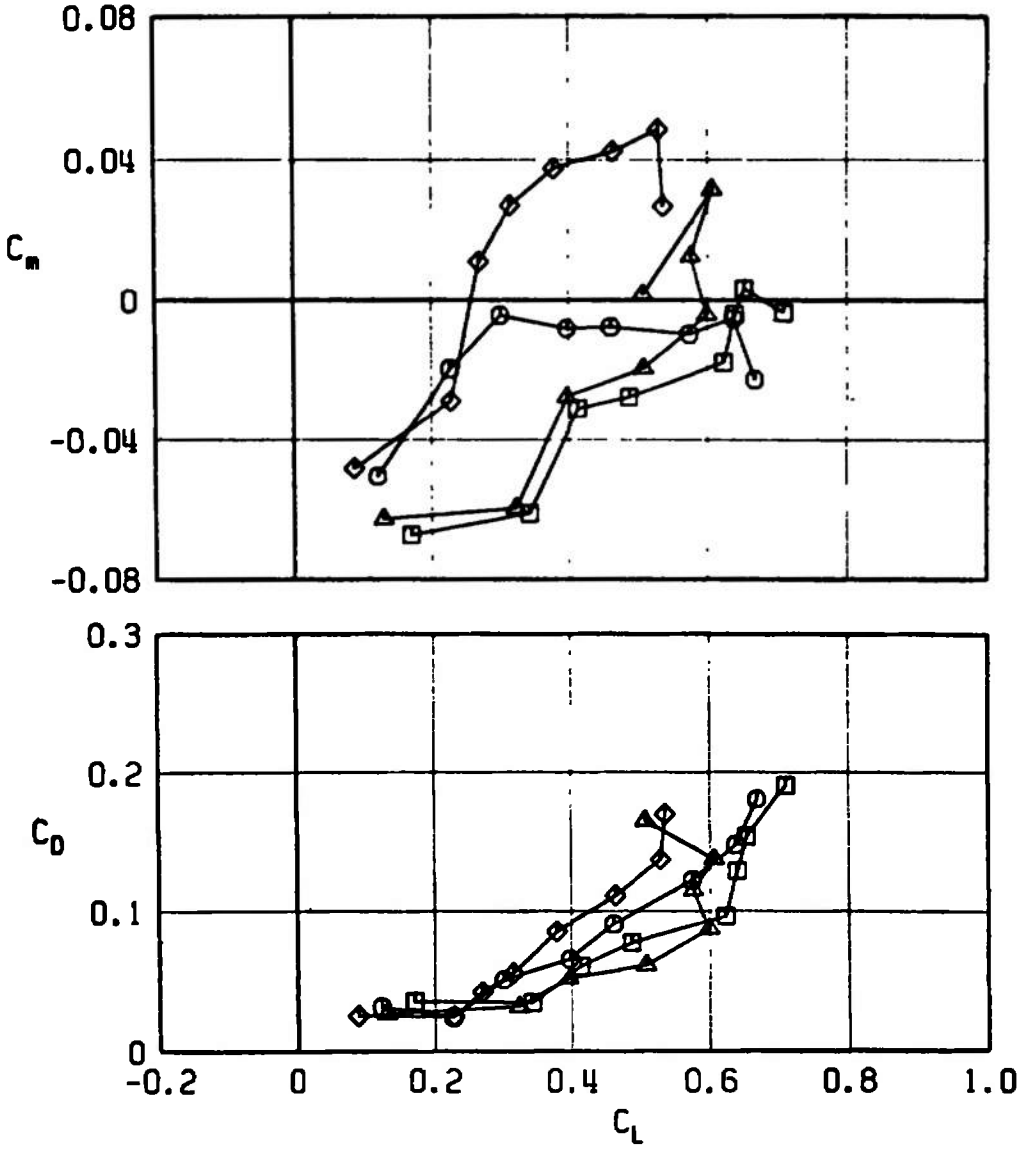

Fig. 44 Concluded

SYMBOL	M_∞	PYLON	STORE	LOC
□	0.85	B	A	0.25
○	0.85	B	B	0.25
△	0.85	B	C	0.25
◇	0.85	B	D	0.25

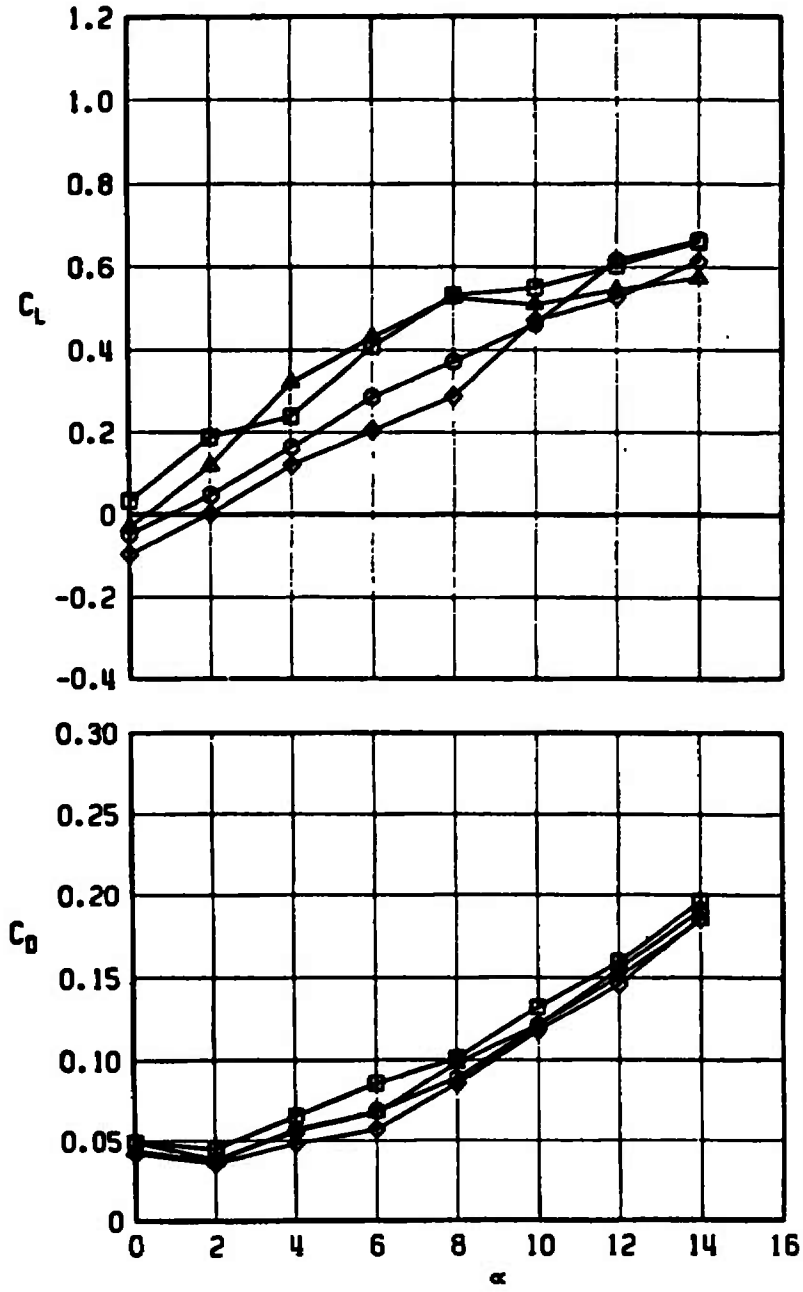

Fig. 45 Effect of Different Stores and B Pylon on the Lift, Drag, and Pitching-Moment Coefficients of the Airfoil, $M_\infty = 0.85$

SYMBOL	M_∞	PYLON	STORE	LOC
□	0.85	B	A	0.25
○	0.85	B	B	0.25
△	0.85	B	C	0.25
◇	0.85	B	D	0.25

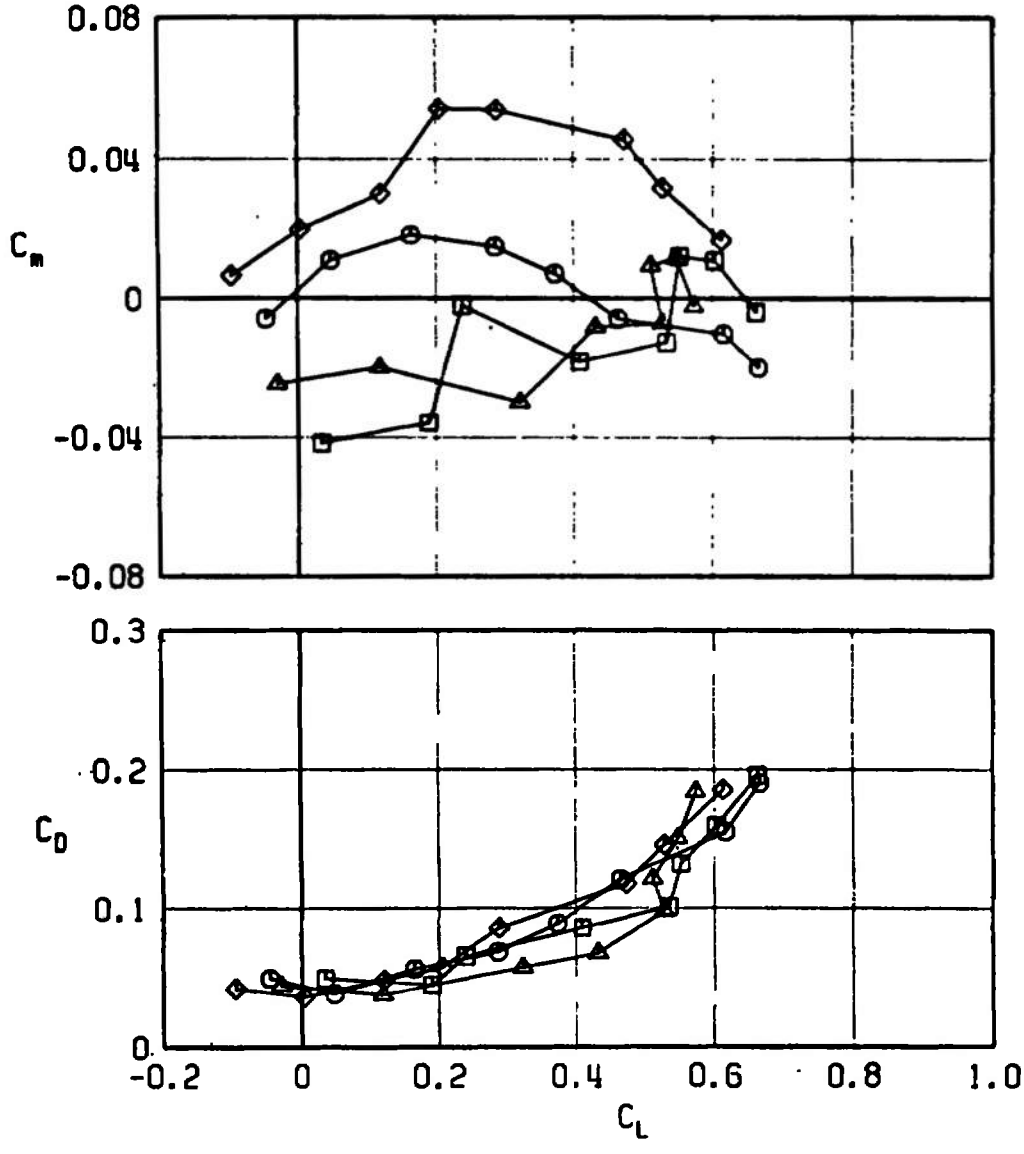

Fig. 45 Concluded

SYMBOL	M_∞	PYLON	STORE	LOC
□	0.90	B	A	0.25
○	0.90	B	B	0.25
△	0.90	B	C	0.25
◇	0.90	B	D	0.25

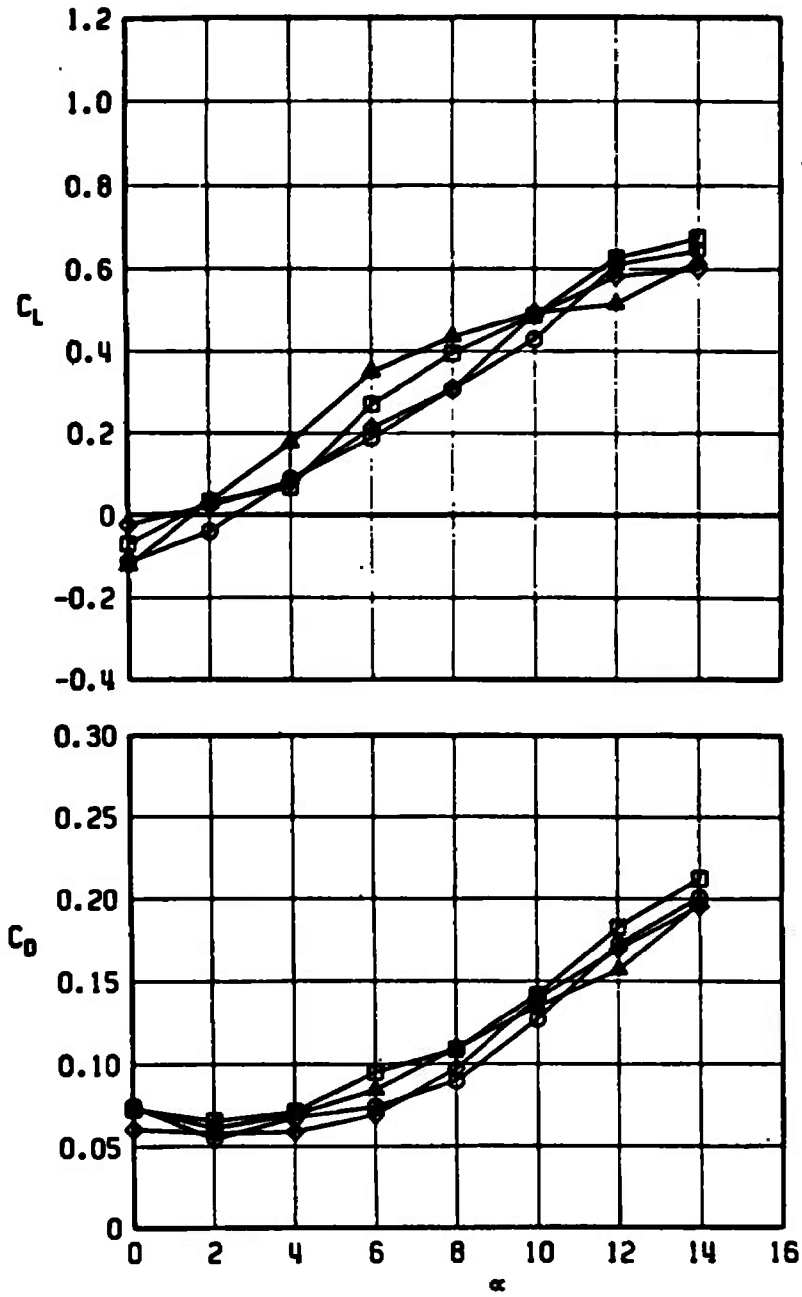

Fig. 46 Effect of Different Stores and B Pylon on the Lift, Drag, and Pitching-Moment Coefficients of the Airfoil, M_∞ = 0.9

SYMBOL	M_∞	PYLON	STORE	LOC
□	0.90	B	A	0.25
○	0.90	B	B	0.25
△	0.90	B	C	0.25
◇	0.90	B	D	0.25

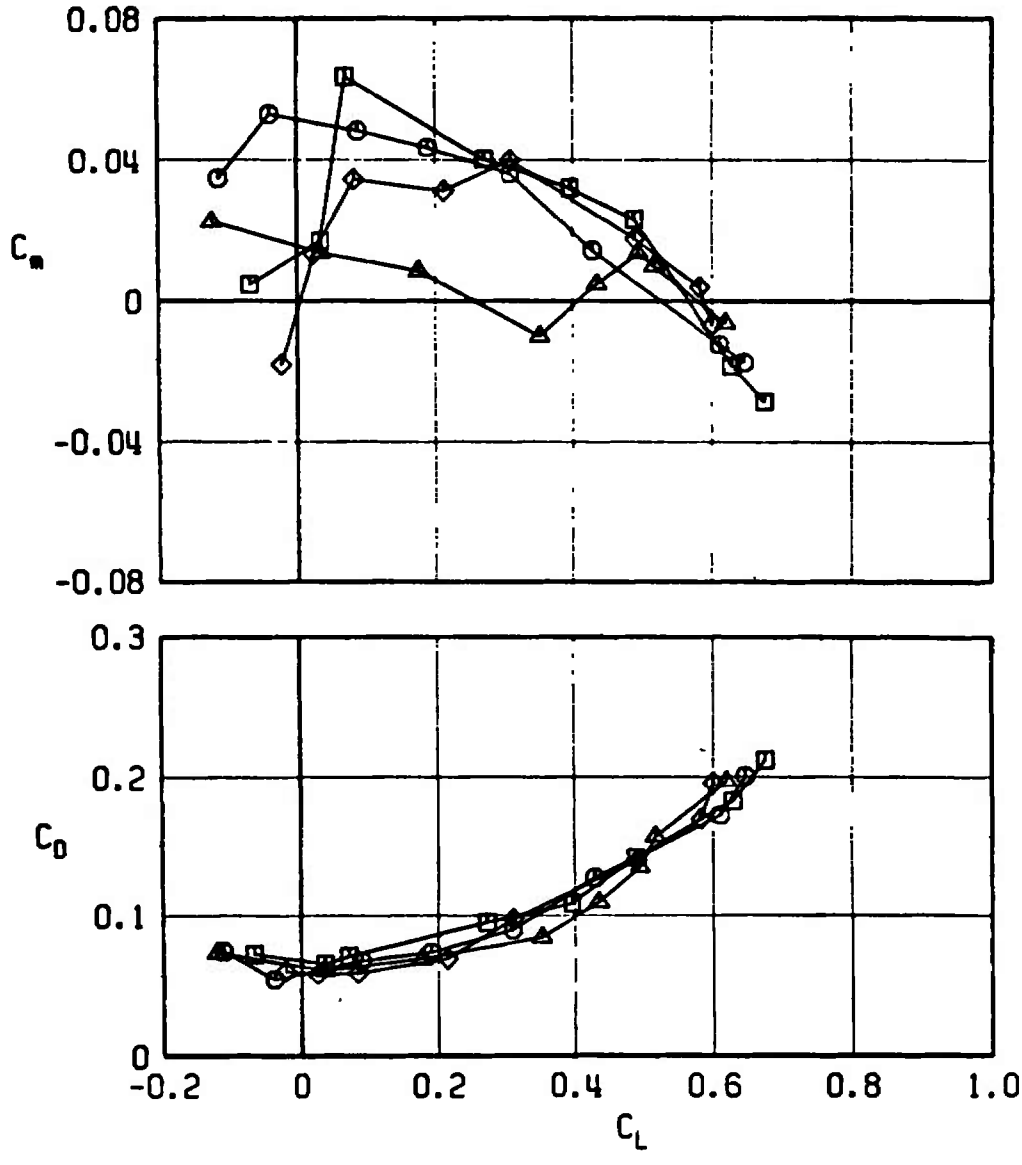

Fig. 46 Concluded

SYMBOL	M_∞	PYLON	STORE	LOC
⊡	0.70	B	C	0.25
⊙	0.70	B	C-1	0.25

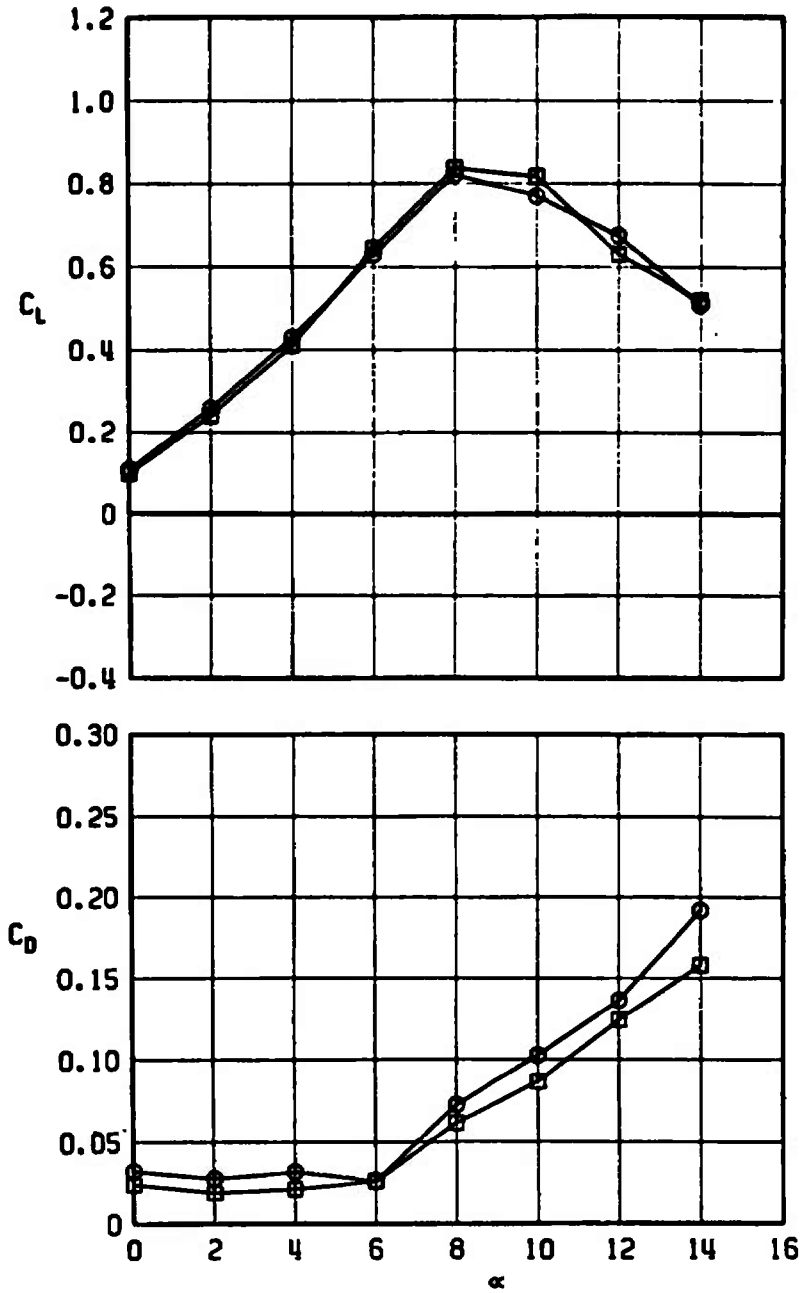

Fig. 47 Effect of C Store Position (Position on B Pylon) on the Lift, Drag, and Pitching-Moment Coefficients of the Airfoil, M_∞ = 0.7

SYMBOL	M_∞	PYLON	STORE	LOC
□	0.70	B	C	0.25
○	0.70	B	C-1	0.25

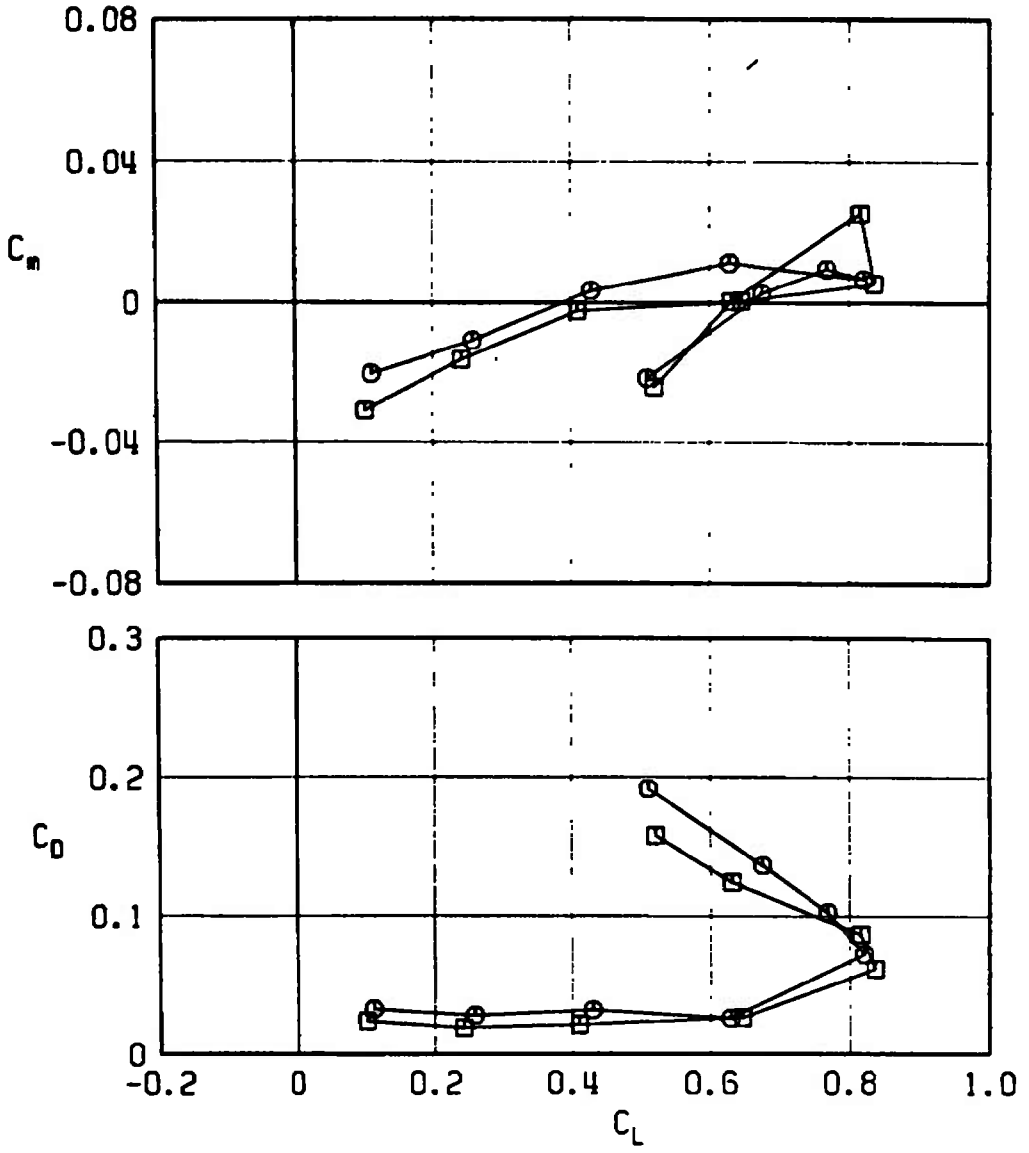

Fig. 47 Concluded

SYMBOL	M_∞	PYLON	STORE	LOC
⊡	0.80	B	C	0.25
⊙	0.80	B	C-1	0.25

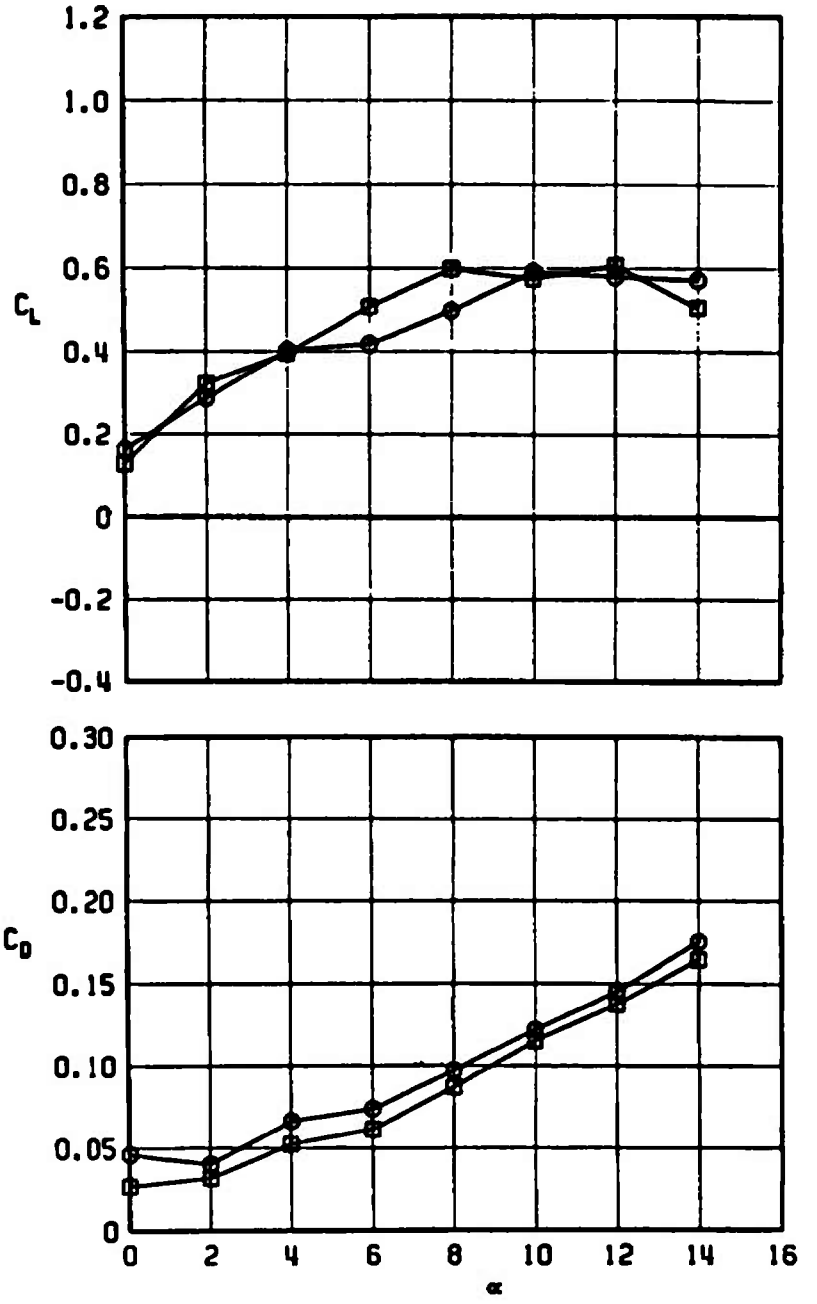

Fig. 48 Effect of C Store Position (Position on B Pylon) on the Lift, Drag, and Pitching-Moment Coefficients of the Airfoil, M_∞ = 0.8

SYMBOL	M_∞	PYLON	STORE	LOC
□	0.80	B	C	0.25
○	0.80	B	C-1	0.25

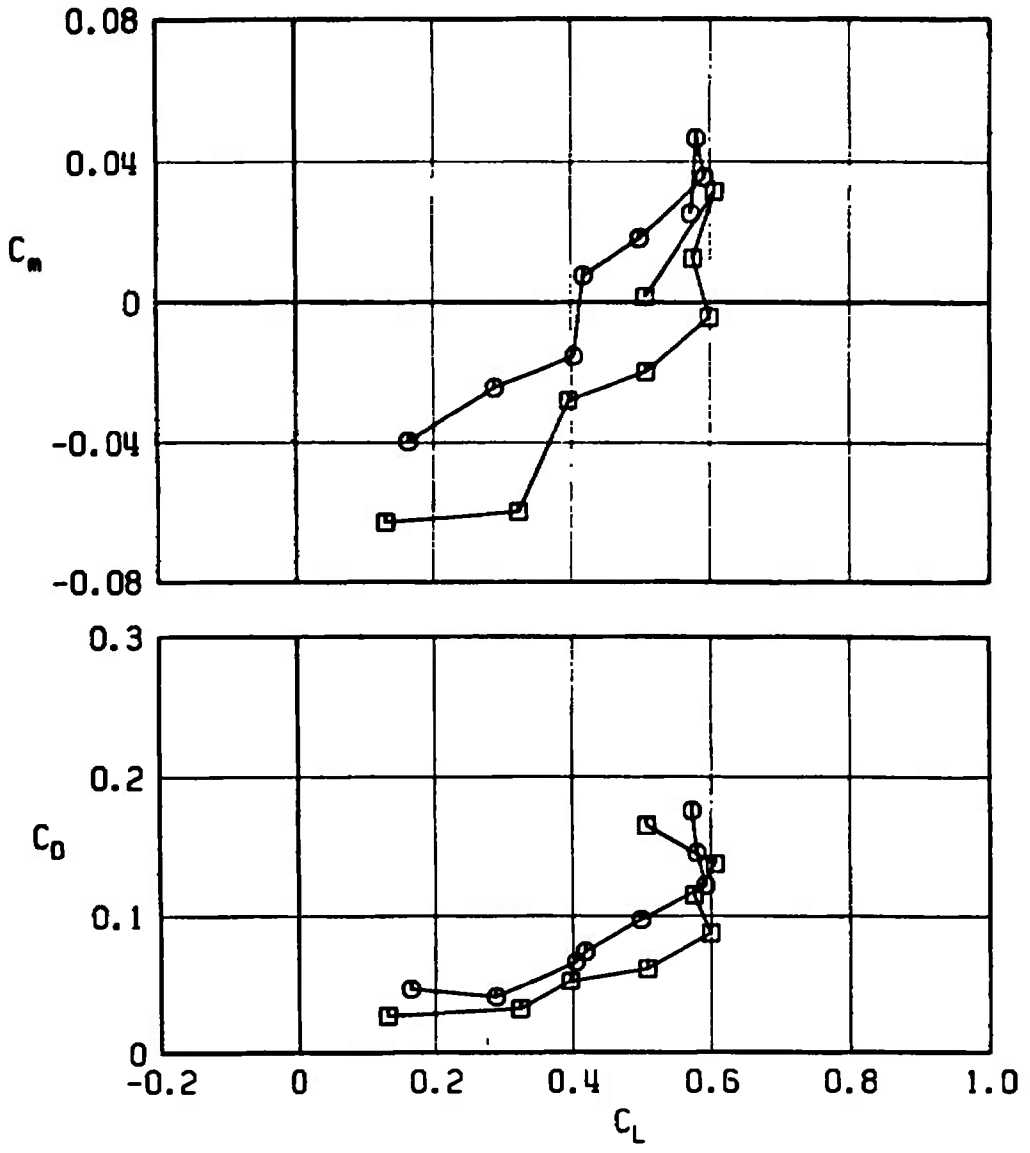

Fig. 48 Concluded

SYMBOL	M_∞	PYLON	STORE	LOC
□	0.85	B	C	0.25
○	0.85	B	C-1	0.25

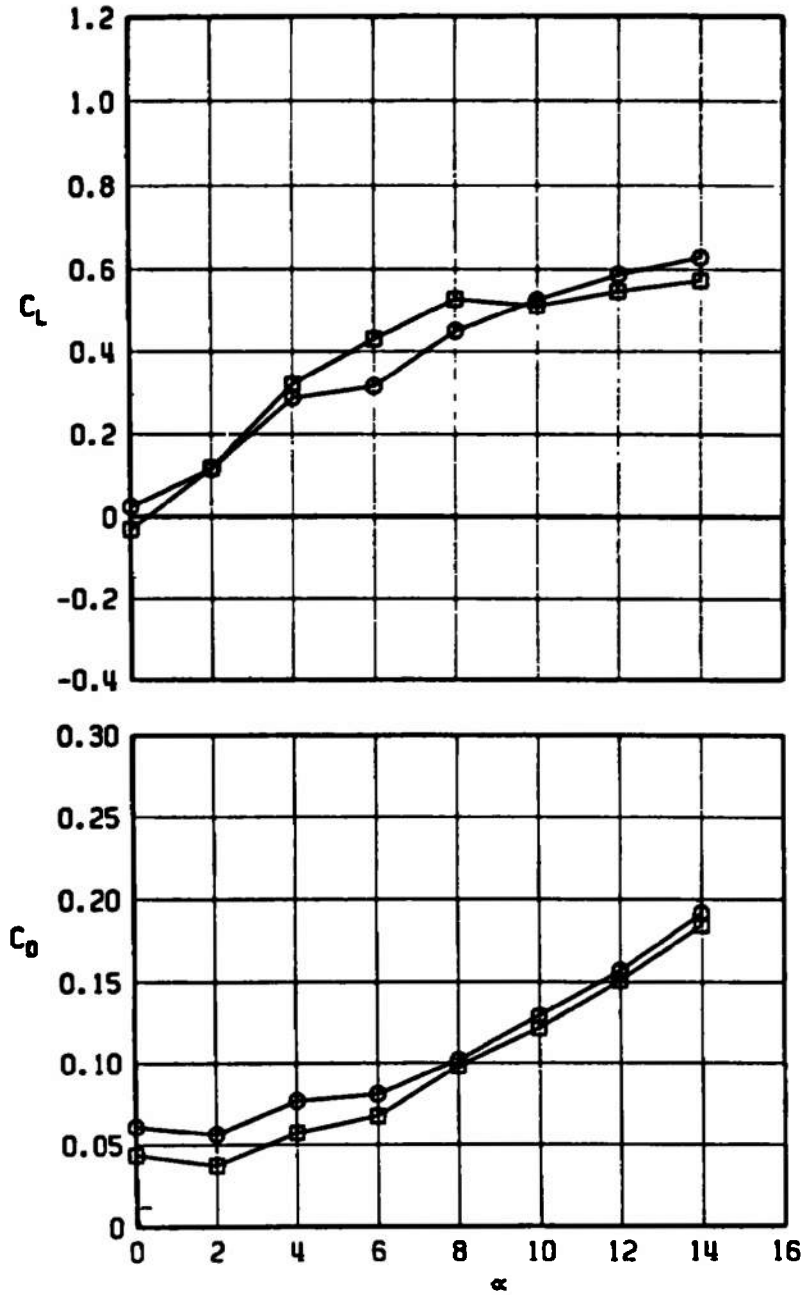

Fig. 49 Effect of C Store Position (Position on B Pylon) on the Lift, Drag, and Pitching-Moment Coefficients on the Airfoil, M_∞ = 0.85

SYMBOL	M_∞	PYLON	STORE	LOC
⊡	0.85	B	C	0.25
⊙	0.85	B	C-1	0.25

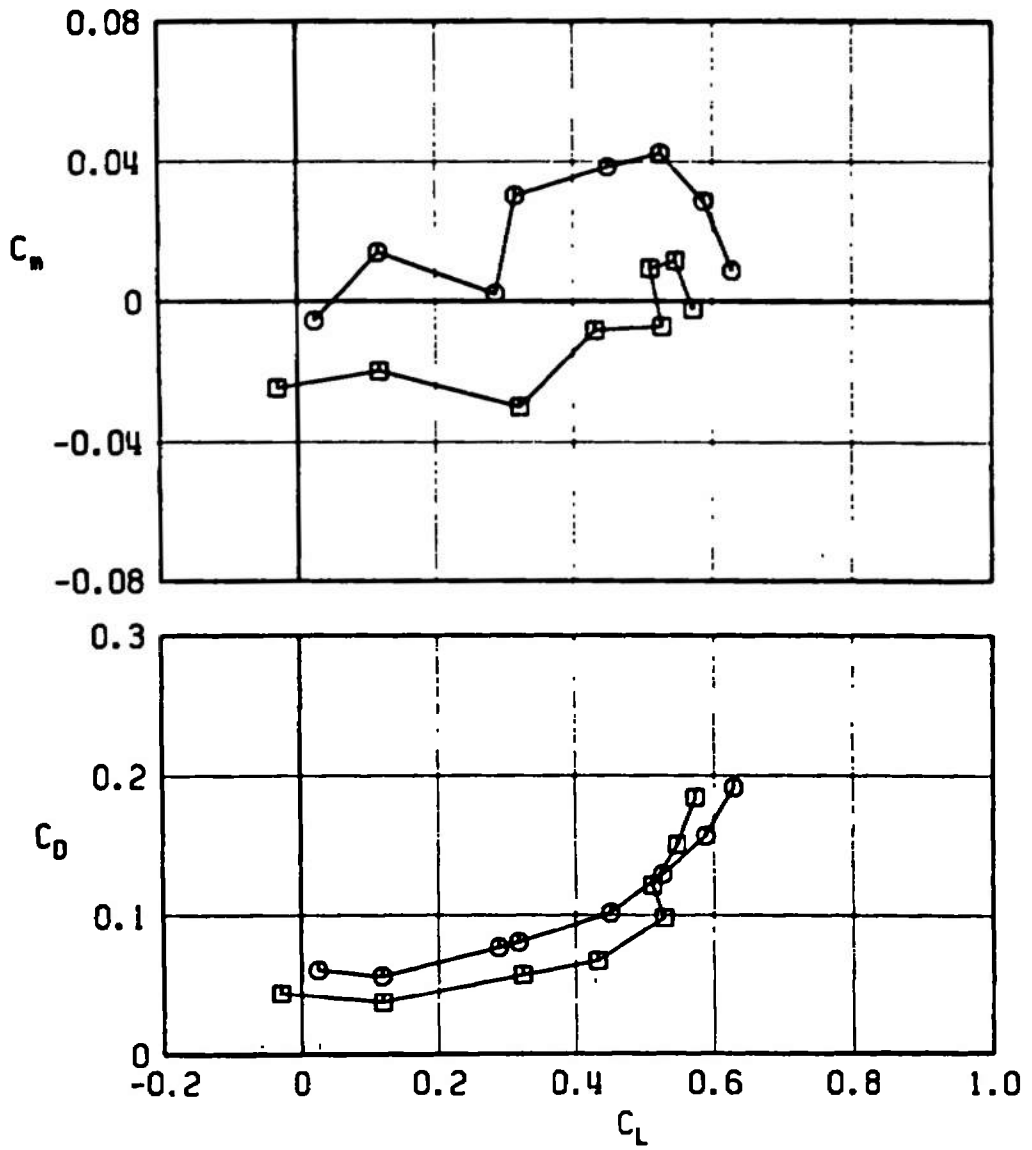

Fig. 49 Concluded

SYMBOL	M_∞	PYLON	STORE	LOC
⊡	0.90	B	C	0.25
⊙	0.90	B	C-1	0.25

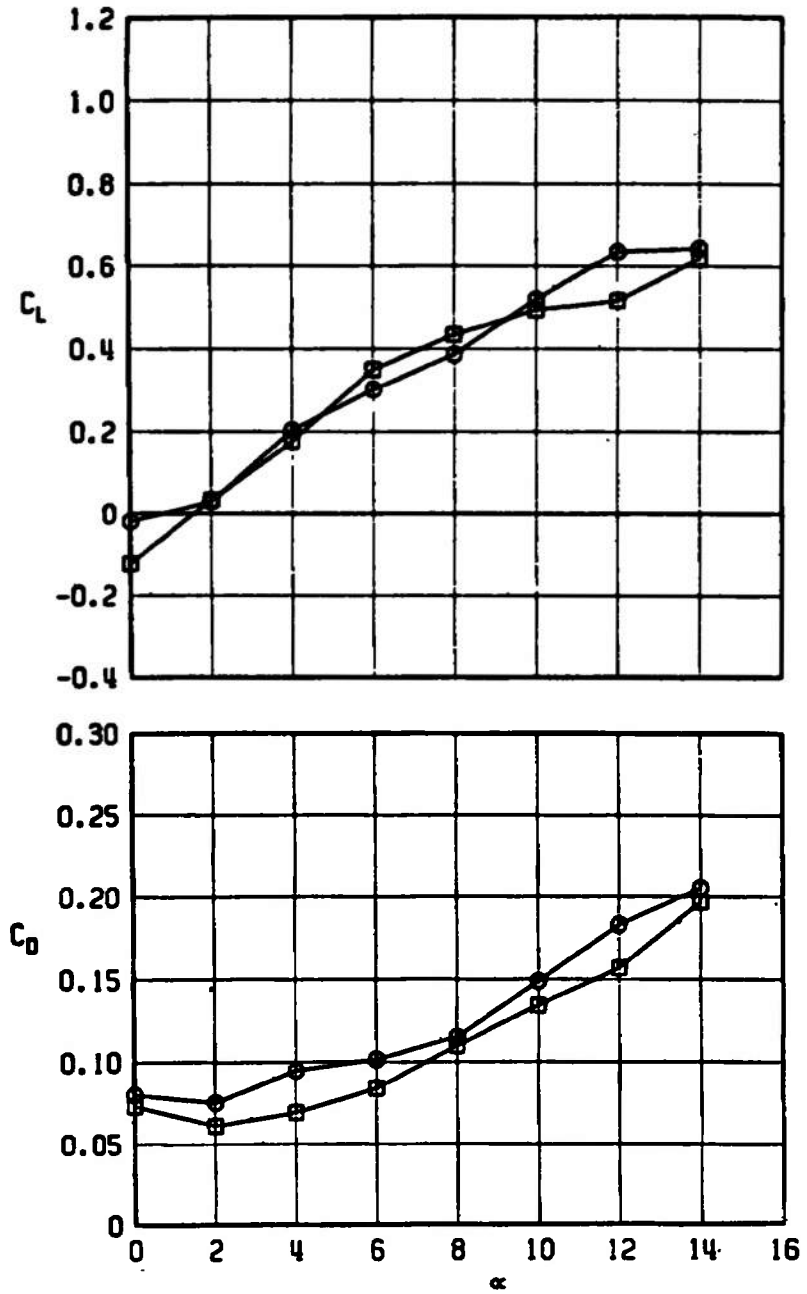

Fig. 50 Effect of C Store Position (Position on B Pylon) on the Lift, Drag, and Pitching-Moment Coefficients of the Airfoil, M_∞ = 0.9

SYMBOL	M_∞	PYLON	STORE	LOC
□	0.90	B	C	0.25
○	0.90	B	C-1	0.25

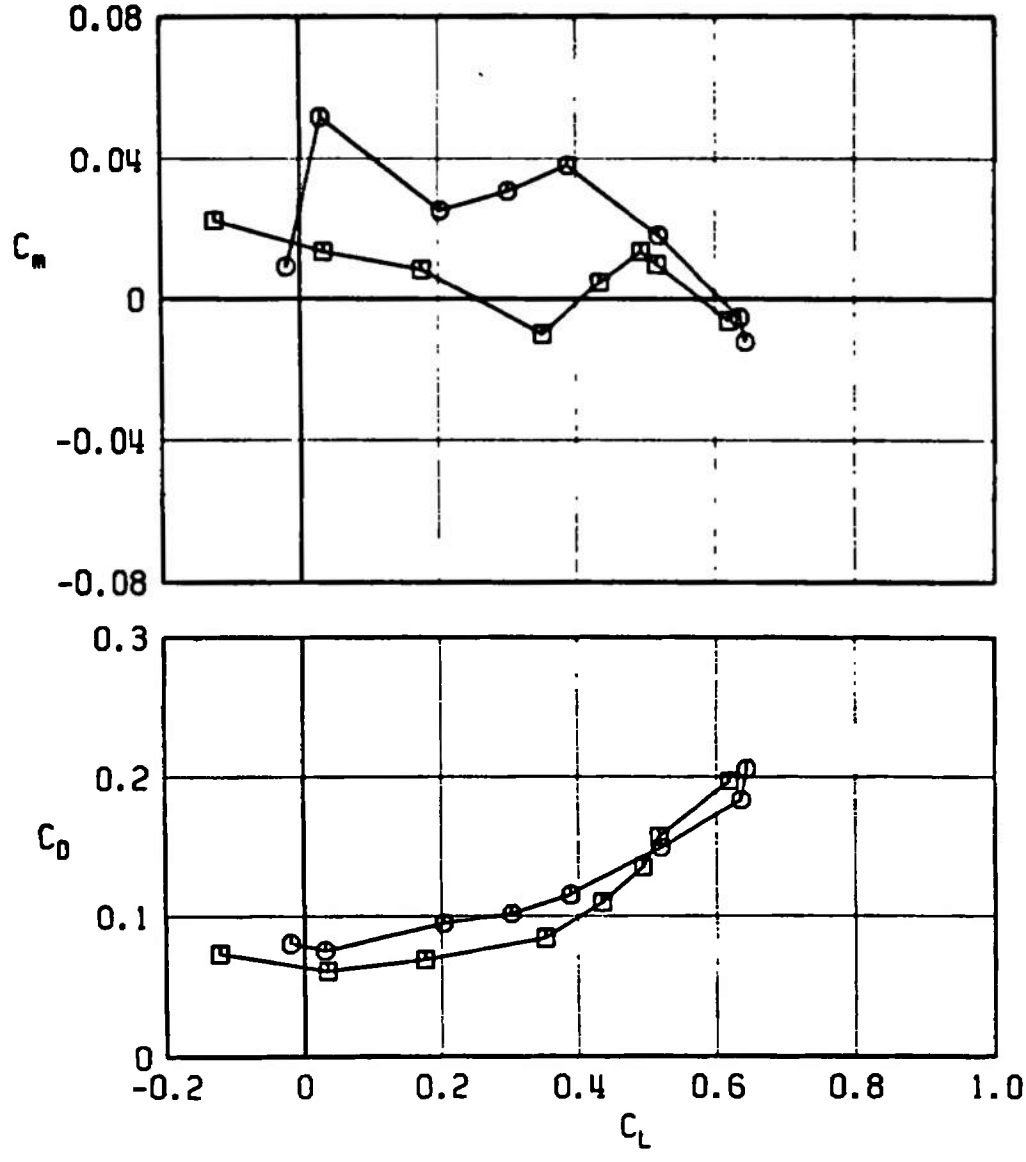

Fig. 50 Concluded

SYMBOL	M_∞	PYLON	STORE	Y
□	0.700	NONE	NONE	NA

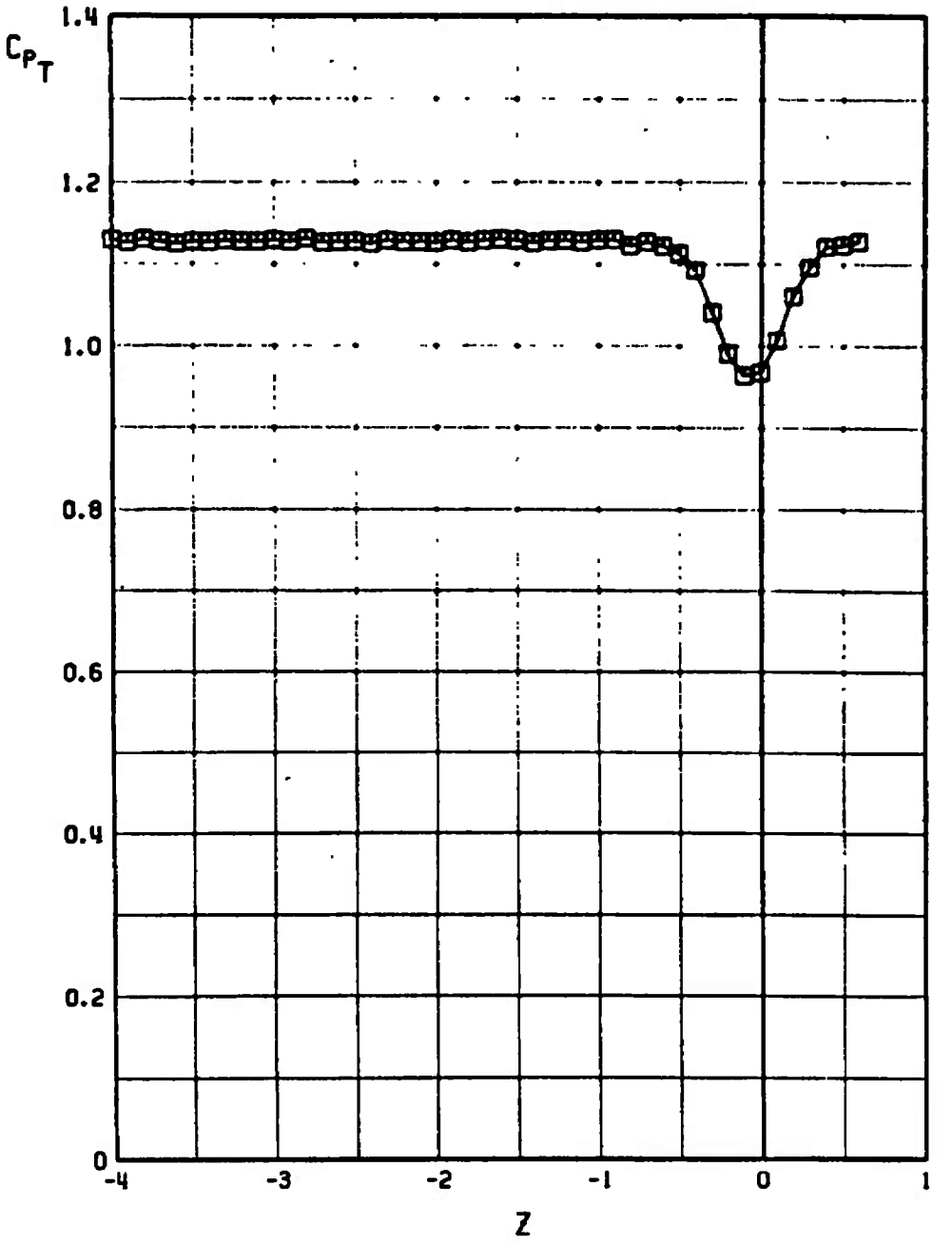

Fig. 51 Total Pressure Wake Survey for the Clean Airfoil

SYMBOL	M_∞	PYLON	STORE	Y
□	0.800	NONE	NONE	NA

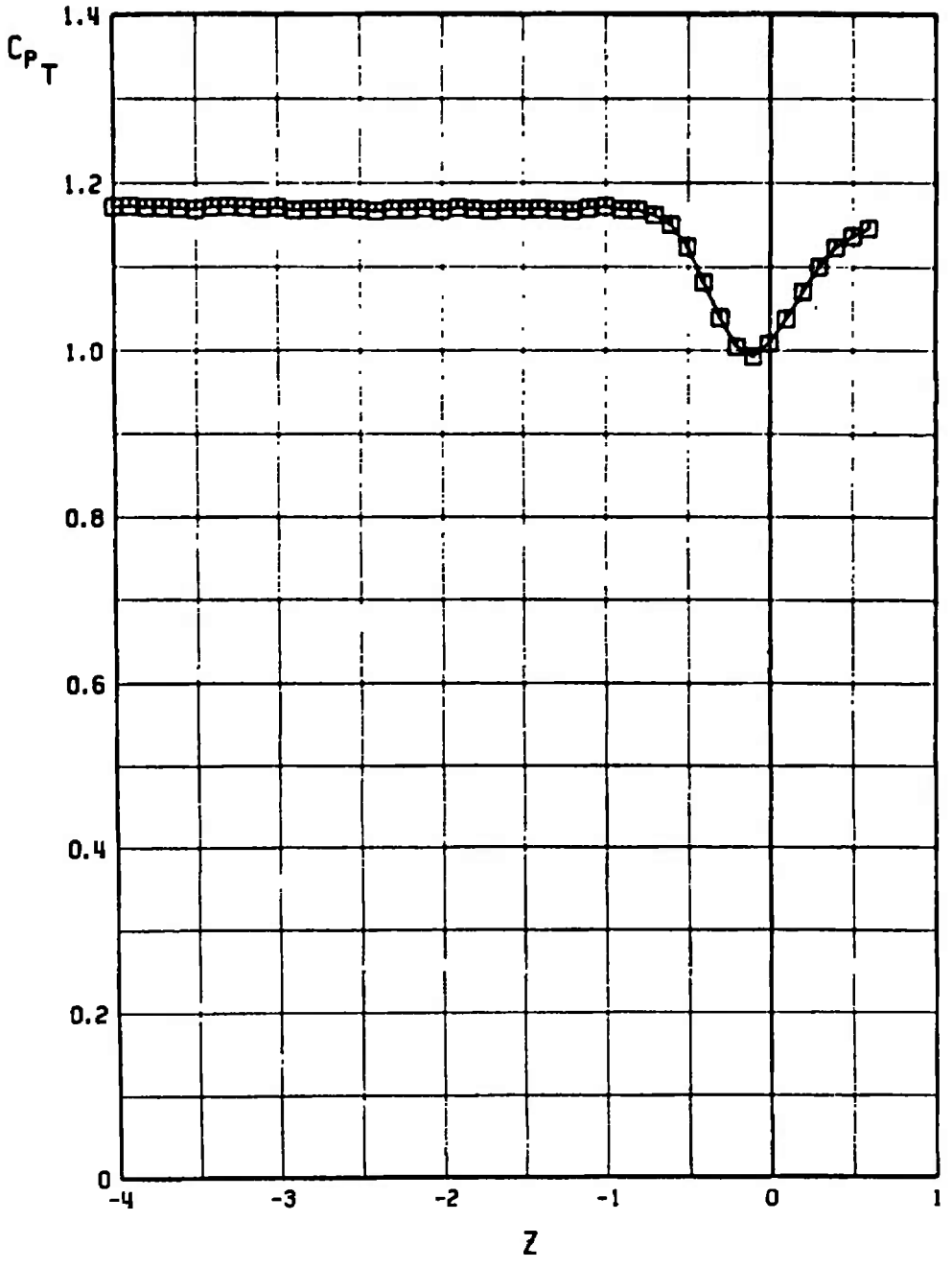

Fig. 51 Continued

SYMBOL	M_∞	PYLON	STORE	Y
□	0.825	NONE	NONE	NA

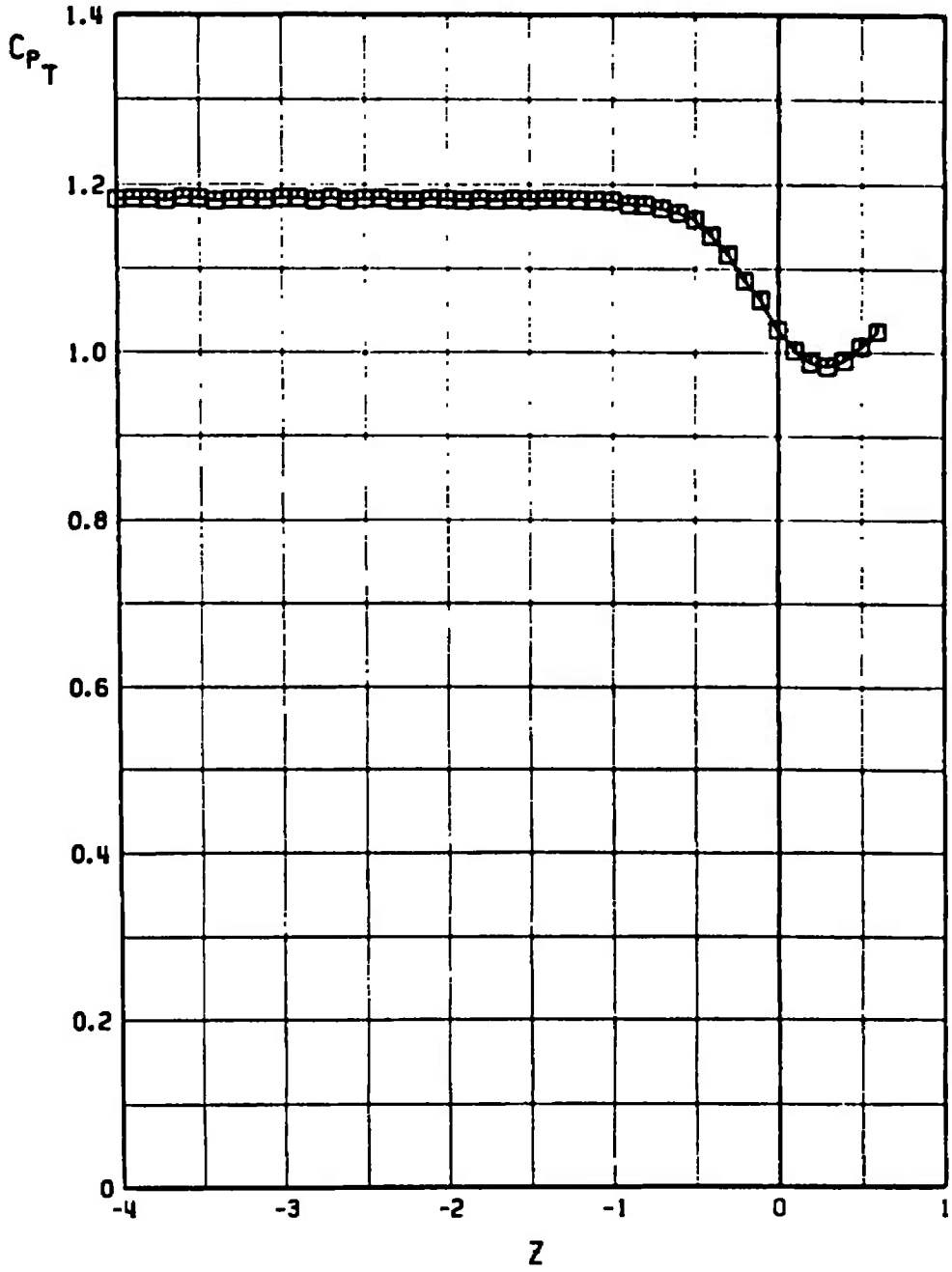

Fig. 51 Continued.

SYMBOL	M_∞	PYLON	STORE	Y
⊙	0.850	NONE	NONE	NA

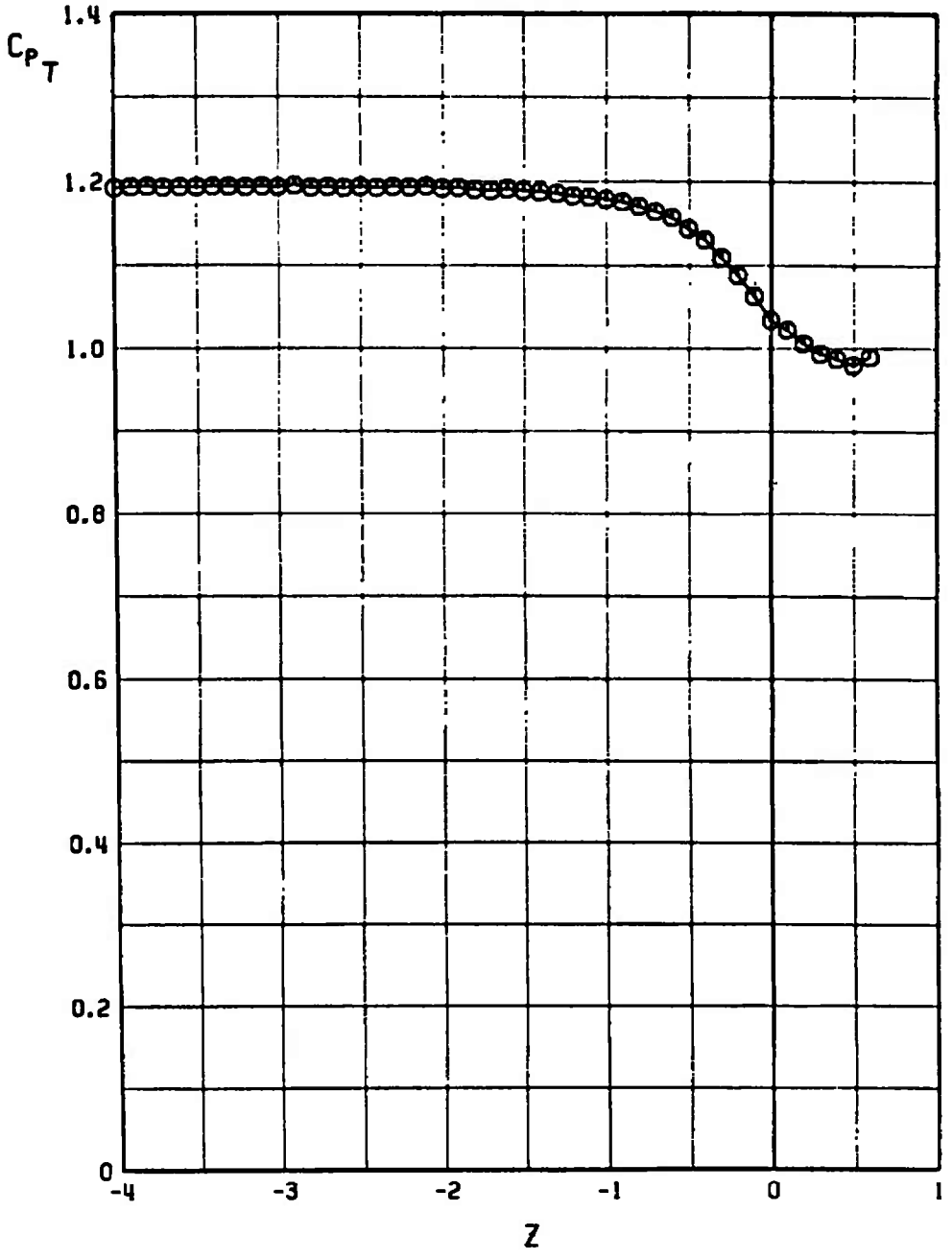

Fig. 51 Continued

SYMBOL	M_∞	PYLON	STORE	Y
□	0.875	NONE	NONE	NA

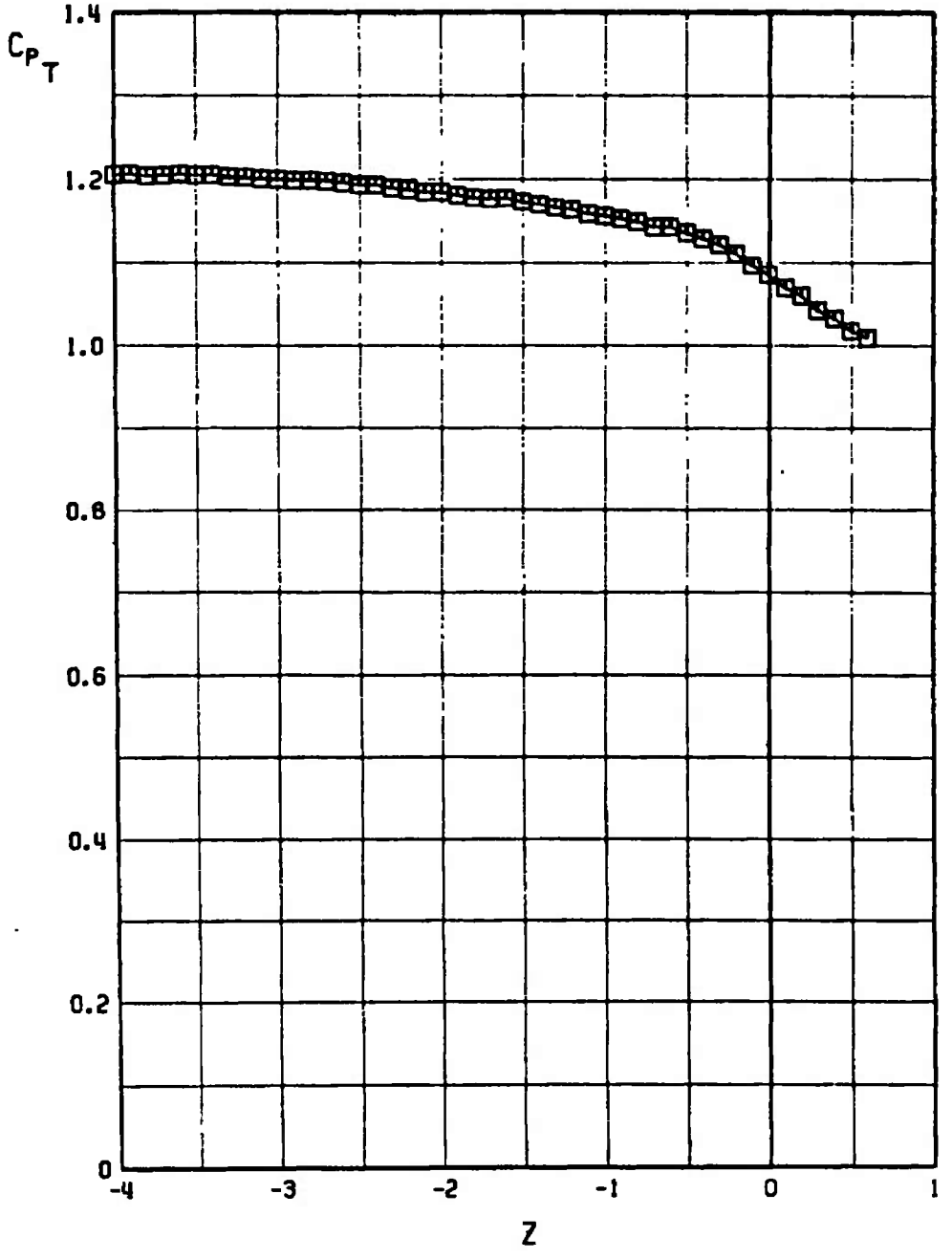

Fig. 51 Continued

SYMBOL	M_∞	PYLON	STORE	Y
⊙	0.900	NONE	NONE	NA

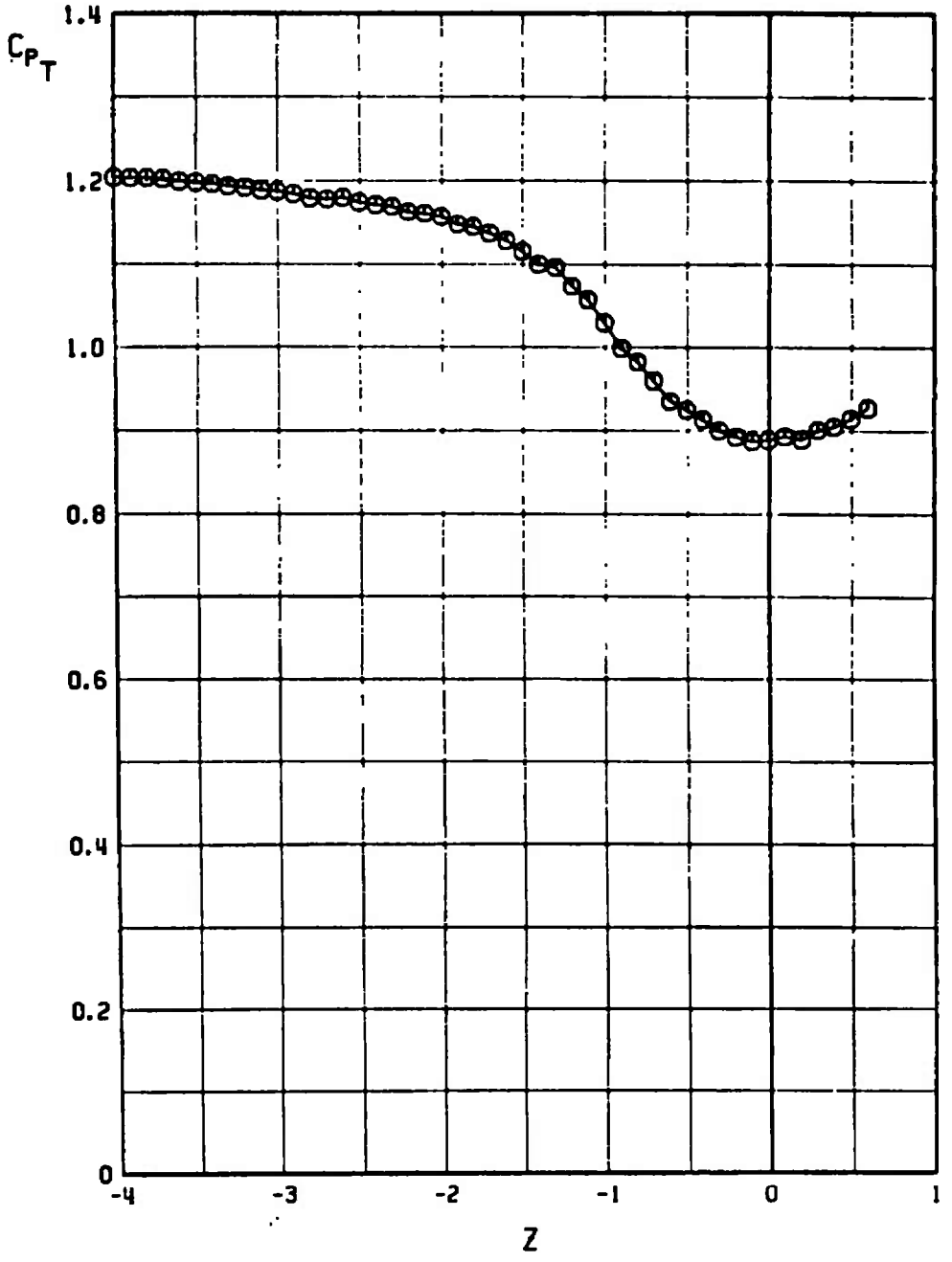

Fig. 51 Continued

SYMBOL	M_∞	PYLON	STORE	Y
□	0.950	NONE	NONE	NA

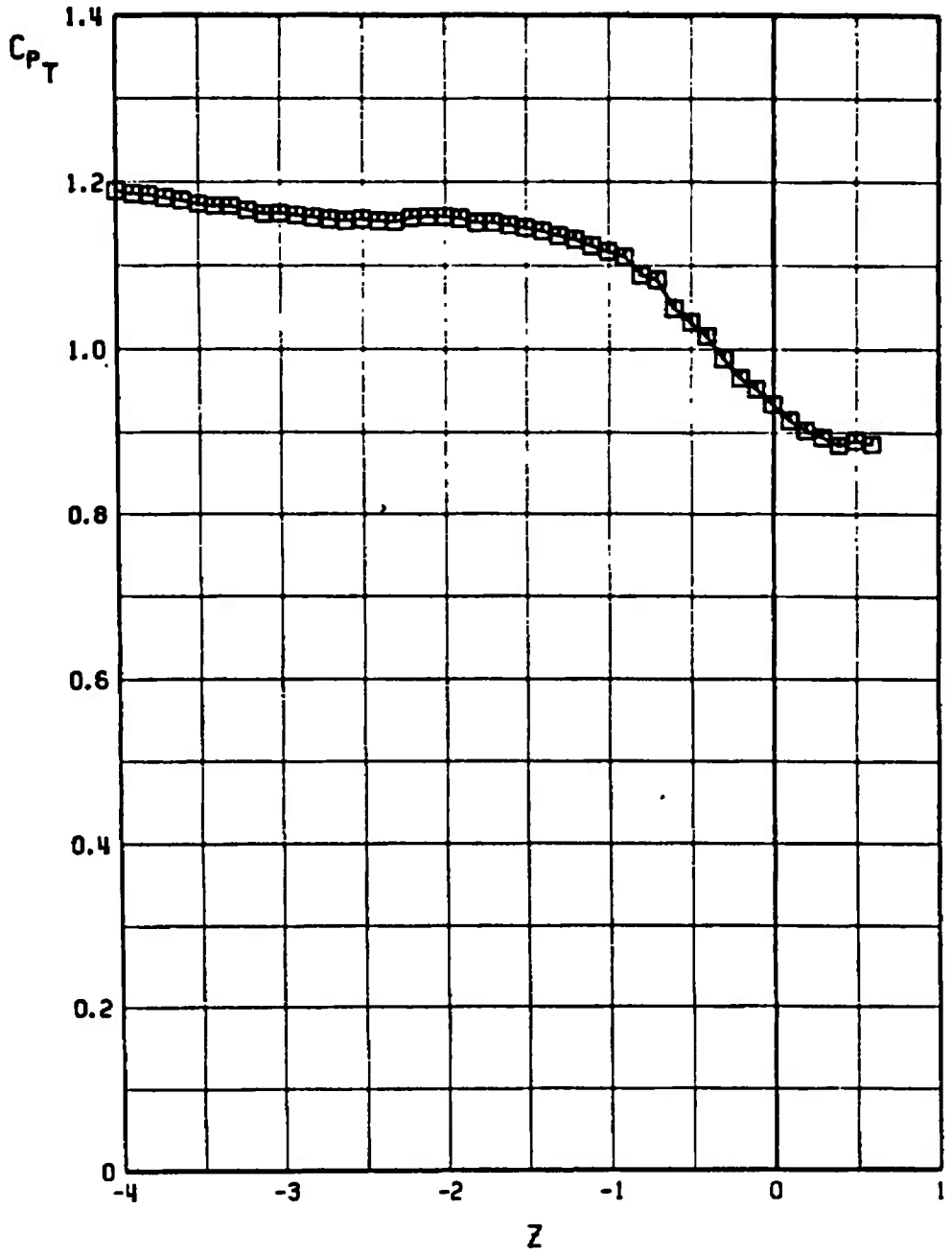

Fig. 51 Concluded

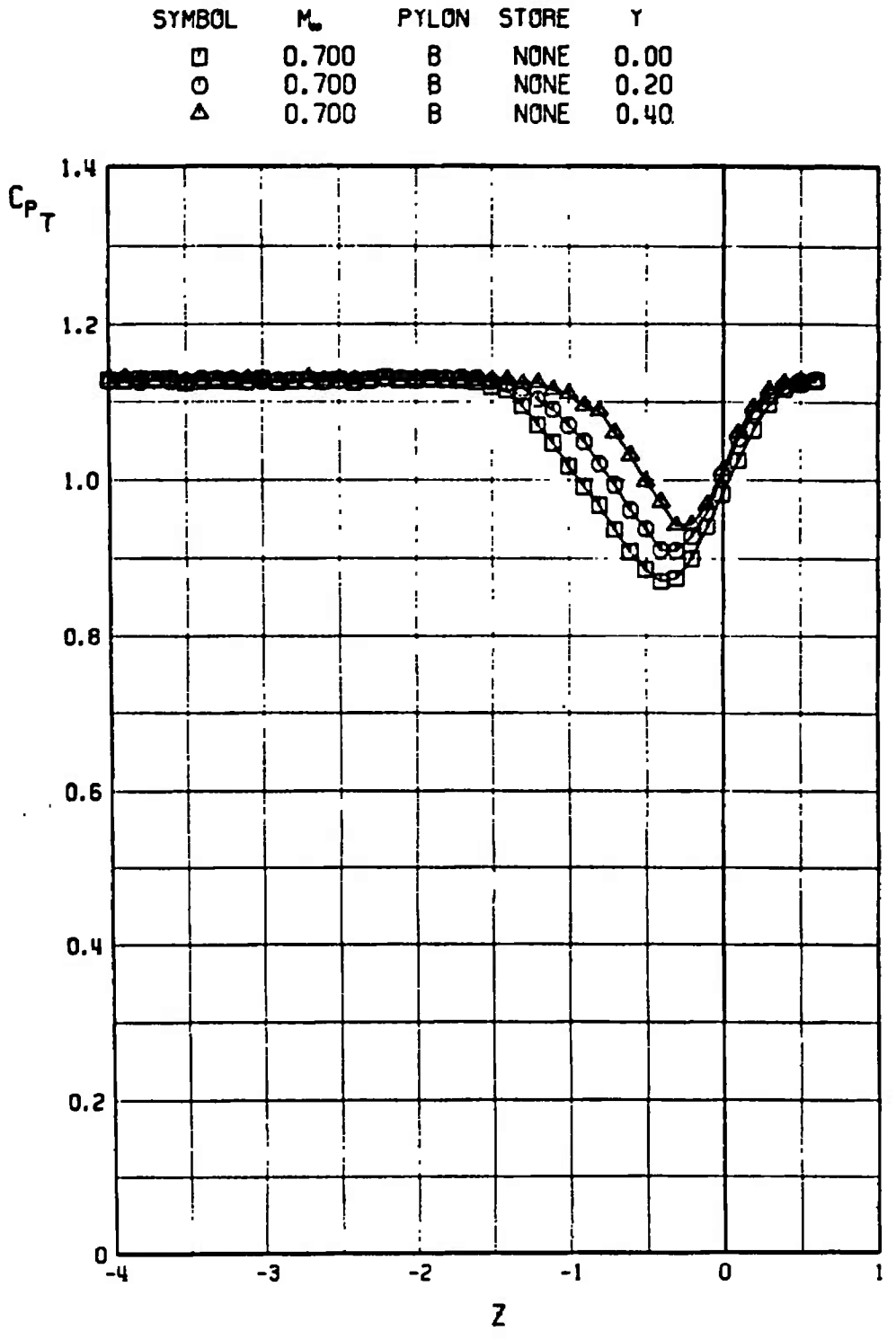

Fig. 52 Total Pressure Wake Survey for the Airfoil with B Pylon

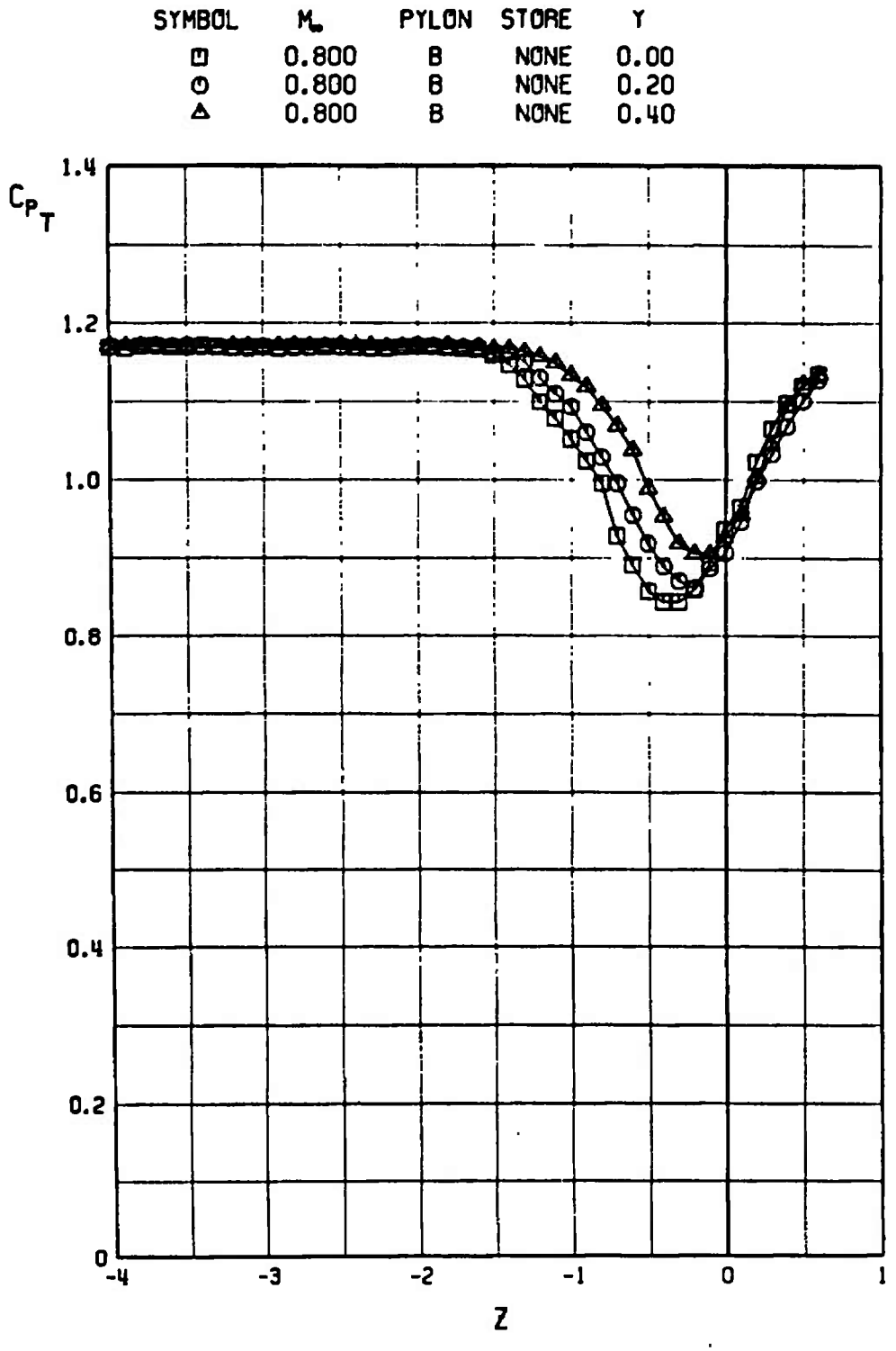

Fig. 52 Continued

SYMBOL	M_∞	PYLON	STORE	Y
□	0.850	B	NONE	0.00
○	0.850	B	NONE	0.20
△	0.850	B	NONE	0.40

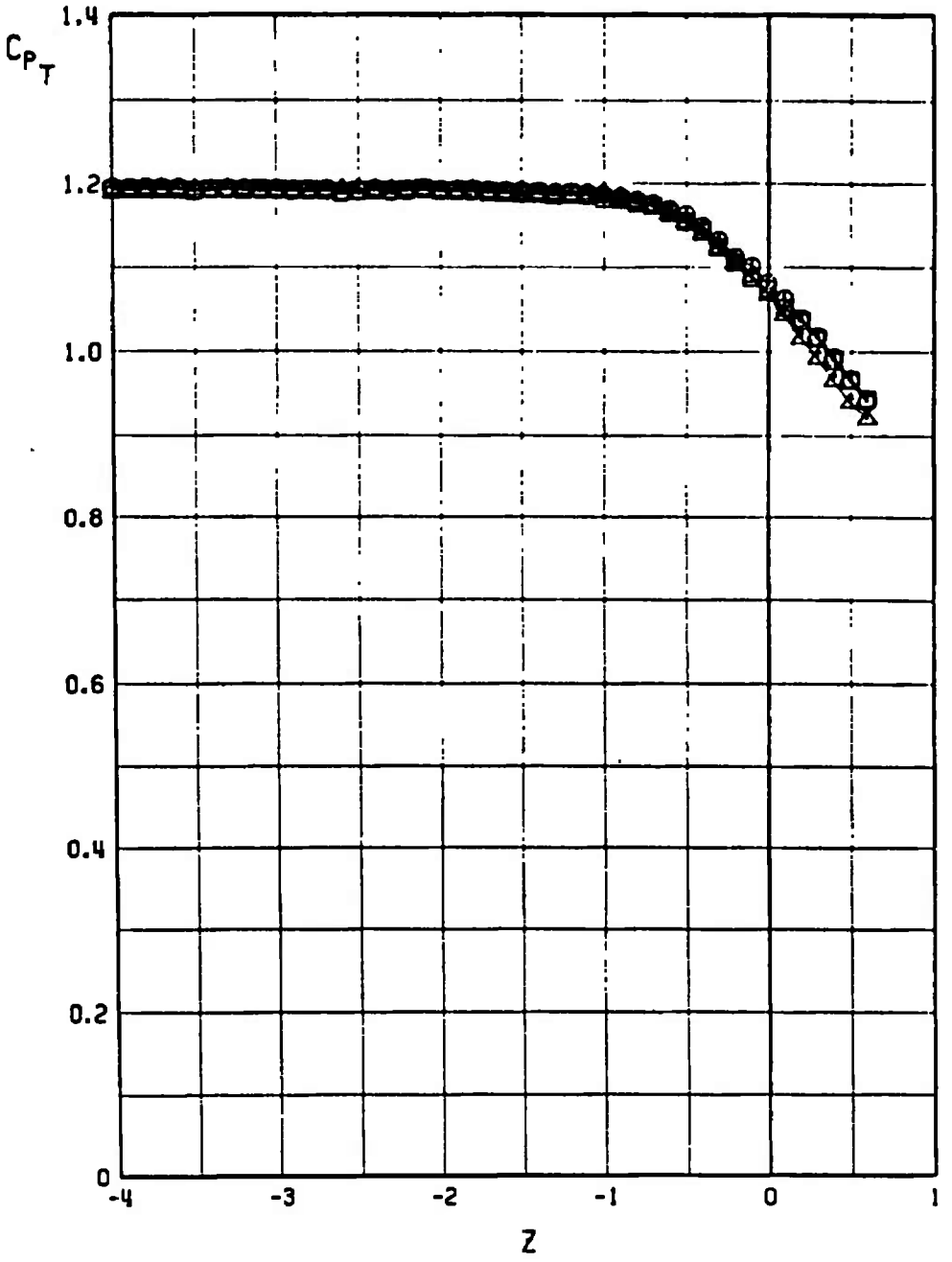

Fig. 52 Continued

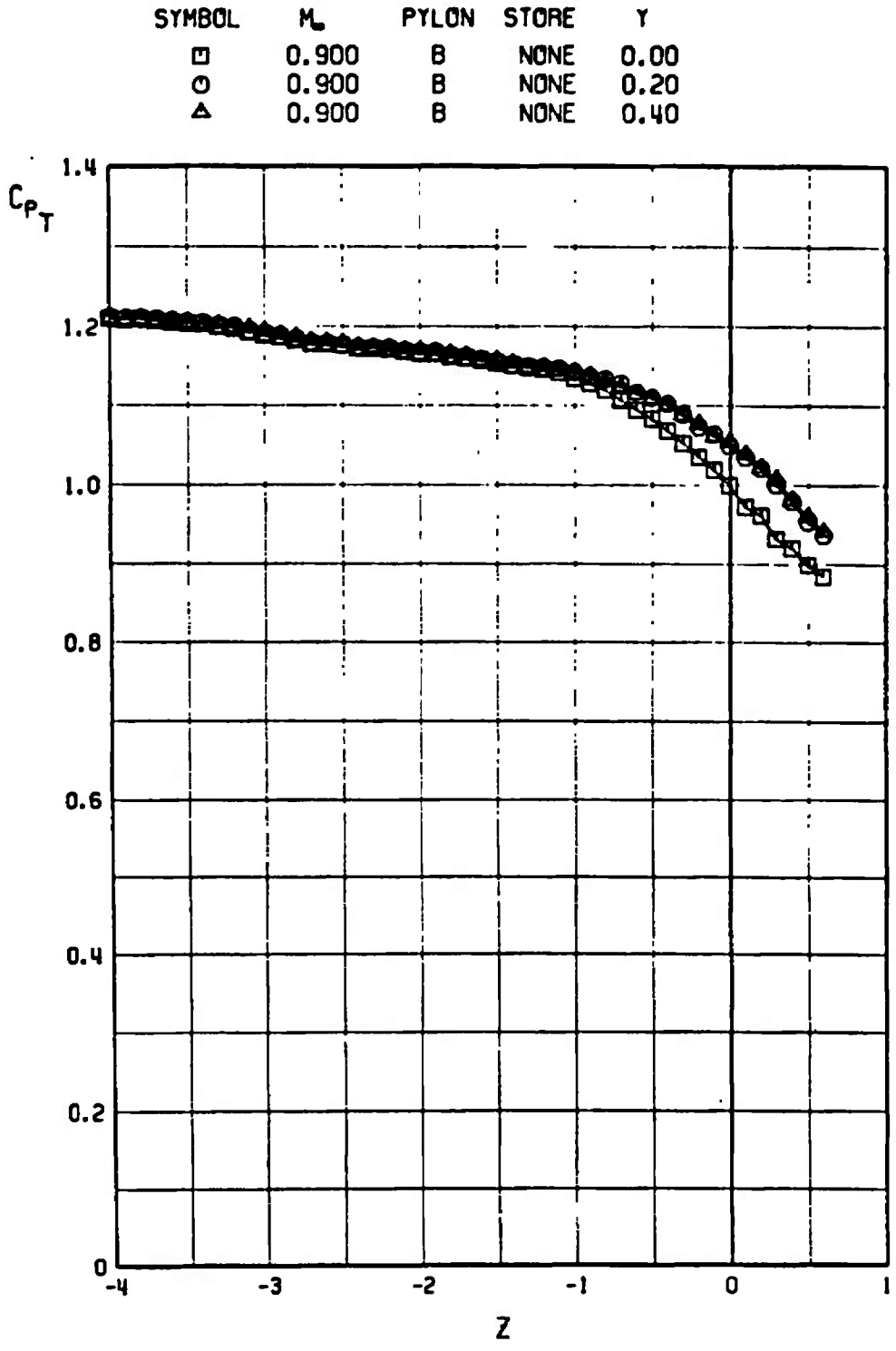

Fig. 52 Concluded

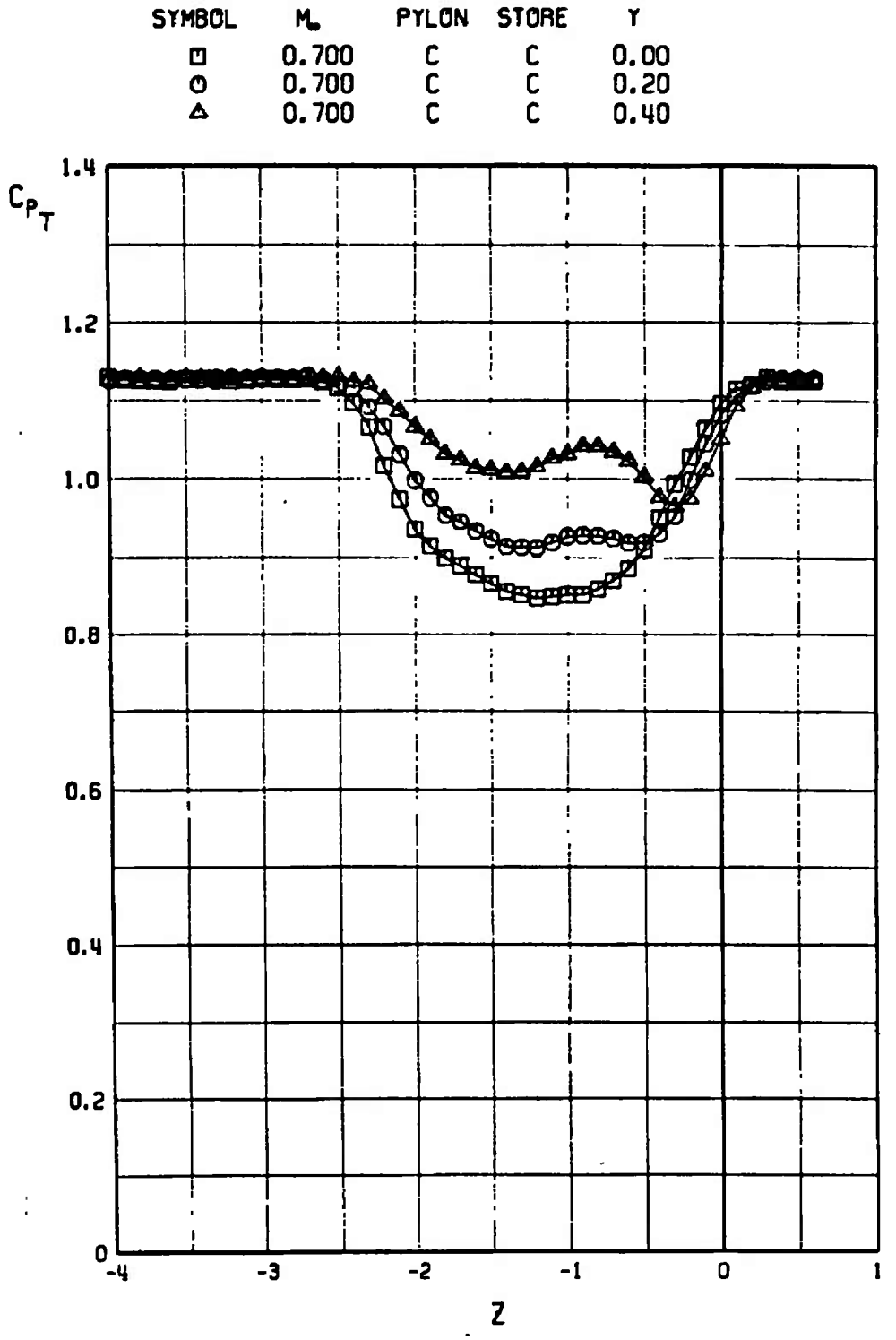

Fig. 53 Total Pressure Wake Survey for the Airfoil with C Pylon and C Store

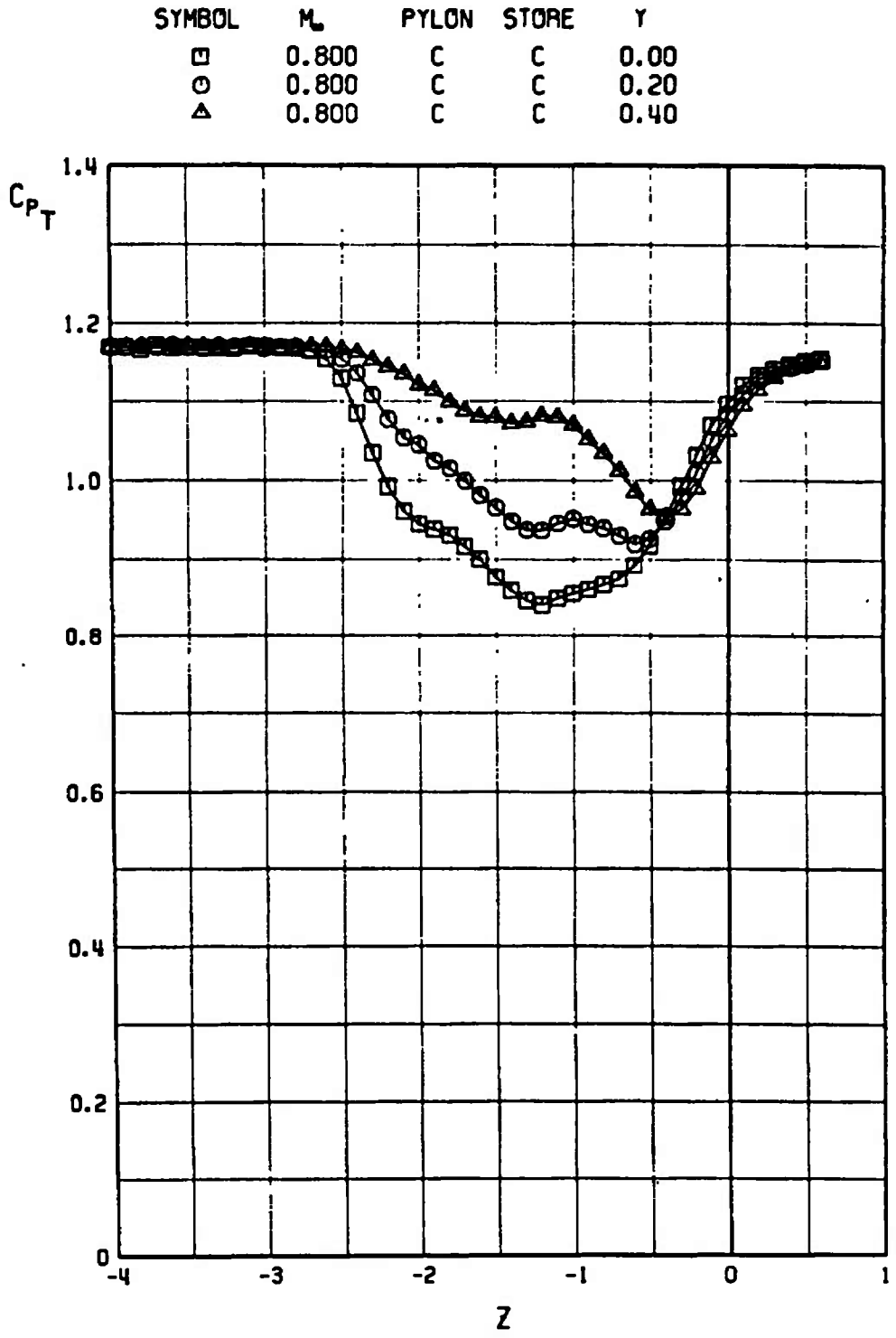

Fig. 53 Continued

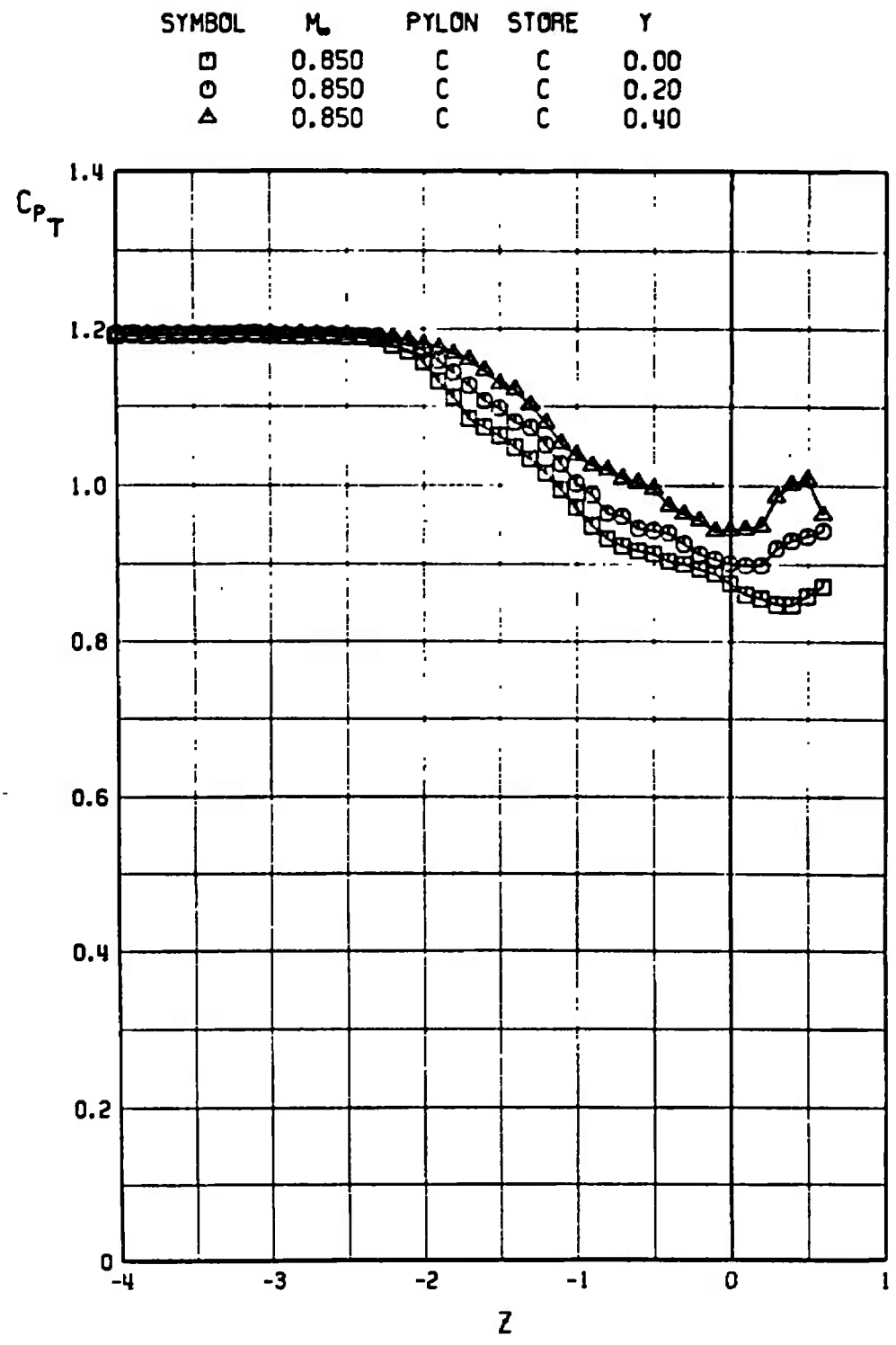

Fig. 53 Continued

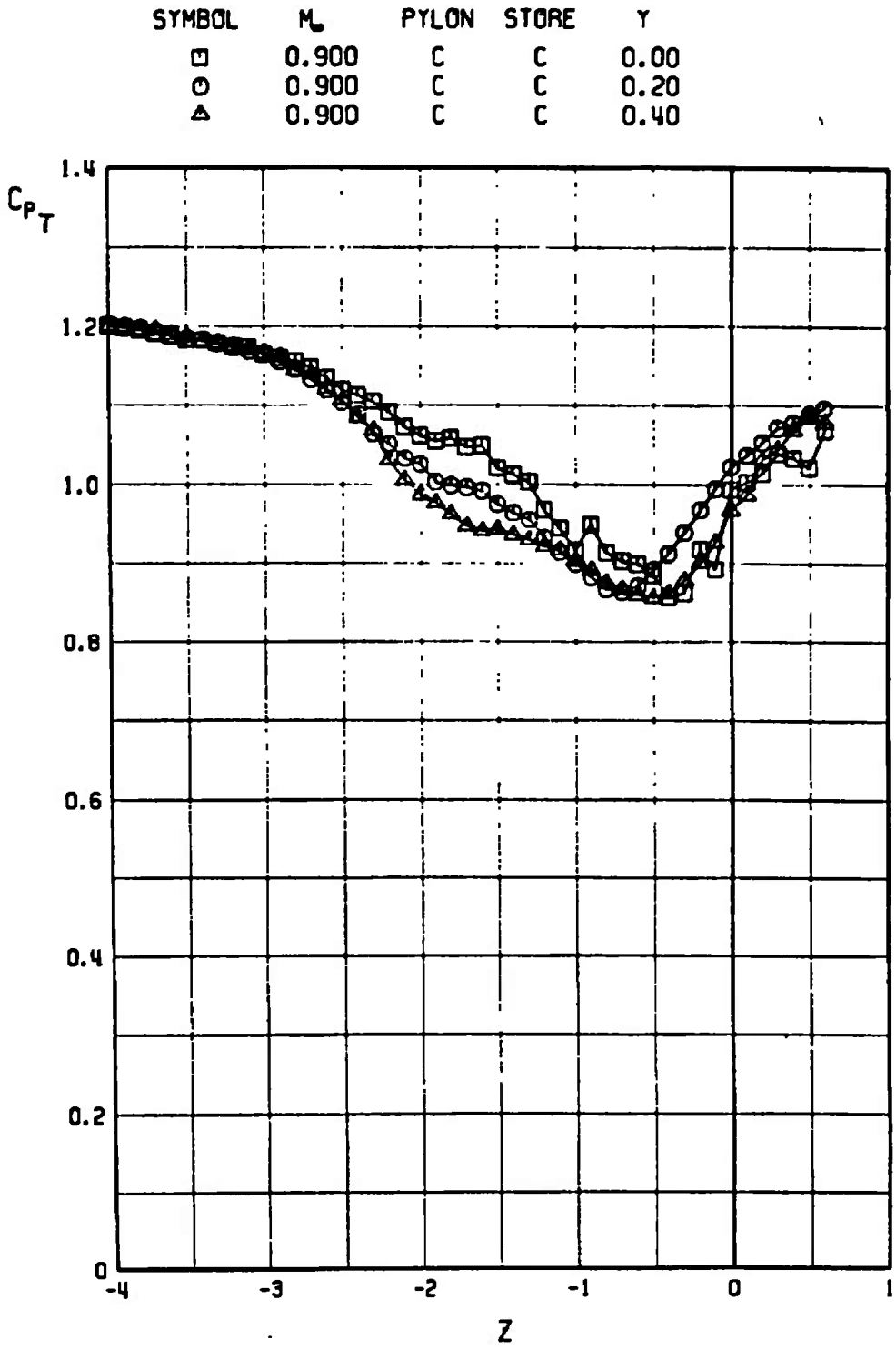

Fig. 53 Concluded

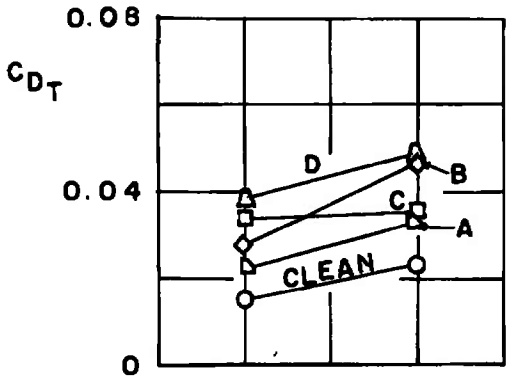

a. Wake Drag Coefficient versus Mach Number for Airfoil with Different Pylons and No Stores

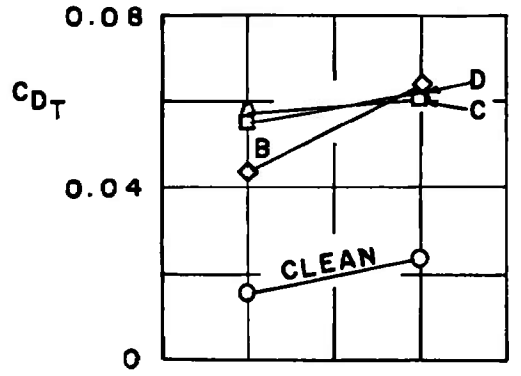

b. Wake Drag Coefficient versus Mach Number for Airfoil with Different Pylons and C Store

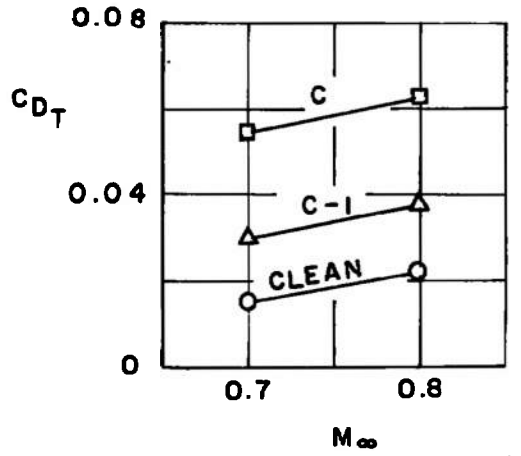

c. Wake Drag Coefficient versus Mach Number for Airfoil with B Pylon and C Store at Different Longitudinal Position on Store

Fig. 54 Wake Survey Drag Coefficient versus Mach Number for the Different Pylon/Store Configurations

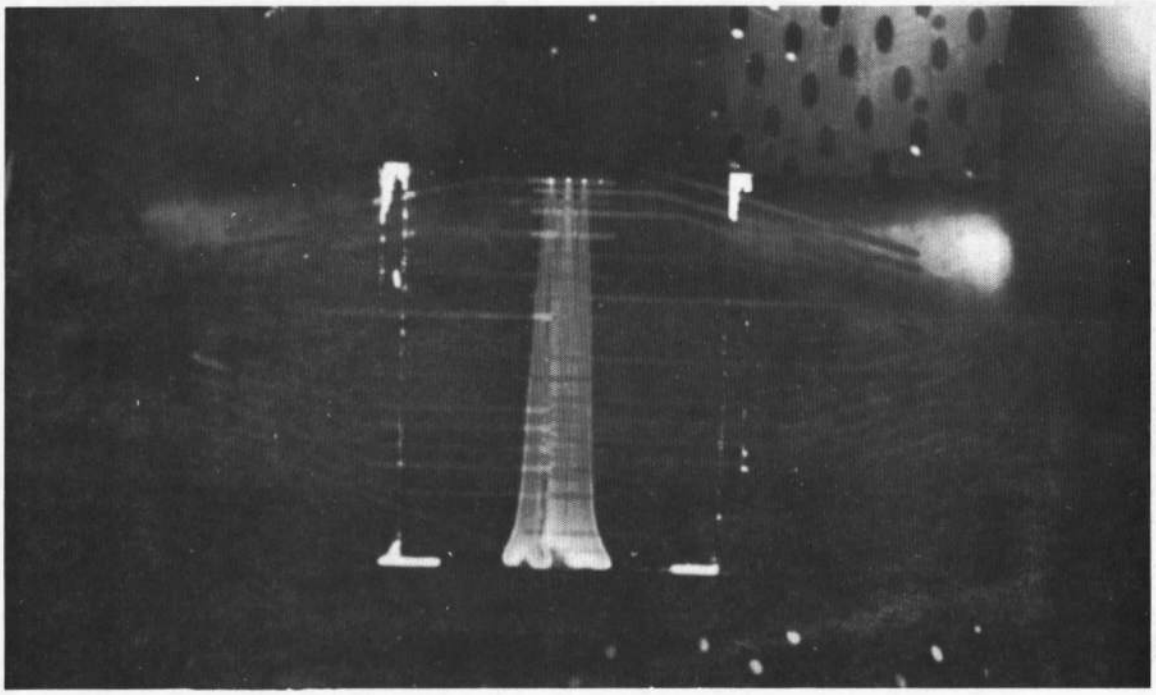

a. $M_\infty = 0.70$

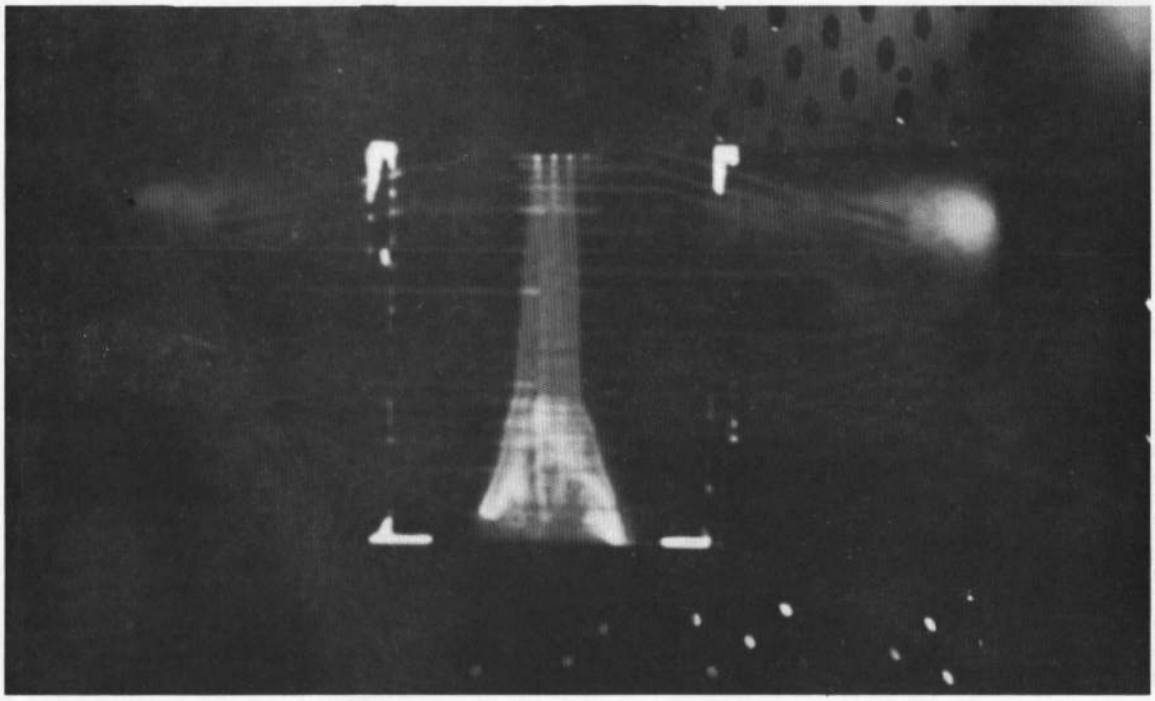

b. $M_\infty = 0.80$

Fig. 55 Photographs of Oil Flow on the Clean Airfoil, Upper Surface

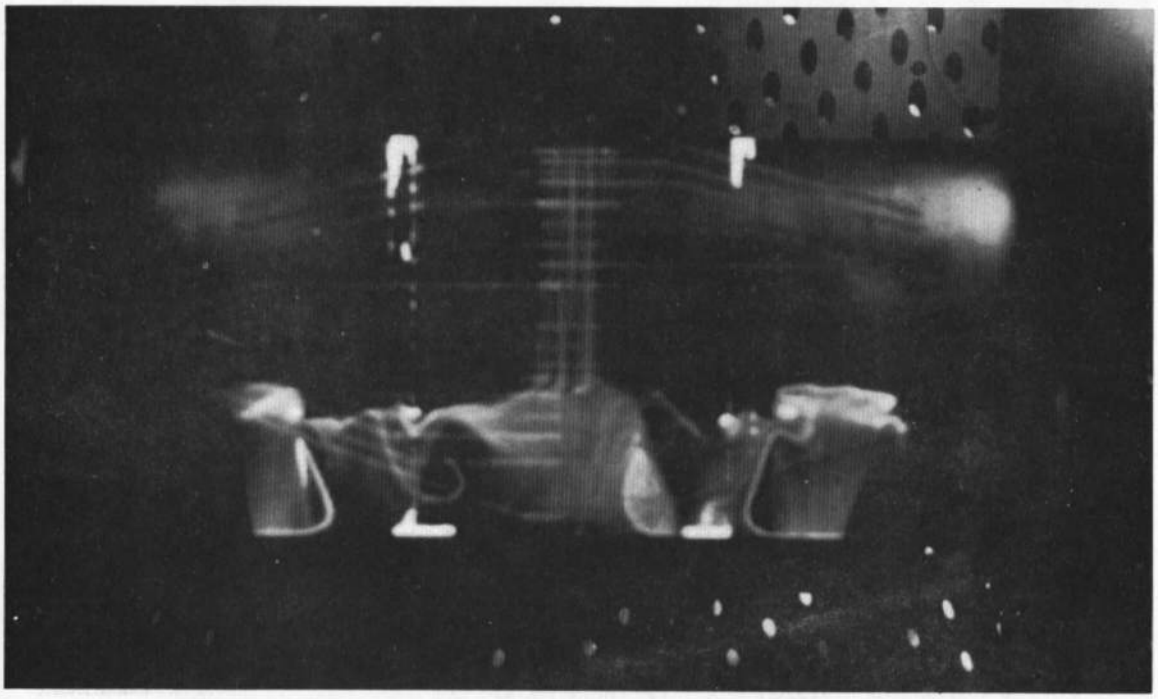

c. $M_\infty = 0.85$

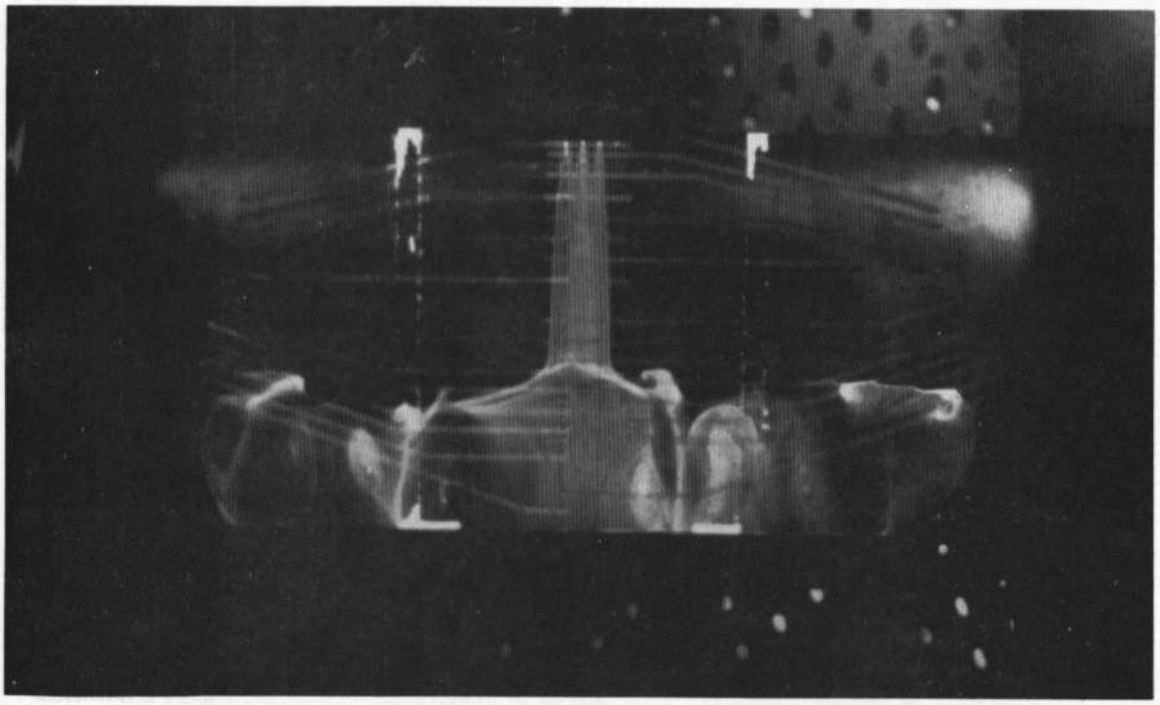

d. $M_\infty = 0.90$

Fig. 55 Concluded

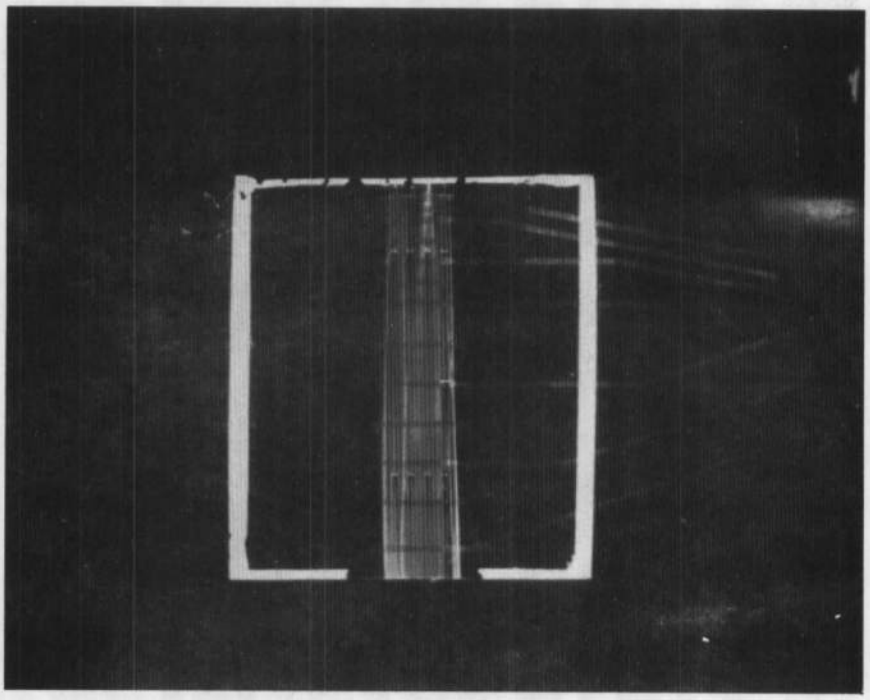

a. $M_\infty = 0.70$

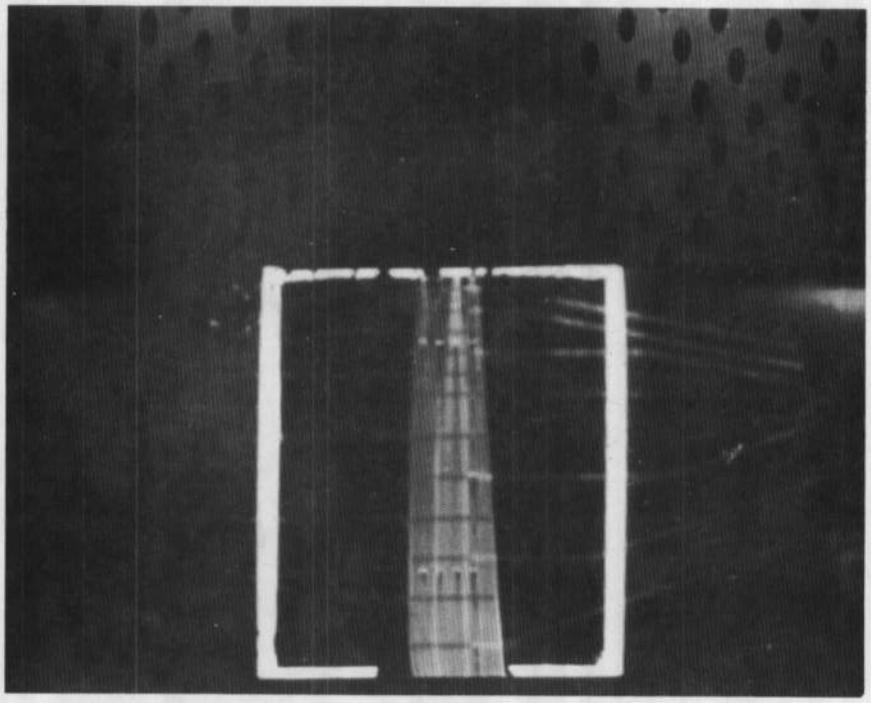

b. $M_\infty = 0.80$

Fig. 56 Photographs of Oil Flow on the Clean Airfoil, Lower Surface

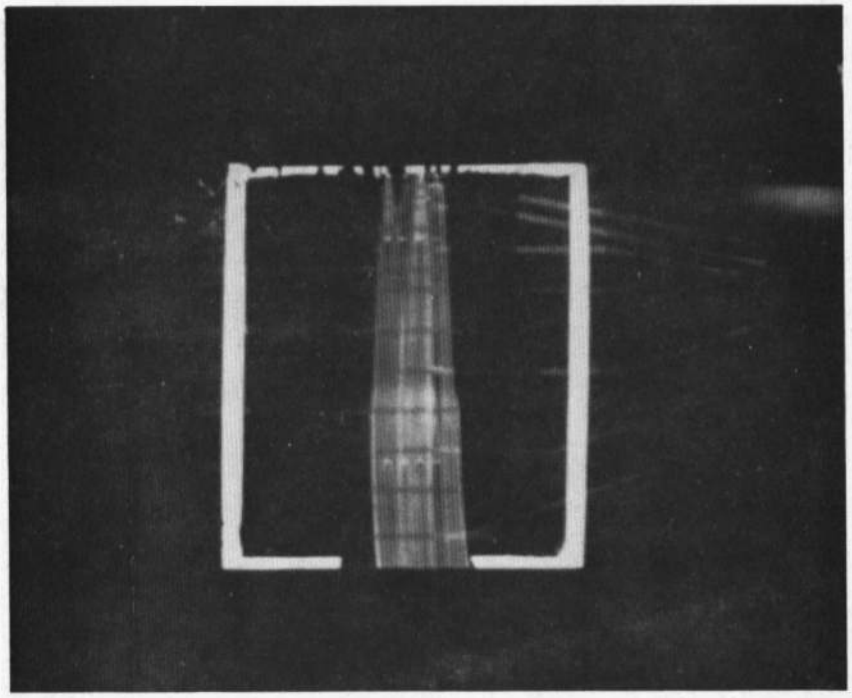

c. $M_\infty = 0.85$

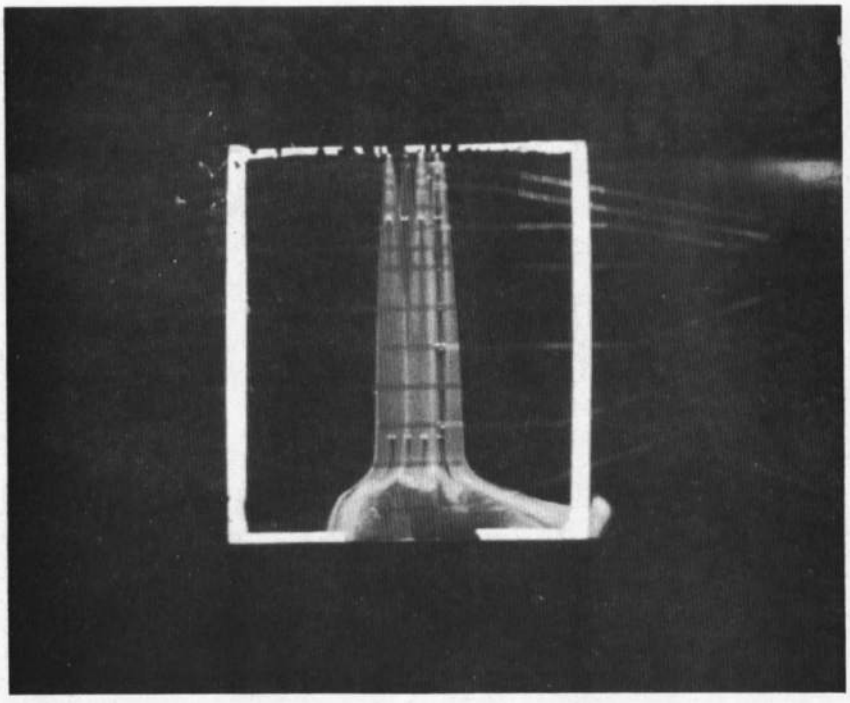

d. $M_\infty = 0.90$

Fig. 56 Concluded

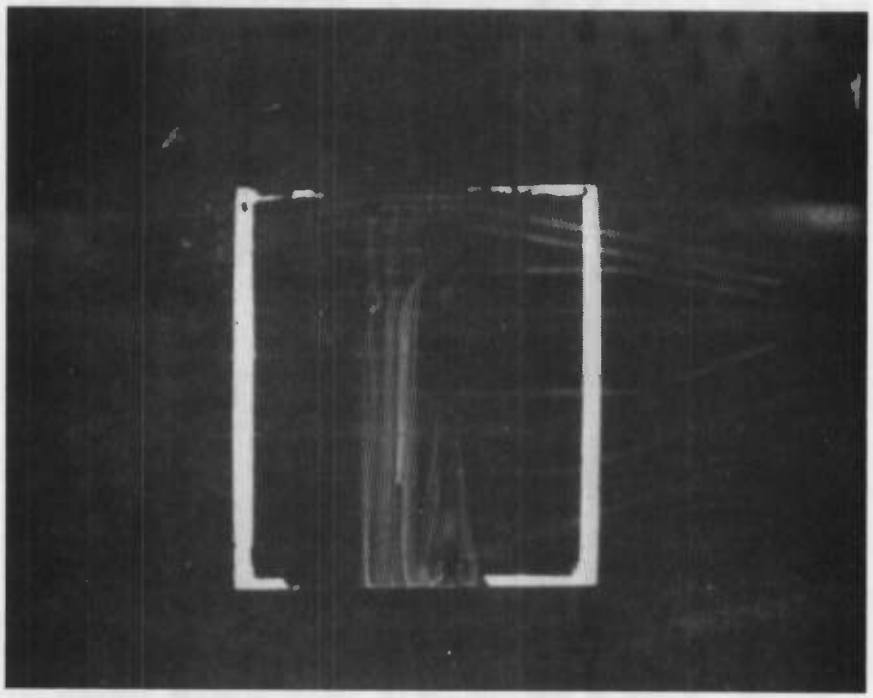

a. $M_\infty = 0.80$

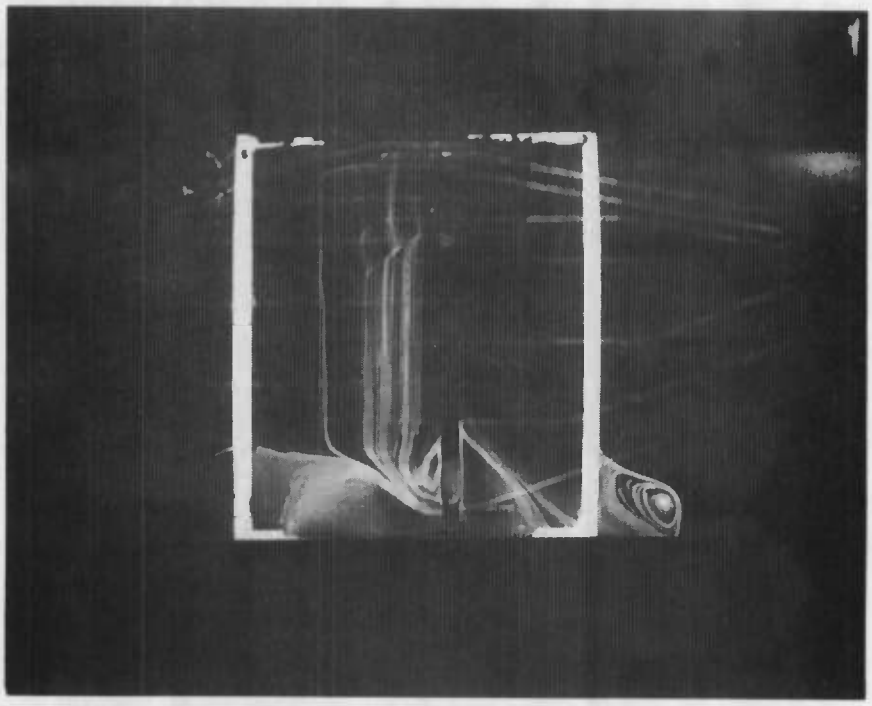

b. $M_\infty = 0.90$

Fig. 57 Photographs of Oil Flow on the Airfoil with B Pylon, Lower Surface

TABLE I
CONFIGURATIONS TESTED

Pressure Distribution Phase			Wake Survey Phase		Oil Flow Visualization Phase	
Pylon	Store	Pylon Location	Pylon	Store	Pylon	Store
None	None	N/A	A	None	None	None
A	↓	0.25	B	↓	B	None
B		0.00, 0.25, 0.50, 0.75	C		A	C
C		0.25	D		B	↓
D		0.25	A	C	C	
A	C	0.00, 0.25, 0.50, 0.75	B	↓	D	
B	↓	↓	C			
C			D			
D			B	C-1		
B	A					
↓	B					
	C					
	D					
	C-1					

*All configurations were tested at Mach numbers of 0.70, 0.80, 0.85, and 0.90; the clean airfoil configuration was also tested at Mach numbers of 0.825, 0.875, 0.925, and 0.95.

UNCLASSIFIED

Security Classification

DOCUMENT CONTROL DATA - R & D

(Security classification of title, body of abstract and indexing annotation must be entered when the overall report is classified)

1 ORIGINATING ACTIVITY *(Corporate author)*
Arnold Engineering Development Center
Arnold Air Force Station, Tennessee 37389

2a. REPORT SECURITY CLASSIFICATION
UNCLASSIFIED

2b. GROUP
N/A

3 REPORT TITLE
WIND TUNNEL INVESTIGATION OF THE PRESSURE DISTRIBUTION ON A TWO-DIMENSIONAL AIRFOIL WITH PYLON-MOUNTED STORES AT MACH NUMBERS FROM 0.7 TO 0.95

4 DESCRIPTIVE NOTES *(Type of report and inclusive dates)*
October 11 to 17, 1972--Final Report

5 AUTHOR(S) *(First name, middle initial, last name)*
D. K. Smith, ARO, Inc.

6 REPORT DATE
April 1973

7a. TOTAL NO OF PAGES
144

7b. NO. OF REFS
1

8a. CONTRACT OR GRANT NO

b. PROJECT NO 2567

c. Program Element 62602F

d.

9a. ORIGINATOR'S REPORT NUMBER(S)
AEDC-TR-73-71
AFATL-TR-73-75

9b. OTHER REPORT NO(S) *(Any other numbers that may be assigned this report)*
ARO-PWT-TR-73-27

10. DISTRIBUTION STATEMENT
Approved for public release; distribution unlimited.

11 SUPPLEMENTARY NOTES
Available in DDC

12 SPONSORING MILITARY ACTIVITY
AFATL/DLGC
Eglin Air Force Base
Florida 32542

13 ABSTRACT

A wind tunnel test was conducted to determine pressure distributions on a two-dimensional airfoil with pylon-mounted stores at Mach numbers from 0.70 to 0.95 and angles of attack from 0 to 14 deg. Four geometrically similar pylon-mounted stores differing in diameter by a factor of about four and four pylons differing in height were tested. Pressure distributions on the airfoil were obtained for the clean airfoil configuration and 12 pylon/store combinations. The pressure distributions were integrated and the lift, drag, and pitching-moment coefficients for the airfoil are presented. Total pressure wake surveys and oil flow photographs were also obtained for the test, and typical data are presented.

DD FORM 1 NOV 65 1473

UNCLASSIFIED

Security Classification

14. KEY WORDS	LINK A		LINK B		LINK C	
	ROLE	WT	ROLE	WT	ROLE	WT
F-4 jet aircraft						
aircraft external stores						
transonic wind tunnels						
separation						
aerodynamic characteristics						

AFSC
Arnold AFS Tenn